Analysis of Nucleocytoplasmic Transport in the Replication Cycle of Human Adenovirus Type 5

Dissertation

zur Erlangung des akademischen Doktorgrades
der Naturwissenschaften (Dr. rer. nat.)

am Department Biologie
der Fakultät für Mathematik, Informatik und Naturwissenschaften
an der Universität Hamburg

vorgelegt von
Melanie Schmid
aus Regensburg

Mai 2011

Genehmigt vom Fachbereich Biologie
der Fakultät für Mathematik, Informatik und Naturwissenschaften
an der Universität Hamburg
auf Antrag von Prof. Dr. T. DOBNER
Weiterer Gutachter der Dissertation:
Prof. Dr. R. GONZÁLES GARCIA CONDE
Tag der Disputation: 08. Juli 2011

Hamburg, den 24. Juni 2011

Professor Dr. Axel Temming
Leiter des Fachbereichs Biologie

Die Arbeit wurde angeleitet von: Prof. Dr. Thomas Dobner

Prüfungsausschuss:	Vorsitzender	Prof. Dr. Michael Böttger
	1. Dissertationsgutachter	Prof. Dr. Thomas Dobner
	2. Dissertationsgutachter	Prof. Dr. Ramón González
	1. Disputationsgutachter	Prof. Dr. Wolfram Brune
	2. Disputationsgutachter	Prof. Dr. Hans-Peter Mühlbach

Meglio una brutta verità che una bella bugia.

Table of contents

1 Abstract

Adenoviral DNA replication and assembly of progeny virions occurs in the nuclear compartment of the host cell. Thus adenoviruses must manipulate cellular transport pathways to import the viral genome and numerous viral proteins into the nucleus, as well as to export viral transcripts and proteins from the nucleus to the cytoplasm. Several adenoviral shuttling proteins apparently contain a nuclear localization signal (NLS) and/or a nuclear export signal (NES). All of these proteins fulfill important regulatory functions throughout the viral life cycle. However, it is still unclear whether the transport signals contribute to the function of these proteins.

Initially, leucine-rich NES sequences of the HIV-1 Rev type were identified in the adenoviral early E1B-55K and E4orf6 proteins. Since these two proteins facilitate the preferential nuclear export of adenoviral transcripts in the late phase of infection, extensive studies previously investigated whether CRM1-dependent transport contributes to this activity. The available data indicate that active CRM1 and/or the E1B-55K NES are not required for viral late mRNA transport. To complete the data, the study presented here set out to elucidate whether either the E1B-55K or E4orf6 NES participate in any of the described functions of the proteins. More precisely, these proteins are known to assemble a Cullin 5-based E3 ubiquitin ligase, which targets specific cellular proteins for proteasomal degradation. Interestingly, this work showed distinct requirements of the NESs for degradation and relocalization of cellular target proteins.

Another NES was identified in early E1A proteins, and it has been suggested that this signal might be required for efficient virus growth. These proteins regulate gene transcription and the cell cycle via interaction with multiple cellular proteins, and predominately fulfill their functions in the nuclear compartment. Thus not surprisingly detailed analysis of adenoviral early and late protein levels, as well as progeny virus production, revealed that a functional E1A NES was not required for efficient adenoviral replication.

Additionally, two regulatory proteins expressed from the late transcription unit contain leucine-rich NES sequences, namely L4-100K and protein VI (pVI). L4-100K mediates Cap-independent translation of viral late mRNA, while both these proteins cooperate in trimerization and subsequent nuclear import of the capsid protein Hexon, a fundamental step during virion assembly. Previously, the L4-100K-NES was shown to be crucial for adenoviral replication. The present work

provides the first evidence that the L4-100K-NES might be required for Hexon metabolism, specifically for trimerization and nuclear import of the capsid protein. Strikingly, the observed phenotype did not depend on active CRM1, indicating that the NES sequence of L4-100K is not a cargo partner of the export receptor CRM1. Most interestingly, although CRM1 itself is seemingly not required for any vital regulatory function of so far identified NES-containing proteins, efficient adenoviral replication does depend on active CRM1. It was shown that CRM1 supports both viral genome replication and nuclear export of early and intermediate viral transcripts. However, during the late phase of infection, export of viral transcripts was shown to depend on TAP, which typically mediates bulk cellular mRNA transport. Data obtained in this study suggest that TAP adaptor proteins are involved in regulating preferential adenoviral mRNA transport, and that this might depend on modification and/or decreased amounts of specific TAP adaptor proteins.

Previous studies proposed a nuclear localization signal in several adenoviral proteins, including E1A, E4orf6, L4-100K, and pVI. However, the import pathway used has only been established for E1A. This work shows binding of E4orf6 to different cellular importins. Surprisingly, this interaction was not required for nuclear localization of the adenoviral protein. In contrast, E4orf6-dependent accumulation of importin α5 was detected in the course of infection, indicating a functional role of the interaction during adenoviral replication.

2 Introduction

2.1 Adenoviruses

2.1.1 Classification

Adenoviruses were first isolated in the early 1950s from adenoid tissue and secretions of patients with respiratory diseases [147, 275]. Generally, adenoviruses cause infections of the respiratory tract [74, 123], the eye [163] or the gastrointestinal tract [349], leading to diseases called acute respiratory disease (ARD), adenoid-pharyngeal-conjunctival (APC), respiratory illness (RI) or adenoid degeneration (AD).

The family of *Adenoviridae* comprises about 100 serologically different virus types and is divided into five genera, depending on their host range: *Aviadenovirus* of avian hosts, *Atadenovirus* of avian, reptile and ruminant hosts, *Mastadenovirus* of mammalian hosts, *Siadenovirus* of amphibian hosts, and *Ichtadenovirus* of fish hosts [19, 73, 150]. To date, 54 human adenovirus types of the *Mastadenovirus* genera have been described and classified into seven subgroups (A-G), according to their sequence homology, hemagglutination, and oncogenicity in immuno-suppressed rodents (Fig. 1) [14, 73, 322, 340]. Since type 2 and 5 are non-oncogenic, they became the most intensively studied human adenoviruses.

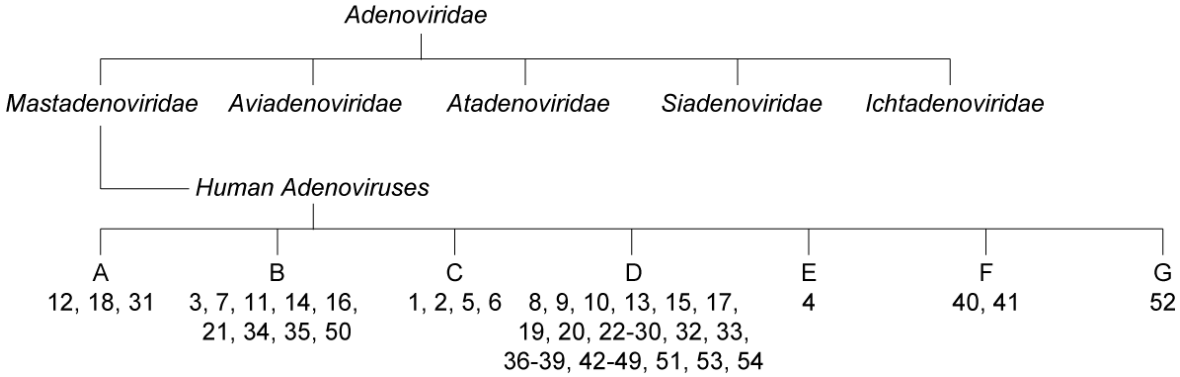

Figure 1: Classification of Adenoviridae. Schematic representation of *Adenoviridae* including human adenovirus types 1-54. Types 1-52 are classified as published by Harrach and associates [73], and types 53 and 54 are classified according to the International Committee of the Taxonomy of Viruses (ICTV).

Human adenoviruses are widely prevalent in the human population and cause lytic as well as persistent infections that are associated with a multitude of clinical symptoms. Although infections are generally respiratory, ocular, or gastro-intestinal, such as ARD, pneumonia, acute follicular conjunctivitis, epidemic

keratoconjunctivitis, or gastroenteritis, the disease pattern also includes hemorrhagic cystitis, urinary tract infection, hepatitis, and meningoencephalitis. Severe systemic infections are described in immunosuppressed patients following allogenic hematopoietic stem cell transplantation. These adenovirus infections can result in death [1, 150, 224].

2.1.2 Structure and genome organization

Adenoviruses are non-enveloped viruses with an icosahedral capsid of 80-110 nm in diameter containing the linear double-stranded DNA genome in a complex with the core proteins V, VII, and µ [297]. The viral capsid comprises 252 structural units (*capsomers*), including 240 Hexons (II) and 12 Pentons (III). This capsid protects the viral genome and plays a substantial role during virus entry into the host cell. Each Penton is non-covalently linked to a Fiber (IV) protein protruding from the capsid structure (*spikes*). Fiber proteins mediate essential steps in the adsorption and internalization of the virus via the Coxsackie virus and Adenovirus receptor (CAR) [20], while interaction of the Penton base protein with additional cell surface proteins (integrins) facilitates efficient uptake of the virus [217, 332, 333]. Other minor components of the viral capsid include proteins IIIa, VI, VIII, and IX [276, 277, 321].

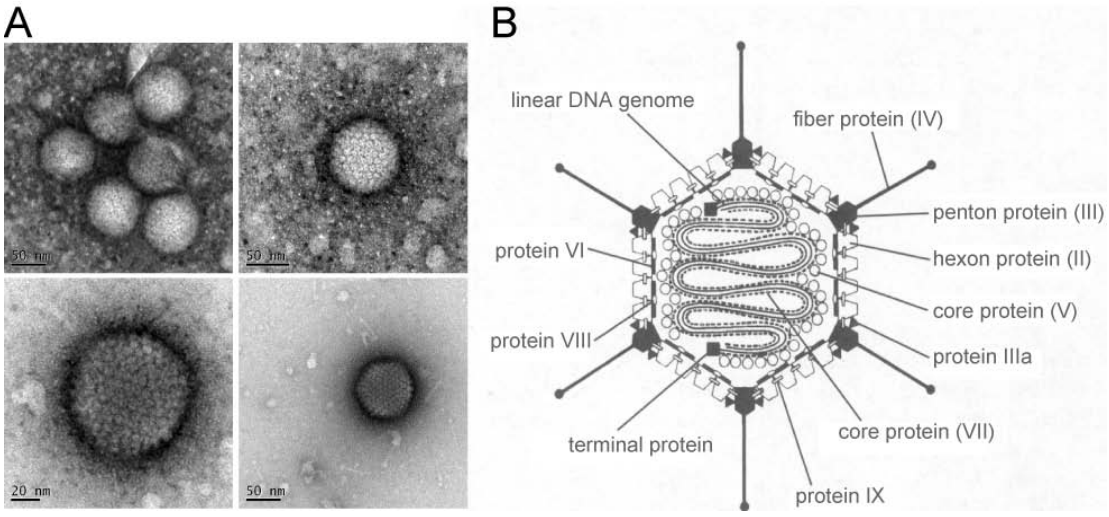

Figure 2: Electron microscope images and schematic representation of adenovirus. (A) The microscope images illustrate the icosahedral structure of adenoviral particles. (B) Schematic illustration of the adenoviral virion including core and capsid proteins (from Modrow and Falke, 2003 [223]).

The adenoviral genome consists of a linear double-stranded DNA that is flanked by inverted terminal repeats (ITR). Both 5´-ends of the genome are linked to a terminal protein (TP) that is essential for initiation of viral DNA replication [73]. The genome of Ad5 shown in Figure 3 comprises nine transcription units that

encode for approximately 40 different regulatory and structural proteins as well as two virus-associated RNAs (VA-RNAs). Transcription units are expressed in a tightly regulated order and are therefore classified as early (E1A, E1B, E2A, E2B, E3, E4), delayed (IX, IVa2) or major late transcription unit (MLTU). All of these units are transcribed by RNA polymerase II, whereas VA-RNAs are transcribed by RNA polymerase III [297].

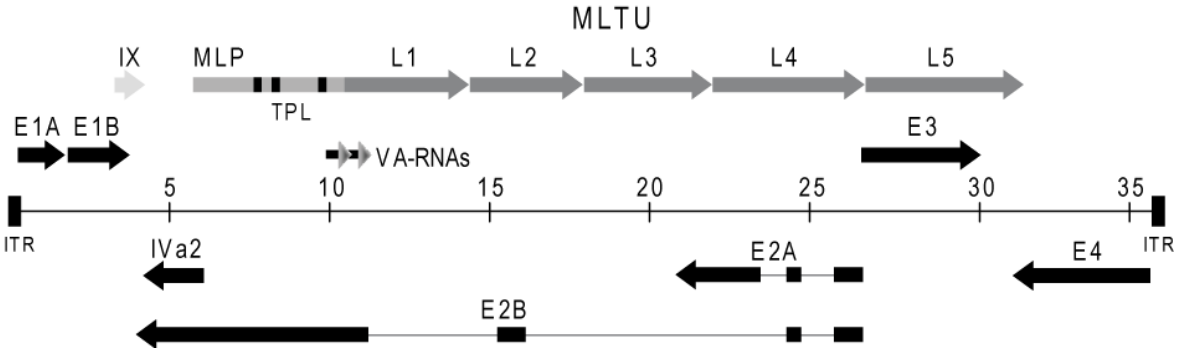

Figure 3: Genome organization of Ad5. Organization of early (E1A, E1B, E2A, E2B, E3, E4), delayed (IX, IVa2) and late (L1-L5; MLTU) transcription units on both DNA strands is illustrated by arrows in relation to the 35.9 kbp DNA genome. Early proteins are involved in DNA replication (E2), immune system modulation (E3), transcription and RNA processing (E1A, E1B, E4), and cell cycle control (E1A, E1B, E4). Late units (L1-L5) mainly encode for structural proteins, with a few exceptions. E: early; ITR: inverted terminal repeat; L: late; MLTU: major late transcription unit; MPL: major late promoter; TPL: tripartite leader; VA-RNAs: virus-associated RNAs.

2.1.3 Oncogenic potential of human adenoviruses

The oncogenic potential of adenoviruses was first described for type 12 after its subcutaneous injection led to development of undifferentiated sarcomas in newborn rodents [314]. Extensive studies have now revealed most of the gene products involved in transformation by human adenoviruses, as well as differences in the oncogenicity among various Ad species [34, 85, 237, 319, 335]. Based on the frequency and time required to establish tumors in rodents, human adenoviruses can be subdivided into highly oncogenic, weakly oncogenic, and non-oncogenic groups (Fig. 4). Types of subgroup A are highly oncogenic, while types of subgroup B are weakly oncogenic and inefficiently form tumors after long incubation times. In contrast, types from subgroups C to F do not cause tumors at all when injected into rodents, except for types 9 and 10 of subgroup D that induce mammary carcinoma in female rats [5, 162, 312].

Interestingly, despite these different oncogenicities in rodent animals, all tested human adenovirus types are able to transform primary rodent cells in culture [237]. Such transformed cells loose contact inhibition and grow in multilayer colonies (*foci*). However, not all of these transformed cells are capable of inducing

tumorigenesis after inoculation into rodents. Consistent with the observed differences in the oncogenic potential of different human adenovirus types in live rodents, the tumorgenicity depends on different factors, such as the type or immune status of the animal [132, 297, 335], which is mainly affected by the thymus-dependent CTL response [24, 64, 265]. Although the molecular mechanisms of transformation are still unclear, the process follows the classical concept of viral oncogenesis, where viral genes persist within the transformed cells maintaining the oncogenic phenotype. Thus, the E1 oncoproteins are retained in all Ad or plasmid transformed cells, underlining the importance of the encoded gene products [34, 85, 237, 319, 335]. Moreover, although the E1 region seems to be indispensable for efficient cell transformation, it was shown that proteins of the E4 region augment this process [85, 309].

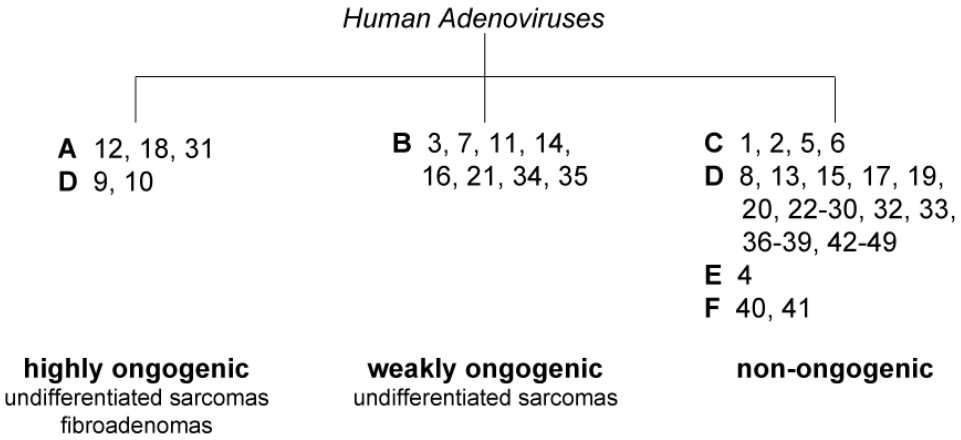

Figure 4: Oncogenic potential of human adenoviruses in rodents. Classification of human adenovirus types according to their oncogenicity in rodents, indicating the induced tumor type. Types 50-54 are not included due to the lack of studies addressing their oncogenic potential.

In contrast to the oncogenicity of human adenoviruses in rodent cells, transformation of primary human cells in culture is a very inefficient process [139]. Thus only a few adenoviral transformed human cell lines are described [48, 95, 96, 118, 133, 286, 331]. To date, malignant diseases in humans could never be convincingly associated with human adenoviruses [57, 209-211, 339]. However, two independent studies recently suggested that adenovirus infections are related to childhood acute lymphoblastic leukemia (ALL) [138] and/or tumorigenesis in brain tissue [182]. A possible relationship between supposed long-term, non-harmful adenovirus infection, persistence, and human malignancies remains to be established.

2.1.4 Productive infection cycle

Human adenoviruses can infect a wide range of cell types *in vivo*, generally post-mitotic resting, differentiated epithelial cells of the respiratory and gastrointestinal tract, and most likely the central nervous system [182]. Additionally, in tissue culture several tumor and primary cell lines can be infected with adenoviruses. In human cells adenoviruses cause a lytic infection, whereas infection of rodent cells results in abortive infection [203, 297]. Recent observations also suggest latent adenovirus infection [120, 138, 182].

The adenoviral replication cycle is classified into two major phases termed *early* and *late*. Conventionally, these phases are separated by the initiation of viral DNA synthesis (Fig. 5). Upon receptor-mediated internalization of the viral particle and import of the viral genome into the cell nucleus, expression of the *immediate early* gene E1A is initiated [9, 10, 227, 285]. Subsequently, E1B and E4 RNAs are transcribed and alternatively spliced to produce the viral early regulatory proteins. These early proteins are multifunctional and provide an optimal environment for virus replication. Hence, these early gene products are responsible for inducing cell cycle progression (E1, E4), inhibiting apoptosis and growth arrest (E1A, E1B), modulating immune response, and maintaining cell viability (E3). The proteins expressed from the E2 transcription unit, i.e. the viral DNA polymerase (E2B), the DNA-binding protein (DBP/E2A-72K), and the precursor of the terminal protein (pTP), function in viral DNA replication [297]. The E4 region encodes at least six different gene products transcribed from several open reading frames (orf), namely E4orf1, E4orf2, E4orf3, E4orf4, E4orf6, and E4orf6/7. These E4 proteins mediate essential functions during the adenoviral replication cycle. To date, the mRNA, but not the protein, of another putative product of this region, E4orf3/4, has been described in Ad infected cells [309, 310].

With the onset of DNA replication, the late phase starts with activation of the major late promoter (MLP), and the consequent expression of the major late transcription unit (MLTU), to produce the late mRNAs from a 29 kb precursor mRNA by differential splicing (Fig. 3). All of these mRNAs (L1-L5) contain a common 5´-non-coding sequence of 201 nucleotides (tripartite leader, TPL). These late mRNAs mainly encode structural proteins of the viral capsid. Another striking feature during the late phase of adenoviral infection is the inhibition of host cell mRNA transport and translation (*host shut-off*). In contrast, viral late mRNAs are efficiently transcribed and exported to the cytoplasm, where they are preferentially translated [297]. Additionally, nuclear structures are rearranged and

centers of viral transcription and DNA replication emerge [258, 259]. Finally, viral late (L4-100K, -33K, -22K, pVI) and early regulatory proteins (E1B-55K, E4orf6, E2A-72K) mediate the encapsidation of the viral genome in the nuclear compartment. Approximately 24 hours post infection up to 10,000 viral particles are released upon host cell lysis (Fig. 5) [297].

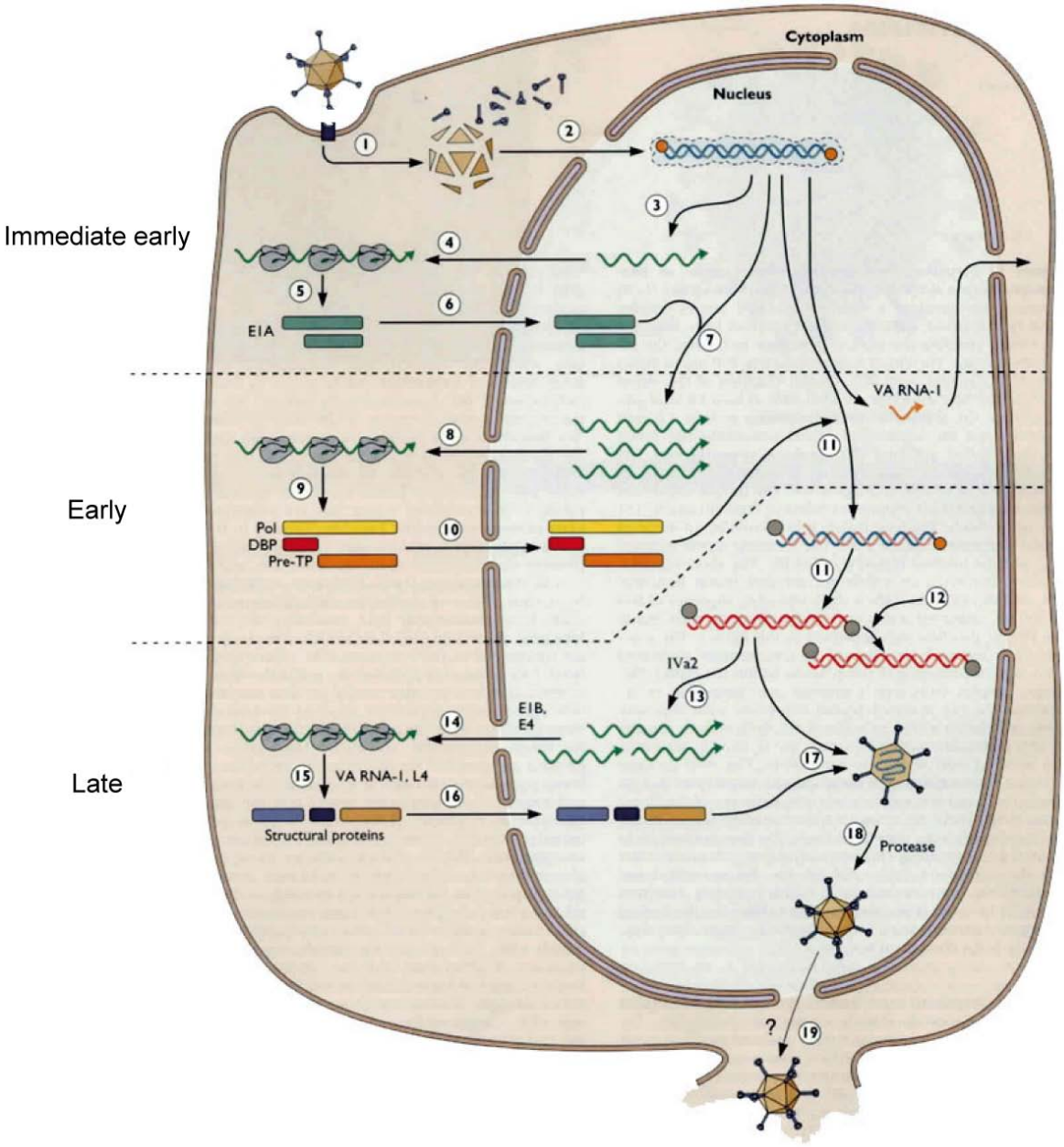

Figure 5: Replication cycle of human adenovirus type 2. (1) Adsorption and endocytosis. (2) Uncoating of the viral particle and import of the viral genome into the nucleus. (3–6) Expression of immediate early E1A genes. (7) The larger E1A protein stimulates transcription of viral early genes. (8–10) Expression of early genes. (11, 12) Viral DNA synthesis. (13–16) Expression of viral late genes. (17) Capsid assembly from structural proteins and progeny viral genomes. (18) Precursor proteins of immature virions are cleaved by the viral L3 protease. (19) Release of progeny viruses (from Flint *et al.*, 2004 [103]).

2.2 Regulatory proteins of adenovirus

2.2.1 Immediate early protein E1A

The E1A region is the first transcription unit expressed after the adenoviral genome has reached the nucleus [32], and encodes five alternatively spliced mRNAs. This generates two major mRNA species, E1A-13S (289 aa) and E1A-12S (243 aa), as well as three additional mRNAs (11S, 10S, 9S) that so far have been assigned no definitive functions. In principle, the gene products are acidic proteins with relatively little secondary structure, and are equally distributed in nuclear and cytoplasmic compartments [113]. E1A proteins mediate important steps during the early phase of the viral life cycle. Both the initiation of unscheduled cell cycle progression and transcriptional activation of viral early gene expression provide optimal conditions for adenoviral DNA and late protein synthesis. By modulating the functions of key regulators of cell cycle progression and programmed cell death, E1A also leads to the immortalization of primary rodent cells, an indispensable step for efficient cell transformation [17, 117]. Through interaction with epigenetic regulators and cellular transcription factors such as pRB, p300/CBP, PCAF, CtBP, $p21^{Cip1/Waf1}$, $p27^{Kip1}$, DYRKs, p400 and TRRAP, E1A proteins are capable of transitorily and temporally modulating approximately 70% of all gene promoters [99, 100, 113]. The most notable example is the exclusive binding of E1A to the phosphorylated form of the retinoblastoma tumor suppressor (pRB) [45, 84, 124, 222]. This leads to dissociation of pRB from the E2F transcription factor and subsequently to the constitutive activation of E2F responsive cellular genes and the viral E2 early promoter [13, 66]. Thus E1A economically induces cell cycle progression as well as expression of the viral proteins required for viral DNA replication. The nuclear localization of E1A has been reported to be mediated via importin α3 binding to a nuclear localization signal (NLS) at the far C-terminus, and is tightly regulated by acetylation at the lysine residue within the NLS [180, 207]. This strong NLS provides rapid localization of E1A to the cell nucleus [186]. However, nuclear export of the protein via the cellular export receptor CRM1 depends on a nuclear export signal (NES) within the conserved region (CR1) domain [164].

2.2.2 Early proteins E1B-55K and E4orf6

The E1 region encodes another multifunctional protein in the second transcription unit (E1B). The E1B-55K phosphoprotein comprises 496 amino acids with a

molecular weight of 55 kDa. It acts in both the early and late phase of the adenoviral replication cycle, thus contributing to transcriptional, post-transcriptional, translational, and post-translational regulation. In the early phase E1B-55K binds to the tumor suppressor protein p53 and subsequently inhibits its function in transcriptional transactivation [284, 296, 346, 347]. Furthermore, E1B-55K and E4orf6, a 34 kDa protein encoded by the E4 region, form a Cullin 5-based E3 ubiquitin ligase that induces the proteasomal degradation of p53 [27, 261]. This, in turn, counteracts E1A-dependent expression of p53, and blocks p53-mediated apoptosis of the host cell [329].

The E1B-55K/E4orf6 ligase complex includes additional cellular proteins (Cullin 5, Rbx1, and Elongin B/C), and is similar to previously described Skp1-Cul1-F-box-protein (SCF) ubiquitin ligases. While E4orf6 mediates complex assembly, E1B-55K likely plays a role in substrate recognition [27, 142, 261]. However, it is still unclear whether the degradation of p53 occurs on nuclear or cytoplasmic proteasomes [142]. Further cellular target proteins of the E3 ubiquitin ligase include Mre11 and DNA-Ligase IV - both involved in DNA double-strand break repair - as well as integrin α3 [15, 72, 304]. Most recently identified is Daxx, whose degradation seems to be independent of E4orf6 [289].

It is well established that during the late phase of infection, both E1B-55K/E4orf6 viral proteins are necessary for the preferential export of viral late mRNAs from the nuclear to the cytoplasmic compartment [11, 39, 140, 198, 254]. Recent studies indicate that the activity of the E1B-55K/E4orf6-complex is required to induce the exclusive nuclear export of the viral TPL-containing mRNAs, whereas bulk cellular mRNA transport is blocked [28, 340]. It has further been reported that inhibition of proteasome activity in infected cells impairs viral late gene expression [65]. Collectively, these observations indicate that degradation of one or more cellular proteins contributes directly or indirectly to the preferential export of viral mRNAs during the late phase of infection. However, to date no such substrate has been identified.

Different data indicate more direct participation of E1B-55K in the transport process of late transcripts. Accordingly, the export of unspliced mRNAs depends more on E1B-55K than the export of short, completely spliced transcripts [196]. Furthermore, the TPL sequence present in all mRNAs transcribed from the MLTU enhances the transcripts´ transport efficiency [151].

Nuclear import and localization of E1B-55K was found to be regulated by its SUMOylation [87, 175] and to depend on the E4orf6 protein [246]. The E4orf6

protein comprises a putative nuclear localization signal at its N-terminus and an amphipathic arginine-rich α-helical nuclear retention signal at its C-terminus [127, 244]. It is proposed that these signals and the interaction of E4orf6 with E1B-55K lead to the localization of E1B-55K at viral transcription and replication centers. Moreover, it has been described that co localization of both proteins in such centers is required for selective mRNA transport. Hence, E1B-55K and/or E4orf6 might recruit a cellular transport factor to the replication centers to promote export of adenoviral mRNAs via unknown mechanisms. Additionally, this would lead to depletion of the transport factor mediating host cell mRNA export [126, 246].

Initial efforts to identify the cellular transport pathway of viral late mRNAs concentrated on the export receptor CRM1. This transport receptor was found to bind to a leucine-rich nuclear export signal in the human immunodeficiency type 1 (HIV-1) Rev protein, mediating the export of unspliced viral transcripts [101, 108, 115, 213]. Studies on E1B-55K and E4orf6 revealed functional NES sequences within both adenoviral proteins [77, 81, 185, 325] and hence led to the assumption that viral late mRNA transport is mediated by CRM1. However, neither blocking CRM1-dependent transport by specific inhibitors [51, 105, 264] nor functional inactivation of NES-dependent transport of E1B-55K and/or E4orf6 during adenoviral infection [175, 288] could confirm this assumption.

Further studies revealed a link between E1B-55K and CRM1-independent shuttling mechanisms. E1B-AP5 (E1B-55K associated protein 5) was identified as a binding partner of E1B-55K *in vitro* as well as in virus-infected cells [116]. The E1B-AP5 gene encodes a nuclear RNA-binding protein of the heterogeneous nuclear ribonucleoprotein (hnRNP) family whose members function in both processing and export of cellular mRNAs [160]. Subsequently, this protein was found to bind TAP (Tip-associated protein) *in vitro*, the major export receptor of bulk mRNA transport [12]. This makes the TAP transport pathway a promising candidate for the shut-off of host cell mRNA transport and preferential export of viral mRNAs during the late phase of adenovirus infection. Recent observations showed a reduction in viral late mRNA transport efficiency when synthesis of TAP was impaired by RNA interference [345], strongly supporting a role of TAP-dependent transport in the export of viral late transcripts.

2.2.3 Late protein L4-100K

One of the rare regulatory proteins encoded by the major late transcription unit (MLTU) is L4-100K. This dumb-bell shaped phosphoprotein comprises 806 amino

acids and has a molecular weight of 100 kDa. Together with two other regulatory proteins of this region, L4-22K and L4-33K, L4-100K supports the early to late switch in adenoviral infection [98, 229].

Besides its regulatory functions in the late phase of infection, L4-100K plays a critical role in counteracting antiviral immune responses. Cytotoxic lymphocytes initiate the immune response against virus-infected cells. These cytotoxic effector cells induce cell death via the Fas receptor pathway or granule exocytosis [301]. One enzyme in these granules is granzyme B [4, 301], mediating the proteolytic cleavage of specific caspases to induce apoptosis of the target cell [279]. Interestingly, although L4-100K is cleaved by this protease, it prevents apoptosis of the infected cell by interacting with granzyme B and inhibiting its function [4].

Adenoviruses have evolved different immunomodulatory mechanisms to overcome both the host cell´s immune and inflammatory responses. In the early phase of infection E1A inhibits interferon-induced gene expression, while VA-RNA blocks interferon PKR (double-stranded RNA-dependent protein kinase) activity [47]. Furthermore, several E3 proteins prevent cytotoxic cell killing [201, 202], and the proteasomal targeting of cellular substrates by the E1B-55K/E4orf6 complex incapacitates several anti-viral mechanisms of the host cell. Degradation of p53 inhibits p53-mediated apoptosis of the host cell [27, 261, 329], while blockage of DNA double strand break repair by reduction of both Mre11 [304] and DNA-Ligase IV [15] prevents concatemerization of the double-stranded viral genome. Moreover, degradation of Daxx, a component of PML (promyelotic leukemia protein) nuclear bodies (PML-NBs), blocks its innate antiviral activities [289].

In addition to its immunomodulatory property, L4-100K is indispensable for efficient completion of lytic viral infection. In the late phase of infection L4-100K stimulates the selective translation of viral late transcripts by specific binding to the TPL sequence via a ribosome shunting mechanism [341, 342]. Thereby, L4-100K interacts with eIF4G, the scaffolding element of the cap-dependent translation initiation complex, and inhibits its phosphorylation by competitively blocking the binding site of MAPK-interacting kinase 1 (MNK1) [67, 68]. This results in inhibition of the cap-dependent translation machinery and hence host cell protein synthesis (*host shut-off*), whereas viral transcripts are efficiently transcribed by ribosome shunting. Such shunting is achieved by the 40S subunit binding to the cap structure and bypassing large segments of the transcript until reaching the initiation codon [79, 80, 352]. The TPL sequence thereby exploits a conspicuous complementarity to 18S rRNA [350].

Another striking feature of L4-100K is its participation in Hexon biogenesis. Early studies described a temperature-sensitive adenovirus mutant that showed impaired nuclear localization and cytoplasmic accumulation of the Hexon protein upon a temperature shift to 39.5°C [171]. Further complementation analysis of this virus mutant identified mutations in the L4-100K protein, and assumed a role of L4-100K in Hexon trimerization [243]. Therefore, L4-100K functions as a chaperone in the trimer formation of the Hexon proteins [55, 56, 149]. This supports the nuclear import, since only Hexon trimers are translocated to the nuclear compartment. However, the import process itself has been reported to depend on the structural protein pVI [149, 337].
Interestingly, L4-100K was found to possess shuttling activity. Previous studies identified both a nuclear export signal of the HIV-1 Rev type [68] and a nuclear localization signal within the L4-100K protein [156, 184].

2.3 Cellular transport pathways

The compartmentalization of eukaryotic cells leads to strict control of gene expression by separating gene transcription in the nucleus from transcript translation in the cytoplasm. This division requires active nucleocytoplasmic transport of macromolecules through nuclear pore complexes (NPC), and signaling pathways that facilitate the exchange of information between the two compartments. Nucleocytoplasmic transport occurs in both directions. Several RNA species that are transcribed and processed in the nuclear compartment are exported to the cytoplasm. Additionally, newly synthesized proteins are transported from the cytoplasm to the site of function. Hence, proteins fulfilling functions in both the nucleus and cytoplasm shuttle between the two compartments via distinct import and export pathways [131]. Mammalian NPCs are large (~120 MDa) proteinaceous assemblies spanning the nuclear envelope. In the absence of unstructured components the central channel is approximately 38 nm in diameter, which matches the known maximal size of actively transported particles. However, the functional diameter of the NPCs is about 9 nm, and allows passive diffusion of macromolecules up to 20 to 60 kDa [3, 239, 268]. The tight regulation of active nucleocytoplasmic transport through the NPCs requires distinct, receptor-mediated import and export pathways [131, 239].

2.3.1 Importin ß-like nuclear transport receptors

Most cellular import and export receptors belong to the importin ß family, comprising approximately 30 putative members in mammals. Importin ß-like

transport receptors interact directly or via an adaptor molecule with the cargo, and bind RanGTP to form a ternary complex that is translocated through the NPC via interaction with the nucleoporins. The transport process is initiated by recognition of specific nuclear localization (NLSs) or nuclear export signals (NESs). Importins bind their cargos in the cytoplasm and translocate to the nucleus in the presence of RanGTP. The trimeric complex dissociates by RanGTP binding to the importin, hence releasing the cargo. Transport in the reverse direction is regulated in a converse manner. Exportins recognizing their substrates in the nucleus form a ternary complex with RanGTP that is transferred to the cytoplasm. Subsequently, GTP hydrolysis results in dissociation of Ran from the complex, and leads to release of the cargo. Both importins and exportins are recycled through re-translocation to the cytoplasmic or nuclear compartment to transport subsequent cargo molecules (Fig. 6). The GTPase-activating protein (RanGAP1) is excluded from the nucleus and mediates the hydrolysis of RanGTP to RanGDP in the cytoplasm, thus depleting RanGTP from the cytoplasm. In contrast, the guanine-nucleotide exchange factor of Ran (RRC1) stimulates the transition from RanGDP to RanGTP in the nucleus. The resulting RanGTP gradient across the nuclear envelope, with high RanGTP concentrations in the nucleus and low levels in the cytoplasm, provides an explanation for the asymmetry of these transport cycles. However, many transport receptors are not essential for cell viability, since cargo transport can access alternative transport pathways [108, 130, 159, 187, 306].

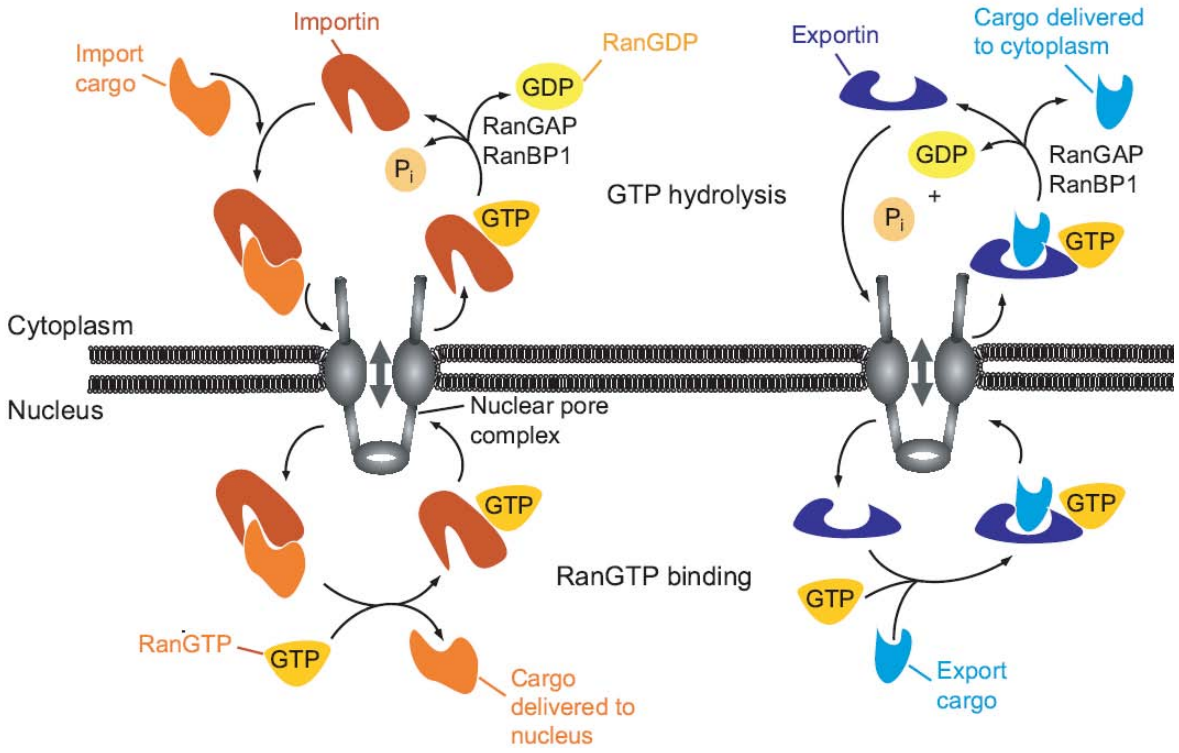

Figure 6: A schematic representation of import and export cycles through the NPC. Importins recognize their cargo in the cytoplasm and translocate through the NPC into the nucleus, where the cargo dissociates from the importin by binding of importin to RanGTP. The importin is recycled back to the cytoplasm for subsequent cargo import. Export of cargos is regulated in a converse manner. Exportins form a trimeric cargo-exportin-RanGTP complex that is transported to the cytoplasm and dissociated upon RanGTP hydrolysis. Subsequently, the exportin is recycled back into the nucleus (from Ström and Weis, 2001 [306]).

2.3.1.1 Classical NLS-dependent nuclear import

Nuclear import by the importin ß family is mediated by approximately ten family members through direct cargo binding [250] or binding of the cargo via adaptor molecules. This heterodimeric complex consists of importin ß and an adaptor protein such as importin α, snurportin 1, XRIPα, importin 7, and RanBP8. Importin α interacts with importin ß via the importin ß binding domain (IBB) [125, 143]. To date, seven importin α proteins are known, classified into three subfamilies: α1 with importin α5, α6 and α7; α2 with importin α1 and α8; as well as α3 with importin α3 and α4. Each importin α is encoded by a different gene, and required for certain steps in differentiation. Interestingly, these adaptor proteins are differentially expressed in distinct tissues and show preferences for specific NLS proteins [172, 231, 232, 257, 293].

The most thoroughly examined import signal is the classical NLS (cNLS), first identified in SV40 large T antigen, and nucleoplasmin [75]. Essentially, cNLS can occur in two varieties. The monopartite NLS comprises a single cluster of basic amino acids, whereas the bipartite NLS contains two clusters of basic residues separated by a variable spacer [62, 63, 106, 192]. Both signals are recognized by the Armadillo (ARM) repeat domain of importin α. This domain consists of ten ARM repeats forming a major and minor cNLS-binding site. The major pocket binds monopartite cNLSs and the larger cluster of basic amino acids in bipartite cNLS. The minor pocket interacts with the smaller stretch of basic residues in bipartite cNLSs [62, 178]. Consequently, importin α forms a heterodimer with importin ß via its IBB domain, and importin ß mediates translocation of the trimeric complex to the nucleus. The complex is released from the NPC, and importin α dissociates from ß by cooperative effects of RanGTP binding to importin ß. The RanGTP-importin ß complex can directly exit the nucleus, whereas importin α requires binding to exportin CAS and RanGTP for its recycling to the cytoplasm [130, 189, 327].

2.3.1.2 CRM1-mediated nuclear export

In contrast to the several classes of characterized NLSs, only one class of nuclear export signal (NES) is known at present. These leucine-rich NESs were first identified in the HIV-1 Rev protein and the cAMP-dependent protein kinase inhibitor [108, 328]. Rev interacts with the Rev responsive element (RRE) in unspliced HIV-1 RNAs, and functions as an adaptor protein for CRM1-dependent export. Like all members of the importin ß family, translocation of CRM1 and cargo depends on formation of a trimeric complex containing RanGTP [108, 115, 272]. However, NES-like sequences have also been identified in proteins not apparently acting as cargo of the export receptor CRM1 [187].

Interestingly, CRM1 is known to be involved in the regulation of cellular processes, such as the downregulation of p53 activity. The nuclear export of the tumor suppressor apparently not only restricts its access to regulatory nuclear targets, but also favors its cytoplasmic degradation [110, 303].

Besides its function in transport of NES-containing proteins, CRM1 mediates the export of cellular ribosomal RNAs (rRNAs), U snRNAs (U-rich small nuclear RNAs) and several specific messenger RNAs (mRNAs). Since CRM1 itself does not bind RNA, it requires specific adaptor proteins as described for the export of HIV-1 full-length mRNA via Rev [108]. Although bulk cellular mRNA transport depends on the export receptor TAP (see 2.3.2) CRM1 is implicated in the translocation of several cellular mRNAs. One example is AU-rich element (ARE)-containing mRNAs. The ARE in the 3´-untranslated region of many mRNAs, including those of proto-oncogenes, cytokines and lymphokines targets them for rapid degradation [49, 295]. However, HuR selectively binds AREs and stabilizes ARE-containing mRNAs in transiently transfected cells [97, 251]. The nucleocytoplasmic shuttling proteins pp32 and APRIL (Acidic protein rich in leucine) both bind HuR and possess a leucine-rich NES, thereby linking ARE-containing mRNAs to CRM1-dependent export [37].

Export via the CRM1 pathway can be blocked by several inhibitors. The fungal metabolite Leptomycin B (LMB) associates covalently with cysteine 528 in the NES binding region of CRM1, thereby irreversibly interferring with both RanGTP and substrate binding to CRM1 [108, 115]. During its translocation through the NPC, CRM1 interacts with the C-terminal FG (phenylalanine, glycine) repeats of the nucleoporin 214 (Nup214), also known as CAN [155]. Overexpression of the C-terminal residues thus leads to competitive inhibition of CRM1-dependent nuclear

export by selectively binding to CRM1, thereby preventing its association with the NPC [29, 354].

2.3.2 RanGTP-independent transport receptors

Further studies revealed that transport substrates can interact directly with NPCs independently of ß-related transport receptors, pointing to a distinct mechanism in NPC passage. One example is nuclear transport factor 2 (NTF2)-like proteins involved in nuclear import as well as export of specific substrates [170, 271, 300]. The NTF2-like factor p15, for example, supports RNA transport via the Tip-associated protein (TAP), also known as nuclear RNA export factor 1 (NXF1). This pathway mediates bulk cellular mRNA transport [35, 158, 195, 266]. Translocation of messenger ribonucleoprotein particles (mRNPs) strictly depends on interplay between pre-mRNA splicing, including the RNA helicase UAP56 involved in the spliceosome assembly, and nuclear export by TAP. The link between the splicing process and the export receptor is achieved by a number of different adaptor proteins that interact with the spliceosome complex [152, 206, 353]. One adaptor protein is Aly/REF, a member of the heterogeneous ribonucleoprotein (hnRNP) family and component of the exon junction complex (EJC) [193]. Previously, serine/arginine-rich (SR) proteins involved in constitutive and alternative mRNA splicing [114, 134, 318], as well as in mRNA transport [153], were also identified as adaptors for TAP-dependent transport [152, 282].
Export of Mason-Pfizer monkey virus (MPMV) unspliced RNAs is achieved by a constitutive transport element (CTE). Interestingly, TAP interacts directly with this CTE and triggers the export of these unspliced RNAs to the cytoplasm [36, 137]. Since a functional export-mediating CTE was identified in an intron of TAP mRNA, it is likely that CTEs are important to facilitate efficient expression of cellular mRNAs with retained introns [200].
The transport of cellular mRNAs via TAP requires two distinct nucleoporins, CAN and RanBP2 (also known as Nup358) [107]. These are components of the cytoplasmic filaments of the NPC, and described to function in translocating cargo-receptor complexes as well as efficient recycling of the transport receptors [274, 278, 320]. However, the translocation and seemingly efficient recycling of TAP to the nuclear compartment only depends on RanBP2 providing major binding sites for the TAP/p15 complex at the NPC and thus supporting TAP-mediated mRNA transport [107]. In contrast to CRM1, the C-terminus of CAN does not interact with TAP; hence TAP-dependent export, predominantly bulk cellular mRNA transport, is unaffected [29, 334].

2.4 Aims and objectives

Compartmentalization in host cells makes it necessary for DNA viruses to use different nucleocytoplasmic transport pathways. Thus adenoviruses depend on cellular shuttling processes not only during the import of their genome and numerous viral proteins into the nucleus, but also for active transport of the viral transcripts and proteins from the nucleus to the cytoplasm.

To date, several adenoviral early (E1A, E1B-55K and E4orf6) and late (L4-100K and pVI) proteins have been reported to contain a leucine-rich nuclear export signal of the HIV-1 Rev-type (see Fig. 7). However, a function besides the nuclear export of these proteins has not been identified for any of these NES sequences.

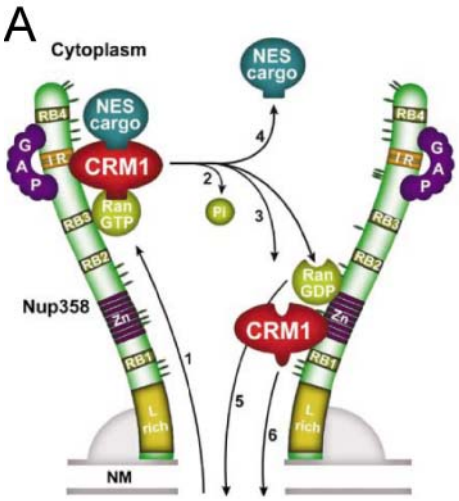

B

Adenoviral protein	NES sequence
E1A	70- VMLAVQEGIDL -80
E1B-55K	83- LYPELRRILTI -93
E4orf6	83- MVLTREELVI -92
L4-100K	383- LCNLVSYLGI -392
pVI	67- LRDKLKEQNFI -76 233- LNSIVGLGV -241
consensus sequence	Φ X2-3 Φ X2-3 Φ X Φ

Figure 7: A model of CRM1 export complex and identified NESs in adenoviral proteins. (A) NES-cargo/CRM1/RanGTP complexes are translocated through the nuclear pore complex and bind to a cargo-dependent CRM1-binding site on cytoplasmic Nup358. With the hydrolysis of GTP, the complex dissociates and the cargo molecule is released into the cytoplasm. CRM1/RanGDP is imported back into the nucleus (from Engelsma *et al.*, 2004 [88]). (B) Comparison of so far identified leucine-rich NES sequences in adenoviral proteins. Numbers refer to amino acid positions (Assembled from several publications cited in the text).

Therefore, this work set out to characterize NES virus mutants, some generated by site-directed mutagenesis, for the individual functions of the altered proteins during the adenoviral life cycle. In addition, one question was whether adenoviruses use CRM1-dependent export for any step of viral replication. Hence, CRM1 was blocked to evaluate early/late protein accumulation, viral DNA and progeny virus synthesis, as well as late mRNA export. Furthermore, the contribution of CRM1 to efficient early mRNA transport was examined, since the transport pathway of the early transcripts has not previously been investigated.

Previous studies proposed a nuclear localization signal in several adenoviral proteins such as E1A, E4orf6, L4-100K, and pVI. However the import pathway used has only been established for E1A. Thus, the aim here was to test the interaction of adenoviral proteins with cellular import receptors, and if these exist, to analyze them further. The results of this study should help to elucidate nucleocytoplasmic shuttling properties of particular adenoviral proteins, as well as their contribution to the proteins´ function in the viral life cycle. Moreover, analyses of viral early and late mRNA export should provide a better understanding of the cellular transport pathways used by adenoviruses.

3 Materials

3.1 Cells

3.1.1 Bacteria strains

STRAIN	CHARACTERISTICS
DH5α	*sup*E44, Δ*lac*U169, (ϕ80d*lac*ZΔM15), *hsd*R17, *rec*A1, *end*A1, *gyr*A96, *thi*-1, *rel*A1 [141].
XL2-Blue	*rec*A1, *end*A1, *gyr*A96, *thi*-1, *hsd*R17, *sup*E44, *rel*A1, lac, [F'*pro*AB, *lac*I^{q}ZΔM15, *Tn10* (Tet^{r}), Amy, Cam^{r}] [46].

3.1.2 Mammalian cell lines

CELL LINE	CHARACTERISTICS
2E2	HEK-293-derived inducible helper cell line expressing the E2 region and E4orf6 under the control of a tetracycline-dependent promoter [54].
A549	Human lung carcinoma cell line expressing wild type p53 [122].
AB120	Established HAd5-transformed rat cell line stably expressing E1A-12S/13S plus E1B-55K [236].
ABS1	Established HAd5-transformed rat cell line stably expressing E1A-12S/13S plus E1B-55K and E4orf6 [236].
BRK1	Spontaneously immortalized BRK cells [86].
E4orf6 NES	A549-derived non-stable cell line expressing the E4orf6-NES protein (this work).
H1299	Human lung carcinoma cell line, p53 negative [221].
HA-TetR	Pseudoprimary human hepatoma cell line expressing EGFPnlsTetR [93, 94].
HA-CANc	HA-TetR-derived inducible cell line expressing CANc under the control of a tetracycline-dependent promoter (this work).
HEK-293	Established HAd5-transformed, human embryonic kidney cell line stably expressing the adenoviral E1A and E1B gene products [133].
HEK-293T	HEK-293-derived inducible helper cell line expressing the SV40 large T antigen [83].
HeLa	Human cervix carcinoma cell line [121].
MRC-5	Fetal human lung fibroblast cell line [161].

3.2 Adenoviruses

ADENOVIRUS	CHARACTERISTICS
***dl*1520**	Ad2/Ad5-chimeric virus with a stop codon at aa position 3 and a 827 bp deletion (nt 2,496-3,323) in the E1B-55K gene [16].
H5*dl*312	E1A null mutant with a 901 bp deletion (nt 448-1,349) within the E1A region [165].
H5*dl*347	E1A mutant with a 254 bp deletion (nt 974-1,228) within the E1A region [336].
H5*dl*348	E1A mutant with a 115 bp deletion (nt 1,113-1,228) within the E1A region [165].
H5*dl*355	E4orf6 mutant with a 14 bp deletion in the E4orf6 gene [140].
H5*pg*4100	Wild type HAd5 with a 1863 bp deletion (nt 28,602-30,465) in the E3 reading frame [175].
H5*pm*4101	E1B-55K mutant carrying 3 aa exchanges (L83/87/91A) within the NES of E1B-55K [175].
H5*pm*4116	E4orf6 mutant carrying 2 aa exchanges (L90A/I92A) within the NES of E4orf6 [288].
H5pm4119	E1B-55K and E4orf6 mutant carrying 3 aa exchanges (L83/87/91A) within the NES of E1B-55K and 2 aa exchanges (L90A/I92A) within the NES of E4orf6 [288].
H5*pm*4149	E1B-55K null mutant carrying four stop codons at aa positions 3, 8, 86 and 88 of the E1B-55K sequence [176].
H5*pm*4154	E4orf6 null mutant carrying a stop codon at aa 66 within E4orf6 [28].
H5*pm*4165	L4-100K mutant carrying 4 aa exchanges (L383A/L386A/L390A/I392A) within the NES of L4-100K (stock of the group).
H5*pm*4201	E1A mutant carrying 1 aa exchange (V74A) within the NES of E1A (this work).
H5*pm*4229	E4orf6 mutant carrying a 423 bp deletion (nt 33,468-33,891) and 1 aa exchange (L245P) within E4orf6 (internal group virus database).

3.3 Nucleic acids

3.3.1 Oligonucleotides

The following oligonucleotides were used as primers for sequencing reactions, PCR amplification, restriction site insertion and site-directed mutagenesis reactions. All oligonucleotides were ordered from Metabion and numbered according to the *Filemaker Pro* database.

#	NAME	SEQUENCE	PURPOSE
64	**E1Bfw bp2043 fwd**	5´-CGCGGGATCCATGGAGCGAAGAAACCCATCTGAGC-3´	viral DNA replication
110	**E1B 361-389 rev :24**	5´-CGGTGTCTGGTCATTAAGCTAAAA-3´	viral DNA replication
330	**E1A fw bp 626 fwd**	5'-CCGAAGAAATGGCCGCCAGTCTTTTGGACCAGC-3'	amplification
331	**E1A rev bp 1290 rev**	5´-GCGTCTCAGGATAGCAGGCGCCATTTTAGGACGG-3´	amplification
390	**E4orf6 Mutante**	5'-CGCGGGAGGAGGCTGTAGCCCTGAGGAAGTGTATGC-3'	mutagenesis
391	**E4orf6 Mutante**	5´-GCATACACTTCCTCAGGGCTACAGCCTCCTCCCGCG-3´	mutagenesis
1110	**L4-100K sqRT-1 for**	5´-AAACTAATGATGGCCGCAGTG-3´	qPCR
1111	**L4-100K sqRT-1 rev**	5´-CGTCTGCCAGGTGTAGCATAG-3´	qPCR
1204	**gapdhFO3**	5´-CATCCTGGGCTACACTGA-3´	qPCR
1205	**gapdhRE3**	5´-TTGACAAAGTGGTCGTTG-3´	qPCR
1371	**18S rRNA fw**	5´-CGGCTACCACATCCAAGGAA-3´	qPCR
1372	**18S rRNA rev**	5´-GCTGGAATTACCGCGGCT-3´	qPCR
1441	**Hexon-qPCR-fw**	5´-CGCTGGACATGACTTTTGAG-3´	qPCR
1442	**Hexon-qPCR-rev**	5´-GAACGGTGTGCGCAGGTA-3´	qPCR
1470	**Fiber fwd**	5´-CGGAGACAAAACTAAACCTGTAACAC-3´	qPCR
1471	**Fiber rev**	5´-TCCCATGAAAATGACATAGAGTATGC-3´	qPCR
1475	**E1-875rev**	5´-GCATAGAAACCGGACCCAAGG-3´	sequencing
1556	**CANc fwd NheI**	5´-GCGCTAGCATGCAGCAATCATCC-3´	mutagenesis
1557	**CANc rev EcoRV**	5´-GCGATATCTCAAGCGTAGTCTGG-3´	mutagenesis
1560	**pLKO fwd EcoRV**	5´-GCGATATCGAATTCTCGACCTCGAGACAAATGG-3´	mutagenesis

1561	**pLKO rev NheI (II)**	5´-GCGCTAGCGGCTCACGAGCGAAGCTTGATCTCTATCACTG-3´	mutagenesis
1569	**E1B-qPCR-fw**	5´-GAGGGTAACTCCAGGGTGCG-3´	qPCR
1570	**E1B-qPCR-rev**	5´-TTTCACTAGCATGAAGCAACCACA-3´	qPCR
1651	**E1A V74A fwd**	5´-CTGTGTAATGTTGGCGGCGCAGGAAGGGATTGAC-3´	mutagenesis
1652	**E1A V74A rev**	5´-GTCAATCCCTCCTGCGCCGCCAACATTACAGAG -3´	mutagenesis
1686	**E1A RT fwd**	5´-GTGCCCCATTAAACCAGTTG-3´	qPCR
1687	**E1A RT rev**	5´-GGCGTTTACAGCTCAAGTCC-3´	qPCR
1688	**DBP RT fwd**	5´-GGTCTGGGCGTTAGGATACA-3´	qPCR
1689	**DBP RT rev**	5´-CAATCAGTTTTCCGGCAAGT-3´	qPCR
1767	**E4orf6-qPCR-new-rev**	5´-GCTGGTTTAGGATGGTGGTG-3´	qPCR
1768	**E4orf6-qPCR-new-fwd**	5´-CCCTCATAAACACGCTGGAC-3´	qPCR
2183	**IVa2 RT fwd**	5´-GAAACCAGAGGGCGAAGACC-3´	qPCR
2184	**IVa2 RT rev**	5´-AGTCTGGGTCACGGTGAAGG-3´	qPCR

3.3.2 Vectors

The following vector plasmids were used for cloning and transfection experiments. All vectors are numbered according to the *Filemaker Pro* database.

#	NAME	CHARACTERISTIC	REFERENCE
136	**pcDNA3**	Expression vector for mammalian cells; CMV promoter.	Invitrogen
234	**LeGO-iBLB2**	Lentiviral expression vector containing neomycin resistance as well as an IRES triggered ORF for BFP.	Weber *et al.*, 2008

3.3.3 Recombinant plasmids

The following recombinant plasmids were used for cloning and transfection experiments. All plasmids are numbered according to the *Filemaker Pro* database.

#	NAME	VECTOR	INSERT	REFERENCE
1154	**Ad5pPG-S2 (Noah)**	pPG-S2	Ad5 genome	Stock of the group
1235	**E1-Box pPG-S3**	pPG-S3	Ad5 E1 region	Stock of the group

1319	**pcDNA3-E1B-55K**	pcDNA3	Ad5 E1B-55K	Stock of the group
1568	**pTL-flag-100K**	pCMV/neo	TL-Ad2-100K	R. Schneider
1581	**Ad5pPG-S2 L4-100k-NES**	pPG-S2	Ad5 genome	Stock of the group
1643	**pTL-flag-100K-NES**	pCMV/neo	TL-Ad2-100K	Stock of the group
1981	**pLKO.DCMV.TetO.cICP0**	pLKO	ICP0	Everett *et al*., 2010; Everett *et al*., 2009
1993	**pcCANc-HA**	pcDNA3	CANc-HA	Schutz *et al*., 2006
2031	**pLKO.DCMV.TetO.CANc-HA**	pLKO	CANc-HA	this work
2044	**E1-Box E1AV74A**	pPG-S3	Ad5 E1 region	this work
2045	**Ad5pPG-S2 E1AV74A**	pPG-S2	Ad5 genome	this work
2112	**LeGO-iBLB2 E4orf6**	LeGO-iBLB2	Ad5 E4orf6	Stock of the group
2311	**LeGO-iBLB2 E4orf6 NES**	LeGO-iBLB2	Ad5 E4orf6	this work

3.4 Antibodies

3.4.1 Primary antibodies

NAME	PROPERTIES
1807	Polyclonal rabbit antibody raised against the C-terminus of E4orf6 [30].
2A6	Monoclonal mouse antibody raised against the N-terminus of Ad5 E1B-55K [284].
3F10	Monoclonal rat antibody raised against the HA-tag (Roche).
6B10	Monoclonal rat antibody raised against the N-terminus of Ad5 L4-100K [190].
7C11	Monoclonal rat antibody raised against the C-terminus of Ad5 E1B-55K [176].
α-Aly/REF (11G5)	Monoclonal mouse antibody raised against Aly/REF (Santa Cruz).
α -ß-actin (AC-15)	Monoclonal mouse antibody raised against ß-actin (Sigma Aldrich).
α-flag (M2)	Monoclonal mouse antibody raised against the flag-tag (Sigma Aldrich).
α-GFP (FL)	Polyclonal rabbit antibody raised against the GFP-tag (Santa Cruz).
α-KPNA2	Polyclonal goat antibody raised against Importin α1 (Abcam).
α-KPNA3	Polyclonal goat antibody raised against Importin α4 (Abcam).
α-KPNA4	Polyclonal goat antibody raised against Importin α3 (Abcam).

α-late (L133)	Polyclonal rabbit antiserum raised against Ad5 late structural proteins [175].
α-Mre11	Polyclonal rabbit antibody raised against the human Mre11 protein (Abcam).
α-protein VI	Polyclonal rabbit antibody raised against Ad5 protein VI [337].
α-SF2/ASF	Monoclonal mouse antibody raised against the N-terminal aa 1-97 of SF2/ASF (Zymed).
α-SRP1	Polyclonal goat antibody raised against Importin α5 (Abcam).
α-TAP	Polyclonal goat antibody raised against a N-terminal peptide of TAP (Santa Cruz).
Ad5 Hexon	Polyclonal rabbit antiserum raised against Ad5 Hexon (Abcam).
B6-8	Monoclonal mouse antibody raised against Ad5 E2A-72K [267].
Do-1	Monoclonal mouse antibody raised against the N-terminal aa 11-25 of human p53 (Santa Cruz).
M73	Monoclonal mouse antibody raised against Ad5 E1A-12S and 13S [144].
RSA3	Monoclonal mouse antibody raised against the N-terminus of Ad5 E4orf6 and E4orf6/7 [215].

3.4.2 Secondary antibodies

The following secondary antibodies were used for Western blot analysis:

NAME	PROPERTIES
HRP-Anti-Mouse IgG	HRP (*horseradish peroxidase*)-coupled antibody raised against mouse IgGs in sheep (Amersham Life Science).
HRP-Anti-Rat IgG	HRP (*horseradish peroxidase*)-coupled antibody raised against Rat IgGs in sheep (Amersham Life Science).
HRP-Anti-Rabbit IgG	HRP (*horseradish peroxidase*)-coupled antibody raised against rabbit IgGs in sheep (Amersham Life Science).
HRP-Anti-Goat IgG	HRP (*horseradish peroxidase*)-coupled antibody raised against goat IgGs in donkey (Santa Cruz).

The following secondary antibodies were used for immunofluorescence analysis:

NAME	PROPERTIES
***Texas Red*-Anti-Mouse IgG**	Texas Red (TR)-coupled antibody raised against mouse IgG in donkey (H + L; Dianova).
Cy™3-Anti mouse IgG	Affinity-purified, Cy™3-coupled antibody raised against mouse IgGs in donkey (H + L; Dianova).

Cy™3-Anti rabbit IgG	Affinity-purified, Cy™3-coupled antibody raised against rabbit IgGs in donkey (H + L; Dianova).
Cy™3-Anti rat IgG	Affinity-purified, Cy™3-coupled antibody raised against rat IgGs in donkey (H + L; Dianova).
Cy™5-Anti rat IgG	Affinity-purified, Cy™5-coupled antibody raised against rat IgGs in donkey (H + L; Dianova).
Alexa™ 488 Anti-Mouse IgG	Alexa™ 488 Antibody raised against mouse IgGs in goat (H + L; $F(ab')_2$ Fragment; Molecular Probes).
Alexa™ 488 Anti-Rabbit IgG	Alexa™ 488 Antibody raised against rabbit IgGs in goat (H + L; $F(ab')_2$ Fragment; Molecular Probes).
Alexa™ 488 Anti-Rat IgG	Alexa™ 488 Antibody raised against rat IgGs in goat (H + L; $F(ab')_2$ Fragment; Molecular Probes).
Alexa™ 555 Anti-Mouse IgG	Alexa™ 555 Antibody raised against mouse IgGs in goat (H + L; $F(ab')_2$ Fragment; Molecular Probes).
Alexa™ 555 Anti-Rabbit IgG	Alexa™ 555 Antibody raised against rabbit IgGs in goat (H + L; $F(ab')_2$ Fragment; Molecular Probes).
Alexa™ 633 Anti-mouse IgG	Alexa™ 633 Antibody raised against mouse IgGs in goat (H + L; $F(ab')_2$ Fragment; Molecular Probes).

3.5 Commercial systems

The following commercial systems were used:

NAME	COMPANY
FireSilver Staining Kit	Proteome Factory
Plasmid Purification Mini, Midi und Maxi Kit	Qiagen
Protein Assay	BioRad
QuikChange™ Site-Directed Mutagenesis Kit	Agilent
Reverse Transcription System	Promega
Pierce SILAC Protein Quantitation Kit	Thermo Scientific
SuperSignal® West Pico Chemiluminescent Substrate	Pierce
Trizol® Reagent	Invitrogen

3.6 Standards and markers

Size determination of DNA fragments on agarose gels was based on a *1 kb* and *100 bp DNA ladder* (New England Biolabs), whereas the molecular weight of

proteins on SDS-polyacrylamide gels was determined by *PageRuler™ Prestained Protein Ladder Plus* (Fermentas).

3.7 Chemicals, reagents, and equipment

Chemicals, enzymes, and reagents used in this study were purchased from Agilent, AppliChem, Biomol, Calbiochem, Enzo Life Science GmbH, InvivoGen, Merck, New England Biolabs, Roche and Sigma Aldrich. Cell culture materials as well as other plastic material and equipment were obtained from BioRad, Biozym, Brand, Engelbrecht, Eppendorf GmbH, Falcon, Gibco BRL, Greiner, Hartenstein, Hellma, LTF Labortechnik, Nunc, Pan, Peqlab, Protean, Sarstedt, Schleicher&Schuell, VWR and Whatman.

3.8 Software and databases

The following software and databases were used in the preparation of this work:

SOFTWARE	PURPOSE	SOURCE
Acrobat 9.0 Pro	PDF data processing	Adobe
BioEdit 7.0.5.2	Sequence data processing	Open Software (provided by *Ibis Therapeutics Carlsbad*)
CLC Main Workbench 5.0	Sequence data processing	CLC bio
6300 Series Ion Trap LC/MS	MS data acquirement and analysis	Agilent
Delta2D	2DE analysis	Decodon
Endnote 9.0	Reference organization	Thomson
Filemaker Pro 8.5	Database management	FileMaker, Inc.
Gene Tools	Quantification of DNA and protein bands	SynGene
Illustrator CS4	Layout processing	Adobe
Mascot	Database for protein identification	Open Software (provided by *Matrix Science*)
Microsoft Office Vista	Text processing	Microsoft
Photoshop CS4	Image processing	Adobe
PubMed	Literature database, open sequence analysis software	Open Software (provided by NCBI)

4 Methods

4.1 Bacteria

4.1.1 Culture and storage

Solid plate culture

Bacteria were plated on solid Luria Bertoni (LB) medium containing 15 g/l agar and the appropriate antibiotics (100 µg/ml ampicillin or 50 µl/ml kanamycin) and incubated overnight at 30 or 37°C. Solid plate cultures sealed with *Parafilm* (Pechiney Plastic Packaging) can be kept for several weeks at 4°C.

Liquid culture

For the liquid culture of *E. coli*, single colonies were picked from plates and inoculated into sterile LB medium containing the appropriate antibiotics. Cultures were incubated overnight at 30 or 37°C in an *Inova 4000 Incubator* (New Brunswick). If necessary, bacteria concentrations were determined by measuring the optical density (OD) of the cultures at 600 nm, wavelength (*SmartSpec™ Plus*, BioRad) against plain media (1 OD_{600} = 8x10^8 cells/ml).

Glycerol culture

For long-term storage of bacteria, liquid cultures of single colonies were centrifuged briefly at 4,000 rpm for 10 min (*Multifuge 3 S-R*; Heraeus). The bacteria pellets were resuspended in 1 ml LB media containing 50% sterile glycerol and transferred into *CryoTubes™* (Nunc). These glycerol stocks can be stored at -80°C for years.

LB Medium	Trypton	10 g/l
	Yeast extract	5 g/l
	NaCl	5 g/l
	• autoclaving	
Antibiotic Solutions	Ampicillin (500 x)	50 mg/ml
	Kanamycin (200 x)	10 mg/ml
	• filter sterilization	
	• storage at –20°C	

4.1.2 Transformation of *E. coli*

4.1.2.1 Electroporation

Electrocompetent *E. coli* cells were prepared as described previously [294]. 1 l YENB medium was inoculated with 10 ml of an overnight culture of bacteria and incubated at 37°C until reaching an OD_{600} of 0.5-0.9. Cells were cooled on ice for

5 min and centrifuged for 10 min at 6,000 rpm at 4°C (*Avanti J-E*; Beckman & Coulter). The bacteria pellet was washed twice with 100 ml ice cold H_20_{dd} and once with 20 ml 10% glycerol. Finally, the bacteria pellet was resuspended in 3 ml 10% glycerol, 50 µl aliquots were frozen in liquid nitrogen and stored at -80°C.

For transformation an aliquot was thawed on ice, mixed with 20-50 ng DNA diluted in H_20_{dd} and placed in a pre-cooled electroporation cuvette (BioRad) with an electrode gap of 1 mm. Electroporation was performed with *GenePulser* (BioRad; 1.25 kV, 25 µF, 200 Ω) for approximately 5 ms. After the pulse, the cells were transferred immediately into a 1.5 ml reaction tube (Eppendorf) with 1 ml SOC medium and incubated for 1 h at 37°C in an *Inova 4000 Incubator* (New Brunswick). After centrifugation, the pellet was resuspended in approximately 50 µl LB, spread on a LB plate containing the appropriate antibiotic and incubated at 30 or 37°C overnight.

YENB	Bacto yeast extract	7.5 g/l
	Bacto nutrient broth	8 g/l
	• autoclaving	
SOC medium	Trypton	20 g/l
	Yeast extract	5 g/l
	NaCl	10 mM
	KCl	2.5 mM
	$MgCl_2$	10 mM
	$MgSO_4$	10 mM
	Glucose	20 mM
	• autoclaving	

4.1.2.2 Chemical transformation

Chemicompetent *E. coli* cells were prepared as described by Hanahan [141]. 200 ml LB medium was inoculated with 2 ml of an overnight culture of bacteria and incubated at 37°C until reaching an OD_{600} of 0.3-0.5 (optimum 0.43). Cells were cooled on ice for 15 min and centrifuged for 5 min at 3,000 rpm at 4°C (*Avanti J-E*; Beckman and Coulter). The bacteria pellet was resuspended with 60 ml TFB I and incubated on ice for 60-90 min. Finally, the bacteria pellet was resuspended in 4 ml TFB II, 100 µl aliquots were frozen in liquid nitrogen and stored at -80°C.

An aliquot of chemically treated competent DH5α/XL2-Blue bacteria was transferred into a 15 ml *Falcon 2059* tube (Falcon). 2 µl of ß-Mercaptoethanol (1.2 M) and 1-10 µl of diluted plasmid DNA (~200 ng) were added to the cells and incubated on ice for 30 min. This mixture was kept at 42°C for 45 s and subsequently transferred to ice for 2 min. After this heat shock, 1 ml of LB or SOC

medium was added to the cells, followed by incubation for 1 h at 37°C in an *Inova 4000 Incubator* (New Brunswick). After centrifugation the bacteria pellet was resuspended in 50 µl LB, plated on LB agar containing the appropriate antibiotics and incubated at 30 or 37°C overnight.

TFB I

Glycerol	15%
$CaCl_2$	10 mM
KOAc	30 mM
$RbCl_2$	100 mM
$MnCl_2$ x $4H_20$	50 mM
• pH 5.8	
• filter sterilization	
• storage at 4°C	

TFB II

Glycerol	15%
MOPS	10 mM
$CaCl_2$	75 mM
$RbCl_2$	10 mM
• filter sterilization	
• storage at 4°C, light protected	

4.2 Mammalian cells

4.2.1 Maintenance and passage of cell lines

Adherent cells were cultured as monolayers in polystyrene cell culture dishes with *Dulbecco´s Modified Eagles Medium* (DMEM; PAA) with 0.11 g/l sodium pyruvate, which was supplemented with 5 -10% fetal calf serum (FCS; Pan) and 1 % of penicillin/streptomycin solution (1,000 U/ml penicillin and 10 mg/ml streptomycin in 0.9% NaCl; Pan). Cultured cells were incubated at 37°C in a CO_2 incubator (Heraeus) in 5% CO_2 atmosphere. To split confluent cells, the medium was removed, cells were washed once with sterile PBS solution and incubated with trypsin/EDTA (Pan). When cells had been efficiently detached from the culture dish, trypsin activity was inhibited by adding 1 volume of medium. Cells were transferred into a 15 or 50 ml tube and pelleted by centrifugation at 2,000 rpm for 3 min (*Multifuge 3S-R*, Heraeus). Cell pellets were resuspended in an appropriate volume of culture medium. If required, the cell number was determined as described in 4.2.3 or split in a constant ratio of 1:2 to 1:20.

PBS

NaCl	140 mM
KCl	3 mM
Na_2HPO_4	4 mM
KH_2PO_4	1.5 mM
• pH 7.0-7.7	
• autoclaving	

4.2.2 Storage of mammalian cells

For long-term storage of mammalian cells, subconfluent cultures were trypsinized and pelleted as described above (4.2.1). The cells were resuspended in 1 ml FCS (Pan), supplemented with 10% DMSO (Sigma) and transferred into a *CryoTube™* (Nunc). The samples were slowly cooled down using "*Mr. Frosty*" (Zefa Laborservice) and either stored at -80°C or in liquid nitrogen. To recultivate frozen cells, the *CryoTube™* (Nunc) was rapidly thawed at 37°C and cells were immediately resuspended in 15 ml of pre-warmed culture medium. Cells were pelleted by centrifugation and seeded in an appropriate cell culture dish at standard conditions (4.2.1).

4.2.3 Determination of total cell number

The total number of viable cells was determined using a Neubauer cell counter (C. Roth). Trypsinized cells were pelleted by centrifugation and resuspended in DMEM (4.2.1). A 50 µl aliquot of cell suspension was mixed with 50 µl trypan blue solution and placed on the Neubauer counter (C. Roth). The mean value of two manual counts (16 squares) under a light microscope (Leica DMIL) was multiplied with the dilution factor and the factor 10^4 to obtain the cell number per ml.

Trypan Blue Solution		
	Trypan blue	0.15% (w/v)
	NaCl	0.85% (w/v)

4.2.4 Transfection of mammalian cells

4.2.4.1 Polyethyleneimine (PEI) method

For efficient transfection of mammalian cells, linear 25 kDa polyethyleneimine (PEI; Polysciences) was generally used. PEI was dissolved in H_2O_{dd} at a concentration of 1 mg/ml, neutralized with 0.1 M HCl (pH 7.2), filter sterilized (0.2 µm), aliquoted and stored at -80°C. For transfection a mixture of DNA, PEI and DMEM was prepared in a ratio of 1:10:100 and incubated for 30 min at RT. After application of this solution to the cells maintained in medium without FCS, cells were incubated for 6 h before replacing the transfection medium with standard culture medium.

4.2.4.2 Polysome method

For maximal transfection efficiency of linearized bacmid DNA, mammalian cells were transfected using *Lipofectamine™2000* reagent (Invitrogen). In this method, cationic lipid vesicles or liposomes bind to the negatively charged DNA and fuse

with the cell membrane, mediating the internalization of DNA. Before addition of the lipid-DNA complexes, prepared according to the manufacturer´s instructions, the cells were washed once with PBS and maintained in DMEM without FCS. This transfection medium was replaced by standard culture medium 6-8 h post transfection.

4.2.5 Harvest of mammalian cells

Transfected or infected adherent mammalian cells were harvested using a cell scraper (Sarstedt). Collected cells were transferred into 15 or 50 ml tubes and centrifuged at 2,000 rpm for 3 min at RT (*Multifuge 3S-R*, Heraeus). After removing the supernatant, the cell pellet was washed once with PBS and stored at -20°C for subsequent experiments.

4.3 Adenovirus

4.3.1 Generating virus from DNA

To generate mutant viruses, the viral genome was released from the recombinant bacmid by *PacI* digestion. After heat inactivation of the restriction enzyme at 65°C for 20 min, 8 µg of linearized DNA per 60 mm dish were transfected into complementing 2E2 cells by the polysome method (4.2.4.2). The transfection medium was changed to normal growth medium 6 to 8 h post transfection. After a maximum of 5 days cells were harvested (4.2.5), pelleted by centrifugation at 2,000 rpm for 5 min (*Multifuge 3S-R*, Heraeus), washed once with PBS, and resuspended in 1 ml DMEM. The viral particles were released by three cycles of freezing in liquid nitrogen and thawing at 37°C in a water bath. Cell debris were separated from virus particles by centrifugation at 4,500 rpm for 10 min (*Multifuge 3S-R*, Heraeus). The supernatant containing the viruses was used for re-infection of a 100 mm petri dish (4.3.4). This procedure was repeated 2 to 5 times until a cytopathic effect was observed in 90% of the cells. After confirmation of the inserted mutations by DNA sequencing (4.4.6.3) the obtained virus solution was used to produce a high-titer virus stock (4.3.2).

4.3.2 Propagation and storage of high-titer virus stocks

In order to produce high-titer virus stocks, several 150 mm petri dishes were infected at a multiplicity of infection (moi) of 5 with the virus obtained as described in 4.3.1. After 3-5 days of incubation, cells were harvested (4.2.5) and centrifuged at 2,000 rpm for 5 min (*Multifuge 3S-R*, Heraeus). The virus-

containing cell pellet was washed once with PBS and resuspended in DMEM. After virus particle release from the cells by freezing and thawing and subsequent centrifugation (4.3.1), the virus-containing supernatant was mixed with 87% sterile glycerol (10% final concentration) for preservation at -80°C.

4.3.3 Titration of virus stocks

The titer of virus stocks was determined in terms of fluorescence forming units (ffu) by immunofluorescence staining of infected cells using an antibody (B6-8) against the adenoviral E2A-72K DNA binding protein (DBP). $5x10^5$ HEK-293 cells seeded in 6-well dishes were infected with 1 ml of virus dilution ranging from 10^{-2} to 10^{-6}. These infected cells were fixed at 20 h p.i. with 1 ml ice-cold methanol by 15 min incubation at -20°C. After removing the methanol, cells were air dried at RT and incubated with 1 ml PBS-Triton for 15 min. Subsequently, the PBS-Triton was removed and each well was blocked with 1 ml TBS-BG for 1 h at RT. Afterwards, each well was incubated with 1 ml solution of the primary B6-8 antibody (1:10 in TBS-BG) for 2 h at RT, washed three times for 15 min with TBS-BG before adding the *Alexa Fluor® 488*-coupled secondary antibody (1:1000 in TBS-BG) for 2 h at RT. Finally the secondary antibody solution was removed, and, after washing the samples three times for 15 min with TBS-BG, infected cells were counted using a fluorescence microscope (Leica). The total number of infectious particles was calculated according to the infected cell number, virus dilutions and microscope magnification.

PBS-Triton	Triton® X-100 • in PBS	0.5 mM

TBS-BG	Tris/HCl, pH 7,6	20 mM
	NaCl	137 mM
	KCl	3 mM
	$MgCl_2$	1.5 mM
	Tween 20	0.05% (v/v)
	Sodium azide	0.05% (w/v)
	Glycine	5 mg/ml
	BSA	5 mg/ml

4.3.4 Infection with adenovirus

Mammalian cells were seeded in appropriate dishes 6-16 h before infection, resulting in a confluence of 60-80%. Growth medium was removed and cells were washed once with PBS. According to the size of the dish, virus dilutions were prepared in an appropriate volume of DMEM and added to cell culture plates. Cells

were incubated with the infection medium for 2 h at 37°C, and the dish was gently shaken every 20 min to achieve efficient and homogenous adsorption of the viral particles. Finally, infection medium was replaced with standard culture medium and infected cells were harvested (4.2.5) or fixed (4.3.3; 4.6.6) according to the experimental procedure at the indicated times post infection.

4.3.5 Determination of virus yield

To determine progeny virus production $2.5x10^5$ cells seeded in a 6-well plate were infected with adenoviruses, harvested at the indicated time points post infection (4.3.4; 4.2.5) and cells were resuspended in an appropriate volume of DMEM. After virus particle release from the cells by freezing and thawing (4.3.1) the titer of the virus solution was determined as described above (4.3.3) and the particle number produced per cell was calculated.

4.4 DNA techniques

4.4.1 Preparation of plasmid DNA from *E. coli*

For large-scale plasmid preparation, 500-1000 ml of liquid bacteria culture were prepared in LB medium containing the appropriate antibiotics. After inoculation of a single bacteria clone, the culture was incubated for 16-20 h at 30 or 37°C in an *Inova 4000 Incubator* (New Brunswick). The bacteria pellet was collected by centrifugation at 6,000 rpm for 10 min (*Avanti J-E*; Beckman and Coulter) and plasmid DNA was isolated according to the manufacturer's instructions using a *MaxiKit* (Qiagen).

For analytic purposes, small volumes of liquid culture (1-5 ml) were inoculated and plasmid DNA was isolated by a modified protocol of Sambrook and Russell [280]. The bacteria pellet of the liquid culture was prepared in a 1.5 ml reaction tube by centrifugation at 11,000 rpm for 3 min (*Eppendorf 5417R*, Eppendorf) and resuspended in 300 µl Buffer P1. This suspension was gently mixed with 300 µl of Buffer P2 to lyse the cells. After incubating for 5 min at RT, 300 µl of Buffer P3 were added and incubated for 5 min on ice for neutralization. Finally, bacterial debris were pelleted by centrifugation at 14,000 rpm for 10 min at 4°C (*Eppendorf 5417R*, Eppendorf), and the plasmid-containing supernatant was transferred to a new 1.5 ml reaction tube with 1 volume of isopropanol and 0.1 volume of 3 M NaAc, and centrifuged at 14,000 rpm for 30 min at 4°C (*Eppendorf 5417R*, Eppendorf) to precipitate the DNA. The pellet was washed once with 1 ml of 75% ethanol and the DNA pellet was dissolved in 20-50 µl of 10 mM Tris-HCl (pH 8.0).

Buffer P1	Tris-HCl, pH 8,0	50 mM
	EDTA	10 mM
	RNAse A	100 µg/ml
	• storage at 4°C	
Buffer P2	NaOH	200 mM
	SDS	1% (w/v)
Buffer P3	Ammonium acetate	7.5 M
	• storage at 4°C	

4.4.2 Quantification of DNA concentration

DNA concentration was determined at a wavelength of 260 nm using a *NanoDrop* spectrophotometer (Peqlab). As described previously [280], an adsorption value of 1 corresponds to an absolute concentration of 50 µg/ml for double-stranded DNA or 33 µg/ml for single-stranded DNA. The purity of DNA was determined by the ratio of OD_{260}/OD_{280} and should be above 1.8 to assure high DNA purity.

4.4.3 Agarose gel electrophoresis

Agarose gels were prepared by dissolving agarose (Seakem LE agarose; Biozym) in TBE to a final concentration of 0.6-2.0% (w/v). The solution was boiled in a microwave oven (Moulinex), allowed to cool and ethidium bromide was added to a final concentration of 0.05 µg/ml. This prepared solution was then poured into an agarose gel tray, and left to set. DNA samples were mixed with 6x loading buffer and subjected to agarose gel electrophoresis in TBE at 5-10 V/cm gel length for approximately 1 h. DNA was visualized by an UV transilluminator at 312 nm (*G:BOX*; SynGene). To minimize harmful UV irradiation for preparative purposes, agarose gels were supplemented with 1 mM guanosine and gel slices were prepared at a wavelength of 365 nm.

TBE	Tris	0.09 M
	Boric acid	0.09 M
	EDTA	2 mM
	• pH 7.8	
6x Loading Buffer	Bromphenol blue	0.25% (w/v)
	Xylene cyanol	0.25% (w/v)
	Glycerol	50% (v/v)
	EDTA	10 mM
Ethidium Bromide Stock Solution	Ethidium bromide	10 mg/ml
	• storage at 4°C, light protected	

4.4.4 Isolation of DNA fragments from agarose gels

Extraction of DNA from agarose gels was performed by centrifugation at 20,000 rpm for 90 min at 10°C (*RC 5B Plus*; Sorvall) and subsequent DNA precipitation from the obtained supernatant, as described previously [136].

4.4.5 Polymerase Chain Reaction (PCR)

4.4.5.1 Standard PCR protocol

For standard PCR amplification of a DNA template, a 50 µl reaction mixture was prepared by mixing 50 ng of DNA, 0.2 µM forward and reverse primers, 1 µl of a dNTP mixture (dATP, dTTP, dGTP, dCTP; each 1 mM), 5 µl of 10x PCR reaction buffer and 2.5 U *Taq*-DNA polymerase (Roche) in a 0.2 ml reaction tube. The thermocycler (*Flexcycler*; Analytic Jena) was programmed as follows:

0.5 - 1 min	95°C	DNA denaturation
0.5 - 1 min	55 – 70°C	Primer annealing
1 min/kb	72°C	Extension

After 20-30 cycles, samples were further incubated at 72°C for 10 min and stored at 4°C. To examine PCR efficiency 5 µl of amplified DNA were analysed by agarose gel electrophoresis (4.4.3).

4.4.5.2 Site-directed mutagenesis

Mutations were inserted into target plasmids using a *QuikChange™ Site-Directed Mutagenesis Kit* (Agilent) according to the manufacturer's instructions. Desired mutations were included with both forward and reverse primer sequences, which were ordered from Metabion. PCR conditions were as follows:

30 s	95°C	DNA denaturation
1 min	55°C	Primer annealing
2 min/kb	68°C	Extension

After 18 cycles, samples were further incubated at 72°C for 10 min and stored at 4°C. To determine the PCR efficiency, 5 µl of amplified DNA were analyzed by agarose gel electrophoresis (4.4.3). Subsequently, the PCR mixture was incubated with *DpnI* for 3 h at 37°C to remove the DNA template and 10 µl were transformed into chemicompetent DH5α (4.1.2.2). Finally, single bacteria clones were picked, cultured in 1-5 ml LB medium (4.1.1) and prepared plasmid DNA (4.4.1) was analyzed by restriction digestion (4.4.6.1), agarose gel electrophoresis (4.4.3) and sequencing (4.4.6.3) before storage (4.1.1).

4.4.5.3 Viral DNA replication assay by PCR

For analysis of viral DNA replication, 10 µg of protein lysate from infected cells (4.3.4; 4.6.1) were mixed with Tween-20 (0.5% final concentration) and Proteinase K (100 µg/ml final concentration) and filled with H_20_{dd} to 25 µl. This digestion reaction mixture was first incubated at 55°C for 1h and then at 95°C for 10 min in a thermoblock (*Eppendorf Thermomixer comfort*, Eppendorf) for enzyme inactivation. Subsequently, a standard PCR reaction (denaturation: 30 s at 95°C, annealing: 1 min at 55°C, polymerization: 2 min at 72°C) was performed with oligonucleotide primers #64 and #100 for 20 cycles to amplify a 389 bp long fragment of the adenoviral E1B-55K gene. PCR products were loaded on an agarose gel (4.4.3) and quantified using the *GeneTools* software (Syngene).

4.4.6 Cloning of DNA fragments

4.4.6.1 Enzymatic restriction of DNA

Restriction enzymes were used according to the manufacturer's instructions in appropriate reaction buffers (New England Biolabs, Roche). For analytic restriction digests, 0.5 µg of DNA were incubated with 3-10 U of enzyme for 2 h at 37°C, unless indicated otherwise. For preparative restriction digests, 5-20 µg of DNA were incubated with 50 U of enzyme for at least 3 h at 37°C. For the cloning of adenoviral bacmid DNA, 25 U of restriction enzyme were used for each µg of DNA. The digested fragments were purified for subsequent procedures (another enzymatic restriction, PCR, ligation) either by preparative agarose gel electrophoresis (4.4.3) or isopropanol/ethanol precipitation (4.4.1).

4.4.6.2 Ligation and transformation

Enzymatically restricted DNA fragments were pretreated for ligation using 5 U of *antarctic phosphatase* (New England Biolabs) for 30 min at 37°C and if required, dephosphorylated with *shrimp alkaline phosphatase* (Roche) for 45 min at 65°C. Before ligation the DNA fragments were purified by either agarose gel electrophoresis (4.4.3) or isopropanol/ethanol precipitation (4.4.1). For a standard ligation reaction 20-100 ng of vector DNA were mixed with 3-5 times more insert DNA in a final volume of 20 µl, including 2 µl of 10x ligation buffer and 1 U of *T4 DNA ligase* (Roche). For ligation the mixture was incubated for 2 h at 13°C, 1 h at 20°C and 30 min at 37°C and subsequently the ligation product was transformed into chemicompetent *E. coli* cells (4.1.2.2). Finally, single bacteria clones were picked, cultured in 1-5 ml LB medium (4.1.1) and prepared plasmid DNA (4.4.1)

was analyzed by restriction digestion (4.4.6.1), agarose gel electrophoresis (4.4.3) and sequencing (4.4.6.3) before storage (4.1.1).

4.4.6.3 DNA sequencing

For DNA sequencing 500 ng of plasmid or 2 µg of bacmid DNA and 20 pmol of sequencing primer were mixed with H_20_{dd} to reach a total volume of 7 µl. Sequencing reactions were performed by Seqlab (Göttingen).

4.5 RNA techniques

4.5.1 Isolation of RNA from mammalian cells

$2.5x10^6$ cells were infected with adenoviruses (4.3.4), harvested (4.2.5) after the indicated times post infection and 1/3 of the pelleted cells was used to extract total RNA, 2/3 to prepare cytoplasmic and nuclear RNA (4.5.1.1). The cell pellet was resuspended in 1 ml of *Trizol® Reagent* (Invitrogen) and total RNA was prepared according to the manufacturer's instructions. The RNA pellet was dissolved in 20-40 µl H_20_{DEPC} and stored at -20°C.

DEPC-treated water was used to prepare buffers and dissolve RNA. DEPC reacts with amin-, hydroxyl- and thiol-groups of proteins (e.g. RNases) and inactivates them. For treatment of H_20_{dd} 0.1% (v/v) DEPC was added, stirred for 1 h at RT on a magnetic stirrer (Heidolph), and incubated overnight at RT followed by autoclaving.

4.5.1.1 Isolation of RNA from fractionated cell lysates

Freshly harvested cells (4.2.5; 4.5.1) were resuspended in 100 µl NP40 buffer supplemented with 1 mM DTT and lysed on ice for a maximum of 2 min. The nuclei were pelleted by centrifugation at 470xg for 5 min at 4°C. 80 µl of the supernatant (cytoplasmic fraction) was transferred into a new 1.5 ml reaction tube and 1 ml of *Trizol® Reagent* (Invitrogen) was added. The nuclei were washed once with 100 µl of the prepared NP40 buffer, and the pellet (nuclear fraction) was resuspended in 1 ml of *Trizol® Reagent* (Invitrogen). Cytoplasmic/nuclear RNA was prepared according to the manufacturer's instructions. Cytoplasmic RNA was dissolved in 10-20 µl, nuclear RNA in 20-40 µl H_20_{DEPC} and both stored at -20°C.

NP40 Buffer

Hepes, pH 7.8	10 mM
KCl	10 mM
Glycerol	20% (v/v)
Nonidet P-40	0.25% (v/v)
• in H_20_{DEPC}	
• storage at 4°C	

4.5.2 Quantification of RNA concentration

The RNA concentration was determined at a wavelength of 260 nm using the *NanoDrop* spectrophotometer (Peqlab). As described previously [280], an adsorption value of 1 corresponds to an absolute concentration of 40 µg/ml RNA. The purity of RNA was determined by the ratio of OD_{260}/OD_{280} and should be above 1.8 to assure high RNA purity.

4.5.3 Reverse transcription

For reverse transcription (RT) of RNA into complementary DNA (cDNA), 1 µg of RNA was transcribed using the *Reverse Transcription System* (Promega). The RT was primed with oligo(dT) to select for processed mRNA and was performed as described by the manufacturer. Samples of cDNA were stored at -20°C.

4.5.4 Real-Time PCR (RT-PCR)

For quantitative PCR (qPCR) of the cDNA samples, a 10 µl reaction mixture was prepared by mixing 1 µl cDNA dilution (1:100 in H_20_{DEPC}), 2.5 pmol forward and reverse primer, and 5 µl *SensiMix Plus SYBR* (Quantace) in a *0.1 ml Strip Tube* (LTF Labortechnik). The qPCR was performed in a *Rotor-Gene 6000* (Corbett Research), and was performed in triplicate for each sample by denaturing at 95 °C for 10 min prior to 40 cycles of PCR reaction as follows:

15 s	95°C	DNA denaturation
30 s	60-68°C	Primer annealing
15 s	72°C	Extension

The average CT (cycle threshold) values were determined and normalized to 18S rRNA (primers # 1371/1372) or glycerolaldehyde 3-phosphatase dehydrogenase (GAPDH; primers #1204/1205; for samples obtained after CRM1 inhibition). The obtained values were used to calculate relative levels of total mRNAs resulting from normalization to wt (H5*pg*4100) mRNA levels (4.5.1) or the cytoplasmic-to-nuclear ratio of fractionated mRNAs (4.5.1.1). Primers for amplification of cDNA were used as follows:

Adenoviral genes	# of primers	Annealing temperature	Product size
IVa2	2183/2184	62°C	119 bp
E1A	1686/1687	60°C	106 bp
E1B	1569/1570	62°C	63 bp
E2A	1688/1689	60°C	113 bp
E4orf6	1767/1768	60°C	120 bp
L3 (Hexon)	1441/1442	60°C	137 bp
L4 (L4-100K)	1110/1111	68°C	199 bp
L5 (Fiber)	1470/1471	60°C	102 bp

Cellular genes	# of primers	Annealing temperature	Product size
18S rRNA	1371/1372	60-68°C	187 bp
GAPDH	1204/1205	60°C	111 bp

4.6 Protein techniques

4.6.1 Preparation of total cell lysates

For analysis of proteins, cell pellets were resuspended in an appropriate volume of lysis buffer supplemented with 1 mM DTT, 0.2 mM PMSF, 1 mg/ml pepstatin A, 5 mg/ml aprotinin, and 20 mg/ml leupeptin. For normal protein analysis RIPA light lysis buffer was used, for immunoprecipitation assays cell pellets were resuspended in NP40 lysis buffer, and for the trimerization assay of H exon cells were lysed in RIPA. After incubation for 30 min on ice, the lysates were sonicated for 30 s (output 0.80; 0.8 impulses/s; *Branson Sonifier 450*, Branson), except for the samples used for the trimerization assay. Subsequently, cellular debris and insoluble components were pelleted by centrifugation at 11,000 rpm for 5 min at 4°C (*Eppendorf 5417R*, Eppendorf), and the protein concentration of the supernatant was determined by spectrometry (4.6.2).

Ripa Light	Tris-HCl, pH 8.0	50 mM
	NaCl	150 mM
	EDTA	5 mM
	Nonidet P-40	0.5% (v/v)
	SDS	0.1% (w/v)
	Triton X-100	0.1% (v/v)
NP40 Lysis Buffer	Tris-HCl, pH 8.0	50 mM
	NaCl	150 mM
	EDTA	5 mM
	Nonidet P-40	0.15% (v/v)
RIPA	Tris-HCl, pH 8.0	50 mM
	NaCl	137 mM
	EDTA, pH 8.0	2 mM
	Glycerol	10% (v/v)
	Nonidet P-40	0.5% (v/v)

4.6.2 Quantitative determination of protein concentration

Protein concentrations in samples were determined using Protein-Assay (BioRad) according to Bradford [33] by measuring the 595 nm absorption of proteins bound to chromogenic substrates. 1 µl of the protein solution was mixed with 800 µl of H_20_{dd} and 200 µl *Bradford Reagent* (BioRad), incubated for 5 min at RT and

measured in a *SmartSpec™ Plus* spectrometer (BioRad) at 595 nm against a blank of 800 µl of H_20_{dd} and 200 µl *Bradford Reagent* (BioRad). Protein concentrations were determined by calculation based on a standard curve with BSA obtained in parallel (concentrations of 1-16 µg/µl; New England Biolabs).

4.6.3 Immunoprecipitation (IP)

For immunoprecipitation equal amounts (0.8 – 2 mg) of cell lysates (4.6.1; 4.6.2) were precleared by addition of 30 µl of *Pansorbin® Cells* (Calbiochem) that was washed three times with NP40 lysis buffer and pelleted by centrifugation at 6,000 rpm for 5 min at 4°C (*Eppendorf 5417R*, Eppendorf) prior to incubation for 2 h at 4°C on a rotator (GFL). Simultaneously, 1 µg of purified antibody per mg sepharose was coupled to 3 mg of protein A -sepharose/IP. Antibody-coupled sepharose beads were washed 3 times with 10 ml NP40 lysis buffer, pelleted by centrifugation at 600xg for 5 min at 4°C (*Eppendorf 5417R*, Eppendorf), and transferred into 1.5 ml reaction tubes. The precleared lysate was added to the sepharose beads after clearing by centrifugation at 600xg for 5 min at 4 °C (*Eppendorf 5417R*, Eppendorf). Immunoprecipitation was performed at 4°C on a rotator (GFL) overnight (approximately 16 h) before sepharose beads were pelleted by centrifugation at 600xg (*Eppendorf 5417R*, Eppendorf) and washed three times with 1 ml NP40 lysis buffer. Finally, 15 µl of 2x SDS sample buffer [280] was added to the samples, which were boiled for 3 min at 95°C to elute the proteins, immediately placed on ice and then centrifuged before loading on gels for SDS-PAGE and Western blotting (4.6.4; 4.6.5).

2x SDS Sample Buffer		
	Tris-HCl, pH 6.8	100 mM
	SDS	4% (w/v)
	DTT	200 mM
	Bromophenol blue	0.2% (w/v)
	Glycerol	20% (v/v)

4.6.4 SDS-polyacrylamide gel electrophoresis (SDS-PAGE)

Protein samples of cell lysates (4.6.1) or immunoprecipitations (4.6.3) were separated by SDS-PAGE according to their molecular weight. Polyacrylamide gels were prepared using a 30% acrylamide/bisacrylamide solution (37.5:1 *Protogel*, National Diagnostics) diluted with H_20_{dd} to give the appropriate final concentration (see receipes below). Acrylamide polymerization was initiated by addition of ammonium persulfate (APS) to a final concentration of 0.1%. All gels were assembled by the *SDS-PAGE system* (Biometra) according to the manufacturer's instructions and run at 20 mA/gel in TGS buffer. Protein samples were prepared

for SDS-PAGE by addition of 2x SDS sample buffer [280] before being heated at 95°C for 5 min or at 55°C for 12 min (for E1B-55K and E4orf6 protein samples) in a thermoblock (*Thermomixer Comfort*, Eppendorf). *PageRuler™ Prestained Protein Ladder Plus* (Fermentas) was used to determine the molecular weight of the proteins. Proteins were first concentrated between a lower percentage stacking gel and a higher percentage separating gel via an artificial pH discrepancy [191]. Afterwards, proteins separated on a SDS-PAGE were transferred to a nitrocellulose membrane by Western blotting (4.6.4; 4.6.5).

30% Acrylamide Stock Solution	Acrylamide	29% (w/v)
	N,N´Methylenebisacrylamide	1% (w/v)
Stacking Gel 5%	Acrylamide stock solution	17% (v/v)
	Tris-HCl, pH 6.8	120 mM
	SDS	0.1% (w/v)
	APS	0.1% (w/v)
	TEMED	0.1% (v/v)
Seperating Gel 8%	Acrylamide stock solution	27% (v/v)
	Tris-HCl, pH 8.8	250 mM
	SDS	0.1% (w/v)
	APS	0.1% (w/v)
	TEMED	0.06% (v/v)
Separating Gel 10%	Acrylamide stock solution	34% (v/v)
	Tris-HCl, pH 8.8	250 mM
	SDS	0.1% (w/v)
	APS	0.1% (w/v)
	TEMED	0.04% (v/v)
TGS Buffer	Tris	25 mM
	Glycine	200 mM
	SDS	0.1% (w/v)

4.6.5 Western blot

For immunoblotting, equal amounts of protein samples were separated by SDS-PAGE and transferred onto nitrocellulose membranes (*Protan®*, Whatman) using *Trans-Blot® Electrophoretic Transfer Cell* (BioRad) in *Towbin* buffer according to the manufacturer's instructions. Briefly, gels and membranes were soaked in *Towbin* buffer, placed upon one another between two pre-soaked blotting papers (Whatman) and two blotting pads in a plastic cassette. The electric transfer was performed in a blotting tank filled with *Towbin* buffer at 400 mA for 90 min. Subsequently, nitrocellulose membranes were incubated for at least 30 min at RT or overnight at 4°C in PBS-Tween containing 5% non-fat dry milk (Frema) or PBS-

Tween with 3% *Bovine Serum Albumin Fraction V* (AppliChem; for primary goat antibodies) on an orbital shaker (GFL) to block unspecific antibody binding to the nitrocellulose membrane. Then membranes were washed briefly to remove residual blocking solution and incubated for 2 h at RT in PBS-Tween containing the primary antibody. The dilutions of primary antibodies as well as the addition of non-fat dry milk (Frema) were determined for each antibody to achieve optimal results. After washing the membranes three times for 15 min in PBS-Tween they were incubated for 2 h at RT or overnight at 4°C with HRP-coupled secondary antibodies (1:10,000; Amersham) containing 3% non-fat dry milk (Frema), and subsequently washed three times for 15 min in PBS-Tween. Protein bands were visualized by enhanced chemiluminescence using *SuperSignal® West Pico Chemiluminescent Substrate* (Pierce) according to the manufacturer's instructions and detected with X-Ray films (*RP New Medical X-Ray Film*, CEA) using *GBX Developer* (Kodak). X-Ray films were scanned and cropped using *Photoshop CS4* (Adobe) and figures were prepared using *Illustrator CS4* (Adobe).

***Towbin* Buffer**	Tris-HCl, pH 8.3	25 mM
	Glycine	200 mM
	SDS	0.05% (w/v)
	Methanol	20% (v/v)
PBS-Tween	Tween 20	0.1% (v/v)
	• in PBS	

4.6.6 Immunofluorescence staining (IF)

$1x10^5$ cells were grown on glass coverslips in 6-wll dishes and fixed at indicated times after transfection (4.2.4.1) or infection (4.3.4) with 1 ml ice-cold methanol for 15 min at -20°C. After removing the methanol, cells were air dried at RT and incubated with 1 ml PBS-Triton for 15 min. Subsequently, the PBS-Triton was removed and each well was blocked with 1 ml TBS-BG for 1 h at RT before adding 50 µl of the appropriate antibody dilutions in PBS-Tween directly onto the glass coverslips. The primary staining was performed in a damp plastic chamber for 1 h at RT. After washing the coverslips three times with PBS for 15 min, cells were further incubated for 1 h with fluorescence-coupled secondary antibodies (dilution 1:100 in PBS or 1:400 in PBS for Alexa™-coupled secondary antibodies) supplemented with 0.5 µg/ml DAPI (4´,6-diamidine-2´-phenylindoldihydrochloride) at RT in a damp plastic chamber (light protected). Finally, coverslips were washed three times for 15 min with PBS, dipped in H_20_{DD}, air-dried and mounted in *Glow Mounting Medium* (EnerGene) on a microscope slide. Digital

images were acquired using *DM6000 fluorescence microscope* (Leica) with a charge-coupled device camera (Leica), cropped and decoded by *Photoshop CS4* (Adobe) and assembled with *Illustrator CS4* (Adobe).

4.7 Proteomic analysis

4.7.1 Stable isotope labeling with amino acids in cell culture (SILAC)

For quantitative analysis of relative changes in the protein abundance of different cell treatments *Pierce® SILAC Protein Quantitation Kit* (Thermo Scientific) was used. Initially A549 cells were cultured in DMEM medium containing $^{13}C_6$ L-lysine to metabolically incorporate the isotope-labeled amino acid into the cellular proteins [242]. After 10 days the incorporation efficiency was tested via mass spectrometry (MS) and compared to an unlabeled control. Then protein lysates (4.6.1) of labeled and unlabeled cells were separated on SDS-PAGE (4.6.4), the gel was Coomassie stained (4.7.3.1), and a protein band was analyzed after tryptic digestion (4.7.4) by MS (4.7.5). A second population of A549 cells was cultured in unlabeled medium. For MS analysis both populations of A549 cells were infected and harvested at indicated times post infection (4.3.4; 4.2.5), cell lysates were prepared (4.7.2.1), the protein concentration was determined and the samples were mixed in a mass ratio of 1:1 before the proteins were separated by 2D gel electrophoresis (4.7.2.2) and subsequently analyzed (4.7.3; 4.7.4; 4.7.5; 4.7.6).

4.7.2 Two dimensional gel electrophoresis (2DE)

4.7.2.1 Preparation of cell lysates

Cell pellets were resuspended in 2DE lysis buffer supplemented with the protease inhibitor cocktail *Complete mini* (Roche). After incubation for 30 min on ice, cellular debris were pelleted by centrifugation at 100,000xg for 30 min at RT and the protein concentration of the supernatant was determined by spectrophotometry according to Lowry [205].

2DE Lysis Buffer		
	Urea	9 M
	DTT	70 mM
	CHAPS	2% (w/v)
	Servalyte 2-4	2% (w/v)

4.7.2.2 Isoelectric focusing and SDS-PAGE

In the first dimension the proteins were separated by isoelectric focusing (IEF) according to their isoelectric point (pI). The protein lysates were applied on an IEF

gel (1.5 mm) with 4% (v/v) acrylamide, and an immobilized pH gradient of 2-11. Proteins migrate according to their isoelectric point (pI) in a separating field of a pI= 3-10. In the second dimension proteins were separated by SDS-PAGE according to their molecular weight. A 15% separating gel was used that efficiently separates proteins with a mass of 8-150 kDa. Finally, the 2D gels were stained with Coomassie *Brilliant Blue* (4.7.3.1) or silver (4.7.3.2). The 2D gel electrophoresis and the subsequent staining of the gels (4.7.2; 4.7.3) were performed by the working group of Dr. Peter Jungblut (Max Planck Institute for Infection Biology, Berlin).

Separating Gel 15%	Acrylamide stock solution	50% (v/v)
	Tris-HCl, pH 8.8	250 mM
	SDS	0.1% (w/v)
	APS	0,1% (w/v)
	TEMED	0.04% (v/v)

4.7.3 Staining of 2DE gels

4.7.3.1 Coomassie Brilliant Blue staining

For Coomassie staining the separating gel was incubated for 30-45 min in Coomassie staining solution. Subsequently, the gel was destained by washing three times for at least 1 h in destaining solution.

Coomassie Staining Solution	*Brilliant Blue R-250*	1 mg/ml
	Methanol	45% (v/v)
	Acetic acid	10% (v/v)
Destaining Solution	Methanol	40% (v/v)
	Acetic acid	10% (v/v)

4.7.3.2 Silver staining

For a more sensitive detection of protein spots the 2D gels were silver stained, using the MS-compatible *FireSilver Staining Kit* (Proteome factory) according to the manufacturer's instructions.

4.7.4 Tryptic in-gel digestion

Excised protein bands and spots from stained SDS-PAGE (4.6.4) or 2D gels (4.7.2.2) were proteolytically digested with trypsin prior to MS analysis (4.7.5). To destain the gel slices, 500 µl of swelling solution was added to the gel pieces in a 1.5 ml reaction tube and incubated for 15 min at RT on a shaker (*Thermomixer 5432*, Eppendorf). Subsequently, the supernatant was removed and the gel pieces

were incubated with 500 µl of shrinking solution for 30 min at RT on a shaker (*Thermomixer 5432*, Eppendorf). The hydration and dehydration step was repeated once, the supernatant was removed, gel pieces were dried for 20 min at 37°C in a vacuum centrifuge with a cooling trap (Thermo Fisher Scientific), and incubated overnight at 37°C with 20 µl of digestion solution for the in-gel digestion with trypsin. To eluate the peptides from the gel, the reaction tubes were centrifuged briefly and the supernatant was collected in a new 1.5 ml reaction tube. The gel pieces were incubated with 30 µl of 65% acetonitrile (ACN) (v/v) and 5% formic acid (FA) (v/v) in H_20_{HPLC} in an ultrasonic bath (*Super RK255H*, Sonorex) for 30 min at RT, and the supernatant was combined with the former one. Subsequently, 30 µl of H_20_{HPLC} was added and the supernatant was collected after 15 min at RT on a shaker (*Thermomixer 5432*, Eppendorf). Again the gel pieces were incubated with 30 µl 65% ACN (v/v) and 5% FA (v/v) in H_20_{HPLC} on a shaker (*Thermomixer 5432*, Eppendorf) for 30 min at RT, and the supernatant was combined with the former ones. Finally, 50 µl of ACN was added to the gel pieces, incubated for 20 min at RT on a shaker (*Thermomixer 5432*, Eppendorf), and the supernatant was combined with the other ones. Subsequently, the peptides in the collected supernatants were dried in a vacuum centrifuge with a cooling trap (Thermo Fisher Scientific) at 37°C for 60-90 min, and the pellets were resuspended in 1 µl of 50% ACN and 0.1% FA in H_20_{HPLC} and diluted with 14 µl of 0.2% FA in H_20_{HPLC}.

Swelling Solution	NH_4CO_3 • in H_20_{HPLC}	100 mM
Shrinking Solution	NH_4CO_3 Acetonitrile • in H_20_{HPLC}	50 mM 60% (v/v)
Digestion Solution	NH_4CO_3 Acetonitrile Trypsin • in H_20_{HPLC}	50 mM 10% (v/v) 10 ng/µl

4.7.5 Mass spectrometry

The tryptically digested peptides (4.7.4) were analyzed by liquid chromatography with tandem mass spectrometry detection (LC-MS/MS). The measurement was performed with nano-HPLC (High Performance Liquid Chromatography) that was directly coupled to an ion trap mass spectrometer (*1100 LC/MSD trap XCT Ultra*; Agilent). The peptides were separated on an HPLC-Chip. The high capacity chip used consists of a 160 nl enrichment column and a 150 mm separation column,

both filled with the reversed phase chromatography material Zorbax C18 300 Å. Using this method the samples were injected into the HPLC system with an auto sampler and a capillary pump at 98% solution A (0.2% FA in H_20_{HPLC}) and 2% solution B (100% ACN) and applied to the enrichment column with a flow rate of 4 µl/min. Non-binding molecules were removed by washing. The elution was carried out using an acetonitrile gradient starting with 2% and up to 40% solution A within 40 min at a flow rate of 0.4 µl/min. The mass spectrometric measurement was performed in the positive ion mode with a voltage of -1.8 kV at the electrospray capillary. To evaporate the solvents, a nitrogen flow of 4 l/min and a temperature of 325°C were applied. The mass spectrometer acquired MS/MS-spectra in the data-dependent modus, whereby the three most intensive precursor ions were automatically selected for the MS/MS-measurement. Doubly charged ions were fragmented preferentially. After three cycles a precursor ion was actively excluded from the fragmentation for one minute.

4.7.6 Identification of proteins via Mascot search database

The peak lists for the MS/MS database request were generated with the Data Analysis software for *6300 Series Ion Trap LC/MS* (Version 3.4; Agilent). The identification was performed with the Mascot search engine [252] and a scan of the human protein database. The request parameters included a mass tolerance of ±1.2 Da for the precursor ions and ±0.6 Da for the fragment ions, trypsin as the enzyme of proteolytic digestion, and a potentially missing trypsin cleavage site.

4.8 Lentivirus

4.8.1 Cloning of lentiviral plasmids

Lentiviral particles were generated based on the system recently described by Fehse and associates [323]. The coding sequences of the adenoviral E4orf6 protein were amplified by PCR, introducing a 5´-*BamHI* site and a 3´-*EcoRI* site (4.4.5.1), purified by agarose gel electrophoresis (4.4.3), sequentially digested with the appropriate enzymes (4.4.6.1) and ligated into LeGo-iBLB2 (4.4.6.2). Mutations within the coding sequences were introduced subsequently via *QuikChange™ Site-Directed Mutagenesis Kit* (Agilent) (4.4.5.2).

4.8.2 Generation and storage of lentiviral particles

To generate a suitable amount of lentiviral particles, HEK-293T cells were seeded on a 150 mm dish to reach a confluence of 70-80% for transfection (4.2.1). The

DNA (8.5 µg LeGo-plasmid, 2.5 µg pRSV-Rev, 2.5 µg pCMV-VSV-G, 4.5 µg pMDLg/pPRE) was transfected using PEI and incubated for 8 h (4.2.4.1). Afterwards the transfection medium was replaced by 15 ml standard culture medium additionally supplemented with 20 mM sterile filtrated HEPES buffer. Two days after transfection, the supernatant was collected, centrifuged shortly at 4,500 rpm for 3 min (*Multifuge 3S-R*, Heraeus) and sterile filtrated (0.45 µm). Finally the supernatant was aliquoted, frozen in liquid nitrogen and stored at -80°C.

4.8.3 Generation of an E4orf6 NES cell line

To transduce A549 cells with lentiviral particles containing the E4orf6-NES coding sequence, $8x10^6$ cells were seeded in 150 mm dishes (4.2.1) and transduced with 3 ml of the obtained and sterile filtrated supernatant (4.8.2). For efficient transduction, adsorption was performed overnight and the medium was supplemented with 8 µg/ml polybrene. Finally, transduction medium was replaced by standard culture medium and 50 µg/ml Blasticidin (InvivoGen) was supplemented to select for E4orf6-NES positive cells. Four days after transduction the cell clones were pooled to obtain a polyclonal E4orf6 NES cell line and further propagated for subsequent experiments.

5 Results

Adenoviruses replicate in the nuclear compartment. Therefore, adenoviral transcripts must be exported to the cytoplasm, while proteins fulfilling functions in both cellular compartments have to shuttle between the nucleus and cytoplasm. To date, several adenoviral proteins have been described to possess a nuclear export signal (NES) of the HIV-1 Rev-type. These include early (E1A, E1B-55K and E4orf6) and late (L4-100K and pVI) proteins [68, 77, 164, 185, 337]. This leucine-rich sequence mediates nuclear export of proteins by the cellular transport receptor CRM1 [188]. However, a function apart from the nuclear export of the specific proteins has not been identified for any of these NES sequences. Furthermore, previous studies proposed a nuclear localization signal in early (E1A and E4orf6) as well as late (L4-100K and pVI) adenoviral proteins [68, 127, 207, 337], although to date use of the import pathway has only been established for E1A [180, 212].

The aim of this work was to elucidate nucleocytoplasmic shuttling properties of particular adenoviral proteins, as well as their contribution to the proteins' function in the viral life cycle. Moreover, examining viral early and late mRNA export should lead to a better understanding of cellular transport pathways used by adenoviruses.

5.1 Nuclear export of E1A is not essential for adenoviral replication

The immediate early proteins of the E1A region are the first expressed adenoviral proteins after the viral genome has reached the nucleus [32]. Due to their function in transcriptional activation of both cellular and adenoviral early genes they are crucial for the life cycle of the virus. This stimulation of gene expression is achieved by interactions with several cellular proteins involved in either transcriptional activation or gene repression. The consequently induced cell cycle progression and entry into the S-phase lead to a substantial increase in cellular RNA and protein synthesis, and provide an optimal environment for adenoviral DNA and protein synthesis [102]. However, a recently identified nuclear export signal (NES) within the conserved region 1 (CR1) domain of E1A proteins led to the assumption that E1A also functions outside the nuclear compartment. Furthermore, the observed reduction in progeny virus production of an E1A NES

mutant indicates a requirement of E1A nuclear export for efficient virus growth, and should be analyzed in more detail [164].

5.1.1 Generation of an E1A NES virus mutant

The most reliable way to study the contribution of E1A nuclear export to the viral infectious cycle is to generate an adenovirus mutant. To insert the point mutation described by Fueyo and colleagues [164], a cloning system already established in our group was used [136]. This system is based on a small region-specific plasmid, in the case of the E1A NES mutant the E1-Box, and a large viral bacmid, the "backbone". Specifically, the V74A mutation was introduced into the E1-Box pPG-S3 using the *Quik ChangeTM Site-Directed Mutagenesis Kit* (Stratagene) and specially designed oligonucleotide primers. After religation of the mutated plasmid into the wild type (wt) backbone pH5*pg*4100, the bacmid was linearized by *Pac*I digestion and transfected into the complementing cell line 2E2 [54] to produce a high titer virus stock. The generated E1A NES mutant H5*pm*4201 contains the same single amino acid exchange V74A in the NES of E1A (Fig. 8A) as described previously [164], located within the CR1 domain present in both the 12S and 13S gene products of the E1A region.

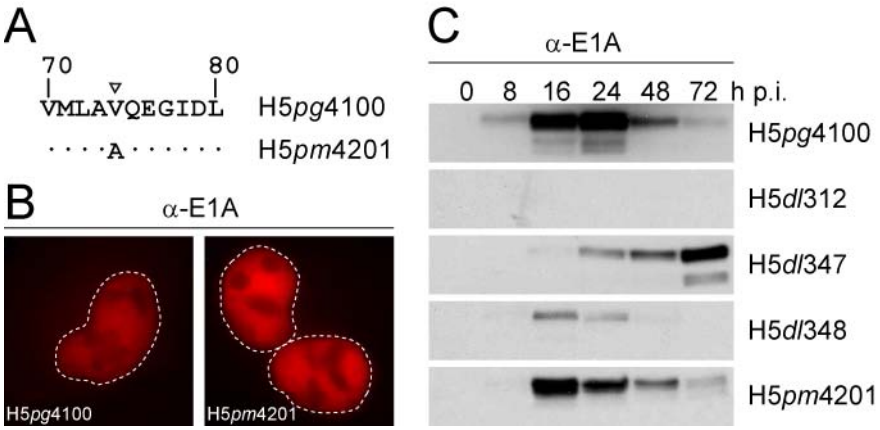

Figure 8: Effect of NES amino acid exchanges on localization and protein stability of E1A. (A) The NES specific residue in E1A is indicated by a triangle. Numbers refer to amino acid residues in the wt E1A protein from H5*pg*4100. The amino acid substitution in the mutated E1A protein from H5*pm*4201 is indicated below. (B) Intracellular localization of E1A in wt and E1A virus mutant-infected cells. A549 cells were infected with wt and E1A mutant viruses at a multiplicity of 10 fluorescence forming units (ffu) per cell and fixed 48 h p.i. Cells were labeled with anti-E1A mouse polyclonal antibody M73 (α-E1A) and Texas red-conjugated secondary antibody. Representative anti-E1A staining patterns are shown. In both panels, nuclei are indicated by a dotted line. (C) Steady-state expression levels of E1A. A549 cells were infected with wt and mutant viruses at a multiplicity of 20 ffu per cell. Cells were harvested at the indicated times post infection (p.i.) and total cell extracts were prepared. Proteins (30 µg samples) from each time point were separated by 10% SDS-PAGE and subjected to immunoblotting using anti-E1A mouse mab M73.

5.1.2 The E1A NES virus mutant supports adenoviral protein synthesis

Intriguingly, E1A was previously observed to not only localize in the nucleus, but also be exported to the cytoplasmic compartment at late times of infection [164]. Therefore, subcellular localization of E1A was tested in A549 cells after infection with wt (H5*pg*4100) and E1A NES mutant (H5*pm*4201). Both wt and mutant virus-infected cells displayed a predominantly nuclear staining pattern of E1A in the early phase of infection that remained unaltered throughout the viral life cycle. The distribution of the E1A proteins at 48 h p.i. was restricted to the nuclear compartment independently of a functional NES (Fig. 8B). To analyze the time course of E1A expression levels, A549 cells were infected with wt (H5*pg*4100) and E1A NES mutant (H5*pm*4201), as well as an E1A null (H5*dl*312), an E1A 13S minus (H5*dl*347) and an E1A 12S minus virus (H5*dl*348). In wt-infected cells E1A started to accumulate 8 h p.i. and steady-state concentrations of the protein increased until the beginning of the late phase (24 h p.i.). At later time points (48 and 72 h p.i) E1A protein levels decreased (Fig. 8C). This expression pattern correlates with the protein's function as a transcriptional activator in the early phase [22]. In the late phase the short half-life of the E1A-proteins [113], due to their degradation [298, 302], leads to a decrease in E1A protein levels. While no E1A was expressed in the E1A null mutant H5*dl*312, the E1A deletion mutant H5*dl*348 accumulated low levels of the 13S splice product at 16 h p.i. that steadily decreased during later time points of infection (Fig. 8C). In contrast, H5*dl*247, which harbors a deletion within the CR3 domain and thus does not express the 13S gene product, accumulated low E1A protein levels starting at 24 h p.i. that further increased until the latest time point of the analysis (72 h p.i.; Fig. 8C). Interestingly, infection with the constructed E1A NES mutant H5*pm*4201 resulted in an E1A expression pattern comparable to Ad5 wt virus. However, E1A accumulated at slightly lower concentrations until 16 h p.i. and decreased in a gradual manner from 24 to 72 h p.i. (Fig. 8C). These results from analyzing subcellular E1A protein localization and expression levels during time course experiments (Fig. 8B and C) do not correlate with published observations on the E1A NES mutant [164]. Here, wt E1A protein is only detected in the nucleus and displays the same localization pattern as the mutated protein (Fig. 8B). Additionally, expression levels of E1A proteins in NES virus-infected cells decreased during the late phase (24-72 h p.i.), whereas Fueyo and colleagues

detected no change in the level of E1A NES protein during adenoviral infection [164].

The different virus mutants were used to evaluate levels of viral early and late proteins (Fig. 9). In wild type-infected A549 cells the early proteins E1B-55K and E4orf6, as well as the structural protein Hexon were expressed in detectable levels 16 h p.i. Proteins of the viral capsid, such as Penton and Fiber, appeared at 24 h p.i., and all structural proteins accumulated in the course of the replication cycle. The complete absence of E1A proteins in H5*dl*312 led to low concentrations of E1B-55K and no detectable levels of E4orf6 or the analyzed proteins of the viral capsids. While the H5*dl*347 virus with a deletion in the 13S mRNA showed delayed and also reduced expression of the examined proteins, expression of the 13S gene product in H5*dl*348-infected cells was sufficient to induce expression of the early viral proteins (E1B-55K and E4orf6) and late structural proteins comparable to wt levels (Fig. 9).

These findings highlight the importance of E1A proteins and especially of the 13S full length gene product for efficient viral protein synthesis [21, 22]. Interestingly, the E1A NES mutant (H5*pm*4201) gave the same expression pattern of the early and structural proteins as detected in wt-infected cells (Fig. 9). This indicates that the NES within E1A is not required for its function in transcriptional activation of early gene expression, and thus together with likely induction of cell cycle progression, promotes the synthesis of the viral capsid proteins.

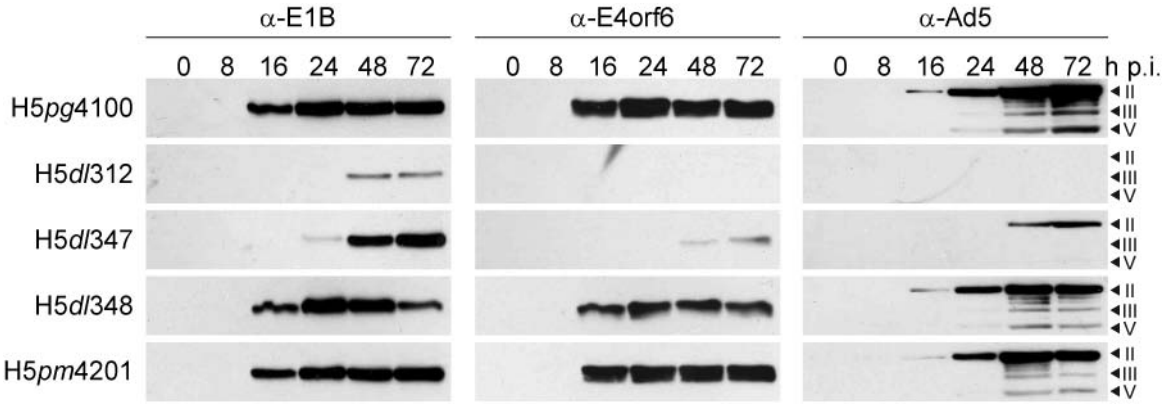

Figure 9: Effect of NES amino acid changes on viral protein synthesis. A549 cells were infected with wt and mutant viruses at a multiplicity of 20 ffu per cell. Cells were harvested at indicated times p.i. and total cell extracts were prepared. Proteins (25 µg samples for E1B-55K and E4orf6; 10 µg samples for capsid proteins) from each time point were separated by 10% SDS-PAGE and subjected to immunoblotting using anti-E1B-55K mouse mab 2A6, anti-E4orf6 mouse mab RSA3 and anti-Ad5 rabbit polyclonal serum L133. Bands corresponding to viral late proteins Hexon (II), Penton (III) and Fiber (V) are indicated on the right.

One of the cellular proteins whose expression is induced by transcriptional activation of E1A upon adenovirus infection is the tumor suppressor protein p53 [330]. In wild type-infected cells the induction of p53 is counteracted by an E3 ubiquitin ligase, assembled by the early adenoviral proteins E1B-55K and E4orf6, that ubiquitinates specific cellular proteins to mark them for proteasomal degradation [27, 142, 261, 263].

As expected, infection of A549 cells with the H5*pg*4100 virus led to degradation of p53, since its levels were clearly reduced after 16 h, and no longer detectable at 48 h post infection (Fig. 10). In contrast, p53 accumulated over the course of an infection with H5*dl*347 virus (Fig. 10), which expresses all E1A proteins except the 13S gene product (Fig. 8C). Hence this virus was not capable of producing sufficient levels of E1B-55K and E4orf6 (Fig. 9) to degrade p53. Also as expected, deletion of the complete E1A region neither induced accumulation of p53 nor its degradation, the latter again due to insufficient E1B-55K and E4orf6 expression levels (Fig. 10). As for the other phenotypes examined (Fig. 8 and 9), the E1A NES mutant (H5*pm*4201) was just as efficient at degrading p53 as the wild type virus.

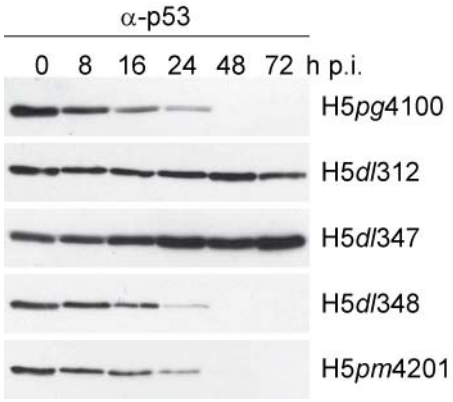

Figure 10: Effect of NES amino acid changes on p53 steady-state concentrations. A549 cells were infected with wt and mutant viruses at a multiplicity of 20 ffu per cell. Cells were harvested at the indicated times post infection p.i. and total cell extracts were prepared. Proteins (50 µg samples) from each time point were separated by 10% SDS-PAGE and subjected to immunoblotting using anti-p53 mouse mab Do-1.

5.1.3 Nuclear export of E1A is not essential for progeny virus production

So far, investigation of the E1A NES virus mutant revealed no requirement of the NES for efficient expression of adenoviral early and late proteins (Fig. 9). In addition, the wt E1A protein was not detected in the cytoplasmic compartment at late times post infection (Fig. 8B). Earlier studies showed a strong impact of the

E1A NES mutation on viral replication when virus yields in serum-starved MRC5 cells were down to 500-fold less, and also significantly lower in E1A complementing HEK-293 cells [133, 164]. Since HEK-293 cells should be capable of complementing a potential defect, virus growth was determined in A549 cells. Additionally, since a stronger effect on progeny virus production was observed in MRC5 cells, the virus yield was determined in these cells under the described conditions [164].

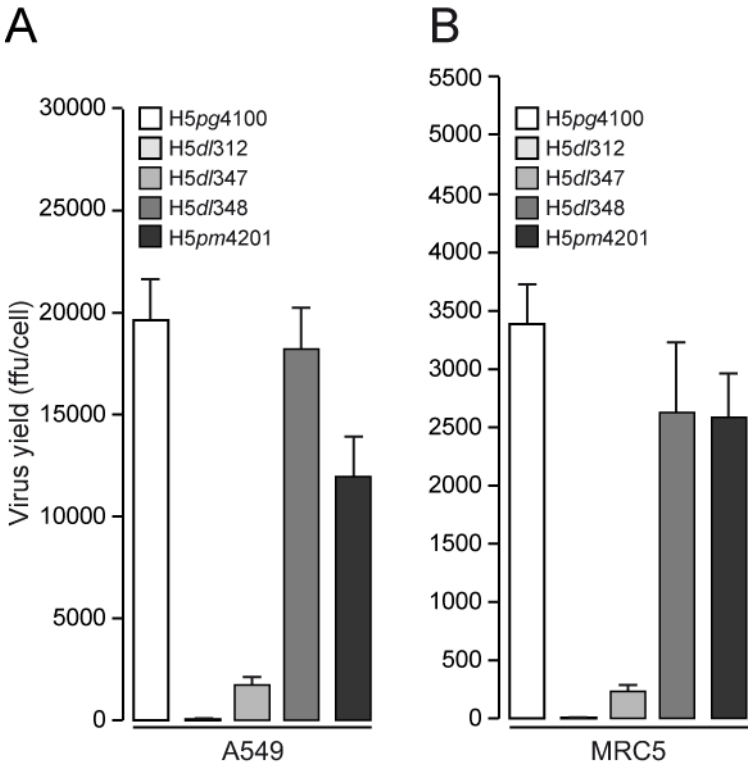

Figure 11: Effect of NES amino acid changes on virus growth. (A) A549 cells were infected with wt and mutant viruses at a multiplicity of 25 ffu per cell. (B) MRC5 cells were grown in medium containing 0.5% FCS 24 h before infection with wt and mutant viruses at a multiplicity of 50 ffu per cell. In both cases viral particles were harvested 48 h p.i. and virus yield was determined by quantitative E2A-72K immunofluorescence staining on HEK-293 cells. All the results represent the averages from three independent experiments. Error bars indicate the standard deviation of the mean.

Although total numbers of progeny virions differed between the two cell types, the effect on virus production displayed a similar pattern. While the deletion mutants H5*dl*312 and H5*dl*347 showed almost no, or severely reduced virus yield, infection of the cells with H5*dl*348 expressing the E1A 13S gene product led to progeny virus production comparable to the wild type virus, H5*pg*4100 (Fig. 11). Progeny virion production in H5*pm*4201-infected A549 cells was reduced by 35% compared to the wild type virus. However, this was less severe than the effect observed by

Fueyo and co-workers [164]. Moreover, in MRC5 cells cultivated under serum starvation, changed to medium containing 0.5% fetal calf serum (FCS) 24 h before infection, the E1A NES mutant (H5*pm*4201) replicated remarkably more efficiently than described previously [164]. Taken together, these data indicate that a functional NES in the E1A protein is not required for efficient replication of the virus, since the NES mutation in H5*pm*4201-infected cells had no significant effect on viral protein synthesis or progeny virus production under the tested conditions (Fig. 9 and 11).

5.2 Neither E1B-55K nor E4orf6 NES are required for efficient viral replication

In the early phase a complex consisting of E1B-55K and E4orf6 is known to assemble a Cullin 5-based E3 ubiquitin ligase to induce proteasomal degradation of various cellular substrates, including p53 and Mre11 [60, 142, 261, 263, 304]. It is well established that during the late phase of infection, both early viral proteins are necessary to preferentially export viral late mRNAs from the nuclear compartment to the cytoplasm [11, 39, 140, 198, 254]. Nevertheless, it is still not understood how the E1B-55K/E4orf6 complex mediates the exclusive nuclear export of viral late mRNAs, nor indeed how export of the complex affects the activity of the E3 ubiquitin ligase, which requires these two early proteins for assembly [28, 340].

Extensive investigations have revealed functional nuclear export signals (NES) within both the E4orf6 and E1B-55K proteins [77, 81, 185, 325]. Since both can shuttle through a NES-dependent pathway, the role of CRM1-mediated export on viral replication was previously examined using the drug leptomycin B, which irreversibly modifies CRM1 [51, 264], as well as a specific peptide inhibitor of CRM1 [105]. These experimental set-ups successfully blocked NES-dependent export of E4orf6 [264] and E1B-55K [51, 105]. In both cases, neither viral late mRNA export [105] nor late protein synthesis were inhibited, indicating that CRM1 does not participate in selective viral mRNA export [51, 105, 264].

Nevertheless, how NES-dependent export of E1B-55K and/or E4orf6 contributes to the viral replication cycle has not been characterized in detail. To address this issue, a set of adenoviral mutants harboring amino acid substitutions within the NES of E1B-55K (H5*pm*4101), E4orf6 (H5*pm*4116), or both (H5*pm*4119) were constructed [175, 288]. In previous analyses mutation of the E4orf6 NES resulted in reduced steady-state concentrations of the protein at late times post infection.

Additionally, defects in viral late protein synthesis and virus progeny production in the E4orf6 NES mutant viruses (H5*pm*4116 and H5*pm*4119) were observed. However, both defects could be due to lower levels of E4orf6 protein expression in these mutants [288].

Levels of the mutated protein were elevated by establishing a semi-stable cell line expressing the E4orf6-NES protein using a lentiviral construct. To produce lentiviral particles the coding sequence of the E4orf6-NES protein was inserted into LeGO-iBLB2. This construct was used to generate lentiviral particles in HEK-293T cells (4.8.2) [323, 324]. Subsequently, the supernatant containing the lentiviral particles was used to transduce A549 cells, which were selected and maintained in medium containing neomycin (250 µg/ml). The established polyclonal cell line, exogenously expressing the mutated E4orf6 protein is subsequently referred to as E4orf6 NES cells.

5.2.1 Mutation of the E4orf6 NES leads to reduced levels of E4orf6

Virus mutants harboring mutations in the leucine-rich nuclear export signals of E1B-55K and/or E4orf6 were generated using our established cloning system [136]. H5*pm*4101 contains three amino acid exchanges in the NES of E1B-55K (L83A, L87A and L91A), while the NES of E4orf6 was mutated (L90A and I92A) in H5*pm*4116. H5*pm*4119 is the double NES mutant (DNES) containing amino acid substitutions in the NES of E1B-55K and E4orf6 (Fig. 12A) [175, 288]. The E4orf6 NES cells were infected with wt (H5*pg*4100), E1B-55K (H5*pm*4149) or E4orf6 (H5*pm*4154) null mutants, as well as with single or double E1B-55K or E4orf6 NES mutants.

Time course analyses were performed for E1B-55K and E4orf6 protein levels. Mock-infected cells displayed a basal expression level of the E4orf6-NES protein, while upon infection with the E4 orf6 minus virus (H5*pm*4154) the protein accumulated to higher levels that decreased at late times post infection (Fig. 12B). The same expression pattern was previously observed after infection of normal A549 cells with both E4orf6 NES virus mutants (H5*pm*4116 and H5*pm*4119, i.e.) [288]. However, infection of the E4orf6 NES cells with the E1B minus virus or with single NES mutants (H5*pm*4101 and H5*pm*4116) resulted in accumulation of E4orf6 similar to that observed in wt-infected cells.

Surprisingly, when the cell line expressing recombinant E4orf6-NES was infected with the double NES mutant, both E1B-55K and E4orf6 protein levels were significantly reduced, whereas infection of cells with H5*pm*4154, H5*pm*4101 and H5*pm*4116 resulted in expression of E1B-55K comparable to wt virus. As

expected, no E1B-55K could be detected upon infection with the E1B minus virus (Fig. 12B). Western blot analysis confirmed that the E4orf6 NES cell line is capable of producing sufficient E4orf6 levels during infection, although the H5*pm*4154 virus encodes no E4orf6.

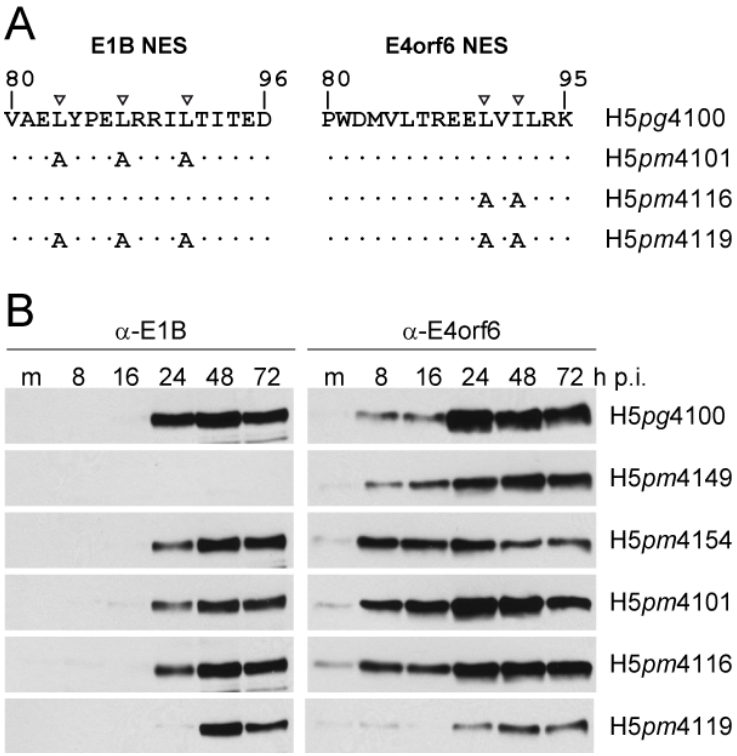

Figure 12: Effect of NES amino acid changes and E1B-55K/E4orf6 protein levels in virus-infected E4orf6 NES cells. (A) Amino acid substitutions in E1B-55K and/or E4orf6 mutant viruses. NES specific residues in E1B-55K and E4orf6 are indicated by triangles. Numbers refer to amino acid residues in the wt E1B-55K and E4orf6 protein from H5*pg*4100. Amino acid changes in the E1B and E4orf6 proteins from H5*pm*4101, H5*pm*4116, and H5*pm*4119 are indicated below. (B) Steady-state expression levels of E1B-55K and E4orf6. E4orf6 NES cells were infected with wt and mutant viruses at a multiplicity of 20 ffu per cell. Infected cells were harvested at the indicated times p.i., non-infected (m = mock) after 72 h p.i. and total cell extracts were prepared. Proteins (25 µg samples) from each time point were separated by 10% SDS-PAGE and subjected to immunoblotting using anti-E1B-55K mouse mab 2A6 or anti-E4orf6 rabbit polyclonal antibody 1807.

5.2.2 Nuclear export of E1B-55K and E4orf6 is not required for efficient virus production

The E4 orf6 NES-expressing cell line was used to evaluate levels of viral late proteins and virus production (Fig. 13). Previous examination of NES virus mutants in normal A549 cells showed low level expression of the mutated E4orf6 protein that was accompanied by reduced L4-100K protein and progeny virus synthesis [288].

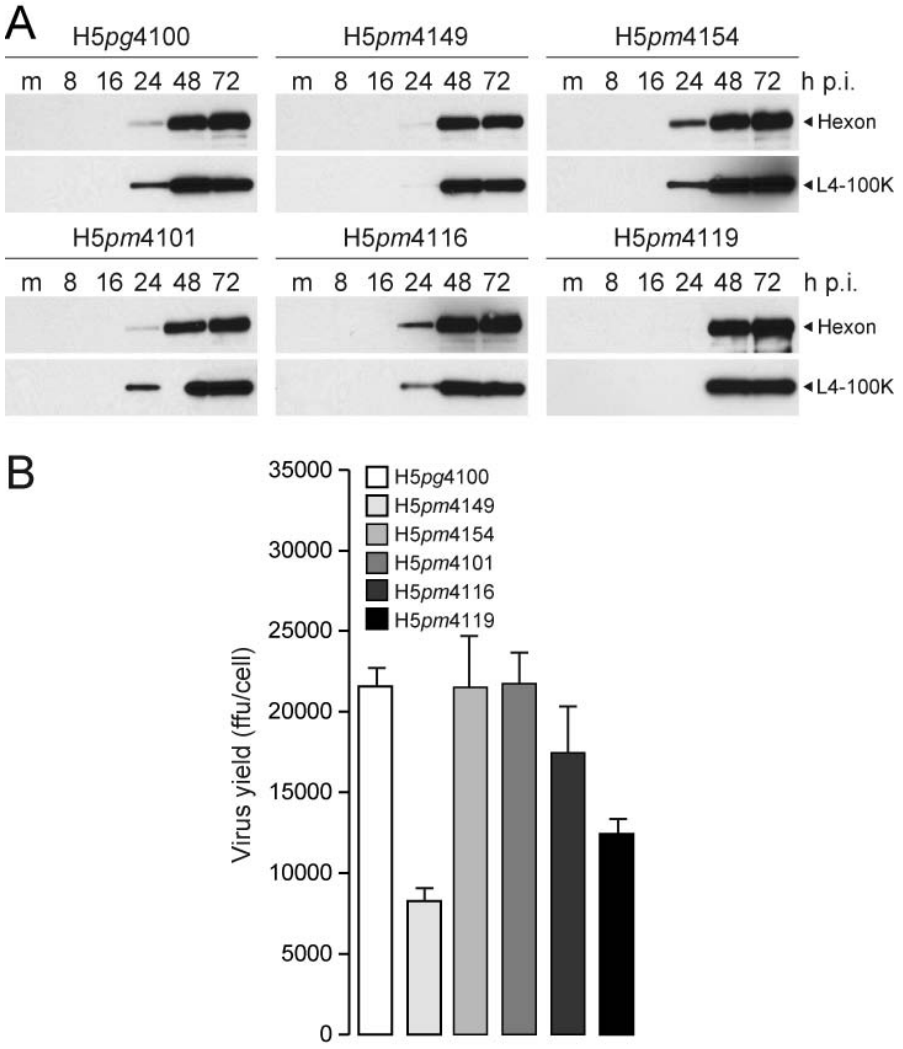

Figure 13: Viral late protein synthesis and virus growth in wt and mutant virus-infected E4orf6 NES cells. (A) Viral late protein synthesis. Total cell extracts from infected cells were prepared at the indicated times and 72 h post infection from non-infected cells (m = mock). Proteins (10 µg samples) were separated by 10% SDS-PAGE, transferred to nitrocellulose membranes and probed with anti-Ad5 rabbit polyclonal serum L133 or anti-L4-100K rat mab 6B10. Bands corresponding to the viral late protein Hexon are indicated on the right. (B) Virus growth. E4orf6 NES cells were infected with wt or mutant viruses at a multiplicity of 10 ffu per cell, harvested 72 h p.i. and virus yield was determined by quantitative E2A-72K immunofluorescence staining on HEK-293 cells. The results represent the average of three independent experiments. Error bars indicate the standard deviation of the mean.

Interestingly, exogenous expression of E4orf6-NES rescued L4-100K protein levels and virus growth in cells infected with the E4 orf6 null virus (H5*pm*4154) to essentially wt levels, indicating that mutation of the protein's NES has no effect on either viral late proteins or virus production. Expression of exogenous E4orf6-NES in the single NES mutants (H5*pm*4101 and H5*pm*4116) led to normal levels of late proteins and virus production; however, virus production did not attain wt levels in

the H5*pm*4116 mutant, suggesting that the lower levels of virus yield displayed by the E4orf6-NES mutants in the absence of the exogenously expressed protein was a result of lower E4orf6 protein levels (Fig. 12B) [288]. Similar low levels of both viral late proteins and progeny viruses were produced in cells infected with the E1B minus and the double NES virus (H5*pm*4149 and H5*pm*4119), emphasizing the importance of sufficient E1B-55K and E4orf6 steady-state concentrations for efficient viral replication (Fig. 13).

5.2.3 NES virus mutants support viral late mRNA transport

The next question was whether E1B-55K NES and/or E4orf6 NES are required for late mRNA synthesis and preferential export during the late phase of infection. For these experiments, NES virus mutants were used to measure both total mRNA levels and nucleocytoplasmic distribution of late transcripts by performing quantitative PCR in the E4orf6-NES expressing A549 cells (Fig. 14).

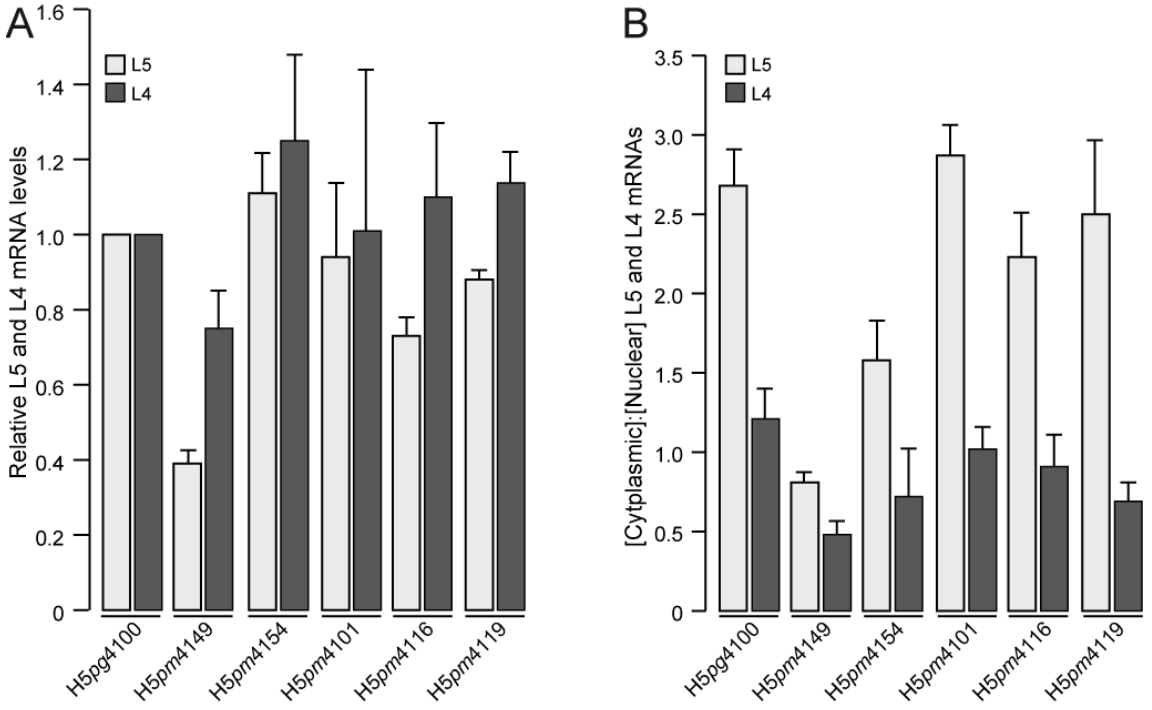

Figure 14: Total amounts and nuclear export efficiency of viral late mRNAs L5 and L4 in wt and mutant virus-infected E4orf6 NES cells. (A) Total amounts of viral late mRNAs L5 and L4. E4orf6 NES cells were infected with wt or mutant viruses at a multiplicity of 10 ffu per cell. Steady-state concentrations of both RNAs were determined by real-time PCR 48 h post infection. Total L5 and L4 values were corrected using 18S rRNA as an internal control and are expressed relative to the wild type value. (B) Nuclear export efficiency of viral late mRNAs L5 and L4. E4orf6 NES cells were infected with wt or mutant viruses at a multiplicity of 10 ffu per cell. Steady-state concentrations of both RNAs in cytoplasm and nucleus were determined by real-time PCR 48 h post infection. Raw numbers were corrected using 18S rRNA as an internal control and used to calculate ratios of cytoplasmic to nuclear L5/L4 mRNAs. All the results represent the average of three independent experiments, each performed in duplicate. Error bars indicate the standard deviation of the mean.

Using H5*pm*4149, we could confirm that E1B-55K is required for efficient synthesis of viral late mRNAs [11, 140, 240]. Absence of this protein led to a significant drop in total viral late mRNA levels compared to H5*pg*4100-infected cells, when measuring L4 or L5 mRNA levels (Fig. 14A). As for virus growth (Fig. 13), viral late mRNA production was completely rescued by exogenously expressed E4orf6-NES in H5*pm*4154-infected cells (Fig. 14A). Similar results were obtained with NES mutants, since none of the NES mutations either in E1B-55K, E4orf6 or both, led to reductions in mRNA production of more than 30% compared to wt levels. These results indicate that the presence of a functional NES in either or both of these early adenoviral proteins is not essential for synthesis or stability of late mRNA (Fig. 14A).

To evaluate efficient nuclear export of late adenoviral mRNAs, L4- and L5-mRNAs were extracted after fractionation of nuclear and cytoplasmic compartments and analyzed them by quantitative PCR (Fig. 14B). As expected, the E1B null mutant was significantly impaired in nuclear export of L4- and L5-mRNA compared to H5*pg*4100. However, the E4orf6 null mutant showed an intermediate phenotype for the export of both viral late transcripts that was not rescued by exogenously expressed E4orf6-NES (Fig. 14B).

As we have shown previously, functional inactivation of the E1B-55K NES does not decrease late mRNA accumulation within the cytoplasm, implicating that mRNA transport does not depend on CRM1-mediated export of E1B-55K [175]. Interestingly, concurrent inactivation of the E4orf6 NES in the H5*pm*4119 virus, as well as mutation of E4orf6 alone in H5*pm*4116 led to a cytoplasmic accumulation of viral late mRNA that was comparable to wt (Fig. 14B). These data indicate that functional inactivation of E1B-55K and/or E4orf6 NES-dependent export does not abrogate viral late mRNA accumulation in the cytoplasm. This is consistent with previous reports where inhibition of CRM1 did not interfere with viral late gene expression [51, 105, 264]. In conclusion, this shows for the first time that NES sequences, which mediate export of both E1B-55K and E4orf6 in the normal context of adenovirus-infected cells, do not contribute to viral late gene expression.

5.2.4 Distinct requirements of the NESs for degradation and relocalization of p53 and Mre11

Since CRM1-dependent export of E1B-55K and E4orf6 is not required for viral late gene expression, the next step was to examine the effect of mutations of both E1B-55K and E4orf6 NES on degradation of p53 and Mre11, two well-known

cellular substrates of the E3 ubiquitin ligase assembled by E1B-55K/E4orf6. Infected A549 cells expressing E4orf6 NES were harvested at various times post infection, and p53 and Mre11 protein levels were analyzed by Western blotting. As expected, infection of A549 cells with the H5*pg*4100 virus led to degradation of p53 and Mre11 [27, 142, 261, 263, 304], since p53 levels declined after 8 h p.i., and Mre11 was clearly reduced by 16 h and no longer detectable at 72 h post infection (Fig. 15). In contrast, Mre11 protein levels were not efficiently reduced and p53 accumulated during the course of infection with the E1B-55K null mutant, H5*pm*4149. Also as expected, mutation of the E1B-55K NES did not interfere with degradation of either cellular protein (Fig. 15) [175]. Interestingly, in H5*pm*4154 or H5*pm*4116, exogenous expression of the E4orf6-NES did not preclude the degradation of Mre11, and p53 did not accumulate to the levels observed in H5*pm*4149-infected cells. As for other phenotypes examined (Fig. 13), the double NES mutant, H5*pm*4119, displayed reduced efficiency for Mre11 and p53 degradation in E4orf6-NES expressing cells (Fig. 15). Taken together, these findings suggest that CRM1-mediated export of either E1B-55K or E4orf6 is not required for degradation of Mre11 or p53.

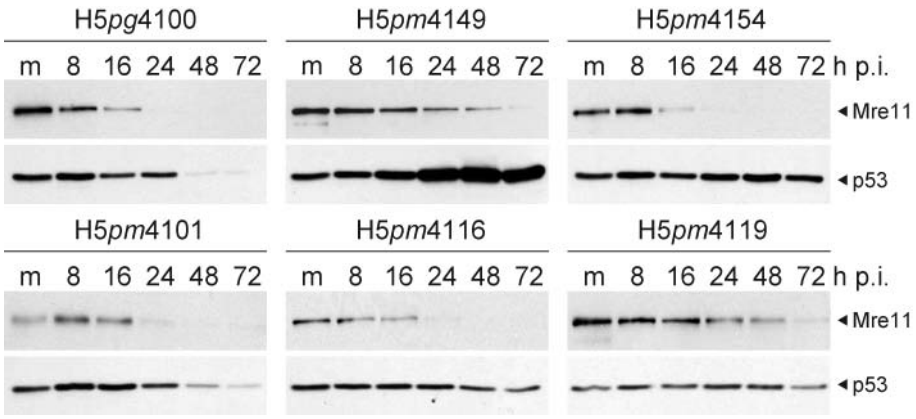

Figure 15: Protein steady-state concentrations of p53 and Mre11 in wt and mutant virus-infected E4orf6 NES cells. E4orf6 NES cells were infected with wt and mutant viruses at a multiplicity of 20 ffu per cell. Non-infected (m = mock) and infected cells were harvested at the indicated times p.i. and whole-cell extracts were prepared. Proteins (40 µg samples) from each time point were separated by 10% SDS-PAGE and subjected to immunoblotting using anti-Mre11 rabbit polyclonal antibody pNB-100-142 and anti-p53 mouse mab DO-1.

Since the results show that degradation of p53 and Mre11 does not require CRM1-dependent export of E1B-55K and E4orf6, it is interesting to examine the effect of NES mutations on the intracellular localization of p53 and Mre11 using triple-label immunofluorescence and confocal microscopy analysis of Ad5-infected cells. It has been proposed that most of E1B-55K and E4orf6 assemble an E3 ubiquitin ligase

that induces polyubiquitylation of p53, Mre11 and other cellular targets. This leads to relocalization of the cellular proteins to cytoplasmic sites that may represent aggregates of misfolded proteins [26, 44, 351]. Relocalization of Mre11 and p53 to these aggregates is induced by E1B-55K [204, 292], while E4orf3 can recruit Mre11 to nuclear tracks and cytoplasmic sites independently of E1B-55K [6, 304].
Analysis of the subcellular distribution of E1B-55K, p53 and Mre11 in A549 cells infected with the wt virus H5*pg*4100 showed reduced nuclear population levels of both p53 and Mre11 (Fig. 16 f, g), compared to mock-infected cells (Fig. 16 b, c), and a clear colocalization of both cellular proteins with E1B-55K in cytoplasmic aggregates (Fig. 16 e-h). In cells infected with the E1B minus mutant neither degradation nor relocalization of p53 were induced, since the protein clearly accumulated in the nuclear compartment, and was not relocalized to cytoplasmic aggregates (Fig. 16 j). The nuclear fraction of Mre11 was relocalized from a homogeneous and diffuse distribution (Fig. 16 c) to numerous nuclear specks. However, the protein was not detected in the cytoplasm (Fig. 16 k) indicating that although nuclear relocalization of Mre11 is independent of E1B-55K, efficient export to the cytoplasm requires this viral protein.
No such requirement was observed for E4orf6, since both p53 and Mre11 could be detected in cytoplasmic aggregates in H5*dl*355-infected cells (Fig. 16 m-p). In H5*pm*4101-infected cells, reduced p53 protein levels were only observed in the nuclear compartment, and intriguingly, no formation of juxta-nuclear cytoplasmic aggregates could be detected (Fig. 16 r). In contrast, Mre11 could be detected in cytoplasmic bodies, indicating that Mre11 can be exported, although with lower efficiency, in the absence of an E1B-55K NES (Fig. 16 s). This redistribution is likely to depend on E4orf3 [6, 304]. It has been shown that E4orf6 is required for degradation of both cellular targets [60, 261, 263, 305]; however, the absence of E4orf6 (in H5*dl*355) did not preclude export of E1B-55K to the cytoplasm, nor was this protein necessary for cytoplasmic localization of either p53 or Mre11 (Fig. 16 m-p). Significantly, mutation of the E4 orf6 NES in H5*pm*4116-infected cells did not block relocalization of p53 or Mre11 to E1B-55K-containing cytoplasmic aggregates (Fig. 16 u-x) indicating that NES-dependent export of E4orf6 does not contribute to cytoplasmic export of either p53 or Mre11.

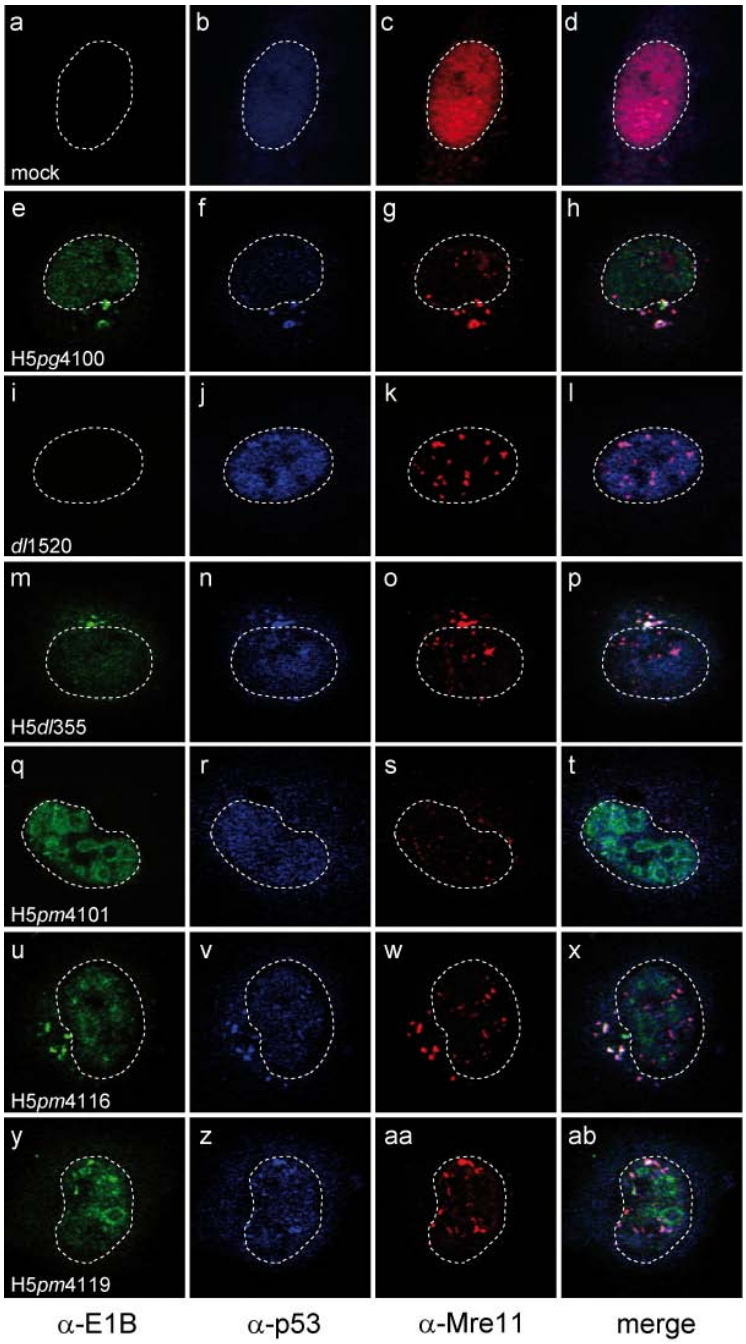

Figure 16: Intracellular localization of E1B-55K, p53 and Mre11 in wt and mutant virus infected cells. A549 cells were uninfected or infected with wt and E1B-55K/E4orf6 mutant viruses at a multiplicity of 20 ffu per cell and fixed at 24 h p.i. Cells were triple-labeled with anti-E1B rat mab 7C11 (α-E1B), anti-p53 mouse mab DO-1 (α-p53) and anti-Mre11 rabbit polyclonal antibody pNB-100-142 (α-Mre11), plus Alexa Fluor 488, 633 and 555 conjugated secondary antibodies, respectively. Representative anti-E1B (green; a, e, i, m, q, u and y), anti-p53 (blue; b, f j, n, r, v and z) and anti-Mre11 (red; c, g, k, o, s, w and aa) staining patterns are shown. The overlays of the green, blue and red images are shown in panels d, h, l, p, t, x and ab (merge). In all panels, nuclei are indicated by a dotted line.

5.2.5 Inhibition of CRM1-dependent transport affects relocalization of p53 to cytoplasmic aggregates

To confirm whether degradation phenotypes exhibited by E1B-55K- and E4orf6-NES mutants correlated with impaired nucleocytoplasmic export, the impact of inhibition of CRM1 on degradation and localization of p53 and Mre11 was examined in the presence of the CRM1 inhibitor leptomycin B (LMB). The LMB concentration used for these assays shows no significant toxic effects for up to 24 hours (Fig. 24B) [51]. Ad-infected cells were treated with LMB, harvested at the indicated times post infection, and protein levels were compared to untreated controls by Western bloting (Fig. 17).

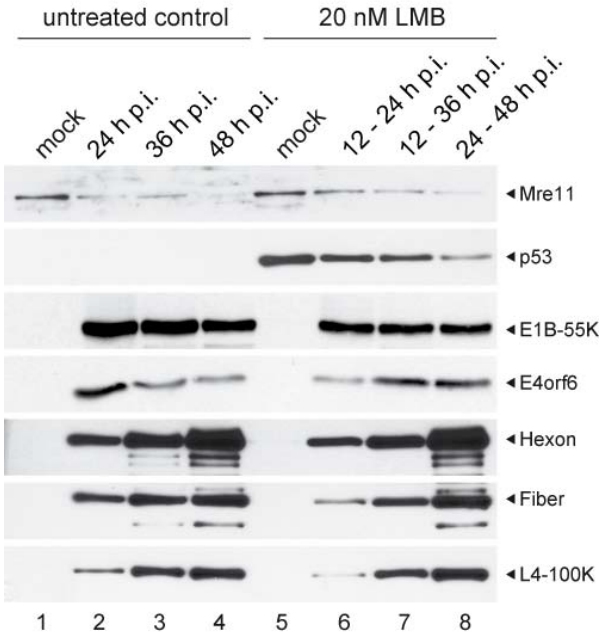

Figure 17: Effect of leptomycin B treatment on steady-state concentrations of Mre11 and p53 in wt-infected cells. A549 cells were infected with wt virus at a multiplicity of 20 ffu per cell, harvested at indicated times p.i. and total cell extracts were prepared. Cells were treated with 20 nM LMB from 12 to 24 (lane 5), 12 to 36 (lane 6) or 24 to 48 h p.i. (lane 7) and compared to untreated controls harvested at the same time points after infection. Proteins (30 µg samples for p53 and Mre11; 20 µg samples for E1B-55K and E4orf6; 10 µg samples for Hexon, Fiber and L4-100K) from each time point were separated bys 10% SDS-PAGE and subjected to immunoblotting using anti-p53 mouse mab DO-1, anti-Mre11 rabbit polyclonal antibody pNB-100-142, anti-E1B-55K mouse mab 2A6, anti-E4orf6 rabbit polyclonal antibody 1807, anti-Ad5 rabbit polyclonal serum L133 and anti-L4-100K rat mab 6B10. Bands corresponding to appropriate proteins are indicated on the right.

As expected, LMB had no effect on late protein synthesis, since steady-state levels of Hexon, Fiber and L4-100K proteins were comparable to those in untreated cells. Furthermore, Mre11 degradation occurred essentially with the same efficiency in LMB-treated or untreated cells, indicating that in agreement with NES virus

mutant results (Fig. 15) [175], CRM1-dependent export is not required for degradation of Mre11 (Fig. 17). Consistent with published observations [194, 233], LMB treatment of mock-infected cells for 24 h led to accumulation of p53 compared to the untreated control (Fig. 17, compare lane 5 with lane 1). Interestingly, p53 levels were efficiently reduced during the course of adenoviral infection (Fig. 17, lanes 5-8), indicating that degradation of p53 occurs in the absence of active CRM1, consistent with the reduction of p53 levels observed in cells infected with NES virus mutants (Fig. 15).

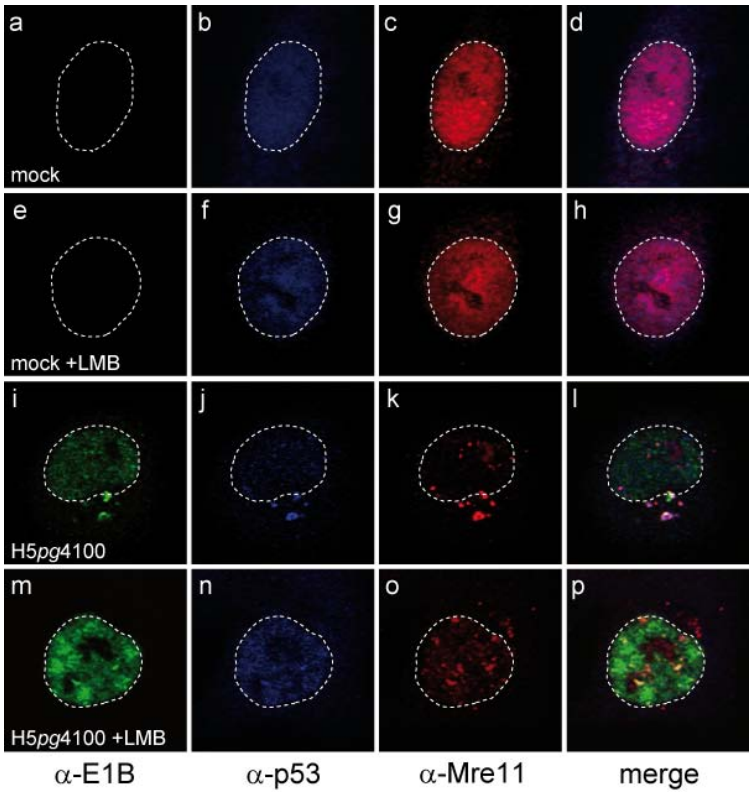

Figure 18: Effect of leptomycin B treatment on intracellular localization of E1B-55K, p53 and Mre11 in wt-infected cells. A549 cells were uninfected or infected with wt virus at a multiplicity of 20 ffu per cell, either untreated or treated with 20 nM LMB from 12 to 24 h p.i. and fixed at 24 h p.i. Cells were triple-labeled with anti-E1B rat mab 7C11 (α-E1B), anti-p53 mouse mab DO-1 (α-p53) and anti-Mre11 rabbit polyclonal antibody pNB-100-142 (α-Mre11), plus Alexa Fluor 488, 633 and 555 conjugated secondary antibodies, respectively. Representative anti-E1B (green; a, e, i and m), anti-p53 (blue; b, f, j and n) and anti-Mre11 (red; c, g, k and o) staining patterns are shown. The overlays of the green, blue and red images are shown in panels d, h, l and p (merge). In all panels, nuclei are indicated by a dotted line.

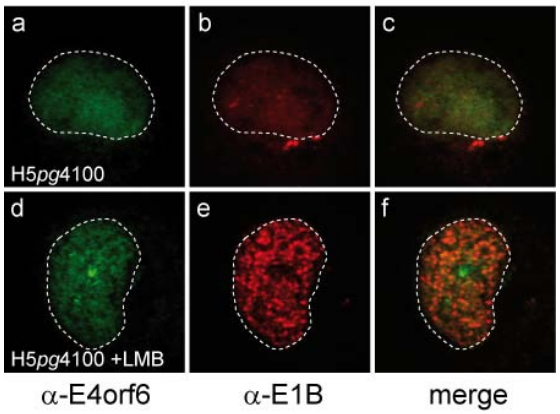

Figure 19: Effect of leptomycin B treatment on intracellular localization of E4orf6 and E1B-55K. A549 cells were infected with wt virus at a multiplicity of 20 ffu per cell, either untreated or treated with 20 nM LMB from 12 to 24 h p.i. and fixed at 24 h p.i. Cells were double-labeled with anti-E4orf6 rabbit polyclonal antibody 1807 (α-E4orf6) and anti-E1B mouse mab 2A6 (α-E1B), plus Alexa Fluor 488 and 555 conjugated secondary antibodies, respectively. Representative anti-E4orf6 (green; a and d) and anti-E1B (red; b and e) staining patterns are shown. Overlays of the green and red images are shown in panels c and f (merge). In all panels, nuclei are indicated by a dotted line.

Immunofluorescence analysis of the intracellular distribution of p53 and Mre11 in Ad-infected cells in the presence of LMB (Fig. 18) confirmed the observed effects of E1B-55K and E4orf6 NES mutations on the relocalization of cellular proteins (Fig. 16). In mock-infected cells, LMB induced no change in p53 or Mre11 distribution: both proteins displayed an essentially nuclear localization (Fig. 18, compare panels a-d with e-h). Treatment of Ad-infected cells with LMB completely inhibited relocalization of both E1B-55K and p53 to cytoplasmic aggregates (Fig. 18 compare panels i, j with m, n), and E1B-55K and E4orf6 displayed the same nucleocytoplasmic distribution as that observed in cells infected with NES mutants (Fig. 19). Similar to the effect observed with the E1B-55K NES mutant, Mre11 levels were reduced (Fig. 17), and the protein was relocalized to both numerous nuclear specks and cytoplasmic aggregates (Fig. 18 o). This indicates that export of Mre11 is not completely blocked by inhibition of CRM1, and is facilitated by E4orf3.

Taken together, these data confirm that CRM1-dependent export of either E1B-55K or E4orf6 is not required for efficient synthesis of viral late proteins, and indicate that while efficient export of p53 depends on the E1B-NES and active CRM1, Mre11 requires neither E1B- nor E4orf6-NES and uses a CRM1-independent export pathway, namely via E4orf3.

5.3 The L4-100K-NES might be required for Hexon trimerization

In addition to the examined adenoviral early proteins E1A, E1B-55K and E4orf6, two late proteins possess a nuclear export signal of the HIV-1 Rev type: the structural protein VI and the regulatory protein L4-100K [68, 337]. Both proteins are described to function in capsid assembly by mediating trimerization of Hexon as well as its nuclear import and integration into the viral capsid [56, 149, 228, 337]. Additionally, L4-100K recognizes viral late transcripts by specifically binding to the tripartite leader (TPL) sequence present in these mRNAs. Subsequently, L4-100K promotes the exclusive translation of viral mRNAs by an initiation mechanism called ribosome shunting [273, 341, 342].

Previous studies on a L4-100K NES virus mutant, with the four hydrophobic amino acids (aa) in the NES substituted by alanines (Fig. 20A), revealed that this nuclear export signal is required for efficient expression of viral late proteins, and crucial for adenoviral replication [183]. However, a specific function of the L4-100K-NES in viral life cycle could not be identified. Although observing only a minor effect on late protein synthesis, virus growth was drastically reduced. This indicates that the substitution mutation results in a downstream encapsidation defect. Therefore the contribution of the L4-100K-NES to viral replication should be analyzed in more detail, especially focusing on the role of L4-100K in capsid assembly.

5.3.1 Mutation of the NES of L4-100K prevents cytoplasmic localization only in transfected but not infected cells

Mutational analysis of the L4-100K protein in transiently transfected cells showed nuclear retention of the L4-100K NES protein, whereas the wild type protein was diffusely distributed in the cytoplasmic and nuclear compartment [68]. After transfection of A549 cells with wt and a NES-mutated L4-100K construct, the wt protein was diffusely localized throughout the cell (Fig. 20B, panels a, b). In parallel the L4-100K NES protein displayed a predominant nuclear distribution pattern (Fig. 20B, panels c, d). However, immunofluorescence analysis of virus-infected A549 cells revealed a distinct localization of the mutated protein (Fig. 20C).

Although wt (H5*pg*4100)-infected A549 cells exhibited the same diffuse distribution (Fig. 20C, panels a, b), amino acid substitutions in the nuclear export signal of L4-100K in the H5*pm*4165 virus did not induce relocalization of the

protein to the nucleus. Surprisingly, the mutated protein localized mainly in the cytoplasm, but in contrast to wt-infected cells in irregularly shaped structures that aggregated around the nuclear membrane (Fig. 20C, panels c, d). This difference compared to transfected cells, where L4-100K NES displayed a predominantly nuclear localization (Fig. 20B, panels c, d), might be due to the modified host cell environment upon virus infection. Although L4-100K is known to be imported into the nucleus [68, 156, 184], previously described functions of L4-100K during adenoviral replication are all restricted to the cytoplasm, including translation initiation of TPL-containing late mRNAs and trimerization of the major capsid component Hexon [56, 67, 145, 149].

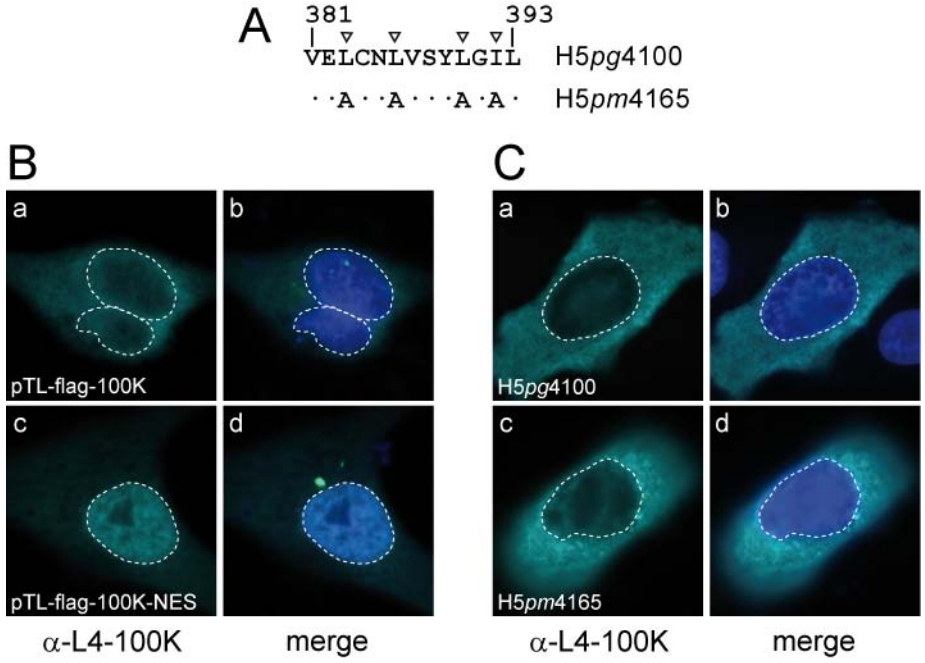

Figure 20: Effect of NES amino acid changes on localization and protein stability of L4-100K. (A) Amino acid substitution L4-100K mutant virus. NES specific residues in L4-100K are indicated by triangles. Numbers refer to amino acid residues in the wt L4-100K protein from H5*pg*4100. Amino acid changes in the L4-100K protein from H5*pm*4165 are indicated below. (B) Intracellular localization of L4-100K in wt and NES-mutant protein transfected cells. A549 cells were transfected with pTL-flag-100K and pTL-flag-100K-NES and fixed 48 h post transfection. Cells were labeled with anti-L4-100K rat mab 6B10 (α-L4-100K) and Cy5 conjugated secondary antibody. Representative anti-L4-100K (green; a and c) staining patterns are shown. Overlays of DAPI staining (blue) with the green images are shown in panels b and d (merge). (C) Intracellular localization of L4-100K in wt and NES-mutant virus-infected cells. A549 cells were infected with wt and L4-100K NES mutant virus at a multiplicity of 10 ffu per cell and fixed at 36 h p.i. Cells were labeled with anti-L4-100K rat mab 6B10 (α-L4-100K) and Cy5 conjugated secondary antibody. Representative anti-L4-100K (green; a and c) staining patterns are shown. Overlays of DAPI staining (blue) with the green images are shown in panels b and d (merge). Nuclei visualized using DAPI are indicated by a dotted line in all panels.

5.3.2 Efficient viral late mRNA transport requires a functional L4-100K-NES

The L4-100K NES mutant virus displayed significantly less viral late protein synthesis of L4-100K as well as structural proteins, most prominently the major capsid protein Hexon [183]. A striking feature of L4-100K is its specific binding to the TPL sequence of viral late mRNAs [145, 342]. Since L4-100K was shown to bind E1B-55K, it was discussed whether this interaction contributes to viral late mRNA export [183], although so far no connection between L4-100K and this process has been established. To examine whether a functional L4-100K-NES contributes to late gene expression at the mRNA level, infected A549 cells were used to measure both total amounts and nucleocytoplasmic distribution of late RNAs by quantitative PCR.

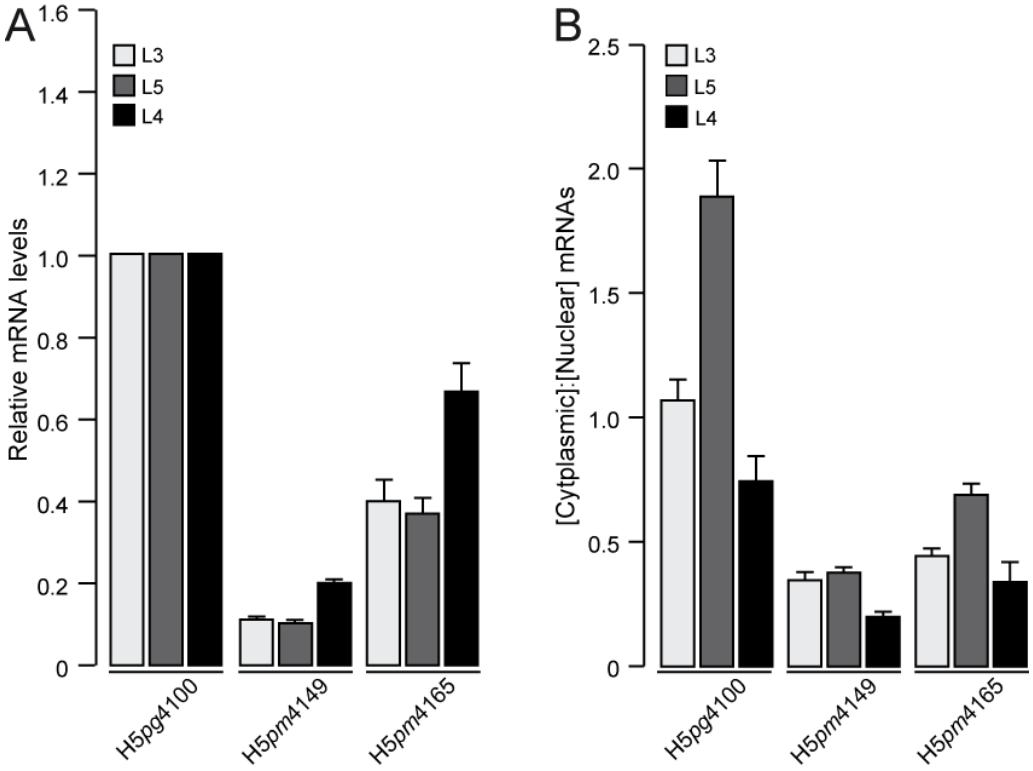

Figure 21: Effect of L4-100K NES mutation on total amounts and nuclear export efficiency of late mRNAs of viral proteins Hexon, Fiber and L4-100K. (A) Total amounts of viral late mRNAs L3, L5 and L4. A549 cells were infected with wt or mutant viruses at a multiplicity of 1 ffu per cell. Steady-state concentrations of RNAs were determined by real-time PCR 48 h p.i. Total L3, L5 and L4 values were corrected using 18S rRNA as an internal control, and are expressed relative to the wild type value. (B) Nuclear export efficiency of viral late mRNAs L3, L5 and L4. A549 cells were infected with wt or mutant viruses at a multiplicity of 1 ffu per cell. Steady-state concentrations of RNAs in cytoplasm and nucleus were determined by real-time PCR 48 h p.i. Raw numbers were corrected using 18S rRNA as an internal control and used to calculate ratios of cytoplasmic to nuclear L3/L5/L4 mRNAs. All results represent the average of three independent experiments, each performed in duplicate. Error bars indicate the standard error of the mean.

The E1B null virus H5*pm*4149 was used as negative control, and as expected, absence of the E1B protein led to a significant drop in both total levels and nuclear export of Hexon, Fiber and L4-100K transcripts compared to H5*pg*4100 infected cells (Fig. 21). Surprisingly, infection of cells with the L4-100K NES mutant (H5*pm*4165) decreased total levels of viral late mRNAs by about 30 to 60%, depending on the mRNA examined (Fig. 21A). However, the effect was less severe than in E1B null mutant-infected cells where levels decreased by about 60 to 90%. In addition, the cytoplasmic accumulation of Hexon, Fiber and L4-100K mRNAs in relation to the nuclear fraction was reduced to approximately 50% compared to wt-infected cells (Fig. 21B). This was unexpected, since to date no involvement of L4-100K in viral late mRNA metabolism, other than its translation, has been seen. Since a functional NES in the L4-100K protein was not required for its predominant localization in the cytoplasm, proposing a role in the export of viral transcripts might be precipitant. Additionally, earlier studies on the export of viral late mRNAs excluded a CRM1-dependent pathway and actually proposed the cellular export receptor TAP as the transport pathway [51, 105, 264, 287, 345]. Nevertheless, mutation of the nuclear export signal (aa position 383 to 392 [68]) could reduce L4-100K´s binding efficiency to the TPL sequences of these mRNAs, since the NES is located in its TPL-RNA binding region (aa position 383–727 [342]), which could affect the stability of these RNAs [273, 341].

5.3.3 Mutation of the L4-100K-NES results in cytoplasmic retention of the Hexon protein

Although reduced accumulation and export efficiency of late transcripts (Fig. 21) provide an explanation for defects in late protein synthesis [183], the drastic effect on virus growth points to an additional encapsidation effect, as discussed above. During the late phase, L4-100K mediates trimerization of the capsid protein Hexon [55, 56]. Since only Hexon trimers are imported [149, 337], subcellular localization of Hexon and L4-100K was examined by immunofluorescence analysis of wt and L4-100K NES mutant virus-infected cells.

The wt L4-100K was diffusely distributed throughout the cytoplasm, while Hexon preferentially localized in the nuclear compartment (Fig. 22A, panels a-c). In contrast, mutation of the nuclear export signal in L4-100K led to a cytoplasmic colocalization of both proteins in distinct, punctuated or filamentous structures around the nucleus (Fig. 22A, panels d-f). Since import of Hexon into the nucleus was only reported after its trimerization [149, 337], this immunofluorescence

analysis (Fig. 22B, panels d-f) suggests that the L4-100K-NES mutation prohibits trimerization of the Hexon protein (Fig. 22A).

The import of Hexon trimers, however, was reported to depend on protein VI [337]. Therefore, localization of protein VI during wt and mutant virus infection was determined. Intriguingly, pVI localized predominantly in the nucleus in wild type (H5*pg*4100)-infected cells (Fig. 22B, panel b), whereas in the L4-100K NES substitution mutation infection a cytoplasmic aggregation of pVI was observed around the nuclear membrane (Fig. 22B, panel e), thus showing a distribution pattern similar to the Hexon protein (Fig. 22B). The aggregation of Hexon and pVI around the nucleus suggests an import defect with both proteins.

Since it has been established that the import process of Hexon is independent of L4-100K, the NES mutation in L4-100K might inhibit trimerization of the capsid protein. To test this idea, infected A549 cells were harvested 48 h p.i. and both Hexon and L4-100K levels were analyzed by Western blotting. L4-100K levels were lower in H5*pm*4165-infected cells than with wt virus (Fig. 22C) as shown recently [183]. To investigate trimerization, samples were either untreated (native) or heated at 55°C for 12 min prior to separating proteins by 8% SDS-PAGE (4.6.4). Staining the nitrocellulose membrane with a Hexon specific antibody revealed a distinct band of approximately ~320 kDa in wt-infected cells, whereas such a band could not be detected after infection with the L4-100K NES mutant (Fig. 22C). Significantly, heating the wt sample led to the appearance of a band at the expected size of Hexon monomers, 114 kDa, and a smear above this band, although the trimeric Hexon band was not diminished.

Thus denaturation of trimers resulted in a clearly stronger staining pattern than observed in native samples, indicating that the Hexon antibody binds the denatured monomeric form of Hexon more efficiently. However, no such band was detected after infection with the H5*pm*4165 virus (Fig. 22C). The absence of a trimeric Hexon band in H5*pm*4165-infected cells and the increased accumulation of denatured Hexon in wild type virus (Fig. 22C), indicates that the L4-100K NES mutation leads to a Hexon trimerization defect.

Taken together, results obtained from immunofluorescence and trimerization analysis (Fig. 22) suggest that the L4-100K NES virus (H5*pm*4165) is not capable of trimerizing the major capsid protein Hexon. Consequently, this might lead to cytoplasmic aggregation of monomeric Hexon proteins that localize in close proximity to the nuclear membrane.

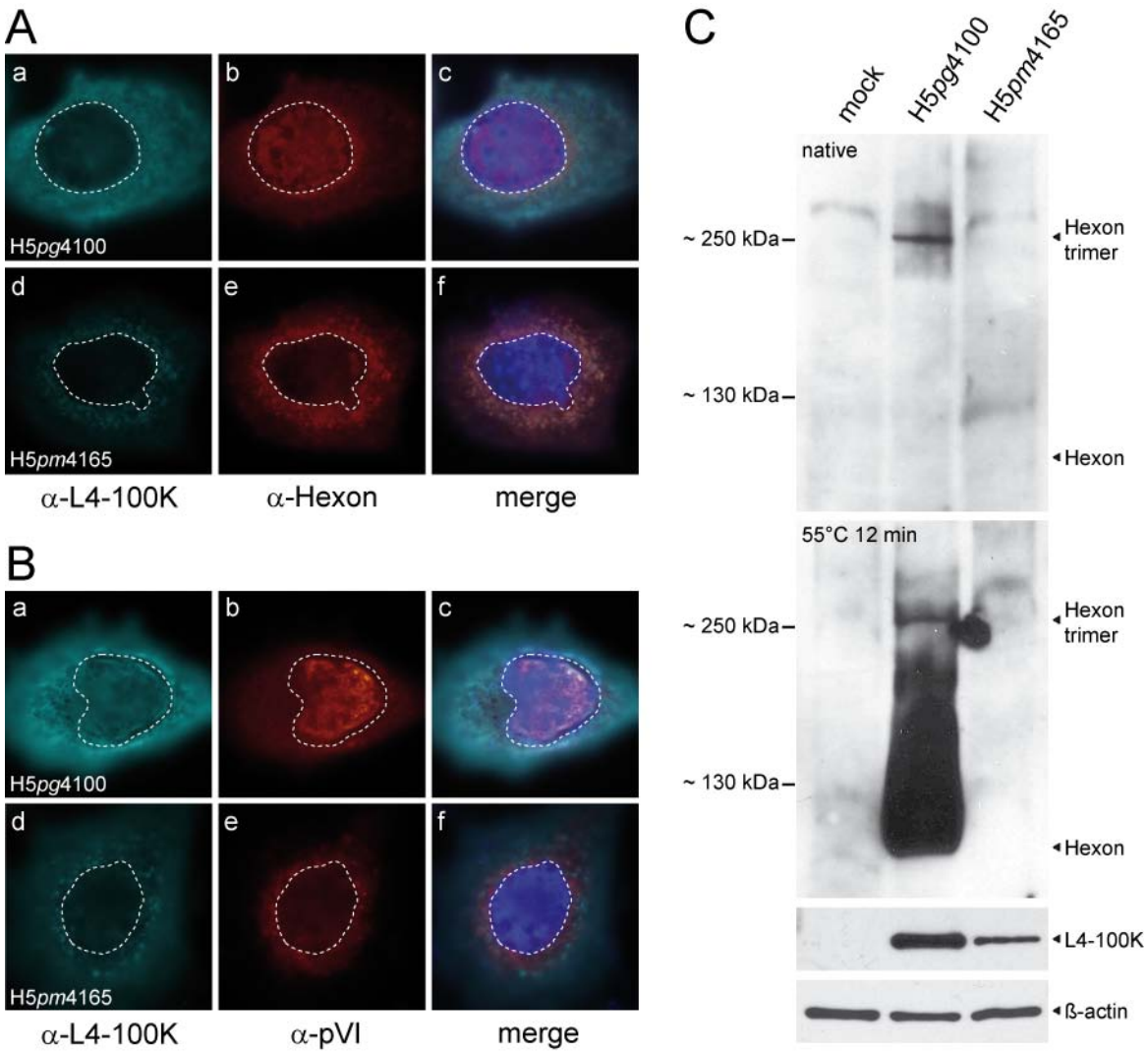

Figure 22: Effect of L4-100K NES mutation on Hexon metabolism. (A, B) I ntracellular localization of L4-100K and Hexon (A) or pVI (B) in wt and L4-100K NES mutant-infected cells. A549 cells were infected with wt and L4-100K NES mutant viruses at a multiplicity of 10 ffu per cell and fixed 36 h p.i. Cells were labeled with anti-L4-100K rat mab 6B10 (α-L4-100K) and anti-Hexon rabbit polyclonal serum Ad5 Hexon (A; α-Hexon) or anti-protein VI rabbit mab pVI (B; α-pVI), plus Cy5 and Cy3 conjugated secondary antibodies, respectively. Representative anti-L4-100K (green; a and d) and anti-Hexon or pVI (red; b and e) staining patterns are shown. Overlays of DAPI staining (blue) with the green and red images are shown in panels c and f (merge). Nuclei visualized using DAPI are indicated by a dotted line in all panels. (C) Hexon trimerization in wt and L4-100K NES mutant virus-infected cells. A549 cells were infected with wt and mutant virus at a multiplicity of 1 ffu per cell, harvested 48 h p.i. and total cell extracts were prepared. Proteins (25 µg samples for Hexon; 10 µg samples for L4-100K and ß-actin) were separated by 8% (for Hexon) or 10% SDS-PAGE (for L4-100K and ß-actin) and subjected to immunoblotting using anti-Hexon rabbit polyclonal serum Ad5 Hexon, anti-L4-100K rat mab 6B10 and anti-ß-actin mouse mab AC-15. Hexon samples were either untreated (native, upper panel) or heated at 55°C for 12 min (lower panel). Bands corresponding to the Hexon monomers or trimers are indicated on the right.

5.3.4 Inhibition of CRM1-dependent transport does not affect L4-100K localization

It should be elucidated whether functional inactivation of the L4-100K-NES, and hence CRM1-dependent transport of the protein led to the observed phenotypes; in other words a distinct localization pattern of the mutated protein in transfected/ infected cells compared to the wt protein (Fig. 20), as well as altered Hexon/pVI localization upon infection with the L4-100K NES virus (Fig. 22). The immunofluorescence analysis was repeated in wild type-infected A549 cells treated with 20 nM LMB 12 h prior to fixation. E1B staining was used as an indicator of functional CRM1 inhibition, since nuclear export of this adenoviral protein depends on CRM1 transport [81, 175, 185]. In addition, a plasmid expressing the L4-100K wt protein was co-transfected with an E1B construct to further analyze the effect of CRM1 inhibition in transfected cells.

Surprisingly, while LMB treatment led to the retention of E1B in the nuclear compartment, the diffuse localization of L4-100K in the nucleus and cytoplasm was unaffected (Fig. 23A compare panels a-c with d-f). This provides new evidence that the export of L4-100K does not depend on CRM1, and might require another cellular export receptor. Similarly, immunofluorescence analysis of infected cells also revealed no effect of LMB treatment on either L4-100K (Fig. 23B to D), Hexon (Fig. 23C) or pVI (Fig. 23D) localization compared to untreated controls. In contrast, E1B was redistributed to the nucleus upon treatment (Fig. 23B).

Taken together, mutations within the NES of L4-100K lead to a strong effect on virus growth [183], probably due to defects in viral late protein synthesis as well as Hexon metabolism. However, since immunofluorescence analysis showed no effect on the subcellular localization of L4-100K after mutation of its NES, or treatment of the cells with LMB, the nuclear export of the protein via its NES or the CRM1 pathway might not be required for efficient viral replication.

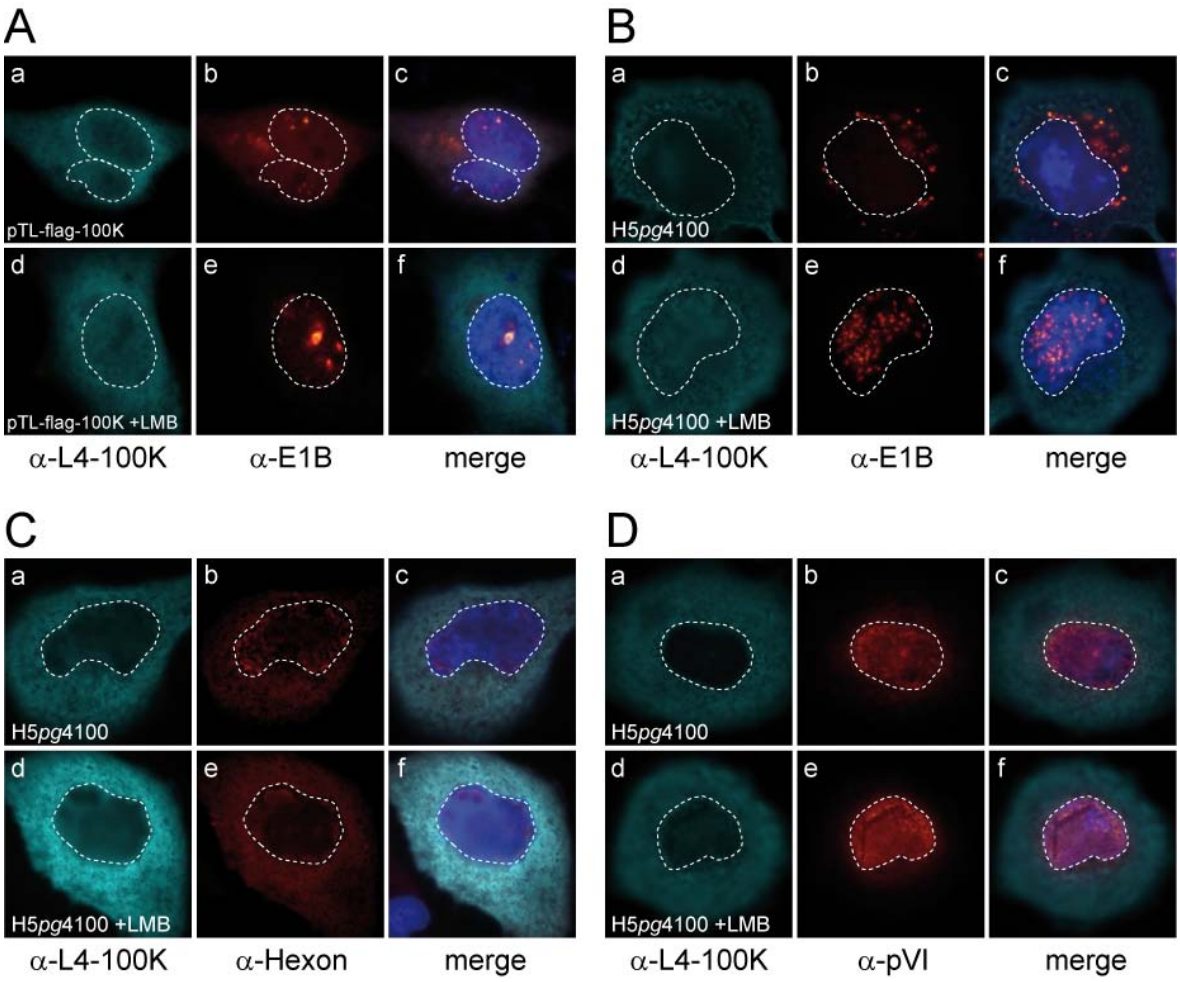

Figure 23: Effect of leptomycin B treatment on intracellular localization of L4-100K, E1B-55K, Hexon and pVI. (A) Intracellular localization of L4-100K and E1B-55K in plasmid transfected and LMB treated cells. A549 cells were transfected with pTL-flag-100K and pcDNA3-E1B-55K, either untreated or treated with 20 nM LMB from 24 to 48 h post transfection, and fixed 48 h post transfection. Cells were labeled with anti-L4-100K rat mab 6B10 (α-L4-100K) and anti-E1B mouse mab 2A6 (α-E1B), plus Cy5 and Cy3 conjugated secondary antibodies, respectively. Representative anti-L4-100K (green; a and d) and anti-E1B (red; b and e) staining patterns are shown. Overlays of DAPI staining (blue) with the green and red images are shown in panels c and f (merge). (B, C, D) Intracellular localization of L4-100K and E1B-55K (B)/Hexon (C)/pVI (D) in wt-infected and LMB treated cells. A549 cells were infected with wt virus at a multiplicity of 10 ffu per cell, either untreated or treated with 20 nM LMB from 24 to 36 h p.i. and fixed at 36 h p.i. Cells were double-labeled with anti-L4-100K rat mab 6B10 (α-L4-100K) and anti-E1B mouse mab 2A6 (B; α-E1B), anti-Hexon rabbit polyclonal serum Ad5 Hexon (C; α-Hexon) or anti-protein VI rabbit mab pVI (D; α-pVI), plus Cy5 and Cy3 conjugated secondary antibodies, respectively. Representative anti-L4-100K (green; a and d) and anti-E1B, Hexon or pVI (red; b and e) staining patterns are shown. Overlays of the green and red images are shown in panels c and f (merge). Nuclei visualized using DAPI are indicated by a dotted line in all panels.

5.4 Inhibition of CRM1-dependent transport prohibits efficient adenoviral replication

This work examined the role of CRM1-dependent transport of four adenoviral proteins, E1A, E1B-55K, E4orf6, and L4-100K, that are known to localize in both the cytoplasm and nucleus at different times of the viral life cycle. However, NESs of E1A, E1B-55K, and E4orf6 that contribute to nucleocytoplasmic shuttling activity have no effect on the efficiency of adenoviral replication. In contrast, mutation of the L4-100K-NES led to a shuttling-independent defect in progeny virus production, since subcellular distribution of the protein was unaffected by the mutation or leptomycin B treatment (Fig. 20, 22 and 23) [68, 183].

Early adenoviral proteins either interact with CRM1 [164] or their subcellular localization is sensitive to inhibition of CRM1 [175, 185]. Interestingly, the structural protein pVI exhibits nucleocytoplasmic shuttling activity, apparently playing an important role in the late phase of infection [337]. Together with L4-100K, the structural protein pVI is described to function in the encapsidation process of the virus, mediating Hexon trimerization, and import into the nucleus, and capsid assembly [55, 56, 149, 337]. To fulfill the role in Hexon trimer nuclear import, pVI contains a nuclear export and localization signal at its C-terminus. Proteolytic cleavage of the protein´s C-terminus transforms the function of pVI into an exclusively structural role in virus assembly [337].

During early stages of adenovirus infection, nuclear targeting of protein pVII and viral DNA into the nucleus is directed by a cellular import mechanism that requires binding of viral particles to the nucleoporin CAN/Nup214 at the nuclear pore complex (NPC) [135, 214, 316]. Interestingly, leptomycin B, a specific inhibitor of CRM1, blocks dissociation of incoming viral particles from microtubules and inhibits their binding to the NPC, suggesting that either CRM1 or CRM1-dependent export is required for the viral genome to reach the nucleus [307].

Thus, multiple CRM1-dependent transport processes may support adenoviral replication; however, previous analyses showed no restrictive effect of CRM1 inhibition on viral late gene expression under the tested conditions [51, 105, 264]. To address the role of CRM1 in viral mRNA export, Bridge and co-workers used the CRM1 inhibitor LMB, which associates covalently with cysteine 528 in the NES binding region of CRM1, irreversibly blocking its interaction with NES containing proteins [108]. Functional inhibition of CRM1 by LMB had only a minor effect on viral late protein synthesis (an indirect measurement of viral late mRNA export), leading to the conclusion that LMB treatment during the late phase of adenoviral

replication does not abrogate viral late mRNA accumulation in the cytoplasm [51, 264].

These findings were supported by a different experimental setup, where a specific peptide inhibitor of CRM1 was used to make direct measurements of viral late mRNA export. Although shuttling of E1B-55K was drastically reduced, viral late mRNA transport was unaffected [105]. Our own studies, using E1B-55K and E4orf6 NES virus mutants, confirmed that stimulation of viral late mRNA transport by these two proteins does not require CRM1-dependent nuclear export (Fig. 14) [175, 288]. Rather the use of leptomycin B or the E1B-55K/E4orf6 NES virus mutant revealed that the NESs present in E1B-55K and E4orf6 are differentially required for export of p53 and Mre11, two important cellular targets of the adenovirus-infected cell-specific E3 ubiquitin ligase. This indicates that although dispensable for viral late mRNA export, CRM1 is required for other activities that depend on E1B-55K/E4orf6 shuttling (Fig. 15-18) [288].

However, adenoviruses are obviously exploiting the functions of CRM1 as an export receptor. Thus it is necessary to test this issue under various conditions in order to more closely examine a possible role of CRM1 in adenoviral replication.

5.4.1 Generation of an inducible cell line expressing CANc, an inhibitor of CRM1-mediated transport

To address the role of CRM1-directed nucleocytoplasmic shuttling in adenoviral replication, experiments were designed to analyze the inhibition of this transport pathway at different stages of the viral life cycle. Therefore, a system was developed that exploits the modular nature of the nucleoporin 214, also known as CAN. The C-terminus of CAN (CANc) includes aa residues 1,864 to 2,090 of this nucleoporin and contains the FG (phenylalanine, glycine) repeats that associate with CRM1 during its translocation through the nuclear pore complex (NPC) (reviewed in reference 155). While treatment with leptomycin B (LMB) blocks CRM1 binding to proteins containing a leucine-rich NES [108], overexpression of CANc leads to dominant-negative inhibition of CRM1-dependent nuclear export by selectively binding to CRM1 and thus preventing its association with the NPC [29, 109, 167, 354]. In contrast to CRM1, TAP does not interact with the C-terminus of CAN, hence TAP-dependent export, predominantly bulk cellular mRNA transport, is unaffected [29, 334].

The function of CRM1 at different steps of viral replication and clearly defined times post infection was studied by generating a tetracycline inducible cell line expressing the C-terminus of CAN (CANc). The CANc coding sequence with an

adjacent hemagglutinin (HA)-tag (CANc-HA) [291], was inserted in a plasmid harboring a tetracycline inducible Tet-On promoter (pLKO.DCMV.TetO) [93, 94] (4.4.5.1 and 4.4.6). To produce tetracycline inducible cells, the non-transformed human hepatocyte HA-TetR cell line, which already expresses the EGFPnlsTetR protein [93, 94], was transfected with the constructed pLKO.DCMV.TetO.CANc-HA plasmid and positive cells were selected for puromycin resistance. The generated cell line was used in subsequent experiments and is referred to as HA-CANc cells. To evaluate expression of CANc, a clone derived from the constructed cell line was analyzed at various times after tetracycline induction. Clearly detectable levels of CANc were obtained at 3 h post tetracycline treatment (Fig. 24A). CANc levels increased to a stable steady-state concentration between 4.5 and 6 h post treatment (Fig. 24A). Significantly, steady-state concentrations of CRM1 were not affected upon CANc expression (Fig. 24A), suggesting that neither expression nor stability of CRM1 are influenced by CANc expression. In addition, expression of CANc did not result in reduced cell viability, since viable cells after 24 or 48 hours post induction decreased only slightly; an effect comparable to 24 hours of LMB treatment in either HeLa or A549 cells (Fig. 24B).

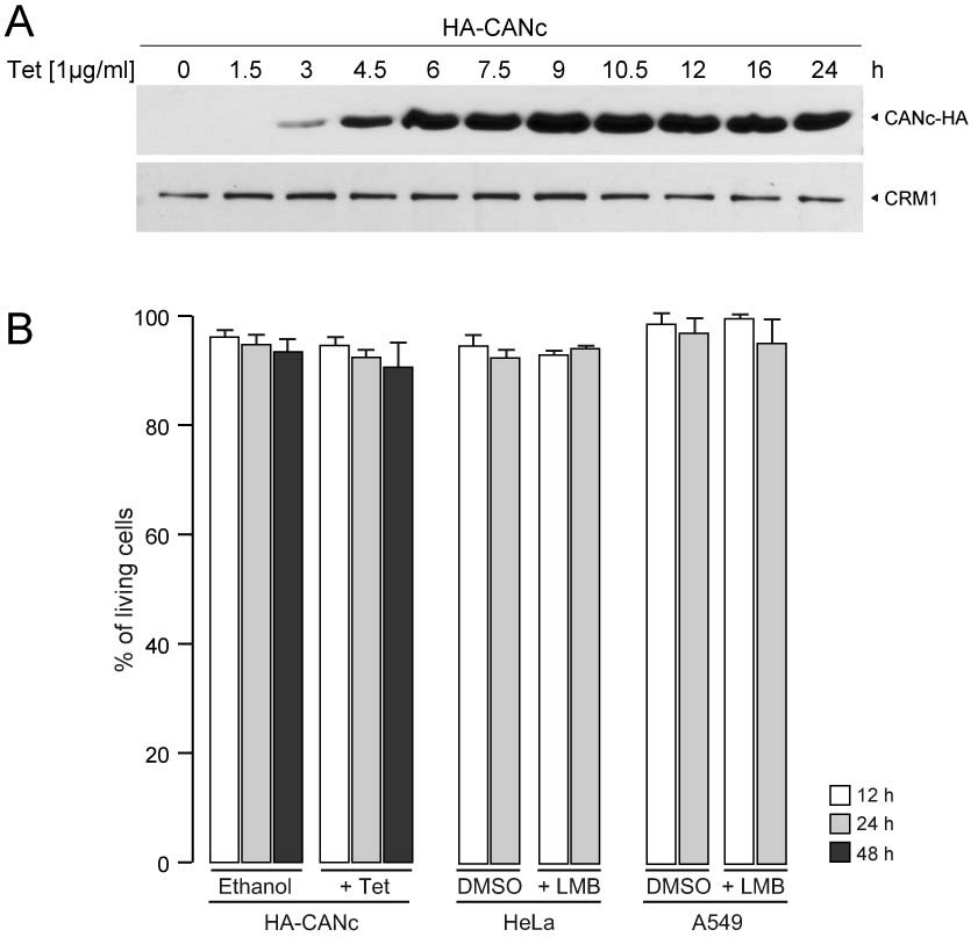

Figure 24: Induction of HA-CANc by tetracycline and the effect of CRM1 inhibition on cell viability. (A) Tetracycline inducible accumulation of HA-CANc. HA-CANc cells were cultivated in the presence of 1 µg/ml tetracycline, harvested after indicated times post treatment and total cell extracts were prepared. Proteins (15 µg) from each time point were separated by 10% SDS-PAGE and subjected to immunoblotting using anti-HA rat mab 3F10 or anti-CRM1 mouse mab Exportin-1 (CRM1). (B) Effect of CRM1 inhibition on the viability of the cells used in this study. HA-CANc cells were treated with 1 µg/ml tetracycline. HeLa and A549 cells were treated with 20 nM leptomycin B. Living cells counted at the indicated times post treatment using cell staining with trypan blue are presented as percentage of total cells. The results represent the average of three independent experiments. Error bars indicate the standard deviation of the mean.

To test the effect of CANc expression on CRM1-dependent nucleocytoplasmic transport, two approaches were used. First HA-CANc cells were transfected with p3_eGFP-CD83complete, a plasmid expressing the mRNA of CD83 linked downstream of a green fluorescent protein (GFP) coding sequence. Since CD83 mRNA depends on CRM1 for export to the cytoplasm [256], the CD83-GFP mRNA was used as a reporter for functional CRM1 transport, visualized by accumulation of GFP. As expected, inhibition of CRM1 transport by CANc resulted in less GFP expression than the untreated control (Fig. 25A), indicating that CANc expression inhibited CRM1-dependent CD83 mRNA export. The constitutively expressed Tet repressor (EGFPnlsTetR) served as a loading control.

A second approach tested the impact of CANc on CRM1-dependent transport of a NES-containing protein by immunofluorescence analysis. As discussed in 5.2 and 5.4, adenoviral E1B-55K contains a CRM1-dependent NES [81, 185]; therefore induced expression of CANc should result in inhibition of E1B-55K export to the cytoplasm. HA-CANc cells were infected with Ad5 wt H5*pg*4100 at a multiplicity of 20 ffu per cell, and tetracycline or ethanol were added 23 h post infection (h p.i.), followed by methanol fixation at 33 h p.i. These times post infection correspond to a period after late phase transition has occurred in adenovirus-infected HepaRG cells, when E1B-55K displays the typical nuclear and cytoplasmic distribution described previously [126, 199, 246]. As expected, induction of CANc led to complete redistribution of the E1B-55K protein to the nuclear compartment (Fig. 25B).

Taken together, these results indicate that, while CANc neither affected expression or stability of CRM1, nor impaired cell viability, its expression abrogated export of *bona fide* CRM1-dependent mRNA and protein cargo. Due to inducible expression of CANc (Fig. 24), the role of CRM1 in early and late phenotypes could be analyzed in detail.

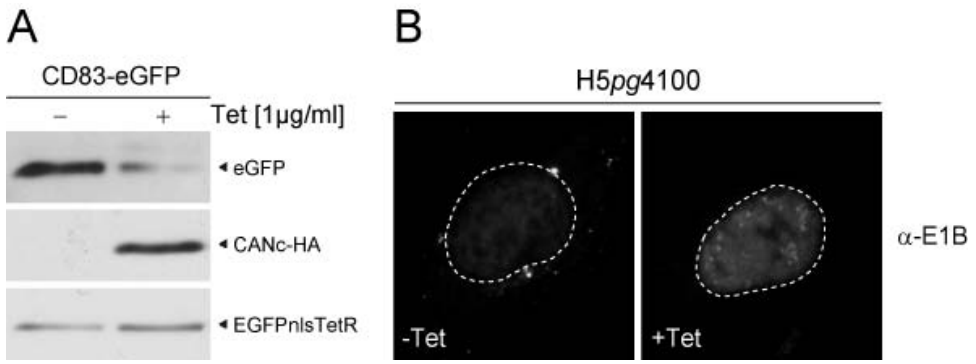

Figure 25: Inhibition of CRM1 mediated transport. (A) 3 x 10^6 HA-CANc cells were transfected with p3_eGFP-CD83complete and treated with either 1 µg/ml tetracycline to induce CANc expression or absolute ethanol as a negative control (- Tet) 4 h post transfection. Cells were harvested 24 h post transfection and total cell extracts were prepared. Proteins (50 µg samples for GFP; 10 µg samples for HA) were separated by 10% SDS-PAGE and subjected to immunoblotting using anti-GFP rabbit polyclonal antibody GFP (FL) and anti-HA rat mab 3F10. (B) HA-CANc cells were infected with Ad5 wild type virus at a multiplicity of 20 ffu per cell, treated with either 1 µg/ml tetracycline (+ Tet) to induce CANc expression or absolute ethanol (- Tet) as a negative control 23 h p.i. and fixed 33 h p.i. Cells were labeled *in situ* with anti-E1B-55K mouse mab 2A6 (α-E1B) and Texas red conjugated secondary antibody. Representative anti-E1B staining patterns are shown. In both panels, nuclei are indicated by a dotted line.

5.4.2 CRM1 activity is required during early and late phase for efficient viral progeny production

Initially, the role of CRM1 was examined at different times post infection, and after viral entry into the nucleus, to evaluate the impact of CRM1 inhibition on virus growth using the inducible expression of CANc in the HepaRG cells. These cells were recently shown to be susceptible and permissive for Ad5 infection, and they fully support the adenoviral life cycle, although with delayed kinetics similar to that observed with other normal human cells [290]. It has been shown that pVII and viral DNA reach the nucleus within the first 60 min post infection [219]. Therefore, to avoid inhibiting viral entry into the nucleus, these experiments were designed to start inhibiting CRM1 activity 2 to 3 h p.i., a post induction time when CANc is first detected. After addition of 1 µg/ml tetracycline to the medium at 0, 5 or 12 h p.i., Ad5-infected HA-CANc cells were harvested 48 h p.i. In parallel, virus growth was also measured in HeLa cells in the presence of LMB. To compensate for the lag in initial CANc expression after induction (Fig. 24A), addition of 20 nM LMB to Ad5-infected HeLa cells was deferred to 2, 8 and 16 h p.i. and cells were harvested 26 h p.i. Virus progeny production was affected in a gradual manner in both HA-CANc (Fig. 26A) and LMB-treated HeLa cells (Fig. 26B). Although total numbers of progeny virions differed between the two cell types, the effect on virus

production displayed a similar pattern. Inhibition of CRM1 either through CANc (HepaRG cells) or LMB (HeLa cells) induced 20 to over 200-fold (Fig. 26A and B) reductions in virus yield when CRM1 was inhibited at times after infection that correspond to the early phase of viral replication (2 to 8 h p.i.). Intriguingly, approximately 30% (HA-CANc) to 60% (HeLa) reductions in virus production were observed when CRM1 was inhibited at later time points, indicating that active shuttling of CRM1 is required during both early and late times post infection.

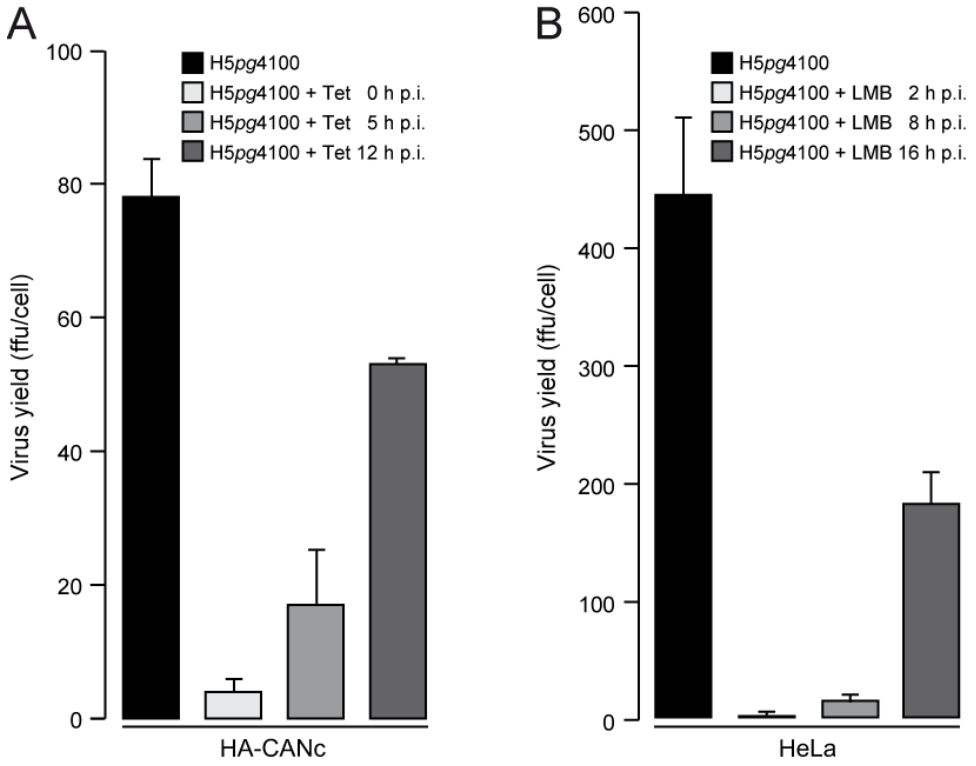

Figure 26: Effect of CRM1 inhibition on virus growth. (A) HA-CANc cells were infected with Ad5 wild type virus at a multiplicity of 50 ffu per cell. Tetracycline was added to the culture medium at different time points after infection as indicated. Viral particles were harvested 48 h p.i. and virus yield was determined by quantitative E2A-72K immunofluorescence staining on HEK-293 cells. The results represent the averages from three independent experiments. Error bars indicate the standard deviation of the mean. (B) HeLa cells were infected with Ad5 wild type at a multiplicity of 10 ffu per cell. Leptomycin B was added to the culture medium at different times after infection as indicated. Viral particles were harvested 26 h p.i. and virus yield was determined by quantitative E2A-72K immunofluorescence staining on HEK-293 cells. The results represent the averages from six independent experiments. Error bars indicate the standard deviation of the mean.

5.4.3 Inhibition of CRM1-mediated transport reduces synthesis of early and late adenoviral proteins

To determine the contribution of CRM1 shuttling on early and late protein synthesis, levels of adenoviral early (E1A, E1B-55K, E2A) as well as late proteins (Hexon, Fiber, L4-100K) were determined in wt-infected cells in the

presence/absence of CANc (Fig. 27A) or LMB (Fig. 27B). After addition of 1 µg/ml tetracycline to the medium at 0, 5, 12 h p.i., Ad5-infected HA-CANc cells were harvested 26 or 48 h p.i., and early and late protein levels were compared to untreated and/or uninfected controls (Fig. 27A). As before, in the case of wt-infected HeLa cells, 20 nM LMB was added at 2, 8 and 16 h p.i. to compensate for delayed CANc expression and cells were harvested at 26 h p.i. (Fig. 27B).

Consistent with previous reports on the effect of LMB in infected HeLa cells during the early phase of adenoviral replication [51, 264], levels of the late proteins Hexon, Fiber and L4-100K were severely reduced when CRM1 shuttling was blocked in the first hours after Ad infection, either with CANc or LMB (Fig. 27). Similar to the relative impact of CANc and LMB on virus growth, this effect was more pronounced in cells treated with LMB than CANc. However, since cell viability was not significantly compromised by either LMB or CANc (Fig. 24), it is possible that differences might result from the mode of action of the inhibitors. Overexpression of C-terminal CAN residues thus leads to a competitive inhibition of CRM1-dependent nuclear export by selectively binding to CRM1 and thereby preventing its association with the NPC [29, 354]. In contrast, LMB associates covalently with the NES binding region of CRM1 and irreversibly blocks CRM1-mediated export [108, 115] thereby providing an explanation for the stronger phenotype upon LMB treatment (Fig. 27B).

CRM1 inhibition by CANc expression at times corresponding to the early phase led to clear reductions of both early and late proteins (Fig. 27A, lane 4, 5). In contrast, inhibition at approximately 15 h p.i. displayed no effect on early proteins. However, late protein levels were still clearly reduced, where this effect was most noticeable with Fiber protein (Fig. 27A, lane 6). LMB induced severe reductions in both early and late proteins when cells were treated at the earliest time after infection (2 h p.i.; Fig. 27B, lane 4). Inhibition of CRM1 close to the onset of viral DNA replication (at approximately 8 h p.i.) led to drastically reduced early and late protein levels (Fig. 27B, lane 6). During CANc expression, this effect was less dramatic than in cells treated at 2 h p.i. (Fig. 27A, compare lane 4 and 5). At a later time post infection (16 h p.i.), inhibition of CRM1 shuttling displayed no effect on further accumulation of early proteins, since E1A, E1B-55K and E2A reached levels comparable to untreated cells (Fig. 27B, compare lane 7 and 8). In contrast to the effect on early proteins, viral late protein levels were clearly reduced (Fig. 27B, lane 8), and as with CANc expressing cells, this effect was most significant for levels of the Fiber protein.

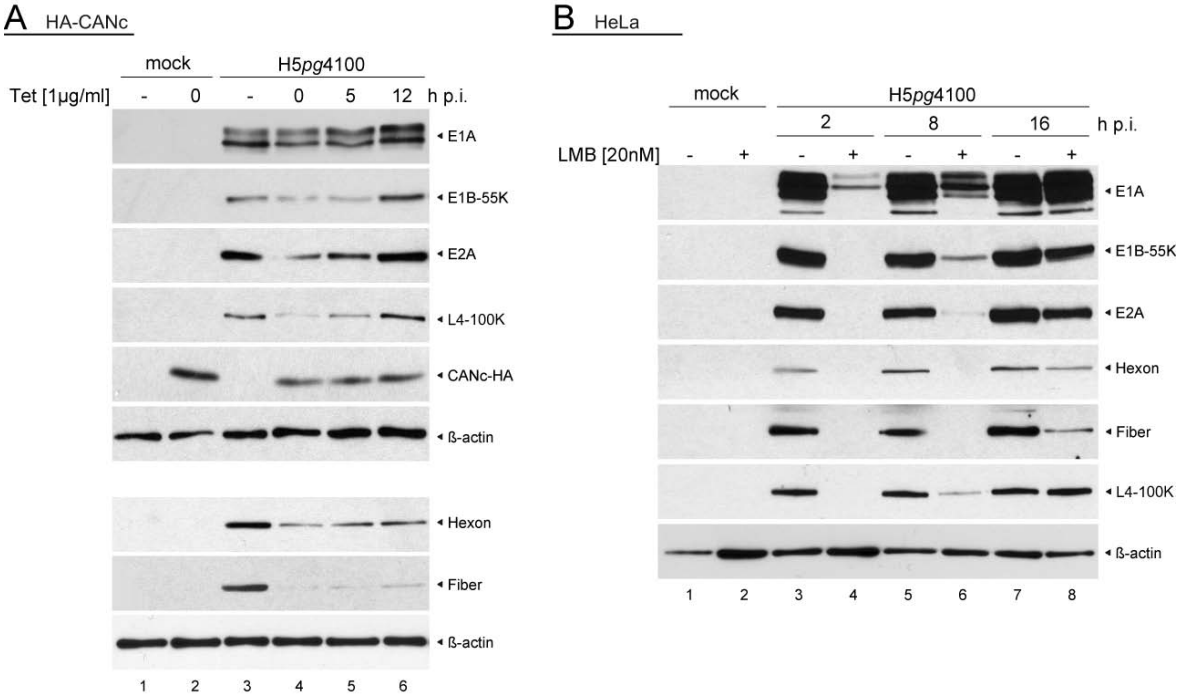

Figure 27: Effect of CRM1 inhibition on viral protein synthesis. Steady-state levels of viral early and late proteins in wild type-infected cells treated with different CRM1 inhibitors. (A) HA-CANc cells were infected with wild type virus at a multiplicity of 50 ffu per cell. Cells were treated with 1 µg tetracycline (lanes 2 and 4 – 6) or absolute ethanol (-; lanes 1 and 3) per ml at the indicated times p.i. and total cell extracts were prepared 26 h p.i. or for Hexon and Fiber proteins 48 h p.i. Proteins (15 µg samples for E1A, Hexon, Fiber, L4-100K and ß-actin; 25 µg samples for E1B-55K; 20 µg samples for E2A; 50 µg samples for CANc-HA) were separated by 10% SDS-PAGE followed by immunoblotting with anti-E1A mouse mab M73, anti-E1B-55K mouse mab 2A6, anti-E2A mouse mab B6-8, anti-L4-100K rat mab 6B10, anti-HA rat mab 3F10 or anti-ß-actin mouse mab AC-15. (B) HeLa cells were infected with Ad5 wild type virus at a multiplicity of 10 ffu per cell. Cells were treated with 20 nM LMB (+; lanes 2, 4, 6 and 8) or DMSO (-; lanes 1, 3, 5 and 7) at the indicated times p.i. and total cell extracts were prepared 26 h p.i. Proteins (10 µg samples for E1A, E2A, Hexon, Fiber and ß-actin; 40 µg samples for E1B-55K) were separated by 12% SDS-PAGE followed by immunoblotting with anti-E1A mouse mab M73, anti-E1B-55K mouse mab 2A6, anti-E2A mouse mab B6-8, anti-Ad5 rabbit polyclonal serum L133 or anti-ß-actin mouse mab AC-15.

For more detailed analysis of the impact of CRM1-inhibition on viral protein accumulation, it was necessary to test whether LMB inhibition of CRM1-dependent transport was functional in these experiments, and to examine whether protein synthesis of both early and late adenoviral proteins was inhibited or only delayed by LMB treatment. Therefore, H1299 cells were infected with H5*pg*4100 6 h post transfection of the p3_eGFP-CD83complete reporter construct for functional CRM1 transport. As before, 20 nM LMB was added 2, 8 and 16 h p.i. to the culture medium and cells were harvested at 26 h p.i. To determine whether inhibition of CRM1-dependent transport abrogates or only delays viral protein synthesis, cell

lysates were also collected at the time point of LMB addition (Fig. 28A, lanes 3, 6 and 9).

LMB inhibited expression of GFP (Fig. 28A, lane 2, 4 and 7) compared to untreated controls (Fig. 28A, lane 1, 5 and 8), demonstrating that functional inhibition of CRM1-dependent transport was functional. Similar GFP levels observed between LMB-treated and untreated cells at 16 h p.i. (Fig. 28A, lanes 10 and 11) likely result from translation of cytoplasmic eGFP-CD83 mRNA that had accumulated before addition of the export inhibitor. Inhibition of CRM1 during the first hours after Ad infection (2 h p.i.) led to severely reduced accumulation of adenoviral early and late proteins compared to the untreated control. Interestingly, treatment at the earliest time point (2 h p.i.) did not block synthesis of E1A, since low but readily detectable levels of the protein accumulated under these conditions (Fig. 28A, compare lanes 3-5).

A similar effect was observed on the accumulation of other early proteins (E1B-55K, E2A) when cells were treated at a time around which DNA replication starts (8 h p.i.) [247]. In contrast, accumulation of late proteins (L4 100K, II, III and V) was still severely reduced when LMB was used at this time post infection (Fig. 28A, lanes 6-8). Addition of LMB at 16 h p.i. did not prevent further accumulation of early proteins, since E1A, E1B-55K and E2A reached similar levels in the LMB-treated and -untreated controls (Fig. 28A, lanes 9-11). However, a clear effect on the expression levels of late adenoviral proteins was observed (Fig. 28A).

Taken together, these results indicate that inhibition of CRM1-dependent transport during the early phase leads to a reduced expression of both early and late proteins. By contrast, its inhibition during the late phase exclusively impacts accumulation of late proteins.

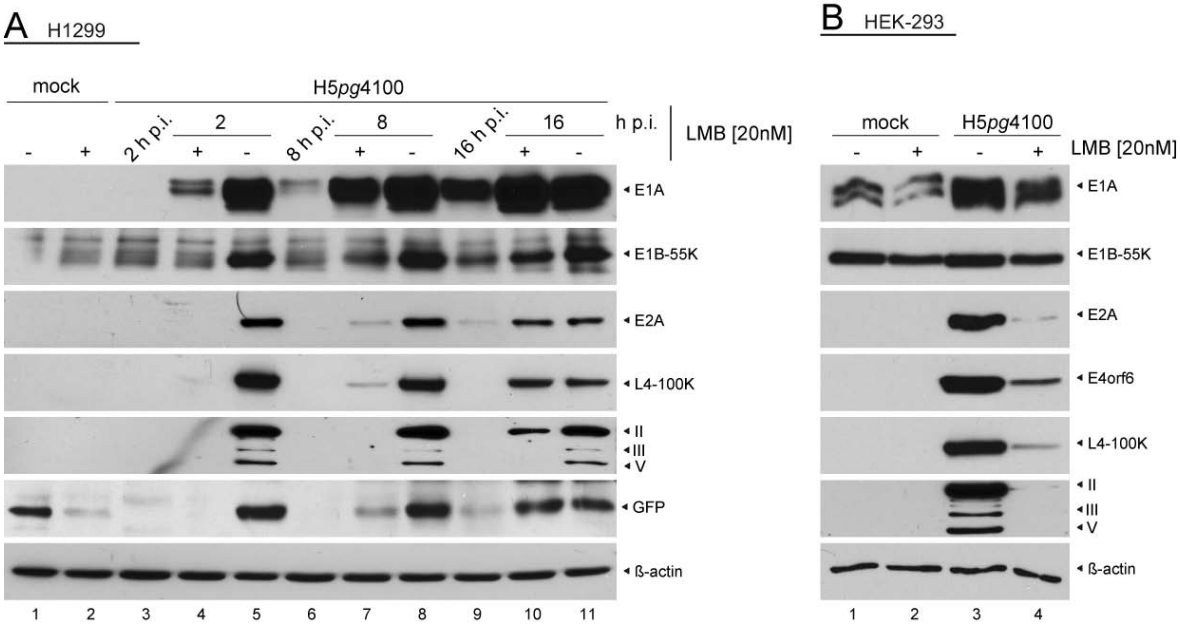

Figure 28: Effect of CRM1 inhibition on viral protein accumulation. (A) H1299 cells were transfected with p3_eGFP-CD83complete and infected with Ad5 wild type virus at a multiplicity of 10 ffu per cell 6 h post transfection. Cells were either harvested before treatment at indicated times p.i. (lanes 3, 6 and 9) or treated with 20 nM LMB (+; lanes 2, 4, 7 and 10) or DMSO (-; lanes 1, 5, 8 and 11) at the indicated times p.i. and total cell extracts were prepared 26 h p.i. Proteins (10 µg samples for E1A, E2A, L4-100K, capsid proteins and ß-actin; 25 µg samples for E1B-55K) were separated by 10% SDS-PAGE followed by immunoblotting with anti-E1A mouse mab M73, anti-E1B-55K mouse mab 2A6, anti-E2A mouse mab B6-8, anti-Ad5 rabbit polyclonal serum L133, anti-L4-100K rat mab 6B10, anti-GFP rabbit polyclonal antibody GFP (FL) or anti-ß-actin mouse mab AC-15. Bands corresponding to viral late proteins Hexon (II), Penton (III) and Fiber (V) are indicated on the right. (B) HEK-293 cells were infected with Ad5 wild type virus at a multiplicity of 10 ffu per cell. Cells were treated with 20 nM LMB (+; 2 and 4) or DMSO (-; 1 and 3) 2 h p.i. and total cell extracts were prepared 26 h p.i. Proteins (10 µg samples for E1A, E2A, L4-100K, capsid proteins and ß-actin; 25 µg samples for E1B-55K and E4orf6) were separated by 10% SDS-PAGE followed by immunoblotting with anti-E1A mouse mab M73, anti-E1B-55K mouse mab 2A6, anti-E2A mouse mab B6-8, anti-E4orf6 mouse mab RSA3, anti-Ad5 rabbit polyclonal serum L133, anti-L4-100K rat mab 6B10 or anti-ß-actin mouse mab AC-15. Bands corresponding to viral late proteins Hexon (II), Penton (III) and Fiber (V) are indicated on the right.

Given that E1A activates transcription of early genes and consequently stimulates the major late transcription unit (MLTU) [23, 230], it should also be examined whether reduced expression of early and late proteins was due to decreased E1A protein levels due to CRM1 inhibition. Therefore, HEK-293 cells (which constitutively express the Ad5 E1 region [133]) were mock-infected or infected with the wild type virus H5*pg*4100, treated with 20 nM LMB or DMSO 2 h p.i. and harvested 26 h p.i. Interestingly, accumulation of early (E2A, E4orf6) and late

proteins (L4-100K, II, III, V) was significantly reduced in LMB-treated HEK-293 cells, despite expression of high levels of E1A and E1B-55K (Fig. 28B).

These results suggest that expression of adenoviral early genes is independent of CRM1 and might occur on a post transcriptional level, leading to reduced early adenoviral protein concentrations even though early gene transcription can be induced by E1A. Nevertheless, the contribution of CRM1 to the accumulation of late proteins required further analysis, since activation of the MLTU does not exclusively depend on E1A but also on the transition to the late phase of infection and expression of other adenoviral late proteins [226, 230, 315].

5.4.4 Inhibition of CRM1 affects viral early mRNA transport

To further address the role of CRM1-directed nucleocytoplasmic shuttling in early adenoviral gene expression, accumulation of viral early mRNA was determined in the absence and presence of leptomycin B. For this purpose A549 cells were infected with H5*pg*4100, 20 nM LMB was added starting from 4 h p.i. and total viral mRNA was prepared 12 h after infection. Levels of E1A, E2A, E1B-55K, and E4orf6 adenoviral transcripts upon LMB treatment, were compared to the untreated control (Fig. 29B).

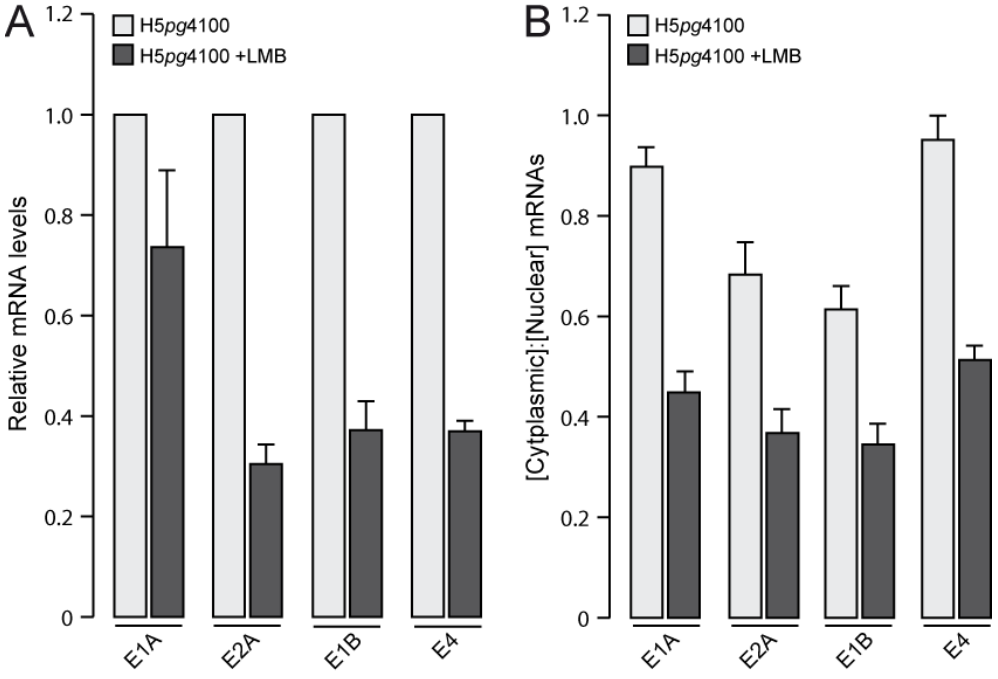

Figure 29: Effect of CRM1 inhibition on accumulation and nuclear export efficiency of viral early mRNAs. (A) A549 cells were infected with Ad5 wild type virus at a multiplicity of 10 ffu per cell. LMB was added to the culture medium 4 h p.i. Steady-state concentrations of both RNAs were determined by real-time PCR at 12 h after infection. Total E1A, E2A, E1B-55K, and E4orf6 values were corrected using GAPDH as an internal control and are expressed relative to the wild type value. (B) A549 cells were infected with Ad5 wild type virus at a multiplicity of 10 ffu per cell. LMB was

added to the culture medium 4 h p.i. Steady-state concentrations of both RNAs in the cytoplasm and nucleus were determined by real-time PCR at 12 h after infection. Raw numbers were corrected using GAPDH as an internal control and used to calculate the ratios of cytoplasmic to nuclear E1A, E2A, E1B-55K, and E4orf6 mRNAs. All the results and standard errors shown are presented for six independent experiments, each performed in duplicate.

Interestingly, the amount of E1A mRNA in LMB treated cells was reduced by about 25% compared to the untreated control. While total E1A mRNA was not severely affected, CRM1 inhibition led to a 60 to 70% decrease of E2A, E1B-55K, and E4orf6 mRNA levels (Fig. 29A). Such an effect could result from the observed reduction in E1A protein levels due to inhibition of CRM1-dependent shuttling (Fig. 27 and 28). The degree of E1A protein reduction did not seem to correlate with the decreased accumulation of the E1A transcript, providing further evidence that transport via CRM1 supports expression of adenoviral early genes, particularly post transcriptionally.

Since no detailed analyses of adenoviral early transcript export have been reported, we decided to examine whether CRM1-dependent transport is required to support export of E1A, E2A, E1B-55K, and E4orf6 mRNA. A549 cells were infected with the wild type virus (H5*pg*4100), 20 nM LMB was added to the culture medium 4 h p.i., and nuclear as well as cytoplasmic mRNA were prepared after cell fractionation 12 h p.i.

The calculated ratio of cytoplasmic to nuclear E1A mRNA was approximately 1:1 (Fig. 29B). This is in perfect agreement with previous studies on the subcellular distribution of newly synthesized E1A mRNA in HEK-293 cells, which revealed the same nuclear to cytoplasmic ratio at both 8 and 14 h p.i. [344]. Notably, treatment of cells with LMB resulted in decreased cytoplasmic accumulation of the E1A transcript to about 50% (Fig. 29B), providing an explanation for lower accumulating E1A protein levels following inhibition of CRM1 transport (Fig. 27 and 28). Surprisingly, blockage of CRM1-dependent shuttling also induced similar reductions in the export efficiency of E2A, E1B-55K, and E4orf6 mRNA compared to untreated controls (Fig. 29B).

Taken together, these data suggest that observed virus replication defects upon CRM1 inhibition during the early phase of the viral life cycle (Fig. 26–28) are a direct consequence of reduced cytoplasmic accumulation of viral early mRNAs (Fig. 29B). Thus, in addition to its role in disassembly of the adenoviral virion and nuclear export of various adenoviral proteins, these experiments provide evidence for a novel function of CRM1 as an export receptor for adenoviral early transcripts.

5.4.5 Inhibition of CRM1-dependent transport blocks adenoviral genome replication and IVa2 expression

CRM1-dependent export of adenoviral early mRNAs could explain defects observed in adenoviral replication upon CRM1 inhibition in the early phase of infection. Nevertheless, CANc induction and LMB treatment of cells at intermediate and late times of infection resulted in reduced virus growth (Fig. 26) and decreased accumulation of viral early and late proteins (Fig. 27 and 28), indicating that CRM1 supports additional steps in the replication cycle of the virus. Viral DNA replication is initiated around 8 h p.i. [247], and is known to be required for transcriptional activation of viral late genes [230]. Therefore, the next question was whether CRM1 inhibition affects the efficiency of viral DNA replication.

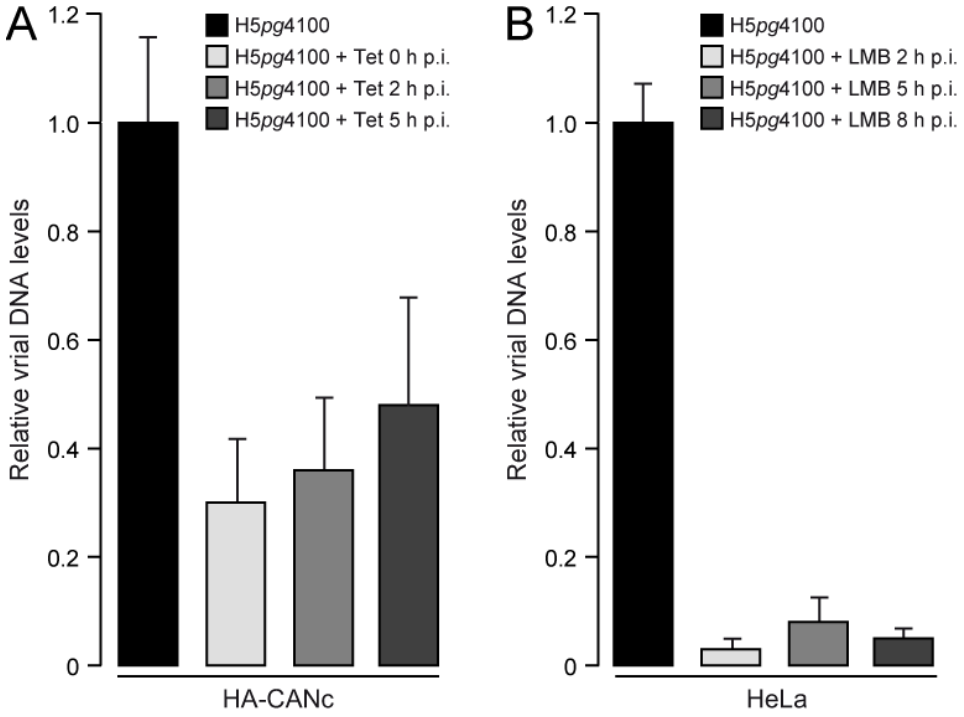

Figure 30: Effect of CRM1 inhibition on viral DNA accumulation. (A) HA-CANc cells were infected with Ad5 wild type virus at a multiplicity of 50 ffu per cell. Cells were treated with 1 µg of tetracycline per ml at the indicated times p.i., total nuclear DNA was isolated 26 h after infection and subjected to quantitative PCR. PCR products were analyzed and quantified using the ChemiDoc system and GeneTools software (Syngene). (B) HeLa cells were infected with Ad5 wild type virus at a multiplicity of 10 ffu per cell. Cells were treated with 20 nM leptomycin B at the indicated times p.i., total nuclear DNA was isolated 26 h after infection and subjected to quantitative PCR. PCR products were analyzed and quantified using the ChemiDoc system and GeneTools software (Syngene). All the results and standard deviations shown represent the averages from three independent experiments.

These experiments were designed to inhibit CRM1-dependent transport during both the early phase of infection and onset of viral DNA replication 8 h p.i. [247],

in other words after the appearance of early mRNAs in the cytoplasm [25]. HA-CANc cells were infected with the wild type virus and CANc expression was induced by addition of 1 µg/ml tetracycline to the medium 0, 2 or 5 h p.i. At 26 h p.i., viral DNA was isolated and subjected to quantitative PCR as described in Materials and Methods (4.4.5.3). In parallel, viral DNA synthesis was measured in LMB-treated HeLa cells. As in previous experiments, addition of 20 nM LMB to Ad5-infected HeLa cells was deferred to 2, 5 and 8 h p.i. to compensate for the lag in initial CANc expression after induction (Fig. 24A), and viral DNA was isolated at 26 h p.i.

Interestingly, inhibition of CRM1-dependent transport in both cell types resulted in reduced accumulation of viral DNA. In HA-CANc cells viral DNA synthesis was affected in a gradual manner, with reductions of 70% to 50% (Fig. 30A). A similar, although more severe effect was induced by LMB treatment of HeLa cells at all times post infection, leading to reduction of more than 90% compared to the untreated controls (Fig. 30B). These results indicate that accumulation of viral DNA is not only affected by CRM1 inhibition during the early phase, which could be explained by reduced export efficiency of viral early mRNAs and hence reduced expression of viral early proteins. Indeed, this can also occur at the onset of viral DNA synthesis, after early mRNAs are exported to the cytoplasm [25, 247].

Initiation of viral DNA replication activates several steps during the late phase of adenoviral life cycle. This includes expression of the intermediate IVa2 protein, hence inducing increased activation of the major late transcription unit (MLTU) [248, 249, 315]. Since lower IVa2 expression could provide a direct link between observed reductions in DNA replication and viral late protein accumulation, observed upon blocking CRM1 transport, IVa2 mRNA levels and export efficiency were measured. After adding 20 nM LMB to wild type-infected A549 cells at 10 h p.i., total as well as nuclear and cytoplasmic mRNA were prepared 18 h p.i.

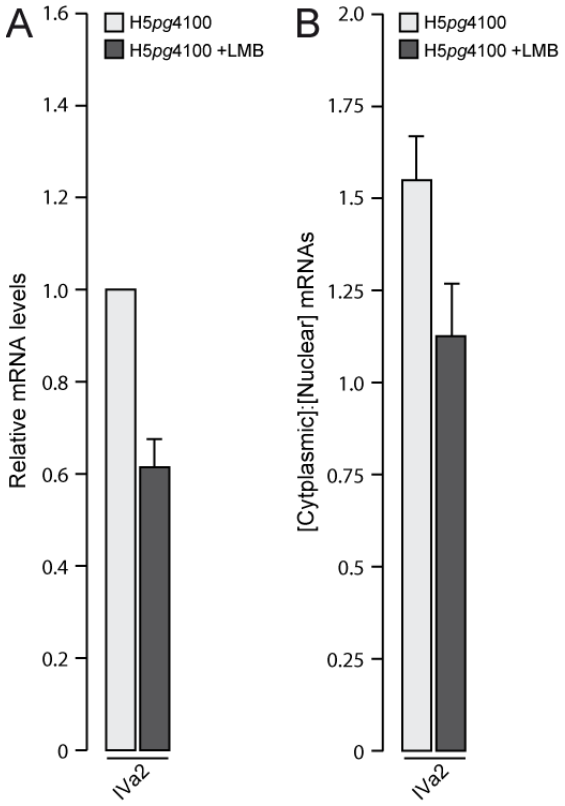

Figure 31: Effect of CRM1 inhibition on accumulation and nuclear export efficiency of IVa2 mRNA. (A) A549 cells were infected with Ad5 wild type virus at a multiplicity of 10 ffu per cell. LMB was added to the culture medium 10 h p.i. Steady-state concentrations of RNA were determined by real-time PCR 18 h after infection. Total IVa2 values were corrected using GAPDH as an internal control and are expressed relative to the wild type value. (B) A549 cells were infected with Ad5 wild type virus at a multiplicity of 10 ffu per cell. LMB was added to the culture medium 10 h p.i. Steady-state concentrations of RNA in the cytoplasm and nucleus were determined by real-time PCR 18 h after infection. Raw numbers were corrected using GAPDH as an internal control and used to calculate the ratios of cytoplasmic to nuclear IVa2 mRNA. All the results and standard errors shown are presented for three independent experiments, each performed in duplicate.

Interestingly, both the total amount of IVa2 transcript (Fig. 31A) and its cytoplasmic accumulation (Fig. 31B) were reduced by about 30 to 40% in LMB-treated cells compared to the controls. While reduced accumulation of viral DNA provides an explanation for the decrease in IVa2 expression levels, the affected export efficiency of the mRNA could result from low levels of the E1B-55K protein, which is known to support the export of IVa2 mRNA [196]. Another possibility might be the requirement of CRM1-dependent shuttling for transport of IVa2 transcripts to the cytoplasm as observed for viral early mRNAs (Fig. 29B).

5.4.6 Inhibition of CRM1 does not block viral late mRNA export, but impairs viral late mRNA accumulation

It was shown recently that selective export of viral late mRNA requires the cellular transport receptor TAP [345] and is independent of CRM1 (Fig. 14) [105, 175, 288]. Since the role of CRM1-mediated export on viral late mRNA transport has only been determined in human tumor cell lines, inducible CANc expression in non-transformed human hepatocytes was used to examine whether the observed effect on late gene expression is a consequence of defective viral late mRNA metabolism.

Since expression of CANc can be induced at any time after infection, HA-CANc cells were used to evaluate the effect of inhibiting CRM1 during the late phase. Initially, the nucleocytoplasmic distribution of L4 and L5 mRNA was analyzed by subcellular fractionation and quantification of the corresponding mRNA using quantitative PCR (4.5). Ad5 wt H5*pg*4100-infected HA-CANc cells were treated with either 1 µg/ml tetracycline or absolute ethanol as a control (Fig. 32A), from 21 to 48 h p.i., a time after infection when CRM1 inhibition should not perturb early protein synthesis (Fig. 27A).

In these experiments, E1B-55K (H5*pm*4149) or E4orf6 (H5*pm*4154) negative viruses confirmed that these early proteins are required for efficient export of viral late mRNAs [11, 39, 140, 198, 254]. The absence of either E1B-55K or E4orf6 led to a 2.5 or 5-fold reduction in the ratio of cytoplasmic to nuclear L4 and L5 mRNA, respectively. In contrast, inhibition of CRM1 shuttling by CANc, had no influence on efficient export of either mRNA species (Fig. 32A).

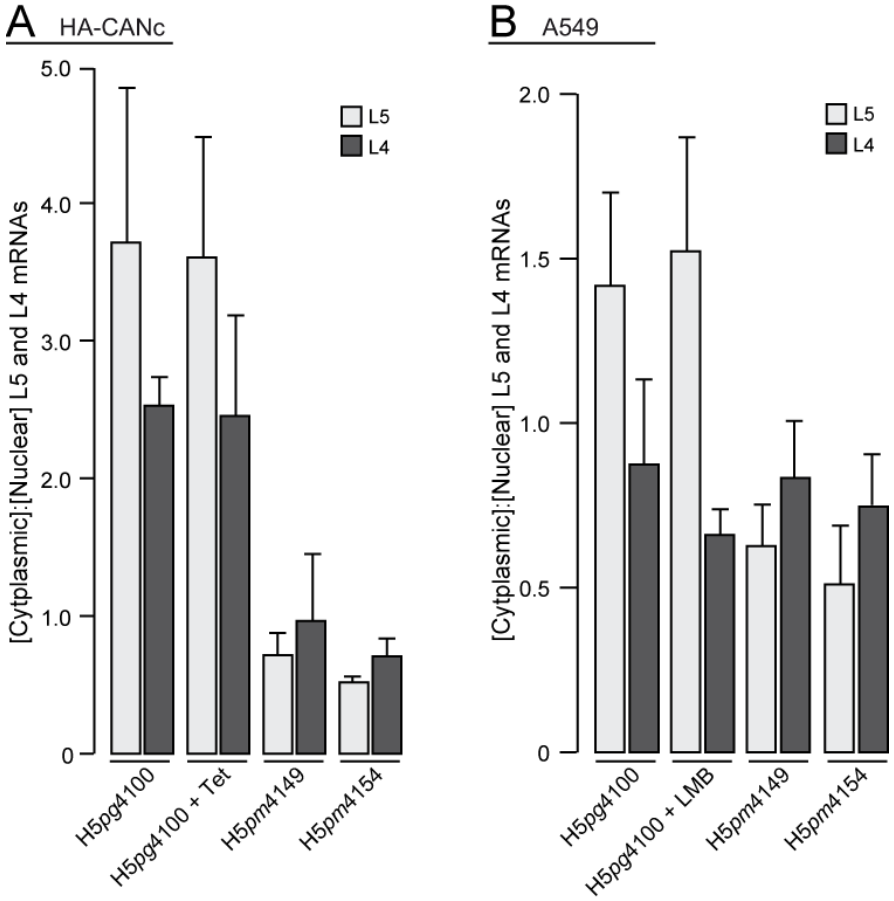

Figure 32: Effect of CRM1 inhibition on nuclear export efficiency of viral late mRNAs. (A) HA-CANc cells were infected with Ad5 wild type virus at a multiplicity of 20 ffu per cell. Tetracycline was added to the culture medium 21 h p.i. Steady-state concentrations of both RNAs in the cytoplasm and nucleus were determined by real-time PCR at 48 h after infection. Raw numbers were corrected using GAPDH as an internal control and used to calculate the ratios of cytoplasmic to nuclear L5/L4 mRNAs. (B) A549 cells were infected with Ad5 wild type virus at a multiplicity of 10 ffu per cell. LMB was added to the culture medium 24 h p.i. Steady-state concentrations of both RNAs in the cytoplasm and nucleus were determined by real-time PCR at 48 h after infection. Raw numbers were corrected using GAPDH as an internal control and used to calculate the ratios of cytoplasmic to nuclear L5/L4 mRNAs. All the results and standard deviations shown are presented for at least three independent experiments, each performed in duplicate.

The effect of CRM1 inhibition by LMB on viral late mRNA export has only been measured indirectly by examining the efficiency of viral late protein synthesis [51, 264]; therefore, in addition to inhibition by CANc, the viral late mRNA export in the presence of LMB was measured (Fig. 32B). H5*pg*4100-infected A549 cells were treated with 20 nM LMB from 24 to 48 h p.i. In agreement with previous reports [51, 264], cell viability was not reduced after the 24 h period of LMB treatment (Fig. 24B). Nuclear and cytoplasmic RNA were extracted and measured 48 h p.i., as described in Materials and Methods (4.5). Consistent with previous

experiments, LMB treatment compared to tetracycline addition reflected the delayed expression of CANc (Fig. 24A). Consistent with results obtained with non-transformed human hepatocytes (Fig. 32A) and with the reported effect of a peptide inhibitor that specifically blocks CRM1 binding to NES-containing proteins [105], export of L4 or L5 mRNAs was not affected by CRM1 inhibition after LMB treatment. As expected, infection of A549 cells with H5*pm*4149 or H5*pm*4154 resulted in approximately 2-fold lower export of L5 mRNA than the wild type virus (Fig. 32B). Nevertheless, no effect could be detected for the export efficiency of L4 mRNA under these conditions.

Collectively, these results are in agreement with previous reports (Fig. 14) [105, 175, 288], since inhibition of CRM1 during the late phase of viral replication did not interfere with viral late mRNA export. However, this extends these observations to non-transformed human hepatocytes.

Sincce viral late mRNA is not exported by CRM1, but inhibition of this export pathway during the late phase reduced DNA and viral progeny production (Fig. 26 and 27), as well as late protein levels (Fig. 27 and 28), the effect of blocking CRM1 on total viral late mRNA levels was examined by treating HA-CANc cells with tetracycline from 21 to 48 h p.i. and A549 cells with LMB from 24 to 48 h p.i. Infection of either HA-CANc or A549 cells with mutant viruses H5*pm*4149 and H5*pm*4154 confirmed that E1B-55K or E4orf6 are required for efficient synthesis of viral late mRNA [11, 140, 240]. Production of L4 and L5 mRNA was reduced by 2 to more than 10-fold (Fig. 33), and in agreement with previous observations this effect was more severe in the absence of E1B-55K than E4orf6 (Fig. 14) [11, 140, 240, 288].

Unexpectedly, although viral late mRNA export was not affected by inhibition of CRM1-dependent shuttling (Fig. 32), accumulation of total L4 and L5 mRNA in both HA-CANc and LMB-treated A549 cells decreased to approximately 50% compared to the untreated controls (Fig. 33), indicating that inhibition of CRM1 affects the efficient expression of viral late mRNA. Since it has been established that active genome replication, viral DNA itself, and IVa2 all stimulate viral late gene expression from the MLTU [230], the reduced levels of viral late transcripts (Fig. 32) could be a consequence of defects in viral DNA synthesis (Fig. 30) and IVa2 expression (Fig. 31).

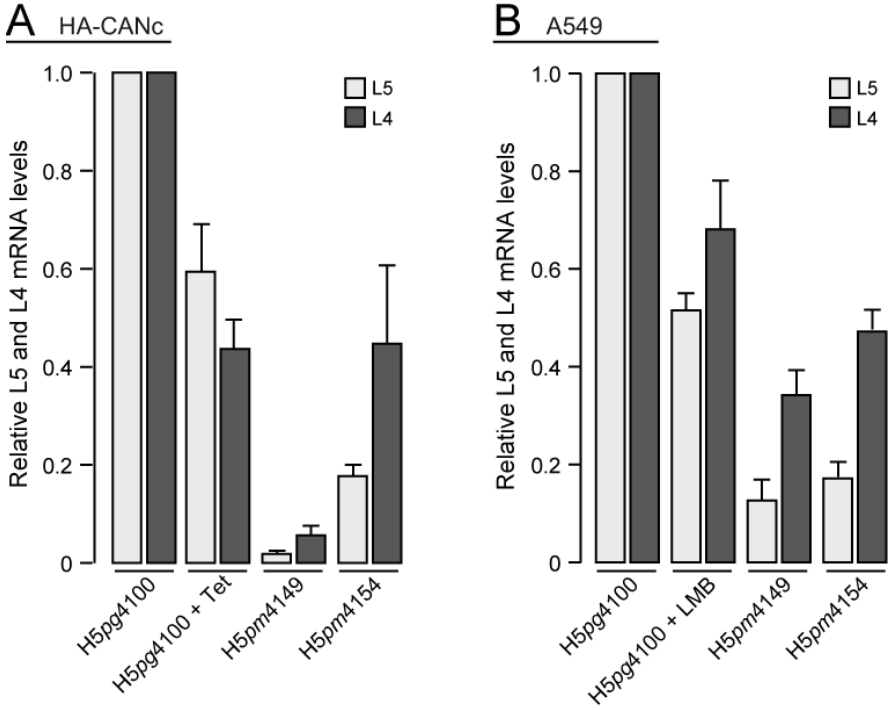

Figure 33: Effect of CRM1 inhibition on total amounts of viral late mRNAs L5 and L4. (A) HA-CANc cells were infected with Ad5 wild type virus at a multiplicity of 20 ffu per cell. Tetracycline was added to the culture medium 21 h p.i. Steady-state concentrations of both RNAs were determined by real-time PCR at 48 h p.i. Total L5 and L4 values were corrected using GAPDH as an internal control and are expressed relative to the wild type value. (B) A549 cells were infected with Ad5 wild type virus at a multiplicity of 10 ffu per cell. LMB was added to the culture medium 24 h p.i. Steady-state concentrations of both RNAs were determined by real-time PCR at 48 h p.i. Total L5 and L4 values were corrected using GAPDH as an internal control and are expressed relative to the wild type value. All the results and standard deviations shown are presented for at least three independent experiments, each performed in duplicate.

5.5 Proteomic approach to identify potential targets of the E3 ubiquitin ligase

Recently, a proteomic approach identified a new substrate of the E3 ubiquitin ligase formed by the early proteins E1B-55K and E4orf6. This approach used two-dimensional difference gel electrophoresis (2DE) and mass spectrometry (MS) to detect and identify cellular proteins whose amount decreased significantly in the presence of E1B-55K and E4orf6 [71, 72]. It has been established that preferential viral late mRNA transport mediated by E1B-55K and E4orf6 depends on the activity of the E3 ubiquitin ligase complex [28, 340]. However, so far no substrate of this complex could be linked to a cellular transport pathway. Subsequent, a similar proteomic approach was used to specifically search for a cellular target of the E3 ubiquitin ligase that is involved in a cellular transport

process. A two-step approach was used: First, cells were infected with the wild type or an E1B minus virus and the cellular lysates analyzed by differential 2DE to identify protein spots that differed in their expression levels. Second, the cellular proteome was marked by SILAC (stable isotope labeling with amino acids in cell culture). Therefore, cells cultured in the presence of heavily labeled lysine were infected with the E1B minus virus, while an unlabeled control was infected with the wild type virus. Subsequently, the protein lysates were pooled, separated on a single 2DE gel, and protein spots detected during the first approach were analyzed by MS to identify potential target proteins of the E1B-55K/E4orf6 complex.

5.5.1 Analysis of protein spots showing higher abundance in E1B minus virus-infected cells

A549 cells were infected with the wild type virus (H5*pg*4100) or the E1B minus mutant (H5*pm*4149). Cell lysates were collected 48 h post infection when degradation of cellular substrates of the E3 ubiquitin ligase is evident [262, 304]. Proteins from each sample were separated by 2DE (4.7.2), and subsequently gels were analyzed using the Delta2D software (Decodon). The overlay of both gels allowed the detection of spots with significantly elevated amounts of protein in either wt or E1B minus virus-infected cell lysates (Fig. 34). Blue dots mark protein spots with three-times or more intensity in wt-infected compared to E1B minus virus-infected cell lysates, while spots marked in pink indicate elevated protein levels in the E1B minus mutant cell lysate (Delta2D, Decodon). Additionally, red circles indicate significantly more intense spots in E1B minus than wt virus-infected cell extracts that were detected manually. The spots marked with orange squares are control spots showing the same protein levels on both 2DE gels (Fig. 34).

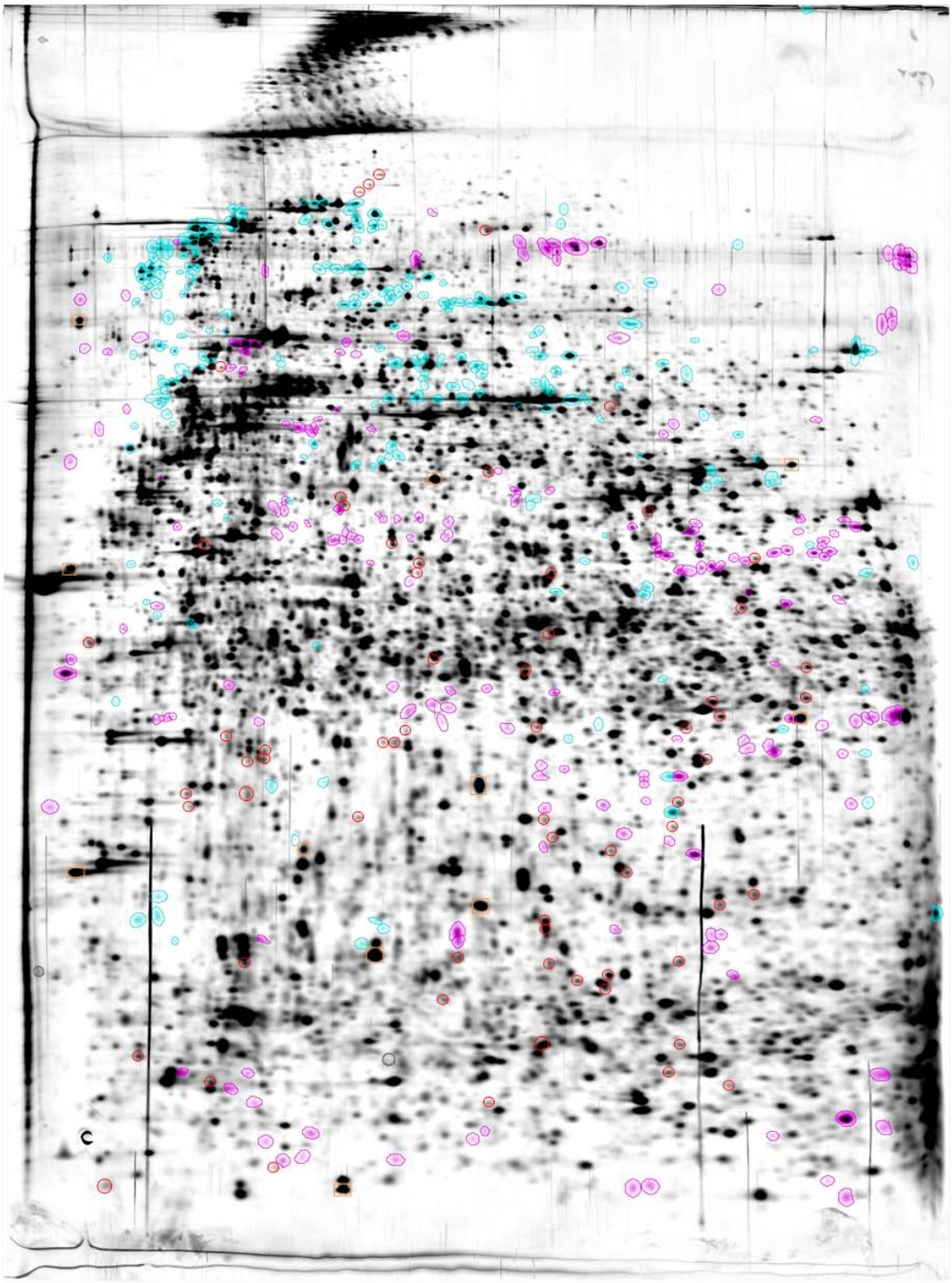

Figure 34: Analysis of differential 2DE gels. A549 cells were infected with wt and E1B minus virus at a multiplicity of 20 ffu per cell. Cells were harvested 48 h p.i. and total cell extracts were prepared. Proteins (60 µg samples) from each sample were separated by 2D gel electrophoresis and protein spots on both 2DE gels were visualized with silver staining. The software Delta2D was used to generate an overlay of the two 2DE gels to detect protein spots that are at least three-times more intense in wt compared to E1B minus virus cell extracts (blue circles) or *vice versa* (pink circles). Red circles indicate more intense spots in E1B minus compared to wt virus cell extracts detected manually, and orange squares indicate control spots showing the same intensities in wt and E1B minus virus.

5.5.2 Identification of possible cellular targets

To identify cellular substrates of the E3 ubiquitin ligase complex, protein spots with higher intensities on the 2DE gel of cell extracts from E1B minus virus infection (Fig. 34, pink and red circles) were tryptically digested and subsequently analyzed by mass spectrometry (MS). To strengthen identification of a possible cellular target, the ratio of protein levels between wt and E1B minus virus-infected cells was also determined. Quantification used the SILAC method, the *in vivo* metabolic incorporation of isotope-labeled amino acids into proteins (*Pierce*® *SILAC Protein Quantitation Kit*, Thermo Scientific): a cell population grown in medium containing unlabeled amino acids is compared to one grown in the presence of $^{13}C_6$-labeled amino acids.

After 100% label incorporation, confirmed via MS, heavily labeled cells were infected with the E1B minus mutant H5*pm*4149, while "light" cells were infected with the wild type virus (H5*pg*4100). Cell lysates from each sample were prepared at 48 h p.i. (4.7.2.1) and mixed with a mass ratio of 1:1. 120 µg of this protein mixture was separated by preparative 2DE, the gel was silver stained (4.7.2 and 4.7.3.2) and screened for interesting protein spots. Recovered spots that were less intense on the differential 2DE of wild type-infected cells (Fig. 34, pink and red circles) were marked in the 2DE of the SILAC labeled sample (Fig. 35, blue circles). Together with the indicated control spots (Fig. 35, orange circles), these samples were further analyzed. To verify our results 400 µg of an independently prepared sample were separated on a second 2DE gel.

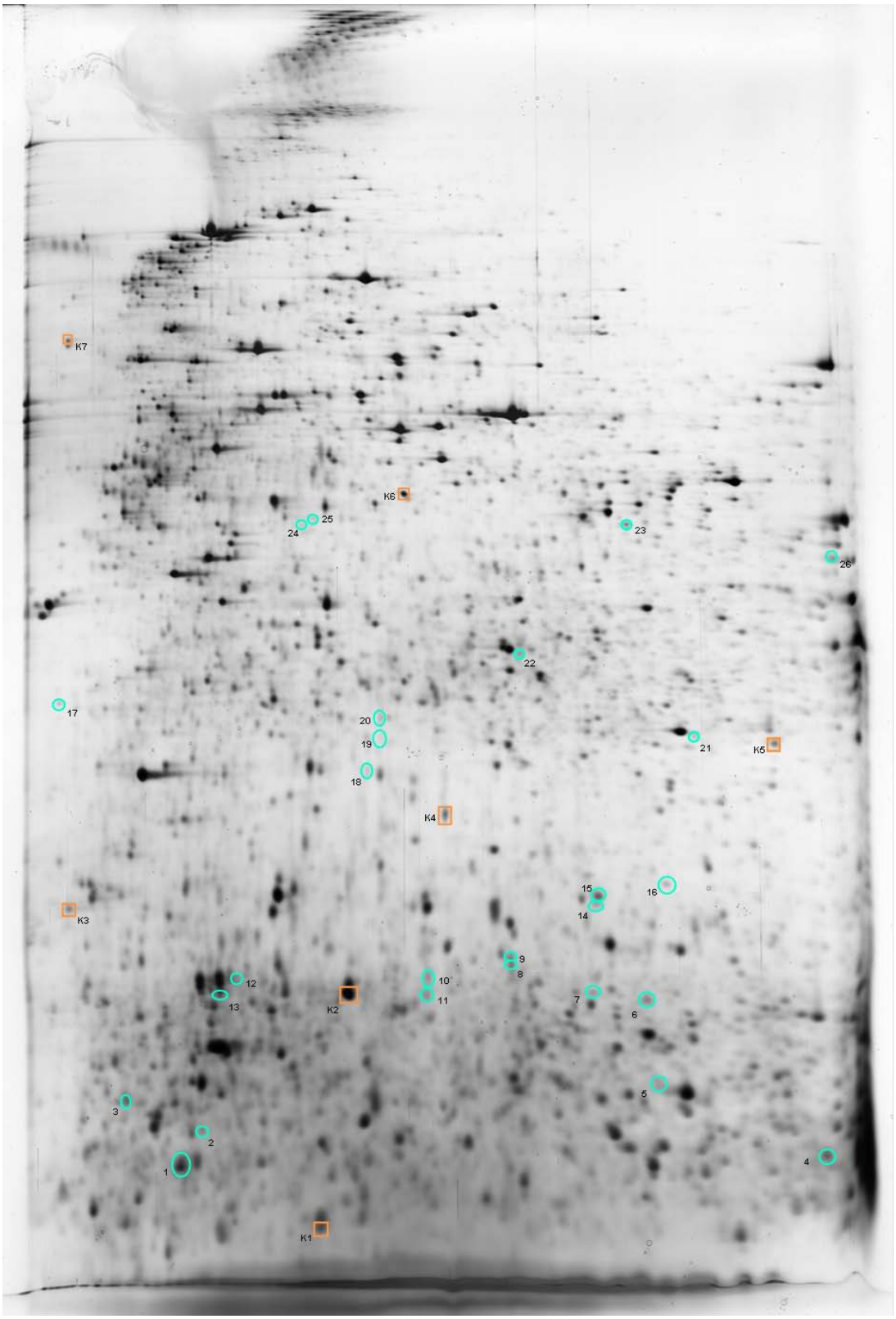

Figure 35: Preparative 2DE gel. A549 cells were infected with wt and E1B minus virus at a multiplicity of 20 ffu per cell. Cells were harvested 48 h p.i. and total cell extracts were prepared. Proteins from each probe were mixed, 120 µg of the mixture was separated by 2DE and protein spots were visualized with silver staining. After comparison of the gel with the one shown in Fig. 34, detectable protein spots (blue circles) were analyzed using tryptic in-gel digestion and mass spectrometric analysis. Results of the identified proteins are shown in Table 1.

Interesting protein spots were excised from the preparative 2DE gels and proteolitically digested with trypsin (4.7.4) cutting specifically behind lysine and arginine amino acids. Incorporation of one $^{13}C_6$ L-Lysine increases the mass of the labeled tryptic peptide by about 6 Da. Since peptides containing unlabeled and labeled amino acids differ only in their isotopic pattern, they are chemically identical. For this reason they show identical behaviour in both reversed phase separation and MS analysis. Peptides derived from both samples appear as two signals with a mass difference of 6 Da and can therefore be quantified by analyzing the ratio of their signal intensities.

The ratio of "heavy" ($^{13}C_6$-labeled peptide of E1B minus-infected cells) to "light" (unlabeled peptide of wt-infected cells) signal intensities were analyzed by MS (Table 1, heavy/light ratio). Possible targets of the E3 ubiquitin ligase complex are listed in Table 1 together with identified proteins of the control spots.

Table 1: Identification of proteins using the Mascot search database. The table lists the analyzed spots (spot; see also Fig. 35), the name of the identified proteins (protein; (2) indicates same spots analyzed on a second 2DE gel (120 µg)) including controls (C1-7), the Mascot score and ratio of signal intensity between analyzed $^{13}C_6$- (heavy; E1B minus virus) and non-labeled (light; Ad5 wt virus) peptides. Only identified proteins with a significant Mascot score of more than 67 are shown.

SPOT	PROTEIN	MASCOT-SCORE	HEAVY/LIGHT RATIO
1	Actin, cytoplasmic 1	76	
	Tubulin alpha-1A chain	75	
2	60 kDa heat shock protein, mitochondrial	96	
3	Actin, cytoplasmic 1	177	1.69
	Alpha-enolase (2)	254	1.65
4	40S ribosomal protein SA	143	
5	Retinal dehydrogenase 1	158	1.04
	Isocitrate dehydrogenase (NADP), mitochondrial	74	
6	T-complex protein 1 subunit eta	95	
7	Glucose-6-phosphate 1-dehydrogenase	139	
	Glyceraldehyde-3-phosphate dehydrogenase	81	
8	Alpha-enolase	100	1.52
	Glycerinaldehyde-3-phosphate dehydrogenase (2)	89	

9	Voltage-dependent a nion-selective channel p rotein 1	124	
10	60 kDa heat shock protein, mitochondrial	172	3.74
	Stomatin-like protein 2	96	
	60 kDa heat shock protein, mitochondrial (2)	99	
11	Calreticulin	103	1.19
12	Annexin A2	139	1.68
	Actin, cytoplasmic 1	138	
	Actin, cytoplasmic 1 (2)	74	
13	Actin, cytoplasmic 1	119	
	Leucine-rich PPR m otif-containing p rotein, mitochondrial	80	
14	UDP-glucose 6-dehydrogenase	167	1.43
	Cofilin-1 (2)	115	
15	Cofilin-1	219	
	Talin-1	92	
	UDP-glucose 6-dehydrogenase	88	1.67
	Cofilin-1 (2)	99	
16	Transketolase	68	2.51
17	Cleavage and polyadenylation specificity factor subunit 6	129	1.50
18	Annexin A1	104	
	Heat shock protein beta-1	73	1.48
19	Profilin-rich protein 4 (2)	98	
	Ig alpha-1 chain c region (2)	85	
20	Stress-70 protein, mitochondrial	132	
	Dynactin subunit 2	126	
21	Peroxiredoxin-1	86	
22	Phosphoglycerate mutase 1	178	
	Annexin A1	177	
	Cytochrome b-c1 complex subunit Rieske	164	
	Malate dehydrogenase	134	

	60 kDa heat shock protein, mitochondrial	101	1.87
23	Annexin A2	385	
	Annexin A2 (2)	200	
24	Protein disulfide-isomerase A6	77	
25	Splicing factor, arginine/serine-rich 1	158	
26	Heterogeneous nuclear ribonucleoprotein A3	75	
C1	Heat shock 70 kDa protein 1A/1B	228	0.86
	Heat shock 70 kDa protein 6	174	
	Heat shock 70 kDa protein 1A/1B (2)	145	1.02
C2	Peroxiredoxin-4	102	1.59
	Galectin-7 (2)	154	
C3	Aldo-keto reductase family 1 member C2	71	
C4	Aldo-keto reductase family 1 member C2	78	
C5	Pyruvate kinase isozymes M1/M2	166	
C6	Pyruvate kinase isozymes M1/M2	118	
	Pyruvate kinase isozymes M1/M2 (2)	237	
C7	Heat shock cognate 71 kDa protein	145	
	Heterogeneous nuclear ribonucleoproteins A2/B1	121	

These analyses led to the identification of 48 proteins with a significant Mascot score of more than 67. However, the heavy/light ratio could only be determined in 13 samples plus three of the controls. Since the two samples are mixed in a mass ratio of 1:1, the expected heavy/light ratio of a control is 1.0 (see C1 of the 120 µg gel in Table 1). Divergent values of control spots (see C1 and C2 of the 400 µg gel in Table 1) might indicate discrepancies in the preparation of the gel. The ratio of the control spots could be used to correct the determined values of the other samples. Since proteins show a Gaussian bell-shaped distribution in 2DE gels, the most abundant protein will cover spots of less abundant proteins. This led to the identification of more than one protein in a single spot, and perhaps not all of these proteins are reduced in wt-infected cells. Nevertheless, the analysis identified one promising candidate, the splicing factor SF2/ASF that is connected with the cellular TAP export pathway (Table 1, protein 25).

5.6 Adenoviruses use the TAP transport pathway

Recent studies provided the first evidence that adenoviruses access the TAP transport pathway to export late mRNA [345]. This pathway also mediates bulk cellular mRNA transport [158, 195, 266]. Therefore a strict interplay is essential between pre-mRNA splicing, including the DEAD-box helicase UAP56 involved in spliceosome assembly, and nuclear export by TAP. The splicing processes and the export receptor are linked by a number of different adaptor proteins [152, 206, 353]. One adaptor protein is Aly/REF, a member of the heterogeneous ribonucleoprotein (hnRNP) family and component of the exon junction complex (EJC) [193]. Previously, serine/arginine-rich (SR) proteins involved in constitutive and alternative mRNA splicing [114, 134, 318] as well as mRNA transport [153], were also identified as adaptors for TAP-dependent transport [152, 282].

Interestingly, data from our group also hint at a role for TAP-dependent transport during the adenoviral life cycle. Recently, we observed an interaction between E1B-55K and the adaptor protein Aly/REF and relocalization of the latter to nuclear structures resembling interchromatin granules (IG) [174]. Since a similar distribution pattern in adenoviral infection was described for other splicing factors [7, 8, 38, 42, 43, 119], the close proximity of IGs to viral transcription and replication centers (RC) might promote processing and export of viral mRNA. So far Aly/REF protein levels have only been investigated during the early phase of infection when they showed a slight accumulation [345]. In addition, the 2DE analysis identified SF2/ASF, a member of the serine/arginine rich splicing factor family, as a potential target of the E3 ubiquitin ligase complex (5.5).

To further analyze the role of Aly/REF and SF2/ASF during adenoviral replication and whether one of these proteins might contribute to the function of TAP in viral late mRNA export, the steady-state levels of both proteins were determined. A549 cells were infected with the wt (H5*pg*4100) as well as the E1B and E4orf6 null viruses (H5*pm*4149 and H5*pm*4154) and cell lysates were prepared at different time points post infection. Protein levels were determined for TAP (Fig. 36A), E1B-55K and E4orf6, as well as two well characterized targets of the E3 ubiquitin ligase complex, Mre11 and p53 (Fig. 36B) [261, 263, 304]. As expected, E1B-55K and E4orf6 accumulated in wild type-infected cells, whereas they were not expressed in either E1B or E4orf6 minus-infected cells. Due to the activity of the ligase complex, levels of Mre11 decreased, and p53 did not accumulate in wild type-infected cells in contrast to the mutant virus infections (Fig. 36B). Consistent with

a previous study, levels of the export receptor TAP were stable during the course of the replication cycle (Fig. 36) [345].

The 2DE analysis pointed to targeting of SF2/ASF for proteasomal degradation induced by the E1B-55K/E4orf6 complex; however, Western blot analysis showed no effect of an adenovirus infection on its steady-state concentrations (Fig. 36A). Possibly, as also observed by Branton and co-workers, only a modified sub-fraction of the protein is degraded, which can not be detected by normal Western blot analysis [71].

Surprisingly, infection of cells with the wt virus (H5*pg*4100) but not with the E1B (H5*pm*4149) and E4orf6 (H5*pm*4154) minus viruses reduced Aly/REF levels at 48 and 72 h p.i. In addition to the observed decrease of the 27 kDa band another band of approximately 18 kDa appeared in these samples (Fig. 36A). A band of the same size was also detected in a longer exposure of E4orf6 minus-infected cells (data not shown). The change in the Aly/REF expression pattern was confirmed by using a second Aly/REF antibody (data not shown). However, the slight increase of Aly/REF observed in the early phase of infection [345] could not be reproduced. This time course experiment and the immunoprecipitation analysis showing binding of E1B-55K to Aly/REF [174] indicate an E1B-55K and E4orf6-dependent alteration of the Aly/REF expression pattern that might involve activity of the E3 ubiquitin ligase complex.

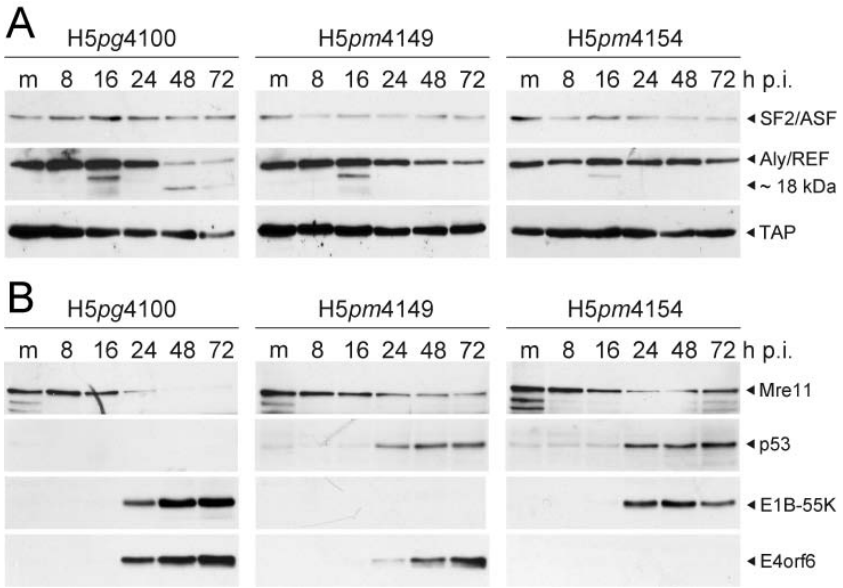

Figure 36: Steady-state concentrations of proteins participating in the TAP transport pathway. A549 cells were infected with wt and E1B/E4orf6 minus viruses at a multiplicity of 20 ffu per cell. Cells were harvested at the indicated times p.i. and whole-cell extracts were prepared. (A) Proteins (20 µg samples for SF2/ASF; 40 µg samples for Aly/REF and TAP) from each time point were separated by 10% SDS-PAGE and subjected to immunoblotting using anti-ASF/SF2 mouse mab SF2/ASF, anti-Aly/REF mouse mab 11G5 or anti-TAP goat polyclonal antibody R-20. (B) Proteins

(20 µg samples for Mre11 and p53; 25 µg samples for E1B-55K and E4orf6) from each time point were separated by 10% SDS-PAGE and subjected to immunoblotting using anti-Mre11 rabbit polyclonal antibody pNB-100-142, anti-p53 mouse mab DO-1, anti-E1B-55K mouse mab 2A6 or anti-E4orf6 rabbit polyclonal antibody 1807.

Although in human cells no second isoform of Aly/REF has been described as yet, an 18 kDa isoform of Aly/REF is known in mouse species [308]. Thus established rat cell lines of immortalized baby rat kidney (BRK) cells, which are more related to the mouse, were tested next. Western blot analysis were performed on protein lysates from spontaneously immortalized BRK cells (BRK1) and BRK cells expressing E1A and E1B-55K (AB120), or E1A, E1B-55K, and E4orf6 (ABS1) [86, 235]. As expected, E1B-55K was expressed in AB120 and ABS1 cells, whereas E4orf6 was only expressed in ABS1 cells. Intriguingly, the expression pattern of Aly/REF was similar to that observed in adenovirus-infected cells (Fig. 36). Although protein levels of Aly/REF were not reduced in AB120 or ABS1 compared to spontaneously immortalized BRK cell line, a band of approximately 18 kDa appeared in both these cell lines (Fig. 37), in other words irrespective of E4orf6 expression. In contrast to infected cells, where E4orf6 was required for efficient accumulation of the 18 kDa band (Fig. 36A), in BRK cells E4orf6 is apparently dispensable for this altered expression pattern (Fig. 37).

Both the expression pattern of Aly/REF during viral infection and the possible degradation of a modified sub-fraction of the SF2/ASF protein are due to the virus affecting the TAP transport pathway. Although the mechanism and function behind these alterations are as yet unclear, the data suggest that adenoviruses may manipulate the TAP transport pathway in favor of their replication.

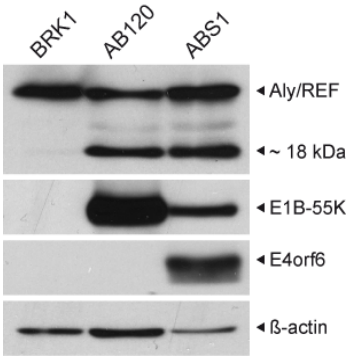

Figure 37: Steady-state concentrations of Aly/REF in BRK cells. BRK1, AB120 and ABS1 cells were harvested and whole cell extracts were prepared. Proteins (50 µg samples for Aly/REF; 25 µg samples for E1B-55K and E4orf6; 20 µg samples for ß-actin) from each cell line were separated by 10% SDS-PAGE and subjected to immunoblotting using anti-Aly/REF mouse mab 11G5, anti-E1B-55K mouse mab 2A6, anti-E4orf6 mouse mab RSA3 or anti-ß-actin mouse mab AC-15.

5.7 Interaction of E4orf6 with importin α

The intracellular localization of adenoviral proteins is critical for their role in the virus life cycle. Generally, the diameter of nuclear pore complexes allows passive diffusion of macromolecules with a molecular size of 20 to 60 kDa [130]. The karyopherin family, including both importins and exportins, mediates bidirectional trafficking of macromolecules in a RanGTP-dependent manner [111, 208]. One member of this family is the export receptor CRM1, which promotes translocation of its cargo proteins by interacting with their nuclear export signal (NES) [101, 108, 328]. Investigating NES sequences within different adenoviral proteins, their importance for the subcellular localization of the respective protein, as well as their contribution to the proteins´ function in viral replication was the main part of this work.

However, proteins that fulfill functions in the nucleus depend on translocation into the nuclear compartment. The nuclear import of proteins is achieved by the action of cellular import receptors that recognize their cargos through a nuclear localization signal (NLS). While in some import pathways importin ß or another family member alone is sufficient to transport the target protein, most cellular proteins use the classical nuclear import pathway. Here, importin α recognizes its cargos via the classical nuclear import signal (cNLS), linking it to importin ß [129, 192].

Although a NLS has been proposed for several adenoviral proteins, including E1A, E4orf6, L4-100K, and pVI [68, 127, 207, 337], the import pathway used has only been established for E1A: Importin α3 binds to E1A and mediates its translocation into the nucleus [180, 212].

5.7.1 E4orf6 interacts with importin α1, α5 and α7

The pathways involved in nuclear translocation of the adenoviral proteins E1B-55K, E4orf6 and L4-100K were characterized by testing binding of these proteins to alpha importins. Specifically, the interaction with ubiquitously expressed alpha importins was analyzed, omitting importin α6, whose mRNA has only been detected in the testis [166, 179, 181, 231, 317]. H1299 cells were transfected with flag-tagged importin α constructs, additionally infected with the wild type adenovirus H5*pg*4100 and co-immunoprecipitation (Co-IP) assays of E1B-55K, E4orf6, and L4-100K were performed using a flag specific antibody. First steady-state concentrations of alpha importins and adenoviral proteins were determined. Whereas the three adenoviral proteins were expressed at similar levels (Fig. 38)

and alpha importins accumulated to a similar extent in the first experiment (Fig. 38A), importin α7 levels were slightly reduced in the second assay (Fig. 38B, lane 7). However, no interaction between E1B-55K or L4-100K and any of the tested alpha importins could be detected in the Co-IP assay (Fig. 38B). Intriguingly, in contrast to E1B-55K and L4-100K, E4orf6 co-immunoprecipitated with three of the importins (importin α1, α5, and α7), the most significant interactions being with importin α5 and α7 (Fig. 38A).

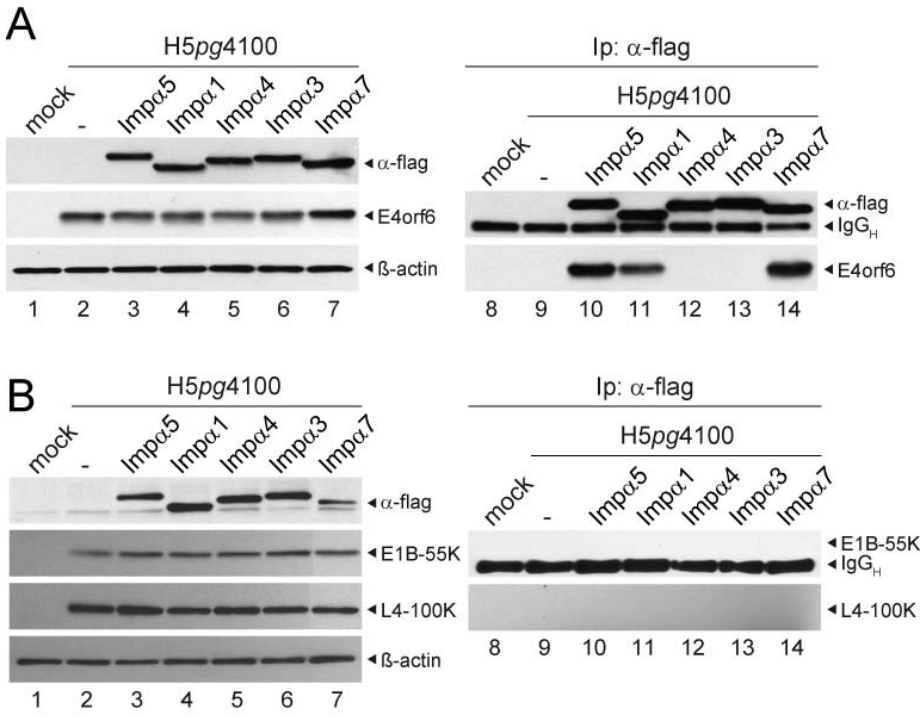

Figure 38: Interaction of Importins with E4orf6, E1B-55K, and L4-100K. Co-immunoprecipitation of E4orf6, E1B-55K or L4-100K with Importins. H1299 cells were transfected with pcDNA3 constructs encoding the flag-tagged importins, 6 h later cells were infected with a multiplicity of 30 (A) or 20 (B) ffu per cell and at 22 h p.i. whole-cell extracts were prepared. For analysis of steady-state concentrations proteins (50 µg samples for importins; 25 µg samples for E4orf6, E1B-55K, and L4-100K; 10 µg for ß-actin) were separated by 12% SDS-PAGE and subjected to immunoblotting using anti-flag mouse mab M2, anti-E4orf6 rabbit polyclonal antibody 1807, anti-E1B mouse mab 2A6, anti-L4-100K rat mab 6B10 or anti-ß-actin mouse mab AC-15. For coimmunoprecipitation with the flag-tagged importins 800 µg (A) or 1 mg samples (B) of protein were coimmunoprecipitated (Ip) with mab M2 (α-flag) and separated by 12% SDS-PAGE followed by immunoblotting with anti-flag mouse mab M2, anti-E4orf6 rabbit polyclonal antibody 1807, anti-E1B mouse mab 2A6 or anti-L4-100K rat mab 6B10.

5.7.2 Immunoprecipitation of the C-Terminus of E4orf6 by importin α1, α5 and α7

No interaction of E4orf6 with an importin or an importin-dependent translocation of the protein has been established in the past. So far only the signals contributing

to the protein´s nuclear localization were described: a putative nuclear localization signal at the N-terminus, between amino acids (aa) 13 and 31, and an amphipathic arginine rich α-helical nuclear retention signal at the C-terminus of E4orf6, between aa 239 and 253 [127, 244]. These signals are believed to be responsible for the nuclear targeting of E4orf6; however, no importin supporting this translocation has been identified. To investigate whether the binding region of importins and the NLS of E4orf6 overlap, Co-IPs were performed with E4orf6 deletion constructs. H1299 cells were co transfected with HA-tagged E4orf6 deletion constructs plus the flag-tagged importins shown to coimmunoprecipitate the E4orf6 protein (Fig. 38).

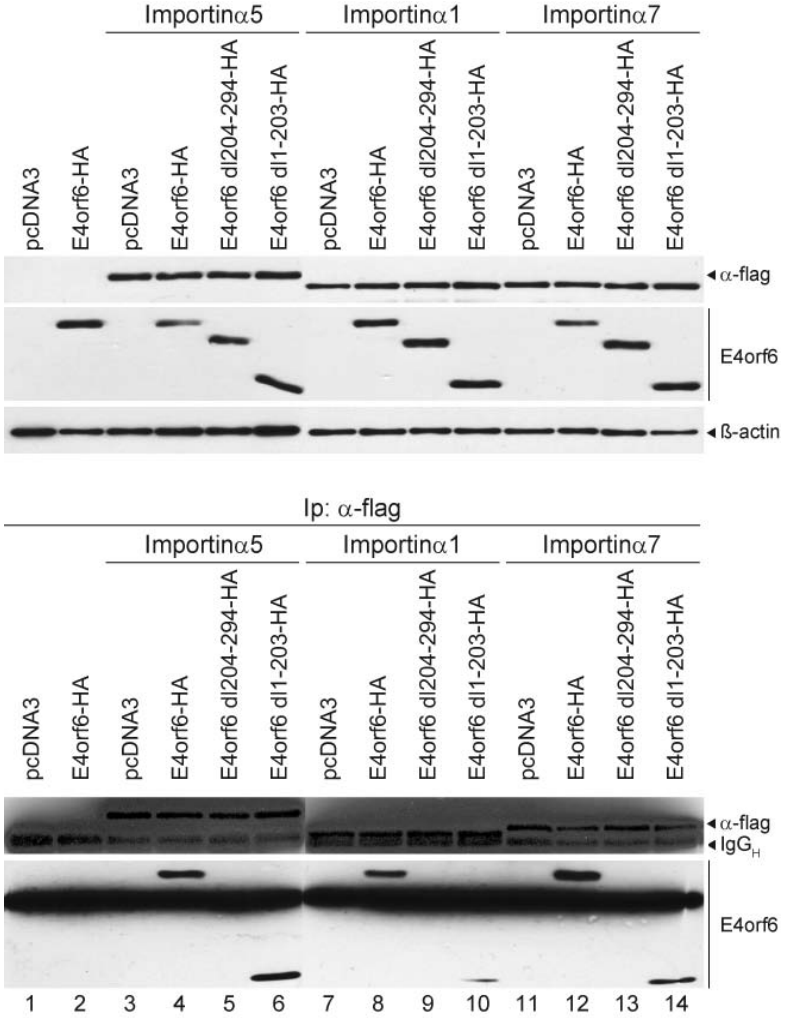

Figure 39: Co-immunoprecipitation of E4orf6 with Importins. H1299 cells were cotransfected with pcDNA3 constructs encoding the flag-tagged importins or E4orf6 wt and mutant proteins. At 24 h post transfection whole-cell extracts were prepared. For analysis of steady-state concentrations proteins (50 µg samples) were separated by 12% SDS-PAGE and subjected to immunoblotting using anti-flag mouse mab M2, and for Eorf6 anti-HA rat mab 3F10 (top panel). For co-immunoprecipitation with the flag-tagged importins 2 mg samples of protein were co-immunoprecipitated (Ip) with mab M2 (α-flag) and separated by 12% SDS-PAGE followed by immunoblotting with anti-flag mouse mab M2 and for E4orf6 anti- HA rat mab 3F10.

Western blot analysis revealed similar steady state concentrations of E4orf6 and importins (Fig. 39, top panel), as well as binding of the E4orf6 full-length protein to the three alpha importins (Fig. 39, lanes 4, 8, 12). Surprisingly, the truncated E4orf6 construct lacking the first 203 aa also co-immunoprecipitated with importin α1, α5 and α7 (Fig. 39, lanes 6, 10, 14). This was unexpected since the NLS was mapped at aa 13 to 31 [127]. In contrast, no binding of the N-terminal fragment (deletion of aa 204-294) containing the putative NLS was detected with any of the importin α constructs (Fig. 39, lanes 5, 9, 13).

The E4orf6-importin binding region was narrowed down further by another Co-IP using E4orf6 constructs with point mutations or deletions in the C-terminus. Again H1299 cells were co transfected with E4orf6 constructs and flag-tagged alpha importins shown to coimmunoprecipitate the E4orf6 protein (Fig. 38). While Western blot analysis revealed similar steady-state concentrations of importins, E4orf6 with a deletion of aa 271-292 showed minor accumulation of the protein compared to the other constructs (Fig. 40, lanes 6, 14, 22). Consistent with previous Co-IPs the E4orf6 full-length protein but not the N-terminal fragment co-immunoprecipitated with importin α5, α1 and α7 (Fig. 40, compare lanes 2, 10, 18 with lanes 4, 12, 20). Interestingly, E4orf6 with a point mutation at aa 245 (L245P; Fig. 40, lanes 3, 11, 19) or deletions of aa 182-213 (Fig. 40, lanes 7, 15, 23), aa 214-228 (Fig. 40, lanes 8, 16, 24), aa 229-248 (Fig. 40, lanes 9, 17, 25) and aa 249-270 (Fig. 40, lanes 5, 13, 21) were co-immunoprecipitated efficiently with all three alpha importins. In contrast, the E4orf6 construct with a deletion of aa 271-292 could not be detected to bind any importins (Fig. 40, lanes 6, 14, 22). However, even longer exposure of the Co-IP to compensate for the poor expression of this construct was negative for an interaction with importins (data not shown). This indicates that the binding region of E4orf6 to importins could be located in the C-terminal amino acids 271 to 294 (Fig. 40).

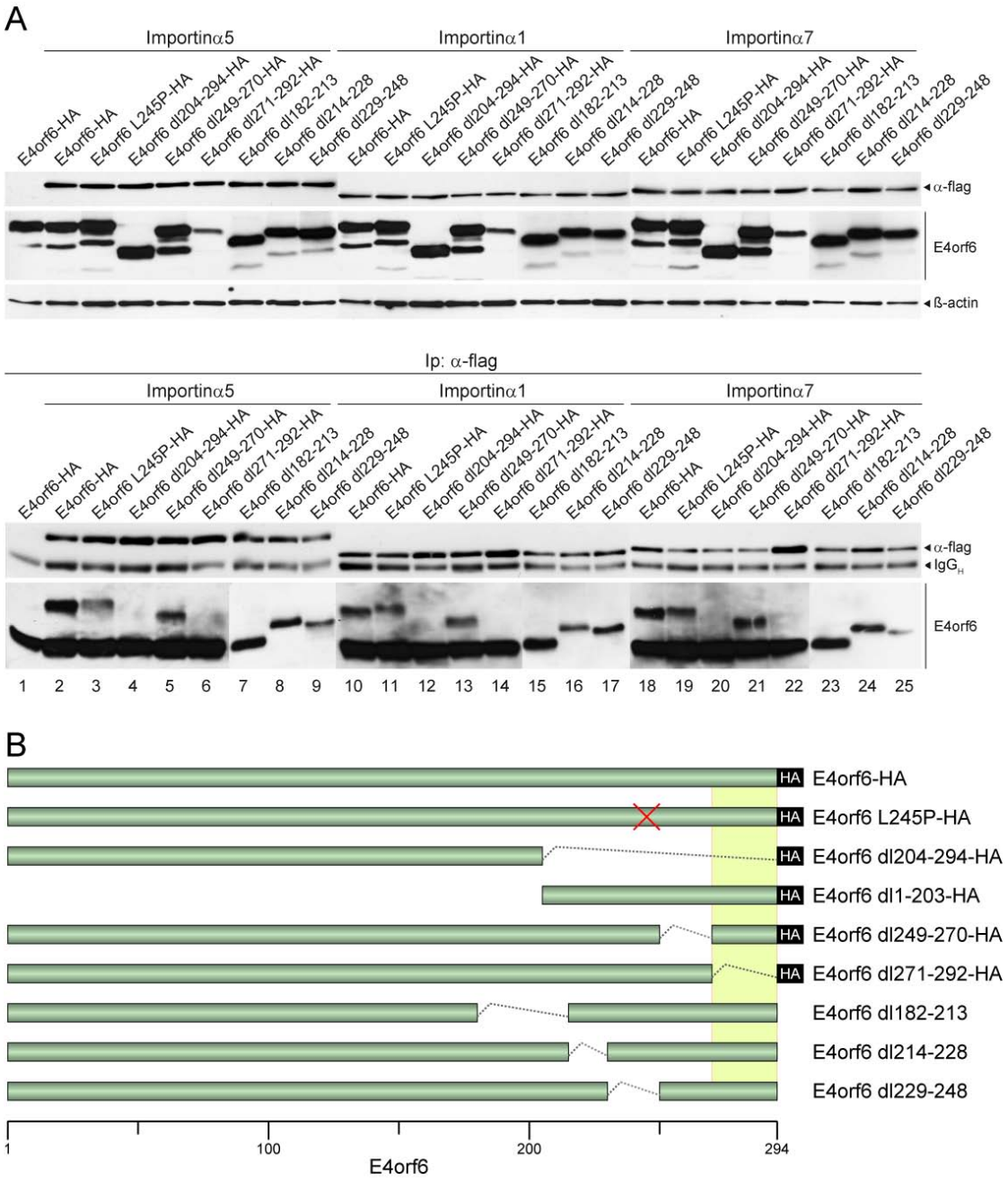

Figure 40: Localization of E4orf6 binding region to Importins (A) Co-immunoprecipitation of E4orf6 with importins. H1299 cells were co-transfected with pcDNA3 constructs encoding the flag-tagged importins or E4orf6 wt and mutant proteins. At 24 h post transfection whole-cell extracts were prepared. For analysis of steady-state concentrations proteins (50 µg samples) were separated by 12% SDS-PAGE and subjected to immunoblotting using anti-flag mouse mab M2 and for Eorf6 either anti-HA rat mab 3F10 (1–6, 10–14 and 18–22) or anti-E4orf6 rabbit polyclonal antibody 1807 (7–9, 15–17 a nd 23 –25). For c o-immunoprecipitation w ith t he f lag-tagged i mportins 1 mg s amples of protein were co-immunoprecipitated (Ip) with mab M2 (α-flag) and separated by 12% SDS-PAGE followed by immunoblotting with anti-flag mouse mab M2 and for Eorf6 either with anti-HA rat mab 3F10 (1–6, 10–14 and 18–22) or anti-E4orf6 rabbit polyclonal antibody 1807 (7–9, 15–17 and 23–25). (B) E4orf6 constructs: deletions in the E4orf6 protein are indicated by lines, point mutations by a red cross. The region of E4orf6 identified as binding to importin α1, α5 and α7 is shaded in green (amino acid residues 271 to 294).

5.7.3 Nuclear import of E4orf6 is independent of binding to importin α1, α5 and α7

The subcellular localization of the E4orf6 constructs was determined by immunofluorescence analysis to test whether binding to alpha importins stimulates the nuclear localization of the E4orf6 protein. A549 cells were transfected with different HA-tagged E4orf6 constructs and probed with HA specific antibody 3F10 at 48 h post transfection.

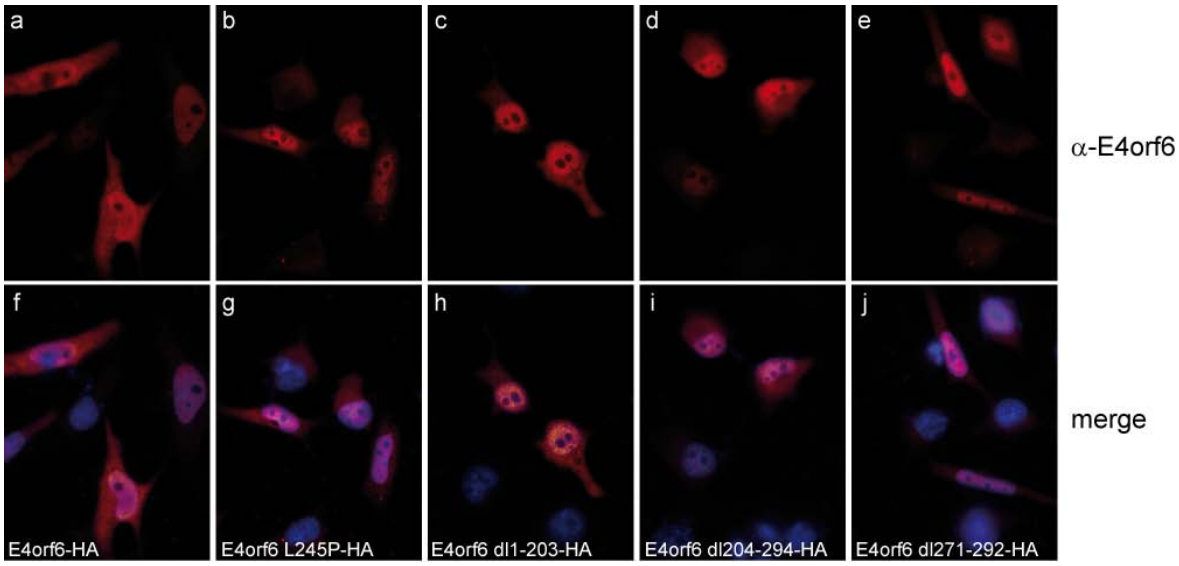

Figure 41: Intracellular localization of E4orf6. A549 cells were transfected with wt and mutant E4orf6 constructs, fixed 48 h post transfection and labeled with anti-HA rat mab 3F10 (α-E4orf6) and Cy3 conjugated secondary antibody to visualize E4orf6 protein. Representative anti-E4orf6 (red; a–e) staining patterns are shown. Overlays of the red images with DAPI staining visualizing the nuclei are shown in panels f–j (merge).

As expected, full length E4orf6 as well as the L245P protein showed predominant nuclear localization in the transfected cells (Fig. 41, panel a, f and b, g) [244]. Intriguingly, E4orf6 with deletions of aa 1-203 (Fig. 41, panel c, h), aa 204-294 (Fig. 41, panel d, i) and aa 271-292 (Fig. 41, panel e, j) localized preferentially in the nuclear compartment. These results suggest that the nuclear translocation of E4orf6 does not depend on binding of the protein to importin α1, α5 or α7. Although surprising, this is in agreement with previous studies where nuclear localization of the E4orf6 protein was also observed in absence of functional NLS or NRS sequences; in other words did not depend on the proposed NLS and NRS sequences. However, these sequences were shown to direct or retain the nuclear localization of E1B-55K in transfected cells [127, 244, 245].

E4orf6 protein is 34 kDa in size, and thus its translocation might border between active and passive transport across the nuclear pore complex [130]. Although the

function of interactions between E4orf6 and importin α1, α5 and α7 remains to be clarified, this might explain why this binding capacity is not required to promote the nuclear translocation of E4orf6. However, E4orf6 might contain signals that mediate its nuclear retention such as the described NLS and NRS sequences [127, 244].

5.7.4 Importin α5 accumulates during adenoviral replication

Together with E1B-55K, E4orf6 is known to form a Cullin 5-based E3 ubiquitin ligase to induce proteasomal degradation of cellular substrates. Here, E4orf6 assembles the complex, while E1B-55K provides substrate recognition [27, 142]. However, since the interaction of E4orf6 with importins did not lead to the nuclear translocation of E4orf6, it might support degradation of importins. To test this A549 cells were infected with wild type (H5*pg*4100) and E4orf6 minus virus (H5*pm*4154) and cells were lysed at various times post infection. Besides importin and E4orf6, Mre11 protein levels were also analyzed by Western blotting to visualize E4orf6-dependent degradation of the substrate (Fig. 42A).

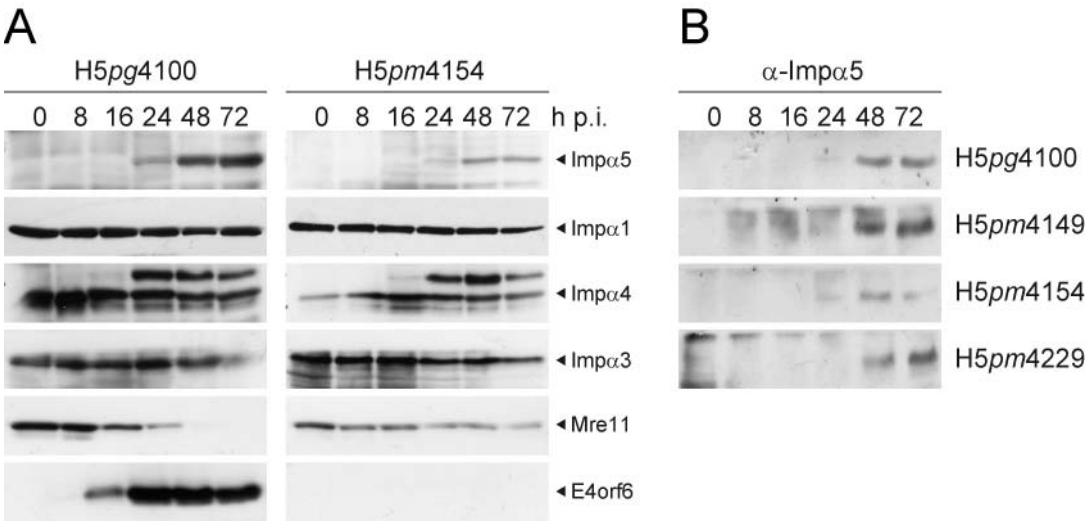

Figure 42: Protein levels of different importins during adenoviral infection. (A) A549 cells were infected with wt and E4orf6 minus virus at a multiplicity of 50 ffu per cell. Cells were harvested at the indicated times p.i. and total cell extracts were prepared. Proteins (25 µg samples) from each time point were separated by 10% SDS-PAGE and subjected to immunoblotting using anti-Importin α5 goat polyclonal antibody α-SRP1, anti-Importin α1 goat polyclonal antibody α-KPNA2, anti-Importin α4 goat polyclonal antibody α-KPNA3, anti-importin α3 goat polyclonal antibody α-KPNA4, anti-Mre11 rabbit polyclonal antibody pNB-100-142, and anti-E4orf6 rabbit polyclonal antibody 1807. (B) A549 cells were infected with wt and mutant viruses at a multiplicity of 25 ffu per cell. Cells were harvested at the indicated times p.i. and total cell extracts were prepared. Proteins (25 µg samples) from each time point were separated by 10% SDS-PAGE and subjected to immunoblotting using anti-Importinα5 goat polyclonal antibody SRP1.

Although in wt-infected cells Mre11 declined 24 h p.i. and E4orf6 accumulated in sufficient levels, no reduction in protein levels was observed for the examined importins (Fig. 42A), independently of their ability to bind to E4orf6 (importin α1 and α5) or not (importin α3 and α4; Fig. 38A). Surprisingly, importin α5 accumulated in the late phase of adenoviral infection starting 24 h p.i.; although faint bands were visible in the E4orf6 minus cell lysates, the protein significantly increased in wild type-infected cells (Fig. 42A).

To test whether E1B-55K is required for importin α5 accumulation, A549 cells were infected with an E1B minus virus (H5*pm*4149). Consistent with the previous time course experiment (Fig. 42A) infection with the wild type virus led to a more significant increase of importin α5 levels than the E4orf6 minus virus (H5*pm*4154; Fig. 42B). Interestingly, H5*pm*4149 (E1B minus) was also capable of inducing this increase, thus e1B-55K was not required for efficient accumulation of importin α5 in the late phase of adenovirus infection (Fig. 42B).

To examine whether the C-terminus of E4orf6 is sufficient to induce importin α5 accumulation, H5*pm*4229 virus expressing only aa 204-294 of E4orf6 protein was tested. In addition, H5*pm*4229 carries a point mutation (L245P) known to result in a non-functional E4orf6 protein during adenovirus infection [244]. Nevertheless, the C-terminal fragment including this mutation was still capable of inducing importin α5 accumulation (Fig. 42B).

These time course experiments indicate a functional role of the E4orf6-importin α5 interaction during the viral life cycle (Fig. 42) that seem not to involve the translocation of E4orf6 protein (Fig. 41). However, the function of the enhanced importin α5 protein levels, as well as the interaction between E4orf6 and three alpha importins, although not contributing to E4orf6 nuclear import, should be examined in future experiments.

6 Discussion

6.1 CRM1 is crucial for the adenovirus life cycle

The life cycle of adenoviruses is divided by convention into early and late phases, separated by the onset of viral genome replication. Early events include virus adsorption, transport of the genome to the nucleus, and the expression of early genes. After the onset of viral DNA replication, transcription of the MLTU and hence synthesis of late proteins is induced. The infectious cycle is completed by encapsidation of the viral genome and virus particle release. These steps are controlled by an orchestra of regulatory processes and require import of the viral genome and numerous viral proteins into the nucleus, as well as active transport of viral transcripts and proteins from the nucleus to the cytoplasm. The latter is achieved by exploiting the shuttling functions of cellular transport receptors that normally stimulate the nuclear export of cellular mRNA and protein cargos.

A set of adenoviral early (E1A, E1B-55K, E4orf6) and late proteins (L4-100K, pVI) contain a leucine-rich NES of the HIV-1 Rev type [68, 77, 175, 185, 337], known to be recognized by the cellular export receptor CRM1 [108]. The identification of these signals led to several studies on the proteins´ shuttling ability and associated functions. Extensive research has focused on the nuclear export of viral late mRNAs [51, 105, 175, 264, 325] known to be mediated by E1B-55K and E4orf6 [11, 39, 140, 198, 254]. However, a role for CRM1-dependent export in supporting adenoviral replication has not been established. To address this issue in detail, the impact of NES mutations and two different CRM1 inhibitors on several steps of the adenoviral life cycle was investigated in the present study.

6.1.1 The NES sequences of E1A, E1B-55K and E4orf6 are not required for efficient adenoviral replication

The early phase of adenoviral infection provides an optimal environment for following DNA replication and synthesis of structural capsid proteins. The regulatory proteins first expressed upon entry of the viral genome into the nucleus are the gene products of the E1A transcription unit. These proteins regulate gene transcription and the cell cycle by interacting with multiple cellular proteins to the advantage of adenoviral replication [113, 283]. Although the majority of identified E1A-binding proteins execute their functions in the nuclear compartment [113, 283], recent observations suggested the existence of a CRM1-dependent nuclear export signal in the CR1 domain of E1A 12S and 13S gene products [164].

Analysis of an adenovirus mutant carrying a substitution mutation in the E1A-NES (V74A) indicated its requirement for efficient progeny virus production. More precisely, virus growth was significantly reduced in serum-starved MRC5 cells and unexpectedly in HEK-293 cells [164]. The latter result is surprising since this cell line stably expresses the E1 region and thus is capable compleming potential defects of E1A and E1B mutant proteins [133]. Moreover, the study could not explain why this mutation affects viral replication. The data neither demonstrated exclusive nuclear localization of the mutated protein nor prohibition of the interaction with the cellular transport receptor CRM1 [164].
In addition, viruses were generated by recombination between cotransfected plasmids, wa method susceptible to further mutations in the viral backbone, and might provide an explanation for the replication defect primarily in complementing HEK-293 cells [133, 164]. However, data of the work presented here revealed that the E1A-NES is not required for efficient adenoviral replication, since E1A levels, expression of early and late proteins (Fig. 8 and 9) as well as virus progeny production were comparable to the wild type virus (Fig. 11). Together with the immunofluorescence analysis showing no difference in the E1A NES mutant virus compared to the wild type (Fig. 8), these data indicate that the nuclear export signal does not contribute to subcellular localization or regulatory functions of the protein.
Since further observations showed a pancellular distribution of the E1A protein sensitive to CRM1 inhibition, CRM1 might translocate the protein by one of the other identified leucine-rich NES sequences [164]. Unfortunately, it remains elusive at this point whether and how the nuclear export of E1A may contribute to the protein's function.

Extensive studies over the last decades revealed multiple functions for the regulatory protein E1B-55K during adenoviral infection. In the early phase interaction of E1B-55K with the tumor suppressor protein p53 inhibits p53-induced cell cycle arrest and apoptosis by repressing its function in transcriptional transactivation [169, 284, 296, 346, 347]. Moreover, E1B-55K and E4orf6 assemble an E3 ubiquitin ligase complex, which mediates the proteasomal degradation of p53, Mre11, and additional cellular target proteins [15, 27, 72, 261, 304]. It is well established that during the late phase of infection both adenoviral proteins accomplish the preferential nuclear export of viral late

transcripts, and thereby contribute to shut-off of host cell protein synthesis (reviewed in references 78, 104).

Interestingly, leucine-rich NES sequences have been identified in both E1B-55K and E4orf6 [77, 81, 185, 325]. However, several studies mostly concentrated on their function in viral late mRNA export, which has been described to be independent of CRM1 [51, 105, 175, 264, 288]. Consistent with data of these analyses using different inhibitors of the CRM1 pathway, mutation of the NES in either E1B-55K or E4orf6 (in H5*pm*4101 or H5*pm*4116), led to cytoplasmic accumulation of late transcripts similar to the wild type virus (Fig. 14). In contrast, further findings indicated that separate and distinct requirements for CRM1-mediated transport of E1B-55K and E4orf6 exist for nucleocytoplasmic transport and degradation of p53 and Mre11 (Fig. 15–18) [288].

The NES mutants directed the synthesis of stable E1B-55K and E4orf6, since protein levels were similar to those produced by the wild type virus during both early and late phases. A clear reduction in E4orf6 steady-state levels was induced by the NES mutation at very late time points post infection [288]. Similar levels were observed upon infection of E4orf6 NES cells with the E4orf6 minus virus, although the E4orf6-NES protein was exogenously expressed (Fig. 12B). The reason(s) for such reduction is not clear, since the substitutions introduced to generate the altered NES not only previously resulted in seemingly stable proteins in transfected cells [51, 77, 264, 325], but do not perturb any known regulatory sequence in E4.

The E4orf6 is known to regulate alternative splicing of the late viral mRNA tripartite leader [240], and a temporal pattern for the production of E4 mRNA splicing has been shown to be influenced by the E1B-55K/E4orf6 proteins [76]. Regulation of E4orf6 mRNA or the role of E4orf6-NES-dependent transport on export or stability of early mRNAs was not implicated in these studies. However, the export efficiency of early mRNAs seems to depend on active CRM1 transport (Fig. 29B). Additionally, fewer transcripts accumulated (Fig. 29A). Whether the latter was a direct effect of CRM1 inhibition or a downstream effect of reduced E1A gene expression remains to be determined.

Thus CRM1-dependent export of viral early mRNAs may be regulated by E4orf6. Nevertheless, transcription of E4 genes declines rapidly upon entry into the late phase (reviewed in reference 237), and the E4orf6 protein half-life is reduced late after infection [70]. Irrespective of the endogenous E4orf6-NES protein levels, exogenous expression of E4orf6-NES completely rescued the defective phenotypes

of an E4orf6 null mutant, H5*pm*4154, in viral late protein and virus production, indicating that the E4orf6-NES protein was functional (Fig. 13). However, for the NES virus mutants, the effect of exogenously expressed E4orf6-NES, resulted in lower accumulation or expression of both the E1B-55K- and E4orf6-NES proteins (Fig. 12B), but only in cells infected with the double NES mutant virus (H5*pm*4119). Such an effect was unexpected and cannot be explained by these experiments. However, the nuclear distribution of E1B-55K and its binding to E4orf6 were affected by mutation of the E4orf6 NES in single and double mutants [288]. Thus, the lower stability of the E4orf6-NES could have a dominant-negative effect, where its overexpresion might lead to formation of a defective, and thereby less stable E1B-55K-NES/E4orf6-NES complex. This is supported by the fact that overexpression of the E4orf6 NES protein in double NES mutant virus infected cells could not rescue the defective properties of the virus.

The complex formed by E1B-55K and E4orf6 ubiquitinylates cellular target proteins to induce their proteasomal degradation [15, 60, 72, 142, 261, 263, 304]. The relocalization to cytoplasmic sites, which may represent aggregates of misfolded proteins [26, 44, 351], further counteracts the functions of these cellular target proteins [204]. Since redistribution of Mre11 to cytoplasmic aggregates not only depends on E1B-55K but also on E4orf3 [6, 204], mutation of the E1B-55K NES plus inhibition of CRM1-dependent transport did not completely block the relocalization of this cellular protein (Fig. 16 and 18). However, the higher efficiency of Mre11 redistribution in the presence of a functional E1B-55K-NES and active CRM1 indicates that E1B-55K-mediated export of Mre11 occurs via CRM1. In agreement with the previously reported effect of E1B-55K-NES mutation on steady-state levels of p53 or Mre11 [175], these data indicate that degradation of either p53 or Mre11 does not require E1B-55K or E4orf6 NES-dependent transport (Fig. 15). Consistently, the levels of Mre11 declined upon inhibition of CRM1 transport (Fig. 17).

In addition, LMB treatment did not block the virus-induced reduction of p53 (Fig. 17), although overall p53 levels were increased through blockage of CRM1-dependent transport [110, 194, 233]. In uninfected cells, MDM2 mediates p53 export via CRM1, which favors the cytoplasmic degradation of p53. Thereby, blockage of CRM1 leads to the stabilization of p53 in the nucleus [110, 253]. Since MDM2-independent degradation of p53 by the human papillomaviurs (HPV) E6 was also sensitive to LMB, a general mechanism to regulate p53 levels via its nuclear export was proposed [110]. However, the decrease of the p53 protein

levels in adenovirus-infected cells occurred independently of a functional E1B-55K and/or E4orf6-NES as well as active CRM1 upon adenovirus infection.
In contrast, although consistent with previous data [292], the relocalization of p53 to cytoplasmic aggregates was reduced by both E1B-55K-NES mutation and LMB treatment (Fig. 16 and 18). Additionally, the distribution pattern of p53 did not depend on E4orf6 (Fig. 16) suggesting that neither the E3 ubiquitin ligase complex nor p53 ubiquitinylation play a role in the nuclear export of p53 to cytoplasmic aggregates.
Taken together, these findings indicate that although CRM1-dependent export of E1B-55K or E4orf6 does not contribute to viral late mRNA export, the relocalization and degradation of cellular targets depending on these viral proteins seem to have distinct requirements. This conclusion is consistent with reports showing that degradation of different cellular proteins can occur independently, and that individual targets require separate substrate recognition events by E1B-55K [50, 292]. Even though E1B-55K may function as a shuttling factor for cellular substrates through the CRM1 pathway, Mre11 can also be exported by E4orf3 [6]. However, this mechanism may involve more than one cellular transport pathway, since blocking CRM1-dependent export does not completely prohibit relocalization of cellular substrates (Fig. 16 and 18).
Besides E4orf3 that possibly shuttles independently of CRM1, E1B-55K has been described to translocate between nuclear and cytoplasmic compartments independently of its NES sequence, depending on its sumoylation status [175]. However, the cellular transport pathway involved remains to be elucidated. Furthermore, the remaining substrates of the E3 ubiquitin ligase should be examined in terms of their degradation and relocalization characteristics in connection with the nuclear export pathways.

6.1.2 Mutation of the L4-100K-NES may block Hexon trimerization

The late phase of adenovirus infection is characterized by massive viral mRNA export to the cytoplasm, vast amounts of structural protein synthesis, and efficient encapsidation of the viral genome in the nucleus. This is accompanied by inhibition of cellular mRNA export and translation, leading to shut-off of host cell protein synthesis [18, 216, 352]. While the selective export of viral late transcripts depends on E1B-55K and E4orf6, the regulatory protein L4-100K plays a vital role in Hexon biogenesis [56, 149, 171, 243] and facilitates the selective translation of viral late mRNAs [67, 273, 342].

Interestingly, recent studies identified a nuclear export signal in this non-structural protein [68] that has further been described to be crucial for adenoviral replication [183]. The mutation of this L4-100K-NES sequence led to reduced late protein synthesis that was most prominent for Hexon levels [183]. Thus, this motif may be required for the selective translation of viral late transcripts achieved by specific binding to the TPL sequence present in these mRNAs [341] in combination with the translation inititation factor eIF4G [342].

Since it was shown that L4-100K binds to E1B-55K, it has been discussed whether this might contribute to viral late mRNA export [183]. Although no connection between L4-100K and this process is established so far, L4-100K remains the only protein known to selectively recognize viral late transcripts via their TPL sequence, which further stimulates export of these mRNAs [151].

It was described recently that the tumor selective potential of the E1B null mutant dl1520 depends on export of viral late transcripts, and that L4-100K might contribute to this selectivity [241]. Interestingly, in the present study a defect in viral late mRNA accumulation and efficient transport to the cytoplasm was detected (Fig. 21). Since L4-100K binding to the TPL sequence stabilizes the late transcripts [273, 341], this might support mRNA export by release from the transport complex.

It would be interesting to investigate the binding potential of L4-100K NES protein to the TPL to clarify the contribution of the NES signal to viral late gene expression. However, diminished binding efficiency of L4-100K to the transcripts is possible, since the nuclear export signal (aa 383-392 [68]) is located in the binding region of the tripartite leader sequence (aa 383-727 [342]), and might explain both inefficient viral late mRNA export and translation.

Nevertheless, inefficient accumulation of viral late proteins alone could not explain the severely reduced amount of progeny virions [183]. This indicates that the NES mutation results in a further effect downstream of viral late protein synthesis. A defect in virus particle assembly, including nuclear import of structural proteins, assembly of the capsid, and encapsidation of the viral genome, could explain the dramatically diminished virus production. L4-100K facilitates trimerization of the major capsid protein Hexon [56, 149, 243], whereas the structural protein pVI binds these trimers to import them into the nucleus [337]. Intriguingly, inactivation of the L4-100K-NES led to cytoplasmic aggregation of L4-100K, Hexon and pVI around the nuclear membrane (Fig. 20 and 22). In contrast, the predominant nuclear localization of Hexon and pVI as seen in wild type-infected

cells was blocked (Fig. 22). This suggests that the Hexon import by pVI into the nucleus is not functional upon inactivation of the L4-100K-NES.

Since it has been established that the import process of Hexon trimers is independent of L4-100K (and depends on pVI), the NES mutation in L4-100K might inhibit trimerization of the capsid protein. This was supported by the absence of Hexon trimers in L4-100K NES mutant-infected cells compared to the wild type virus (Fig. 22). However, since it has been shown that the L4-100K NES protein was still able to bind the Hexon protein [183], the inability to trimerize the monomers might induce the colocalization of both proteins in cytoplasmic aggregates. In addition, this inability could also explain the aggregation of the protein VI in similar cytoplasmic structures. pVI might still bind to Hexon but is not able to import the monomers. Furthermore, the cytoplasmic accumulation of these proteins may represent aggregates of misfolded proteins and subsequently induce their degradation. This, in turn, could explain the observed reductions of L4-100K and Hexon protein levels upon infection with the L4-100K NES virus mutant (Fig. 22C).

Earliest analysis on Hexon trimerization indicated a self-assembly mechanism of partially digested Hexons [31]. A low rate of Hexon trimer self-assembly during infection with the L4-100K NES virus might provide an explanation for production of small amounts of progeny virions [183].

In contrast to transfection experiments (Fig. 20) [68], the predominant cytoplasmic localization of L4-100K after adenovirus infection was not abolished by substitution mutations in the NES sequence (Fig. 20). Moreover, LMB treatment of infected cells did not induce redistribution of the L4-100K protein to the nuclear compartment (Fig. 23). A seemingly nuclear retention of the L4-100K protein upon mutation or CRM1 inhibition was only detected in dead cells, where comparison with the phase contrast revealed a cytoplasm that was enclosed around the nucleus (data not shown).

The distinct subcellular localization pattern between transfected and infected cells (Fig. 20) might be due to a modified host cell environment upon virus infection. In cells transfected with a L4-100K plasmid carrying the NES mutation, a predominant nuclear localization was observed (Fig. 20) [68]. However, use of LMB demonstrated that this redistribution to the nucleus is independent of active CRM1 (Fig. 20). This indicates that in transfected cells the NES sequence triggers export of the protein to the cytoplasm via a CRM1-independent transport pathway. Since NES-like sequences have also been identified in proteins that are seemingly

not cargo of the export receptor CRM1 [187], a CRM1-independent shuttling mechanism of L4-100K is not unfounded.

Interestingly, the subcellular localization of pVI is not altered upon LMB treatment, although this protein has been described to contain at least one functional nuclear export signal [337]. During virus entry into the host cell it might mediate the import of the viral genome into the nucleus [338]. However, in the late phase of infection the Hexon import via pVI, re-export of pVI, and finally, integration of pVI into the viral capsid is a tightly regulated process. A C-terminal fragment comprising both a nuclear localization and export signal allows shuttling of pVI for several rounds of Hexon import. Proteolytical cleavage of the C-terminal segment triggers the functional transition of pVI from an import adaptor to a structural protein of the viral capsid [337]. Both Hexon and pVI display a predominantly nuclear distribution that is unaltered after LMB treatment (Fig. 23). This indicates that nuclear import of the Hexon protein via pVI is efficient, although CRM1-dependent transport is inhibited. Moreover, this provides evidence that the NES sequence of pVI is no cargo of the export receptor CRM1. The localization of the NES sequence in the L4-100K protein (aa 383-392 [68]) is located in the region binding to TPL-containing RNAs (aa 383-727 [342]) and the Hexon binding region (aa 215-420; aa 614-806 [183]). This leads to the assumption that the NES mutation prohibits efficient viral late gene expression and trimerization of the Hexon protein. Thus, the mutation might lead to a dominant-negative phenotype affecting the replication of the virus by shuttling-independent mechanisms.

Taken together, the data suggest a crucial function of the L4-100K-NES for several steps in adenoviral replication, including late gene expression and virus particle assembly. Interestingly, these effects and the translocation of L4-100K to the cytoplasm are independent of the cellular export receptor CRM1. Moreover, the results underline the important interplay between L4-100K and pVI during the encapsidation process.

6.1.3 CRM1 facilitates early and IVa2 mRNA export

While transport of early proteins (E1A, E1B-55K, E4orf6) can be driven by CRM1, and late proteins (L4-100K, pVI) also possess leucine-rich NESs, export of viral late mRNA requires an unrelated cellular mechanism that depends on Nxf1/TAP [345]. Notably, cytoplasmic accumulation of viral late mRNA also requires E1B-55K and E4orf6 proteins [11, 39, 140, 198, 254], but neither active CRM1 nor the NES present in either of these early proteins participate in viral late mRNA export (Fig. 14 and 32) [51, 105, 264, 288]. Rather, the E1B-55K and E4orf6 NESs seem

to be required for at least some of these proteins' activities associated with the adenovirus-infected cell specific E3 ubiquitin ligase (Fig. 15–18) [175, 204, 288, 292].

The available data suggest that the activity of mRNA export receptors, such as Nxf1/TAP, and that of karyopherins, such as CRM1, may participate in a coordinated transport of viral proteins and mRNA at different stages of adenoviral replication. The requirement for Nxf1/TAP in viral mRNA export was only recently elucidated [345]. In contrast, several studies have addressed the role of NES-dependent CRM1 export of adenoviral proteins [51, 68, 77, 105, 164, 175, 264, 288, 337]. Although the majority of these studies have examined the participation of this export pathway in viral late mRNA transport [51, 105, 175, 264, 288], the role of CRM1 during different stages of viral replication is only partially understood.

This study provides new evidence that active CRM1-dependent transport is required during both the early and late phases of viral replication. Significantly, the data indicate that the defects observed upon CRM1 inhibition are direct consequences of reduced viral early mRNA export and viral DNA replication.

Expression of the dominant-negative form of CANc in non-transformed hepatocytes efficiently inhibited export of well characterized CRM1-dependent mRNA and protein cargos (the CD83 mRNA and the E1B-55K protein; Fig. 25), without compromising CRM1 expression or stability, nor cell viability (Fig. 24). This made it possible to evaluate the role of CRM1 at defined times post infection. Diminished production of viral progeny (Fig. 26) could result from the additive and pleiotropic effects of CRM1 inhibition on early and late gene expression, viral DNA replication and viral late protein assembly. The effects of either CANc or LMB, which in these studies displayed similar phenotypes and no significant toxicity, were more severe during the earlier stages, when both viral early proteins and viral DNA replication were clearly reduced (Fig. 27, 28 and 30).

Although as expected, inhibition of CRM1 did not perturb export of viral late mRNA [105], it did considerablely reduce their total steady-state concentrations (Fig. 32). Furthermore, while CRM1 inhibition during the early stages of infection led to low expression levels of both early and late proteins, only late proteins were reduced when CRM1 was inhibited during the late phase (Fig. 27 and 28), indicating that active CRM1 shuttling is also required for efficient expression or accumulation of viral late mRNA. It was initially found that LMB treatment at a late stage of infection had only a minor effect on accumulation of viral late proteins

[51, 264]. Subsequently, direct measurement of total viral late mRNA synthesis and export efficiency after CRM1 transport was blocked by a peptide inhibitor, led to the conclusion that CRM1 inhibition does not affect viral late mRNA production [105]. These discrepancies could be consequences of the treatment time-span used in the different experiments. In these studies, CRM1 was inhibited at later times post infection (from 24 to 48 h p.i.) to examine viral late mRNA synthesis and export, while in the previous reports late proteins or mRNA were measured using treatments from 12 to 24 or 14 to 18 h p.i. [51, 105].

The effects observed on viral late mRNA and protein production in these experiments could be caused by reduced viral DNA replication, activation of transcription from the ML promoter by IVa2, or posttranscriptional processing of late mRNA. Such defects could in turn be explained by the observed reduction in E2A (DBP), E1B-55K or E4orf6 protein levels (Fig. 27), since each contributes to either DNA replication (E2A) or postranscriptional processing of late mRNA (E1B-55K and E4orf6) [104, 297, 310]. It is also possible that expression of other early genes, such as additional E2 and E4 encoded mRNA, which were not measured, is reduced and could account for the observed effects.

The reduced expression level of the IVa2 intermediate protein (Fig. 31A), which is responsible for the increased activation of the MLTU induced upon initiation of viral DNA replication [248, 249, 315], provides an explanation for the reduced accumulation of viral late mRNAs. Additionally, the affected export of the IVa2 mRNA (Fig. 31B) could be a consequence of low E1B-55K protein levels (Fig. 27 and 28) since it has been shown that E1B-55K is required for efficient transport of IVa2 mRNA [196]. Alternatively, as in the case of the viral early transcripts (Fig. 29), CRM1 inhibition may directly restrict export of the IVa2 mRNA (Fig. 31B).

The reduction of viral DNA synthesis induced by restricted CRM1 shuttling might be a consequence of lower early gene expression. Inhibition of CRM1 at the earlier time points, approximately 2 to 8 h p.i., resulted in lower E2A mRNA and protein levels (Fig. 27–29) and could account for a similar reduction in DNA. The effect of CRM1 inhibition on viral DNA was significantly more severe in HeLa cells treated with LMB than in the hepatocytes expressing CANc (Fig. 30). The reason(s) for this difference are not clear, but it is possible that the covalent modification of CRM1 by LMB may have a more stable effect than the dynamic/transient interaction that could be established between CANc and CRM1. The effect of LMB treatment could therefore result in stronger phenotypes, as was indeed observed

for viral protein synthesis and progeny production (Fig. 26–28).

The contribution of CRM1 to viral DNA replication remains to be determined, but it is possible that shuttling of both early viral and cellular proteins that participate, directly or indirectly, in viral DNA synthesis could be affected by CRM1 inhibition. It is well established that upon entry into the nucleus viral DNA colonizes specific nuclear sites associated with structures known as PML oncogenic domains (PODs) or nuclear domain 10 (ND10) [157]. The PML protein and other components of the ND10 are reorganized from a spherical distribution to filamentous structures during the early phase of infection [52, 82]. Such reorganization precedes viral DNA replication and is induced by the E4orf3 protein [52, 82, 157, 197], which is known to be required for efficient viral DNA replication, presumably through recruitment of the MRN (Mre11, Nbs1, Rad50) complex and consequent inactivation of the DNA damage response [91, 92]. In addition to E4orf3, other E4 gene products are known to be indirectly implicated in efficient viral DNA replication [40, 140, 326]. Furthermore, after reorganization of the cell nucleus, the E2 gene products directly responsible for viral genome replication (pTP, DBP and the viral polymerase), as well as cellular transcription factors NFI, NFII and NFIII that stimulate viral DNA synthesis, must be recruited to the viral genome (reviewed in reference 297). Since leptomycin B (LMB) blocks dissociation of incoming viral particles from microtubules and inhibits their binding to the NPC, entry of the viral DNA into the nucleus requires active CRM1 shuttling [307]. Although the experiments were designed to inhibit CRM1 after the viral genome reaches the nucleus, it is possible that localization or activity of any of the viral or cellular proteins participating in genome replication may require CRM1 shuttling.

The primary effect of CRM1 inhibition can be linked directly to reduced early mRNA export: E2A (and E4orf6) protein levels were reduced upon LMB treatment in HEK-293 cells, i.e. in the presence of high levels of E1A, indicating that at early times post infection a post transcriptional block is induced by CRM1 inhibition (Fig. 28B). This conclusion is supported by the fact that E1A mRNA export efficiency decreased significantly, whereas the quantities of total E1A mRNA were only slightly affected, when CRM1 was inhibited from 4 to 12 h p.i. (Fig. 29).

The novel finding that adenoviral early mRNA requires active CRM1 for export raises the question of whether this pathway provides a selective advantage over cellular mRNA. It is well established that viral late mRNA has a competitive advantage over cellular mRNA, both at the level of translation and export [104, 341, 342]. Significantly, while efficient viral late mRNA export is accompanied by

concomitant inhibition of most cellular mRNA export, viral early mRNAs do not seem to benefit from a selective export process. However, since adenovirus infection does not perturb export of cellular snRNAs or ribosomal RNAs [53, 299], which are exported by the CRM1 pathway, it is possible that export of the early mRNA through this pathway may be advantageous. Thus adenoviruses would avoid competition with bulk cellular mRNA, which exit the nucleus through the Nxf1/TAP pathway.

The features of early mRNA that may be recognized by the cellular machinery directing export through CRM1 remain to be determined. Since CRM1 does not bind RNA directly, it requires adaptor proteins, such as HuR and eukaryotic initiation factor 4E (eIF4E) for mRNA export [37, 69, 256]. The subset of cellular mRNA exported through CRM1 includes certain early response genes that contain an AU-rich element in their 3' untranslated region. However, the export of the IFN-alpha 1 mRNA through CRM1 is not mediated by ARE sequences [173], suggesting that other features, unrelated to ARE sequences, can be recognized by adaptor proteins that associate with CRM1. Therefore, as with the viral late mRNA, it will be interesting to determine which cellular adaptor proteins may be responsible for recognizing the viral early mRNA.

In summary, these results demonstrate that export via the cellular transport receptor CRM1 supports several steps of adenoviral replication. Significantly, the data provide new evidence for CRM1 as the export receptor for viral early mRNAs. The defects observed upon CRM1 inhibition are direct consequences of reduced nucleocytoplasmic translocation of early transcripts and viral DNA replication. Thus, the early-to-late switch, characterized by the onset of viral genome replication and transcriptional activation of the MLTU, is blocked. It would be interesting to investigate whether the defect in IVa2 expression as well as in viral genome replication are direct or downstream effects of CRM1 inhibition.

6.2 Adenoviral interference with the TAP transport pathway

A recent study on the preferential export of major late transcripts revealed possible participation of the cellular transport receptor TAP [345], which mediates export of bulk cellular mRNA [35, 158, 195, 266]. A first link to this pathway emerged with the identification of E1B-AP5 (E1B-55K-associated protein 5), which specifically bound to a GST-E1B-55K fusion protein, and interestingly, exhibited RNA binding activity *in vitro* [116]. This heterogeneous nuclear ribonucleoprotein

(hnRNP) interacts with TAP, and thus may facilitate recruitment of the export receptor to the mRNP (messenger ribonucleoprotein particle) [12]. Impaired binding of E1B-AP5 to E1B-55K led to reduced efficiency of mRNA transport in Ad5-infected cells, accompanied by destabilization and/or mislocalization of the E1B-55K protein [116, 126, 348]. Thus, it still remains unclear whether this interaction contributes to regulation of adenoviral mRNA transport.

indeed, this and other studies revealed a connection to the TAP pathway via different adaptor proteins. Previous data identified a critical role for several serine/arginine (SR)-rich proteins in the early to late switch of adenoviral infection [90, 168]. Further candidates are SR proteins, essential splicing factors, that mediate recognition of splice sites during spliceosome assembly [146]. The initiation of complex formation requires SR protein phosphorylation [220, 343], while dephosphorylation occurs during splicing progression [154]. Interestingly, it has been established that SR proteins are targeted by adenoviral E4orf4 in the late phase of infection, resulting in their dephosphorylation by the cellular phosphatase PP2A [168, 177]. Together with titration of SR proteins and L4-33K [313], this regulates recognition of specific splice sites in favor of alternative spliced early and late mRNAs during the late phase of infection [2, 148, 238].

Recently, a continuative role of shuttling SR proteins as adaptors for TAP-dependent nuclear export of mRNA cargos has been suggested. Therefore dephosphorylation of SR proteins is likely to mediate nucleocytoplasmic translocation, whereas cytoplasmic rephosphorylation may trigger disassembly of the export complex and contribute to re-import of SR proteins [152, 154]. Thus, it is interesting that the prototypical SR protein SF2/ASF was identified as a possible target of the E3 ubiquitin ligase complex via mass spectrometric (MS) analysis (Table 1, probe 25).

Unlike MS analysis, Western blot analysis detected unaltered protein levels in wild type-infected cells during the course of adenoviral infection that were comparable to levels of the E1B minus virus (Fig. 36). Possibly, as observed by Branton and co-workers, only a modified sub-portion of the protein is degraded, which can not be detected by immunoblot analysis [71]. However, previous studies revealed that overexpression of SF2/ASF not only prevents the early to late shift in mRNA expression but additionally blocks cytoplasmic accumulation of major late mRNAs [225]. In context with the accumulated data, results of this work suggest a critical role of SF2/ASF in selective export of late transcripts via the TAP transport pathway, and that this depends on E1B-55K but is independent of E4orf4.

Moreover, this study provided new evidence for Aly/REF as a further cellular target protein during adenoviral infection. Aly/REF is a member of the hnRNP family and component of the exon junction complex (EJC) [193]. Like SR proteins, Aly/REF functions as an adaptor protein for TAP-dependent transport and links the export receptor TAP to the splicing process [206, 353]. Steady-state analysis of Aly/REF displayed altered protein levels in an E1B- and E4orf6-dependent manner late in infection. Specifically, a 27 kDa band, which has been assigned to the described human Aly/REF isoform, declined at 48 h post wild type infection. Simultaneously, another band of approximately 18 kDa appeared (Fig. 36). An isoform of exactly the same size has been described for *Mus musculus* [308]. Thus, it seems likely that this band may be assigned to a second yet unidentified isoform of *Homo sapiens*.

Intriguingly, a band of 18 kDa was also detected in immunoblot analysis of immortalized baby rat kidney (BRK) cells expressing E1A and E1B-55K (Fig. 37). In contrast to adenovirus-infected cells, where E4orf6 was required for efficient accumulation of the 18 kDa band (Fig. 36), in BRK cells E4orf6 was dispensable for this altered expression pattern (Fig. 37). A previous study observed an interaction between E1B-55K and Aly/REF in immunoprecipitation analysis and relocalization of the cellular protein in close proximity to viral transcription and replication centers [174]. This distribution pattern is characteristic for several splicing factors [7, 41, 43, 119] and consistent with the observation that viral transcription occurs primarily at the periphery of replication centers [255, 260].

Together these results suggest that Aly/REF may be a new target of the virus-induced E3 ubiquitin ligase leading to decreased steady-state concentrations of the protein; E1B-55K may provide substrate recognition. Whether the reduction of Aly/REF protein levels depends on E4orf6 or not remains to be tested. However, recent data provided the first evidence for E4orf6-independent assembly of the ligase complex and subsequent degradation of the target protein [289]. It might be conceivable that Aly/REF undergoes a post translational modification distinct from ubiquitinylation by the ligase complex. Proteolytic cleavage of Aly/REF could provide an explanation for both reduction of the full-length protein and appearance of the 18 kDa band (Fig. 36 and 37). Furthermore, the existence of a second murine Aly/REF isoform, which is likely to be generated by alternative splicing [308], suggests another possibility. Aly/REF mRNAs might be alternatively spliced during the late phase of adenovirus infection, leading to the observed alteration in the protein expression pattern (Fig. 36). Although the mechanism

behind the modified protein expression and localization of Aly/REF [174] remains unclear, it is entirely feasible that adenoviruses utilize Aly/REF and its link to the TAP transport pathway in favor of their replication.

The efficient export of herpesviral mRNA is mediated by ICP27. Interestingly, this protein can access both the CRM1 and TAP pathway for its nucleocytoplasmic translocation [59, 281]. However, the export of viral mRNA by ICP27 strictly depends on the export receptor TAP [59], and is achieved by interaction with either Aly/REF [58] or SR proteins [89].

Parallels between ICP27 and the adenoviral E1B-55K protein are remarkable. These include the nuclear export of the protein via CRM1 [81, 185], which in turn was excluded for the adenoviral late transcript transport (Fig. 14 and 32) [105, 175, 288], and the recently identified role of TAP as export receptor of late mRNAs [345]. Typically, TAP facilitates translocation of mRNA cargo via interaction with specific adaptor proteins [152, 193, 282]. As with herpesviral mRNA, results of this study (Table 1; Fig. 36 and 37) in conjunction with previous observations [174, 225] suggest a role for Aly/REF and/or SR proteins in preferential export of viral mRNAs via TAP in the late phase of adenoviral infection. Thus, usurping TAP adaptor proteins might block cellular mRNA export and/or support adenoviral late mRNA transport. However, the mechanism and function behind these alterations are as yet unclear, and remain to be elucidated, together with the contribution of TAP to the preferential export of viral mRNA.

6.3 E4orf6 interacts with specific alpha importins

Proteins that fulfill functions in the nucleus depend on their translocation into the nuclear compartment. A subset of the so far discussed adenoviral shuttling proteins contain a putative nuclear localization signal (NLS), including E1A, E4orf6, L4-100K and pVI [68, 127, 207, 337]. However, the nuclear import pathway used has only been identified for E1A: Importin α3 interacts with E1A and mediates its translocation into the nucleus [180, 212]. Intriguingly, this study revealed distinct binding efficiencies between E4orf6 and three alpha importins (Fig. 38). The most efficient interaction was observed with importin α5 and α7, which are both members of the importin α1 subfamily. The third binding partner, importin α1, is the single tested importin of subfamily α2, whereas no interaction could be detected with importins of the subfamily α3 (Fig. 38) [172, 179].

The three importin subfamilies share up to 50% sequence similarity, while within each subfamily the sequence similarity reaches more than 80% [179]. This

suggests that each subfamily may bind a similar set of NLS-containing proteins. Thus, interaction of E4orff6 with different importins from more than one subfamily is surprising. Interestingly, the herpesviral Orf57 shuttling protein has also been described to interact with importin α1 and α5, which represent members of two distinct importin subfamilies (α2 and α1). These two importins both bind the protein via its NLS sequence and facilitate its translocation [128].

Together this indicated that the importins binding to E4orf6 might also be capable of directing its nuclear import. However, the identified binding region (Fig. 40; aa 271–294) is distinct from the proposed NLS (aa 13-31 [127]) or nuclear retention signal (NRS; aa 239-253 [244]). In addition, neither the binding region comprised a common NLS sequence nor did the nuclear import of E4orf6 dependent on the availability of this region (Fig. 41). Although it is surprising that the nuclear translocation of E4orf6 does not depend on binding of the protein to importins, this is in agreement with previous studies that observed E4orf6 in the nuclear compartment in the absence of a functional NLS or NRS sequence.

In contrast, these E4orf6 sequences were proposed because they direct or retain the nuclear localization of E1B-55K in transfected cells [127, 244, 245]. Since the nuclear pore complex (NPC) allows passive diffusion of macromolecules up to 20 to 60 kDa [130], it is possible that the 34 kDa protein E4orf6 enters the nucleus without being actively transported. However, E4orf6 might contain signals that ensure its nuclear retention such as the previously described NLS or NRS sequences [127, 244].

Altogether, results of this work suggest a shuttling-independent function of the interaction between E4orf6 and importins. Interestingly, it has been established that viruses and parasites target alpha importins to inhibit distinct cellular proteins involved in the host cell immune response [61, 112, 218, 269, 270, 311]. The haantanviral nucleocapsid protein, for example, inhibits release of cytokines, specifically tumor necrosis factor alpha (TNF-α)-induced activation of nuclear factor kappa B (NF-κB). This is likely achieved by inhibiting the nuclear translocation of p65, a subunit of NF-κB, via blocking binding to its import receptors [311]. Another more common mechanism to counteract the host cell immune response is inhibiting cellular interferon (IFN) signaling. Therefore, different viral and parasite proteins target alpha importins that mediate the nuclear translocation of STAT1, which resembles a key step in IFN signaling [112, 218, 269, 270]. Although no role in the inhibition of cellular immune response has been described for E4orf6, it is possible that its interaction with distinct alpha

importins competes with and/or blocks the nuclear import of specific cellular target proteins.

Surprisingly, steady-state levels of importin α5, a strong E4orf6 binder, were elevated in the late phase of infection in an E4orf6-dependent manner. Moreover, expression of the C-terminal 90 aa of E4orf6 was sufficient to induce this increase. In contrast, the amphipathic α-helix, which mediates nuclear localization of E1B-55K [244], did not contribute to accumulation of importin α5 (Fig. 42). This indicates that the binding region of E4orf6 to importin α5 located in the C-terminal 24 aa (Fig. 40) might induce the elevated importin α5 levels. Interestingly, the binding region is located within the so called Oncodomain (aa 204-294), which in cooperation with Ad5 E1 proteins is responsible for induction of morphological hypertransformation in BRK cells by E4orf6 [234]. Hence, the importin α1, α5 and α7 / E4orf6 interaction and/or the elevated levels of importin α5 (Fig. 38 and 42) might contribute to the oncogenic potential of the E4orf6 protein.

Taken together, importin α5 accumulation during adenovirus infection provides a first hint for a functional role of E4orf6 interaction with alpha importins that seems not to involve the translocation of E4orf6 protein to the nucleus. However, the function of the binding as well as enhanced importin α5 protein levels remains to be elucidated. It is conceivable that E4orf6 competitively inhibits binding of cellular substrates to alpha importins, and hence their translocation into the nuclear compartment. Furthermore, this might be essential for the function of E4orf6 in adenoviral replication and/or for its oncogenic potential.

7 References

1. Abe, S., K. Miyamura, T. Oba, S. Terakura, M. Kasai, K. Kitaori, T. Sasaki, and Y. Kodera. 2003. Oral ribavirin for severe adenovirus infection after allogeneic marrow transplantation. Bone Marrow Transplant 32:1107-8.
2. Akusjarvi, G., and J. Stevenin. 2003. Remodelling of the host cell RNA splicing machinery during an adenovirus infection. Curr Top Microbiol Immunol 272:253-86.
3. Alber, F., S. Dokudovskaya, L. M. Veenhoff, W. Zhang, J. Kipper, D. Devos, A. Suprapto, O. Karni-Schmidt, R. Williams, B. T. Chait, A. Sali, and M. P. Rout. 2007. The molecular architecture of the nuclear pore complex. Nature 450:695-701.
4. Andrade, F., H. G. Bull, N. A. Thornberry, G. W. Ketner, L. A. Casciola-Rosen, and A. Rosen. 2001. Adenovirus L4-100K assembly protein is a granzyme B substrate that potently inhibits granzyme B-mediated cell death. Immunity 14:751-61.
5. Ankerst, J., and N. Jonsson. 1989. Adenovirus type 9-induced tumorigenesis in the rat mammary gland related to sex hormonal state. J Natl Cancer Inst 81:294-8.
6. Araujo, F. D., T. H. Stracker, C. T. Carson, D. V. Lee, and M. D. Weitzman. 2005. Adenovirus type 5 E4orf3 protein targets the Mre11 complex to cytoplasmic aggresomes. J Virol 79:11382-91.
7. Aspegren, A., and E. Bridge. 2002. Release of snRNP and RNA from transcription sites in adenovirus-infected cells. Exp Cell Res 276:273-83.
8. Aspegren, A., C. Rabino, and E. Bridge. 1998. Organization of splicing factors in adenovirus-infected cells reflects changes in gene expression during the early to late phase transition. Exp Cell Res 245:203-13.
9. Avvakumov, N., M. Sahbegovic, Z. Zhang, M. Shuen, and J. S. Mymryk. 2002. Analysis of DNA binding by the adenovirus type 5 E1A oncoprotein. J Gen Virol 83:517-24.
10. Avvakumov, N., R. Wheeler, J. C. D'Halluin, and J. S. Mymryk. 2002. Comparative sequence analysis of the largest E1A proteins of human and simian adenoviruses. J Virol 76:7968-75.
11. Babiss, L. E., H. S. Ginsberg, and J. E. Darnell, Jr. 1985. Adenovirus E1B proteins are required for accumulation of late viral mRNA and for effects on cellular mRNA translation and transport. Mol Cell Biol 5:2552-8.
12. Bachi, A., I. C. Braun, J. P. Rodrigues, N. Pante, K. Ribbeck, C. von Kobbe, U. Kutay, M. Wilm, D. Gorlich, M. Carmo-Fonseca, and E. Izaurralde. 2000. The C-terminal domain of TAP interacts with the nuclear pore complex and promotes export of specific CTE-bearing RNA substrates. Rna 6:136-58.
13. Bagchi, S., P. Raychaudhuri, and J. R. Nevins. 1990. Adenovirus E1A proteins can dissociate heteromeric complexes involving the E2F transcription factor: a novel mechanism for E1A trans-activation. Cell 62:659-69.
14. Bailey, A., and V. Mautner. 1994. Phylogenetic relationships among adenovirus serotypes. Virology 205:438-52.
15. Baker, A., K. J. Rohleder, L. A. Hanakahi, and G. Ketner. 2007. Adenovirus E4 34k and E1b 55k oncoproteins target host DNA ligase IV for proteasomal degradation. J Virol 81:7034-40.
16. Barker, D. D., and A. J. Berk. 1987. Adenovirus proteins from both E1B reading frames are required for transformation of rodent cells by viral infection and DNA transfection. Virology 156:107-21.
17. Barral, P. M., A. Rusch, A. S. Turnell, P. H. Gallimore, P. J. Byrd, T. Dobner, and R. J. Grand. 2005. The interaction of the hnRNP family member E1B-AP5 with p53. FEBS Lett 579:2752-8.
18. Beltz, G. A., and S. J. Flint. 1979. Inhibition of HeLa cell protein synthesis during adenovirus infection. Restriction of cellular messenger RNA sequences to the nucleus. J Mol Biol 131:353-73.
19. Benkö, M., B. Harrach, and W. C. Russell. 2000. Family Adenoviridae. In Virus Taxonomy. 7th Report of the International Committee on Taxonomy of Viruses, pp. 227-38. Edited by M. H. V. van Regenmortel, C. M. Fraquet, D. H. L. Bishop, E. B. Carstens, M. K. Estes, S. M. Lemon, J. Maniloff, M. A. Mayo, D. J. McGeoch, C.R. Pringle and R. B. Wickner. New York, San Diego: Academic Press.
20. Bergelson, J. M., J. A. Cunningham, G. Droguett, E. A. Kurt-Jones, A. Krithivas, J. S. Hong, M. S. Horwitz, R. L. Crowell, and R. W. Finberg. 1997. Isolation of a common receptor for Coxsackie B viruses and adenoviruses 2 and 5. Science 275:1320-3.
21. Berk, A. J. 1986. Functions of adenovirus E1A. Cancer Surv 5:367-87.
22. Berk, A. J. 2005. Recent lessons in gene expression, cell cycle control, and cell biology from adenovirus. Oncogene 24:7673-85.
23. Berk, A. J., F. Lee, T. Harrison, J. Williams, and P. A. Sharp. 1979. Pre-early adenovirus 5 gene product regulates synthesis of early viral messenger RNAs. Cell 17:935-44.
24. Bernards, R., P. I. Schrier, A. Houweling, J. L. Bos, A. J. van der Eb, M. Zijlstra, and C. J. Melief. 1983. Tumorigenicity of cells transformed by adenovirus type 12 by evasion of T-cell immunity. Nature 305:776-9.
25. Binger, M. H., and S. J. Flint. 1984. Accumulation of early and intermediate mRNA species during subgroup C adenovirus productive infections. Virology 136:387-403.
26. Blair Zajdel, M. E., and G. E. Blair. 1988. The intracellular distribution of the transformation-associated protein p53 in adenovirus-transformed rodent cells. Oncogene 2:579-84.
27. Blanchette, P., C. Y. Cheng, Q. Yan, G. Ketner, D. A. Ornelles, T. Dobner, R. C. Conaway, J. W. Conaway, and P. E. Branton. 2004. Both BC-box motifs of adenovirus protein E4orf6 are required to efficiently assemble an E3 ligase complex that degrades p53. Mol Cell Biol 24:9619-29.
28. Blanchette, P., K. Kindsmuller, P. Groitl, F. Dallaire, T. Speiseder, P. E. Branton, and T. Dobner. 2008. Control of mRNA export by adenovirus E4orf6 and E1B55K proteins during productive infection requires E4orf6 ubiquitin ligase activity. J Virol 82:2642-51.

29. Bogerd, H. P., A. Echarri, T. M. Ross, and B. R. Cullen. 1998. Inhibition of human immunodeficiency virus Rev and human T-cell leukemia virus Rex function, but not Mason-Pfizer monkey virus constitutive transport element activity, by a mutant human nucleoporin targeted to Crm1. J Virol 72:8627-35.
30. Boivin, D., M. R. Morrison, R. C. Marcellus, E. Querido, and P. E. Branton. 1999. Analysis of synthesis, stability, phosphorylation, and interacting polypeptides of the 34-kilodalton product of open reading frame 6 of the early region 4 protein of human adenovirus type 5. J Virol 73:1245-53.
31. Boulanger, P. A. 1975. Adenovirus assembly: self-assembly of partially digested hexons. J Virol 16:1678-82.
32. Boulanger, P. A., and G. E. Blair. 1991. Expression and interactions of human adenovirus oncoproteins. Biochem J 275 (Pt 2):281-99.
33. Bradford, M. M. 1976. A rapid and sensitive method for the quantitation of microgram quantities of protein utilizing the principle of protein-dye binding. Anal Biochem 72:248-54.
34. Branton, P. E., S. T. Bayley, and F. L. Graham. 1985. Transformation by human adenoviruses. Biochim Biophys Acta 780:67-94.
35. Braun, I. C., A. Herold, M. Rode, and E. Izaurralde. 2002. Nuclear export of mRNA by TAP/NXF1 requires two nucleoporin-binding sites but not p15. Mol Cell Biol 22:5405-18.
36. Bray, M., S. Prasad, J. W. Dubay, E. Hunter, K. T. Jeang, D. Rekosh, and M. L. Hammarskjold. 1994. A small element from the Mason-Pfizer monkey virus genome makes human immunodeficiency virus type 1 expression and replication Rev-independent. Proc Natl Acad Sci U S A 91:1256-60.
37. Brennan, C. M., I. E. Gallouzi, and J. A. Steitz. 2000. Protein ligands to HuR modulate its interaction with target mRNAs in vivo. J Cell Biol 151:1-14.
38. Bridge, E., M. Carmo-Fonseca, A. Lamond, and U. Pettersson. 1993. Nuclear organization of splicing small nuclear ribonucleoproteins in adenovirus-infected cells. J Virol 67:5792-802.
39. Bridge, E., and G. Ketner. 1990. Interaction of adenoviral E4 and E1b products in late gene expression. Virology 174:345-53.
40. Bridge, E., S. Medghalchi, S. Ubol, M. Leesong, and G. Ketner. 1993. Adenovirus early region 4 and viral DNA synthesis. Virology 193:794-801.
41. Bridge, E., and U. Pettersson. 1996. Nuclear organization of adenovirus RNA biogenesis. Exp Cell Res 229:233-9.
42. Bridge, E., K. U. Riedel, B. M. Johansson, and U. Pettersson. 1996. Spliced exons of adenovirus late RNAs colocalize with snRNP in a specific nuclear domain. J Cell Biol 135:303-14.
43. Bridge, E., D. X. Xia, M. Carmo-Fonseca, B. Cardinali, A. I. Lamond, and U. Pettersson. 1995. Dynamic organization of splicing factors in adenovirus-infected cells. J Virol 69:281-90.
44. Brown, C. R., S. J. Doxsey, E. White, and W. J. Welch. 1994. Both viral (adenovirus E1B) and cellular (hsp 70, p53) components interact with centrosomes. J Cell Physiol 160:47-60.
45. Buchkovich, K., N. Dyson, P. Whyte, and E. Harlow. 1990. Cellular proteins that are targets for transformation by DNA tumour viruses. Ciba Found Symp 150:262-71; discussion 271-8.
46. Bullock, W. O., J. M. Fernandez, and J. M. Short. 1987. Xl1-Blue: a high efficiency plasmid transforming recA Escherichia coli strain with beta-galactosidase selection. BioTechniques 5:376-378.
47. Burgert, H. G., Z. Ruzsics, S. Obermeier, A. Hilgendorf, M. Windheim, and A. Elsing. 2002. Subversion of host defense mechanisms by adenoviruses. Curr Top Microbiol Immunol 269:273-318.
48. Byrd, P., K. W. Brown, and P. H. Gallimore. 1982. Malignant transformation of human embryo retinoblasts by cloned adenovirus 12 DNA. Nature 298:69-71.
49. Caput, D., B. Beutler, K. Hartog, R. Thayer, S. Brown-Shimer, and A. Cerami. 1986. Identification of a common nucleotide sequence in the 3'-untranslated region of mRNA molecules specifying inflammatory mediators. Proc Natl Acad Sci U S A 83:1670-4.
50. Carson, C. T., R. A. Schwartz, T. H. Stracker, C. E. Lilley, D. V. Lee, and M. D. Weitzman. 2003. The Mre11 complex is required for ATM activation and the G2/M checkpoint. Embo J 22:6610-20.
51. Carter, C. C., R. Izadpanah, and E. Bridge. 2003. Evaluating the role of CRM1-mediated export for adenovirus gene expression. Virology 315:224-33.
52. Carvalho, T., J. S. Seeler, K. Ohman, P. Jordan, U. Pettersson, G. Akusjarvi, M. Carmo-Fonseca, and A. Dejean. 1995. Targeting of adenovirus E1A and E4-ORF3 proteins to nuclear matrix-associated PML bodies. J Cell Biol 131:45-56.
53. Castiglia, C. L., and S. J. Flint. 1983. Effects of adenovirus infection on rRNA synthesis and maturation in HeLa cells. Mol Cell Biol 3:662-71.
54. Catalucci, D., E. Sporeno, A. Cirillo, G. Ciliberto, A. Nicosia, and S. Colloca. 2005. An adenovirus type 5 (Ad5) amplicon-based packaging cell line for production of high-capacity helper-independent deltaE1-E2-E3-E4 Ad5 vectors. J Virol 79:6400-9.
55. Cepko, C. L., and P. A. Sharp. 1983. Analysis of Ad5 hexon and 100K ts mutants using conformation-specific monoclonal antibodies. Virology 129:137-54.
56. Cepko, C. L., and P. A. Sharp. 1982. Assembly of adenovirus major capsid protein is mediated by a nonvirion protein. Cell 31:407-15.
57. Chauvin, C., M. Suh, C. Remy, and A. L. Benabid. 1990. Failure to detect viral genomic sequences of three viruses (herpes simplex, simian virus 40 and adenovirus) in human and rat brain tumors. Ital J Neurol Sci 11:347-57.
58. Chen, I. H., L. Li, L. Silva, and R. M. Sandri-Goldin. 2005. ICP27 recruits Aly/REF but not TAP/NXF1 to herpes simplex virus type 1 transcription sites although TAP/NXF1 is required for ICP27 export. J Virol 79:3949-61.
59. Chen, I. H., K. S. Sciabica, and R. M. Sandri-Goldin. 2002. ICP27 interacts with the RNA export factor Aly/REF to direct herpes simplex virus type 1 intronless mRNAs to the TAP export pathway. J Virol 76:12877-89.

60. Cheng, C. Y., P. Blanchette, and P. E. Branton. 2007. The adenovirus E4orf6 E3 ubiquitin ligase complex assembles in a novel fashion. Virology 364:36-44.
61. Chung, K. M., J. Lee, J. E. Kim, O. K. Song, S. Cho, J. Lim, M. Seedorf, B. Hahm, and S. K. Jang. 2000. Nonstructural protein 5A of hepatitis C virus inhibits the function of karyopherin beta3. J Virol 74:5233-41.
62. Conti, E., and J. Kuriyan. 2000. Crystallographic analysis of the specific yet versatile recognition of distinct nuclear localization signals by karyopherin alpha. Structure 8:329-38.
63. Conti, E., M. Uy, L. Leigthon, G. Blobel, and J. Kuriyan. 1998. Crystallographic Analysis of the Recognition of a Nuclear Localization Signal by the Nuclear Import Factor Karyopherin α. Cell 94:193-204.
64. Cook, J. L., and A. M. Lewis, Jr. 1987. Immunological surveillance against DNA-virus-transformed cells: correlations between natural killer cell cytolytic competence and tumor susceptibility of athymic rodents. J Virol 61:2155-61.
65. Corbin-Lickfett, K. A., and E. Bridge. 2003. Adenovirus E4-34kDa requires active proteasomes to promote late gene expression. Virology 315:234-44.
66. Cress, W. D., and J. R. Nevins. 1996. Use of the E2F transcription factor by DNA tumor virus regulatory proteins. Curr Top Microbiol Immunol 208:63-78.
67. Cuesta, R., Q. Xi, and R. J. Schneider. 2000. Adenovirus-specific translation by displacement of kinase Mnk1 from cap-initiation complex eIF4F. Embo J 19:3465-74.
68. Cuesta, R., Q. Xi, and R. J. Schneider. 2004. Structural basis for competitive inhibition of eIF4G-Mnk1 interaction by the adenovirus 100-kilodalton protein. J Virol 78:7707-16.
69. Culjkovic, B., I. Topisirovic, L. Skrabanek, M. Ruiz-Gutierrez, and K. L. Borden. 2006. eIF4E is a central node of an RNA regulon that governs cellular proliferation. J Cell Biol 175:415-26.
70. Cutt, J. R., T. Shenk, and P. Hearing. 1987. Analysis of adenovirus early region 4-encoded polypeptides synthesized in productively infected cells. J Virol 61:543-52.
71. Dallaire, F., P. Blanchette, and P. E. Branton. 2009. A proteomic approach to identify candidate substrates of human adenovirus E4orf6-E1B55K and other viral cullin-based E3 ubiquitin ligases. J Virol 83:12172-84.
72. Dallaire, F., P. Blanchette, P. Groitl, T. Dobner, and P. E. Branton. 2009. Identification of integrin alpha3 as a new substrate of the adenovirus E4orf6/E1B 55-kilodalton E3 ubiquitin ligase complex. J Virol 83:5329-38.
73. Davison, A. J., M. Benko, and B. Harrach. 2003. Genetic content and evolution of adenoviruses. J Gen Virol 84:2895-908.
74. Dingle, J. H., and A. D. Langmuir. 1968. Epidemiology of acute, respiratory disease in military recruits. Am Rev Respir Dis 97:Suppl:1-65.
75. Dingwall, C., and R. A. Laskey. 1991. Nuclear targeting sequences--a consensus? Trends Biochem Sci 16:478-81.
76. Dix, I., and K. N. Leppard. 1993. Regulated splicing of adenovirus type 5 E4 transcripts and regulated cytoplasmic accumulation of E4 mRNA. J Virol 67:3226-31.
77. Dobbelstein, M., J. Roth, W. T. Kimberly, A. J. Levine, and T. Shenk. 1997. Nuclear export of the E1B 55-kDa and E4 34-kDa adenoviral oncoproteins mediated by a rev-like signal sequence. Embo J 16:4276-84.
78. Dobner, T., and J. Kzhyshkowska. 2001. Nuclear export of adenovirus RNA. Curr Top Microbiol Immunol 259:25-54.
79. Dolph, P. J., J. T. Huang, and R. J. Schneider. 1990. Translation by the adenovirus tripartite leader: elements which determine independence from cap-binding protein complex. J Virol 64:2669-77.
80. Dolph, P. J., V. Racaniello, A. Villamarin, F. Palladino, and R. J. Schneider. 1988. The adenovirus tripartite leader may eliminate the requirement for cap-binding protein complex during translation initiation. J Virol 62:2059-66.
81. Dosch, T., F. Horn, G. Schneider, F. Kratzer, T. Dobner, J. Hauber, and R. H. Stauber. 2001. The adenovirus type 5 E1B-55K oncoprotein actively shuttles in virus-infected cells, whereas transport of E4orf6 is mediated by a CRM1-independent mechanism. J Virol 75:5677-83.
82. Doucas, V., A. M. Ishov, A. Romo, H. Juguilon, M. D. Weitzman, R. M. Evans, and G. G. Maul. 1996. Adenovirus replication is coupled with the dynamic properties of the PML nuclear structure. Genes Dev 10:196-207.
83. DuBridge, R. B., P. Tang, H. C. Hsia, P. M. Leong, J. H. Miller, and M. P. Calos. 1987. Analysis of mutation in human cells by using an Epstein-Barr virus shuttle system. Mol Cell Biol 7:379-87.
84. Dyson, N., K. Buchkovich, P. Whyte, and E. Harlow. 1989. Cellular proteins that are targetted by DNA tumor viruses for transformation. Princess Takamatsu Symp 20:191-8.
85. Endter, C., and T. Dobner. 2004. Cell transformation by human adenoviruses. Curr Top Microbiol Immunol 273:163-214.
86. Endter, C., B. Hartl, T. Spruss, J. Hauber, and T. Dobner. 2005. Blockage of CRM1-dependent nuclear export of the adenovirus type 5 early region 1B 55-kDa protein augments oncogenic transformation of primary rat cells. Oncogene 24:55-64.
87. Endter, C., J. Kzhyshkowska, R. Stauber, and T. Dobner. 2001. SUMO-1 modification required for transformation by adenovirus type 5 early region 1B 55-kDa oncoprotein. Proc Natl Acad Sci U S A 98:11312-7.
88. Engelsma, D., R. Bernad, J. Calafat, and M. Fornerod. 2004. Supraphysiological nuclear export signals bind CRM1 independently of RanGTP and arrest at Nup358. Embo J 23:3643-52.
89. Escudero-Paunetto, L., L. Li, F. P. Hernandez, and R. M. Sandri-Goldin. 2010. SR proteins SRp20 and 9G8 contribute to efficient export of herpes simplex virus 1 mRNAs. Virology 401:155-64.

90. Estmer Nilsson, C., S. Petersen-Mahrt, C. Durot, R. Shtrichman, A. R. Krainer, T. Kleinberger, and G. Akusjarvi. 2001. The adenovirus E4-ORF4 splicing enhancer protein interacts with a subset of phosphorylated SR proteins. Embo J 20:864-71.
91. Evans, J. D., and P. Hearing. 2003. Distinct roles of the Adenovirus E4 ORF3 protein in viral DNA replication and inhibition of genome concatenation. J Virol 77:5295-304.
92. Evans, J. D., and P. Hearing. 2005. Relocalization of the Mre11-Rad50-Nbs1 complex by the adenovirus E4 ORF3 protein is required for viral replication. J Virol 79:6207-15.
93. Everett, R. D., C. Boutell, C. McNair, L. Grant, and A. Orr. 2010. Comparison of the biological and biochemical activities of several members of the alphaherpesvirus ICP0 family of proteins. J Virol 84:3476-87.
94. Everett, R. D., M. L. Parsy, and A. Orr. 2009. Analysis of the functions of herpes simplex virus type 1 regulatory protein ICP0 that are critical for lytic infection and derepression of quiescent viral genomes. J Virol 83:4963-77.
95. Fallaux, F. J., A. Bout, I. van der Velde, D. J. van den Wollenberg, K. M. Hehir, J. Keegan, C. Auger, S. J. Cramer, H. van Ormondt, A. J. van der Eb, D. Valerio, and R. C. Hoeben. 1998. New helper cells and matched early region 1-deleted adenovirus vectors prevent generation of replication-competent adenoviruses. Hum Gene Ther 9:1909-17.
96. Fallaux, F. J., O. Kranenburg, S. J. Cramer, A. Houweling, H. Van Ormondt, R. C. Hoeben, and A. J. Van Der Eb. 1996. Characterization of 911: a new helper cell line for the titration and propagation of early region 1-deleted adenoviral vectors. Hum Gene Ther 7:215-22.
97. Fan, X. C., and J. A. Steitz. 1998. Overexpression of HuR, a nuclear-cytoplasmic shuttling protein, increases the in vivo stability of ARE-containing mRNAs. Embo J 17:3448-60.
98. Farley, D. C., J. L. Brown, and K. N. Leppard. 2004. Activation of the early-late switch in adenovirus type 5 major late transcription unit expression by L4 gene products. J Virol 78:1782-91.
99. Ferrari, R., A. J. Berk, and S. K. Kurdistani. 2009. Viral manipulation of the host epigenome for oncogenic transformation. Nat Rev Genet 10:290-4.
100. Ferrari, R., M. Pellegrini, G. A. Horwitz, W. Xie, A. J. Berk, and S. K. Kurdistani. 2008. Epigenetic reprogramming by adenovirus e1a. Science 321:1086-8.
101. Fischer, U., J. Huber, W. C. Boelens, I. W. Mattaj, and R. Luhrmann. 1995. The HIV-1 Rev activation domain is a nuclear export signal that accesses an export pathway used by specific cellular RNAs. Cell 82:475-83.
102. Flint, J., and T. Shenk. 1989. Adenovirus E1A protein paradigm viral transactivator. Annu Rev Genet 23:141-61.
103. Flint, S. J., L. W. Enquist, V. R. Racaniello, and A. M. Skalka. 2004. Molecular Biology and Pathogenesis. Principles of Virology, 2nd ed. Edited by ASM Press.
104. Flint, S. J., and R. A. Gonzalez. 2003. Regulation of mRNA production by the adenoviral E1B 55-kDa and E4 Orf6 proteins. Curr Top Microbiol Immunol 272:287-330.
105. Flint, S. J., W. Huang, J. Goodhouse, and S. Kyin. 2005. A peptide inhibitor of exportin1 blocks shuttling of the adenoviral E1B 55 kDa protein but not export of viral late mRNAs. Virology 337:7-17.
106. Fontes, M. R., T. Teh, and B. Kobe. 2000. Structural basis of recognition of monopartite and bipartite nuclear localization sequences by mammalian importin-alpha. J Mol Biol 297:1183-94.
107. Forler, D., G. Rabut, F. D. Ciccarelli, A. Herold, T. Kocher, R. Niggeweg, P. Bork, J. Ellenberg, and E. Izaurralde. 2004. RanBP2/Nup358 provides a major binding site for NXF1-p15 dimers at the nuclear pore complex and functions in nuclear mRNA export. Mol Cell Biol 24:1155-67.
108. Fornerod, M., M. Ohno, M. Yoshida, and I. W. Mattaj. 1997. CRM1 is an export receptor for leucine-rich nuclear export signals. Cell 90:1051-60.
109. Fornerod, M., J. van Deursen, S. van Baal, A. Reynolds, D. Davis, K. G. Murti, J. Fransen, and G. Grosveld. 1997. The human homologue of yeast CRM1 is in a dynamic subcomplex with CAN/Nup214 and a novel nuclear pore component Nup88. Embo J 16:807-16.
110. Freedman, D. A., and A. J. Levine. 1998. Nuclear export is required for degradation of endogenous p53 by MDM2 and human papillomavirus E6. Mol Cell Biol 18:7288-93.
111. Fried, H., and U. Kutay. 2003. Nucleocytoplasmic transport: taking an inventory. Cell Mol Life Sci 60:1659-88.
112. Frieman, M., B. Yount, M. Heise, S. A. Kopecky-Bromberg, P. Palese, and R. S. Baric. 2007. Severe acute respiratory syndrome coronavirus ORF6 antagonizes STAT1 function by sequestering nuclear import factors on the rough endoplasmic reticulum/Golgi membrane. J Virol 81:9812-24.
113. Frisch, S. M., and J. S. Mymryk. 2002. Adenovirus-5 E1A: paradox and paradigm. Nat Rev Mol Cell Biol 3:441-52.
114. Fu, X. D. 1995. The superfamily of arginine/serine-rich splicing factors. Rna 1:663-80.
115. Fukuda, M., S. Asano, T. Nakamura, M. Adachi, M. Yoshida, M. Yanagida, and E. Nishida. 1997. CRM1 is responsible for intracellular transport mediated by the nuclear export signal. Nature 390:308-11.
116. Gabler, S., H. Schutt, P. Groitl, H. Wolf, T. Shenk, and T. Dobner. 1998. E1B 55-kilodalton-associated protein: a cellular protein with RNA-binding activity implicated in nucleocytoplasmic transport of adenovirus and cellular mRNAs. J Virol 72:7960-71.
117. Gallimore, P. H., P. J. Byrd, and R. J. A. Grand. 1985. Adenovirus genes involved in transformation. What determines the oncogenic phenotype? Symp. Soc. Gen. Microbiol. 37:126-72.
118. Gallimore, P. H., R. J. Grand, and P. J. Byrd. 1986. Transformation of human embryo retinoblasts with simian virus 40, adenovirus and ras oncogenes. Anticancer Res 6:499-508.
119. Gama-Carvalho, M., I. Condado, and M. Carmo-Fonseca. 2003. Regulation of adenovirus alternative RNA splicing correlates with a reorganization of splicing factors in the nucleus. Exp Cell Res 289:77-85.

120. Garnett, C. T., G. Talekar, J. A. Mahr, W. Huang, Y. Zhang, D. A. Ornelles, and L. R. Gooding. 2009. Latent species C adenoviruses in human tonsil tissues. J Virol 83:2417-28.
121. Gey, G. O., W. D. Coffman, and M. T. Kubicek. 1952. Tissue culture studies of the proliferative capacity of cervical carcinoma and normal epithelium. Cancer Res 12:264-65.
122. Giard, R. J., S. A. Aaronson, G. J. Todaro, P. Arnstein, J. H. Kersey, H. Dosik, and W. P. Parks. 1973. In vitro cultivation of human tumors: establishment of cell lines derived from a series of solid tumors. J Natl Cancer Inst 51:1417-23.
123. Ginsberg, H. S., E. Gold, W. S. Jordan, Jr., S. Katz, G. F. Badger, and J. H. Dingle. 1955. Relation of the new respiratory agents to acute respiratory diseases. Am J Public Health Nations Health 45:915-22.
124. Giordano, A., C. McCall, P. Whyte, and B. R. Franza, Jr. 1991. Human cyclin A and the retinoblastoma protein interact with similar but distinguishable sequences in the adenovirus E1A gene product. Oncogene 6:481-5.
125. Goldfarb, D. S., A. H. Corbett, D. A. Mason, M. T. Harreman, and S. A. Adam. 2004. Importin alpha: a multipurpose nuclear-transport receptor. Trends Cell Biol 14:505-14.
126. Gonzalez, R. A., and S. J. Flint. 2002. Effects of mutations in the adenoviral E1B 55-kilodalton protein coding sequence on viral late mRNA metabolism. J Virol 76:4507-19.
127. Goodrum, F. D., T. Shenk, and D. A. Ornelles. 1996. Adenovirus early region 4 34-kilodalton protein directs the nuclear localization of the early region 1B 55-kilodalton protein in primate cells. J Virol 70:6323-35.
128. Goodwin, D. J., and A. Whitehouse. 2001. A gamma-2 herpesvirus nucleocytoplasmic shuttle protein interacts with importin alpha 1 and alpha 5. J Biol Chem 276:19905-12.
129. Gorlich, D., S. Kostka, R. Kraft, C. Dingwall, R. A. Laskey, E. Hartmann, and S. Prehn. 1995. Two different subunits of importin cooperate to recognize nuclear localization signals and bind them to the nuclear envelope. Curr Biol 5:383-92.
130. Gorlich, D., and U. Kutay. 1999. Transport between the cell nucleus and the cytoplasm. Annu Rev Cell Dev Biol 15:607-60.
131. Gorlich, D., and I. W. Mattaj. 1996. Nucleocytoplasmic transport. Science 271:1513-8.
132. Graham, F. L. 1984. Transformation by and Oncogenicity of Human Adenoviruses. In The Adenoviruses, pp. 339-98. Edited by H. S. Ginsberg. Plenum Press, New York.
133. Graham, F. L., J. Smiley, W. C. Russell, and R. Nairn. 1977. Characteristics of a human cell line transformed by DNA from human adenovirus type 5. J Gen Virol 36:59-74.
134. Graveley, B. R. 2000. Sorting out the complexity of SR protein functions. Rna 6:1197-211.
135. Greber, U. F., P. Webster, J. Weber, and A. Helenius. 1996. The role of the adenovirus protease on virus entry into cells. Embo J 15:1766-77.
136. Groitl, P., and T. Dobner. 2007. Construction of adenovirus type 5 early region 1 and 4 virus mutants. Methods Mol Med 130:29-39.
137. Gruter, P., C. Tabernero, C. von Kobbe, C. Schmitt, C. Saavedra, A. Bachi, M. Wilm, B. K. Felber, and E. Izaurralde. 1998. TAP, the human homolog of Mex67p, mediates CTE-dependent RNA export from the nucleus. Mol Cell 1:649-59.
138. Gustafsson, B., W. Huang, G. Bogdanovic, F. Gauffin, A. Nordgren, G. Talekar, D. A. Ornelles, and L. R. Gooding. 2007. Adenovirus DNA is detected at increased frequency in Guthrie cards from children who develop acute lymphoblastic leukaemia. Br J Cancer 97:992-4.
139. Hahn, W. C., C. M. Counter, A. S. Lundberg, R. L. Beijersbergen, M. W. Brooks, and R. A. Weinberg. 1999. Creation of human tumour cells with defined genetic elements. Nature 400:464-8.
140. Halbert, D. N., J. R. Cutt, and T. Shenk. 1985. Adenovirus early region 4 encodes functions required for efficient DNA replication, late gene expression, and host cell shutoff. J Virol 56:250-7.
141. Hanahan, D. 1983. Studies on transformation of Escherichia coli with plasmids. J Mol Biol 166:557-80.
142. Harada, J. N., A. Shevchenko, A. Shevchenko, D. C. Pallas, and A. J. Berk. 2002. Analysis of the adenovirus E1B-55K-anchored proteome reveals its link to ubiquitination machinery. J Virol 76:9194-206.
143. Harel, A., and D. J. Forbes. 2004. Importin beta: conducting a much larger cellular symphony. Mol Cell 16:319-30.
144. Harlow, E., B. R. Franza, Jr., and C. Schley. 1985. Monoclonal antibodies specific for adenovirus early region 1A proteins: extensive heterogeneity in early region 1A products. J Virol 55:533-46.
145. Hayes, B. W., G. C. Telling, M. M. Myat, J. F. Williams, and S. J. Flint. 1990. The adenovirus L4 100-kilodalton protein is necessary for efficient translation of viral late mRNA species. J Virol 64:2732-42.
146. Hertel, K. J., K. W. Lynch, and T. Maniatis. 1997. Common themes in the function of transcription and splicing enhancers. Curr Opin Cell Biol 9:350-7.
147. Hilleman, M. R., and J. H. Werner. 1954. Recovery of new agents from patients with acute respiratory illness. Proc Soc Exp Biol Med 85:183-88.
148. Himmelspach, M., Y. Cavaloc, K. Chebli, J. Stevenin, and R. Gattoni. 1995. Titration of serine/arginine (SR) splicing factors during adenoviral infection modulates E1A pre-mRNA alternative splicing. Rna 1:794-806.
149. Hong, S. S., E. Szolajska, G. Schoehn, L. Franqueville, S. Myhre, L. Lindholm, R. W. Ruigrok, P. Boulanger, and J. Chroboczek. 2005. The 100K-chaperone protein from adenovirus serotype 2 (Subgroup C) assists in trimerization and nuclear localization of hexons from subgroups C and B adenoviruses. J Mol Biol 352:125-38.
150. Horwitz, M. S. 1996. Adenoviruses. In Fields Virology, 3rd ed, pp. 2149-71. Edited by B. N. Fields, D. M. Knipe and P. M. Howley. Lippincott Williams & Wilkins.

151. Huang, W., and S. J. Flint. 1998. The tripartite leader sequence of subgroup C adenovirus major late mRNAs can increase the efficiency of mRNA export. J Virol 72:225-35.
152. Huang, Y., R. Gattoni, J. Stevenin, and J. A. Steitz. 2003. SR splicing factors serve as adapter proteins for TAP-dependent mRNA export. Mol Cell 11:837-43.
153. Huang, Y., and J. A. Steitz. 2001. Splicing factors SRp20 and 9G8 promote the nucleocytoplasmic export of mRNA. Mol Cell 7:899-905.
154. Huang, Y., T. A. Yario, and J. A. Steitz. 2004. A molecular link between SR protein dephosphorylation and mRNA export. Proc Natl Acad Sci U S A 101:9666-70.
155. Hutten, S., and R. H. Kehlenbach. 2007. CRM1-mediated nuclear export: to the pore and beyond. Trends Cell Biol 17:193-201.
156. Iacovides, D. C., C. C. O'Shea, J. Oses-Prieto, A. Burlingame, and F. McCormick. 2007. Critical role for arginine methylation in adenovirus-infected cells. J Virol 81:13209-17.
157. Ishov, A. M., and G. G. Maul. 1996. The periphery of nuclear domain 10 (ND10) as site of DNA virus deposition. J Cell Biol 134:815-26.
158. Izaurralde, E. 2002. Nuclear export of messenger RNA. Results Probl Cell Differ 35:133-50.
159. Izaurralde, E., U. Kutay, C. von Kobbe, I. W. Mattaj, and D. Gorlich. 1997. The asymmetric distribution of the constituents of the Ran system is essential for transport into and out of the nucleus. Embo J 16:6535-47.
160. Izaurralde, E., and I. W. Mattaj. 1995. RNA export. Cell 81:153-9.
161. Jacobs, J. P., C. M. Jones, and J. P. Baille. 1970. Characteristics of a human diploid cell designated MRC-5. Nature 227:168-70.
162. Javier, R., K. Raska, Jr., G. J. Macdonald, and T. Shenk. 1991. Human adenovirus type 9-induced rat mammary tumors. J Virol 65:3192-202.
163. Jawetz, E. 1959. The story of shipyard eye. Br Med J 1:873-6.
164. Jiang, H., M. V. Olson, D. R. Medrano, O. H. Lee, J. Xu, Y. Piao, M. M. Alonso, C. Gomez-Manzano, M. C. Hung, W. K. Yung, and J. Fueyo. 2006. A novel CRM1-dependent nuclear export signal in adenoviral E1A protein regulated by phosphorylation. Faseb J 20:2603-5.
165. Jones, N., and T. Shenk. 1979. Isolation of adenovirus type 5 host range deletion mutants defective for transformation of rat embryo cells. Cell 17:683-9.
166. Kamei, Y., S. Yuba, T. Nakayama, and Y. Yoneda. 1999. Three distinct classes of the alpha-subunit of the nuclear pore-targeting complex (importin-alpha) are differentially expressed in adult mouse tissues. J Histochem Cytochem 47:363-72.
167. Kang, Y., and B. R. Cullen. 1999. The human Tap protein is a nuclear mRNA export factor that contains novel RNA-binding and nucleocytoplasmic transport sequences. Genes Dev 13:1126-39.
168. Kanopka, A., O. Muhlemann, S. Petersen-Mahrt, C. Estmer, C. Ohrmalm, and G. Akusjarvi. 1998. Regulation of adenovirus alternative RNA splicing by dephosphorylation of SR proteins. Nature 393:185-7.
169. Kao, C. C., P. R. Yew, and A. J. Berk. 1990. Domains required for in vitro association between the cellular p53 and the adenovirus 2 E1B 55K proteins. Virology 179:806-14.
170. Katahira, J., K. Strasser, A. Podtelejnikov, M. Mann, J. U. Jung, and E. Hurt. 1999. The Mex67p-mediated nuclear mRNA export pathway is conserved from yeast to human. Embo J 18:2593-609.
171. Kauffman, R. S., and H. S. Ginsberg. 1976. Characterization of a temperature-sensitive, hexon transport mutant of type 5 adenovirus. J Virol 19:643-58.
172. Kelley, J. B., A. M. Talley, A. Spencer, D. Gioeli, and B. M. Paschal. 2010. Karyopherin alpha7 (KPNA7), a divergent member of the importin alpha family of nuclear import receptors. BMC Cell Biol 11:63.
173. Kimura, T., I. Hashimoto, T. Nagase, and J. Fujisawa. 2004. CRM1-dependent, but not ARE-mediated, nuclear export of IFN-alpha1 mRNA. J Cell Sci 117:2259-70.
174. Kindsmüller, K. 2006. Analysen zur Funktion des E1B-55K-Proteins von Adenovirus Typ 5 im lytischen Replikationszyklus. Dissertation, Universität Regensburg.
175. Kindsmuller, K., P. Groitl, B. Hartl, P. Blanchette, J. Hauber, and T. Dobner. 2007. Intranuclear targeting and nuclear export of the adenovirus E1B-55K protein are regulated by SUMO1 conjugation. Proc Natl Acad Sci U S A 104:6684-9.
176. Kindsmuller, K., S. Schreiner, F. Leinenkugel, P. Groitl, E. Kremmer, and T. Dobner. 2009. A 49-kilodalton isoform of the adenovirus type 5 early region 1B 55-kilodalton protein is sufficient to support virus replication. J Virol 83:9045-56.
177. Kleinberger, T., and T. Shenk. 1993. Adenovirus E4orf4 protein binds to protein phosphatase 2A, and the complex down regulates E1A-enhanced junB transcription. J Virol 67:7556-60.
178. Kobe, B. 1999. Autoinhibition by an internal nuclear localization signal revealed by the crystal structure of mammalian importin alpha. Nat Struct Biol 6:388-97.
179. Kohler, M., S. Ansieau, S. Prehn, A. Leutz, H. Haller, and E. Hartmann. 1997. Cloning of two novel human importin-alpha subunits and analysis of the expression pattern of the importin-alpha protein family. FEBS Lett 417:104-8.
180. Kohler, M., D. Gorlich, E. Hartmann, and J. Franke. 2001. Adenoviral E1A protein nuclear import is preferentially mediated by importin alpha3 in vitro. Virology 289:186-91.
181. Kohler, M., C. Speck, M. Christiansen, F. R. Bischoff, S. Prehn, H. Haller, D. Gorlich, and E. Hartmann. 1999. Evidence for distinct substrate specificities of importin alpha family members in nuclear protein import. Mol Cell Biol 19:7782-91.
182. Kosulin, K., C. Haberler, J. A. Hainfellner, G. Amann, S. Lang, and T. Lion. 2007. Investigation of adenovirus occurrence in pediatric tumor entities. J Virol 81:7629-35.
183. Koyuncu, O. Ö. 2009. Role of the Adenovirus Type 5 L4-100K Protein During Lytic infection. Dissertation, Universität Hamburg.

184. Koyuncu, O. O., and T. Dobner. 2009. Arginine methylation of human adenovirus type 5 L4 100-kilodalton protein is required for efficient virus production. J Virol 83:4778-90.
185. Kratzer, F., O. Rosorius, P. Heger, N. Hirschmann, T. Dobner, J. Hauber, and R. H. Stauber. 2000. The adenovirus type 5 E1B-55K oncoprotein is a highly active shuttle protein and shuttling is independent of E4orf6, p53 and Mdm2. Oncogene 19:850-7.
186. Krippl, B., B. Ferguson, M. Rosenberg, and H. Westphal. 1984. Functions of purified E1A protein microinjected into mammalian cells. Proc Natl Acad Sci U S A 81:6988-92.
187. Kutay, U., F. R. Bischoff, S. Kostka, R. Kraft, and D. Gorlich. 1997. Export of importin alpha from the nucleus is mediated by a specific nuclear transport factor. Cell 90:1061-71.
188. Kutay, U., and S. Guttinger. 2005. Leucine-rich nuclear-export signals: born to be weak. Trends Cell Biol 15:121-4.
189. Kutay, U., E. Izaurralde, F. R. Bischoff, I. W. Mattaj, and D. Gorlich. 1997. Dominant-negative mutants of importin-beta block multiple pathways of import and export through the nuclear pore complex. Embo J 16:1153-63.
190. Kzhyshkowska, J., E. Kremmer, M. Hofmann, H. Wolf, and T. Dobner. 2004. Protein arginine methylation during lytic adenovirus infection. Biochem J 383:259-65.
191. Laemmli, U. K. 1970. Cleavage of structural proteins during the assembly of the head of bacteriophage T4. Nature 227:680-5.
192. Lange, A., R. E. Mills, C. J. Lange, M. Stewart, S. E. Devine, and A. H. Corbett. 2007. Classical nuclear localization signals: definition, function, and interaction with importin alpha. J Biol Chem 282:5101-5.
193. Le Hir, H., E. Izaurralde, L. E. Maquat, and M. J. Moore. 2000. The spliceosome deposits multiple proteins 20-24 nucleotides upstream of mRNA exon-exon junctions. Embo J 19:6860-9.
194. Lecane, P. S., T. M. Kiviharju, R. G. Sellers, and D. M. Peehl. 2003. Leptomycin B stabilizes and activates p53 in primary prostatic epithelial cells and induces apoptosis in the LNCaP cell line. Prostate 54:258-67.
195. Lei, E. P., and P. A. Silver. 2002. Protein and RNA export from the nucleus. Dev Cell 2:261-72.
196. Leppard, K. N. 1993. Selective effects on adenovirus late gene expression of deleting the E1b 55K protein. J Gen Virol 74 (Pt 4):575-82.
197. Leppard, K. N., and R. D. Everett. 1999. The adenovirus type 5 E1b 55K and E4 Orf3 proteins associate in infected cells and affect ND10 components. J Gen Virol 80 (Pt 4):997-1008.
198. Leppard, K. N., and T. Shenk. 1989. The adenovirus E1B 55 kd protein influences mRNA transport via an intranuclear effect on RNA metabolism. Embo J 8:2329-36.
199. Lethbridge, K. J., G. E. Scott, and K. N. Leppard. 2003. Nuclear matrix localization and SUMO-1 modification of adenovirus type 5 E1b 55K protein are controlled by E4 Orf6 protein. J Gen Virol 84:259-68.
200. Li, Y., Y. C. Bor, Y. Misawa, Y. Xue, D. Rekosh, and M. L. Hammarskjold. 2006. An intron with a constitutive transport element is retained in a Tap messenger RNA. Nature 443:234-7.
201. Lichtenstein, D. L., K. Doronin, K. Toth, M. Kuppuswamy, W. S. Wold, and A. E. Tollefson. 2004. Adenovirus E3-6.7K protein is required in conjunction with the E3-RID protein complex for the internalization and degradation of TRAIL receptor 2. J Virol 78:12297-307.
202. Lichtenstein, D. L., K. Toth, K. Doronin, A. E. Tollefson, and W. S. Wold. 2004. Functions and mechanisms of action of the adenovirus E3 proteins. Int Rev Immunol 23:75-111.
203. Liebermann, H., R. Mentel, L. Dohner, S. Modrow, and W. Seidel. 1996. Inhibition of cell adhesion to the virus by synthetic peptides of fiber knob of human adenovirus serotypes 2 and 3 and virus neutralisation by anti-peptide antibodies. Virus Res 45:111-22.
204. Liu, Y., A. Shevchenko, A. Shevchenko, and A. J. Berk. 2005. Adenovirus exploits the cellular aggresome response to accelerate inactivation of the MRN complex. J Virol 79:14004-16.
205. Lowry, O. H., N. J. Rosebrough, A. L. Farr, and R. J. Randall. 1951. Protein measurement with the Folin phenol reagent. J Biol Chem 193:265-75.
206. Luo, M. L., Z. Zhou, K. Magni, C. Christoforides, J. Rappsilber, M. Mann, and R. Reed. 2001. Pre-mRNA splicing and mRNA export linked by direct interactions between UAP56 and Aly. Nature 413:644-7.
207. Lyons, R. H., B. Q. Ferguson, and M. Rosenberg. 1987. Pentapeptide nuclear localization signal in adenovirus E1a. Mol Cell Biol 7:2451-6.
208. Macara, I. G. 2001. Transport into and out of the nucleus. Microbiol Mol Biol Rev 65:570-94, table of contents.
209. Mackey, J. K., M. Green, W. S. Wold, and P. Rigden. 1979. Analysis of human cancer DNA for DNA sequences of human adenovirus type 4. J Natl Cancer Inst 62:23-6.
210. Mackey, J. K., P. M. Rigden, and M. Green. 1976. Do highly oncogenic group A human adenoviruses cause human cancer? Analysis of human tumors for adenovirus 12 transforming DNA sequences. Proc Natl Acad Sci U S A 73:4657-61.
211. Mackey, J. K., W. S. Wold, P. Rigden, and M. Green. 1979. Transforming region of group A, B, and C adenoviruses: DNA homology studies with twenty-nine human adenovirus serotypes. J Virol 29:1056-64.
212. Madison, D. L., P. Yaciuk, R. P. Kwok, and J. R. Lundblad. 2002. Acetylation of the adenovirus-transforming protein E1A determines nuclear localization by disrupting association with importin-alpha. J Biol Chem 277:38755-63.
213. Malim, M. H., D. F. McCarn, L. S. Tiley, and B. R. Cullen. 1991. Mutational definition of the human immunodeficiency virus type 1 Rev activation domain. J Virol 65:4248-54.

214. Martin-Fernandez, M., S. V. Longshaw, I. Kirby, G. Santis, M. J. Tobin, D. T. Clarke, and G. R. Jones. 2004. Adenovirus type-5 entry and disassembly followed in living cells by FRET, fluorescence anisotropy, and FLIM. Biophys J 87:1316-27.
215. Marton, M. J., S. B. Baim, D. A. Ornelles, and T. Shenk. 1990. The adenovirus E4 17-kilodalton protein complexes with the cellular transcription factor E2F, altering its DNA-binding properties and stimulating E1A-independent accumulation of E2 mRNA. J Virol 64:2345-59.
216. Mathews, M. B., and T. Shenk. 1991. Adenovirus virus-associated RNA and translation control. J Virol 65:5657-62.
217. Mathias, P., T. Wickham, M. Moore, and G. Nemerow. 1994. Multiple adenovirus serotypes use alpha v integrins for infection. J Virol 68:6811-4.
218. Matte, C., and A. Descoteaux. 2010. Leishmania donovani amastigotes impair gamma interferon-induced STAT1alpha nuclear translocation by blocking the interaction between STAT1alpha and importin-alpha5. Infect Immun 78:3736-43.
219. Mirza, M. A., and J. Weber. 1979. Uncoating of adenovirus type 2. J Virol 30:462-71.
220. Misteli, T., J. F. Caceres, J. Q. Clement, A. R. Krainer, M. F. Wilkinson, and D. L. Spector. 1998. Serine phosphorylation of SR proteins is required for their recruitment to sites of transcription in vivo. J Cell Biol 143:297-307.
221. Mitsudomi, T., S. M. Steinberg, M. M. Nau, D. Carbone, D. D'Amico, S. Bodner, H. K. Oie, R. I. Linnoila, J. L. Mulshine, J. D. Minna, and et al. 1992. p53 gene mutations in non-small-cell lung cancer cell lines and their correlation with the presence of ras mutations and clinical features. Oncogene 7:171-80.
222. Mittnacht, S., J. A. Lees, D. Desai, E. Harlow, D. O. Morgan, and R. A. Weinberg. 1994. Distinct sub-populations of the retinoblastoma protein show a distinct pattern of phosphorylation. Embo J 13:118-27.
223. Modrow, S., and D. Falke. 2003. Molekulare Virologie. 2. Auflage. Spektrum Akademischer Verlag.
224. Modrow, S., and D. Falke. 2010. Molekulare Virologie. 3. Auflage. Spektrum Akademischer Verlag.
225. Molin, M., and G. Akusjarvi. 2000. Overexpression of essential splicing factor ASF/SF2 blocks the temporal shift in adenovirus pre-mRNA splicing and reduces virus progeny formation. J Virol 74:9002-9.
226. Mondesert, G., C. Tribouley, and C. Kedinger. 1992. Identification of a novel downstream binding protein implicated in late-phase-specific activation of the adenovirus major late promotor. Nucleic Acids Res 20:3881-9.
227. Moran, E., T. Grodzicker, R. J. Roberts, M. B. Mathews, and B. Zerler. 1986. Lytic and transforming functions of individual products of the adenovirus E1A gene. J Virol 57:765-75.
228. Morin, N., and P. Boulanger. 1986. Hexon trimerization occurring in an assembly-defective, 100K temperature-sensitive mutant of adenovirus 2. Virology 152:11-31.
229. Morris, S. J., and K. N. Leppard. 2009. Adenovirus serotype 5 L4-22K and L4-33K proteins have distinct functions in regulating late gene expression. J Virol 83:3049-58.
230. Morris, S. J., G. E. Scott, and K. N. Leppard. 2010. Adenovirus late-phase infection is controlled by a novel L4 promoter. J Virol 84:7096-104.
231. Nachury, M. V., U. W. Ryder, A. I. Lamond, and K. Weis. 1998. Cloning and characterization of hSRP1 gamma, a tissue-specific nuclear transport factor. Proc Natl Acad Sci U S A 95:582-7.
232. Nadler, S. G., D. Tritschler, O. K. Haffar, J. Blake, A. G. Bruce, and J. S. Cleaveland. 1997. Differential expression and sequence-specific interaction of karyopherin alpha with nuclear localization sequences. J Biol Chem 272:4310-5.
233. Naniwa, J., J. Kigawa, R. Akeshima, Y. Kanamori, H. Itamochi, T. Oishi, T. Iba, and N. Terakawa. 2003. Leptomycin B enhances CDDP-sensitivity via nuclear accumulation of p53 protein in HPV-positive cells. Cancer Sci 94:1099-103.
234. Nevels, M., S. Rubenwolf, T. Spruss, H. Wolf, and T. Dobner. 2000. Two distinct activities contribute to the oncogenic potential of the adenovirus type 5 E4orf6 protein. J Virol 74:5168-81.
235. Nevels, M., T. Spruss, H. Wolf, and T. Dobner. 1999. The adenovirus E4orf6 protein contributes to malignant transformation by antagonizing E1A-induced accumulation of the tumor suppressor protein p53. Oncogene 18:9-17.
236. Nevels, M., B. Tauber, E. Kremmer, T. Spruss, H. Wolf, and T. Dobner. 1999. Transforming potential of the adenovirus type 5 E4orf3 protein. J Virol 73:1591-600.
237. Nevins, J. R. 1987. Regulation of early adenovirus gene expression. Microbiol Rev 51:419-30.
238. Nevins, J. R., and M. C. Wilson. 1981. Regulation of adenovirus-2 gene expression at the level of transcriptional termination and RNA processing. Nature 290:113-8.
239. Nigg, E. A. 1997. Nucleocytoplasmic transport: signals, mechanisms and regulation. Nature 386:779-87.
240. Nordqvist, K., K. Ohman, and G. Akusjarvi. 1994. Human adenovirus encodes two proteins which have opposite effects on accumulation of alternatively spliced mRNAs. Mol Cell Biol 14:437-45.
241. O'Shea, C. C., L. Johnson, B. Bagus, S. Choi, C. Nicholas, A. Shen, L. Boyle, K. Pandey, C. Soria, J. Kunich, Y. Shen, G. Habets, D. Ginzinger, and F. McCormick. 2004. Late viral RNA export, rather than p53 inactivation, determines ONYX-015 tumor selectivity. Cancer Cell 6:611-23.
242. Ong, S. E., B. Blagoev, I. Kratchmarova, D. B. Kristensen, H. Steen, A. Pandey, and M. Mann. 2002. Stable isotope labeling by amino acids in cell culture, SILAC, as a simple and accurate approach to expression proteomics. Mol Cell Proteomics 1:376-86.
243. Oosterom-Dragon, E. A., and H. S. Ginsberg. 1981. Characterization of two temperature-sensitive mutants of type 5 adenovirus with mutations in the 100,000-dalton protein gene. J Virol 40:491-500.
244. Orlando, J. S., and D. A. Ornelles. 1999. An arginine-faced amphipathic alpha helix is required for adenovirus type 5 e4orf6 protein function. J Virol 73:4600-10.

245. Orlando, J. S., and D. A. Ornelles. 2002. E4orf6 variants with separate abilities to augment adenovirus replication and direct nuclear localization of the E1B 55-kilodalton protein. J Virol 76:1475-87.
246. Ornelles, D. A., and T. Shenk. 1991. Localization of the adenovirus early region 1B 55-kilodalton protein during lytic infection: association with nuclear viral inclusions requires the early region 4 34-kilodalton protein. J Virol 65:424-9.
247. Osborne, T. F., and A. J. Berk. 1983. Far upstream initiation sites for adenovirus early region 1A transcription are utilized after the onset of viral DNA replication. J Virol 45:594-9.
248. Pardo-Mateos, A., and C. S. Young. 2004. A 40 kDa isoform of the type 5 adenovirus IVa2 protein is sufficient for virus viability. Virology 324:151-64.
249. Pardo-Mateos, A., and C. S. Young. 2004. Adenovirus IVa2 protein plays an important role in transcription from the major late promoter in vivo. Virology 327:50-9.
250. Pemberton, L. F., and B. M. Paschal. 2005. Mechanisms of receptor-mediated nuclear import and nuclear export. Traffic 6:187-98.
251. Peng, S. S., C. Y. Chen, N. Xu, and A. B. Shyu. 1998. RNA stabilization by the AU-rich element binding protein, HuR, an ELAV protein. Embo J 17:3461-70.
252. Perkins, D. N., D. J. Pappin, D. M. Creasy, and J. S. Cottrell. 1999. Probability-based protein identification by searching sequence databases using mass spectrometry data. Electrophoresis 20:3551-67.
253. Piette, J., H. Neel, and V. Marechal. 1997. Mdm2: keeping p53 under control. Oncogene 15:1001-10.
254. Pilder, S., M. Moore, J. Logan, and T. Shenk. 1986. The adenovirus E1B-55K transforming polypeptide modulates transport or cytoplasmic stabilization of viral and host cell mRNAs. Mol Cell Biol 6:470-6.
255. Pombo, A., J. Ferreira, E. Bridge, and M. Carmo-Fonseca. 1994. Adenovirus replication and transcription sites are spatially separated in the nucleus of infected cells. Embo J 13:5075-85.
256. Prechtel, A. T., J. Chemnitz, S. Schirmer, C. Ehlers, I. Langbein-Detsch, J. Stulke, M. C. Dabauvalle, R. H. Kehlenbach, and J. Hauber. 2006. Expression of CD83 is regulated by HuR via a novel cis-active coding region RNA element. J Biol Chem 281:10912-25.
257. Prieve, M. G., K. L. Guttridge, J. E. Munguia, and M. L. Waterman. 1996. The nuclear localization signal of lymphoid enhancer factor-1 is recognized by two differentially expressed Srp1-nuclear localization sequence receptor proteins. J Biol Chem 271:7654-8.
258. Puvion-Dutilleul, F., J. P. Bachellerie, N. Visa, and E. Puvion. 1994. Rearrangements of intranuclear structures involved in RNA processing in response to adenovirus infection. J Cell Sci 107 (Pt 6):1457-68.
259. Puvion-Dutilleul, F., M. K. Chelbi-Alix, M. Koken, F. Quignon, E. Puvion, and H. de The. 1995. Adenovirus infection induces rearrangements in the intranuclear distribution of the nuclear body-associated PML protein. Exp Cell Res 218:9-16.
260. Puvion-Dutilleul, F., and E. Puvion. 1991. Sites of transcription of adenovirus type 5 genomes in relation to early viral DNA replication in infected HeLa cells. A high resolution in situ hybridization and autoradiographical study. Biol Cell 71:135-47.
261. Querido, E., P. Blanchette, Q. Yan, T. Kamura, M. Morrison, D. Boivin, W. G. Kaelin, R. C. Conaway, J. W. Conaway, and P. E. Branton. 2001. Degradation of p53 by adenovirus E4orf6 and E1B55K proteins occurs via a novel mechanism involving a Cullin-containing complex. Genes Dev 15:3104-17.
262. Querido, E., R. C. Marcellus, A. Lai, R. Charbonneau, J. G. Teodoro, G. Ketner, and P. E. Branton. 1997. Regulation of p53 levels by the E1B 55-kilodalton protein and E4orf6 in adenovirus-infected cells. J Virol 71:3788-98.
263. Querido, E., M. R. Morrison, H. Chu-Pham-Dang, S. W. Thirlwell, D. Boivin, and P. E. Branton. 2001. Identification of three functions of the adenovirus e4orf6 protein that mediate p53 degradation by the E4orf6-E1B55K complex. J Virol 75:699-709.
264. Rabino, C., A. Aspegren, K. Corbin-Lickfett, and E. Bridge. 2000. Adenovirus late gene expression does not require a Rev-like nuclear RNA export pathway. J Virol 74:6684-8.
265. Raska, K., Jr., and P. H. Gallimore. 1982. An inverse relation of the oncogenic potential of adenovirus-transformed cells and their sensitivity to killing by syngeneic natural killer cells. Virology 123:8-18.
266. Reed, R., and E. Hurt. 2002. A conserved mRNA export machinery coupled to pre-mRNA splicing. Cell 108:523-31.
267. Reich, N. C., P. Sarnow, E. Duprey, and A. J. Levine. 1983. Monoclonal antibodies which recognize native and denatured forms of the adenovirus DNA-binding protein. Virology 128:480-4.
268. Reichelt, R., A. Holzenburg, E. L. Buhle, Jr., M. Jarnik, A. Engel, and U. Aebi. 1990. Correlation between structure and mass distribution of the nuclear pore complex and of distinct pore complex components. J Cell Biol 110:883-94.
269. Reid, S. P., L. W. Leung, A. L. Hartman, O. Martinez, M. L. Shaw, C. Carbonnelle, V. E. Volchkov, S. T. Nichol, and C. F. Basler. 2006. Ebola virus VP24 binds karyopherin alpha1 and blocks STAT1 nuclear accumulation. J Virol 80:5156-67.
270. Reid, S. P., C. Valmas, O. Martinez, F. M. Sanchez, and C. F. Basler. 2007. Ebola virus VP24 proteins inhibit the interaction of NPI-1 subfamily karyopherin alpha proteins with activated STAT1. J Virol 81:13469-77.
271. Ribbeck, K., U. Kutay, E. Paraskeva, and D. Gorlich. 1999. The translocation of transportin-cargo complexes through nuclear pores is independent of both Ran and energy. Curr Biol 9:47-50.
272. Richards, S. A., K. L. Carey, and I. G. Macara. 1997. Requirement of guanosine triphosphate-bound ran for signal-mediated nuclear protein export. Science 276:1842-4.

273. Riley, D., and S. J. Flint. 1993. RNA-binding properties of a translational activator, the adenovirus L4 100-kilodalton protein. J Virol 67:3586-95.
274. Rout, M. P., and J. D. Aitchison. 2001. The nuclear pore complex as a transport machine. J Biol Chem 276:16593-6.
275. Rowe, W. P., R. J. Hübner, L. K. Gilmore, R. H. Parrot, and T. G. Ward. 1953. Isolation of a cythopathogenic agent from human adenoids undergoing spontaneous degeneration in tissue culture. Proc Soc Exp Biol Med 84:570-73.
276. Russell, W. C. 2009. Adenoviruses: update on structure and function. J Gen Virol 90:1-20.
277. Russell, W. C., and D. A. Matthews. 2003. Nuclear perturbations following adenovirus infection. Curr Top Microbiol Immunol 272:399-413.
278. Ryan, K. J., and S. R. Wente. 2000. The nuclear pore complex: a protein machine bridging the nucleus and cytoplasm. Curr Opin Cell Biol 12:361-71.
279. Salvesen, G. S., and V. M. Dixit. 1997. Caspases: intracellular signaling by proteolysis. Cell 91:443-6.
280. Sambrook, J., and D. W. Russell. 2001. Molecular cloning: A laboratory manual. Cold Spring Harbor Laboratory Press.
281. Sandri-Goldin, R. M. 1998. ICP27 mediates HSV RNA export by shuttling through a leucine-rich nuclear export signal and binding viral intronless RNAs through an RGG motif. Genes Dev 12:868-79.
282. Sanford, J. R., N. K. Gray, K. Beckmann, and J. F. Caceres. 2004. A novel role for shuttling SR proteins in mRNA translation. Genes Dev 18:755-68.
283. Sang, N., J. Caro, and A. Giordano. 2002. Adenoviral E1A: everlasting tool, versatile applications, continuous contributions and new hypotheses. Front Biosci 7:d407-13.
284. Sarnow, P., C. A. Sullivan, and A. J. Levine. 1982. A monoclonal antibody detecting the adenovirus type 5 -E1b-58Kd tumor antigen: characterization of the E1b-58Kd tumor antigen in adenovirus-infected and -transformed cells. Virology 120:510-7.
285. Schaeper, U., T. Subramanian, L. Lim, J. M. Boyd, and G. Chinnadurai. 1998. Interaction between a cellular protein that binds to the C-terminal region of adenovirus E1A (CtBP) and a novel cellular protein is disrupted by E1A through a conserved PLDLS motif. J Biol Chem 273:8549-52.
286. Schiedner, G., S. Hertel, and S. Kochanek. 2000. Efficient transformation of primary human amniocytes by E1 functions of Ad5: generation of new cell lines for adenoviral vector production. Hum Gene Ther 11:2105-16.
287. Schmid, M., R. A. Gonzalez, and T. Dobner. CRM1-dependent transport supports cytoplasmic accumulation of adenoviral early transcripts. J Virol. Submitted for publication.
288. Schmid, M., K. Kindsmüller, P. Wimmer, P. Groitl, R. A. Gonzalez, and T. Dobner. The E3 ubiquitin ligase activity associated with the adenoviral E1B-55K-E4orf6 complex does not require CRM1-dependent export. J Virol. Accepted for publication.
289. Schreiner, S., P. Wimmer, H. Sirma, R. D. Everett, P. Blanchette, P. Groitl, and T. Dobner. 2010. Proteasome-dependent degradation of Daxx by the viral E1B-55K protein in human adenovirus-infected cells. J Virol 84:7029-38.
290. Schreiner, S., P. Wimmer, H. Sirma, R. D. Everett, P. Blanchette, P. Groitl, and T. Dobner. Proteasome-dependent degradation of Daxx by the viral E1B-55K protein in human adenovirus-infected cells. J Virol 84:7029-38.
291. Schutz, S., J. Chemnitz, C. Spillner, M. Frohme, J. Hauber, and R. H. Kehlenbach. 2006. Stimulated expression of mRNAs in activated T cells depends on a functional CRM1 nuclear export pathway. J Mol Biol 358:997-1009.
292. Schwartz, R. A., S. S. Lakdawala, H. D. Eshleman, M. R. Russell, C. T. Carson, and M. D. Weitzman. 2008. Distinct requirements of adenovirus E1b55K protein for degradation of cellular substrates. J Virol 82:9043-55.
293. Sekimoto, T., N. Imamoto, K. Nakajima, T. Hirano, and Y. Yoneda. 1997. Extracellular signal-dependent nuclear import of Stat1 is mediated by nuclear pore-targeting complex formation with NPI-1, but not Rch1. Embo J 16:7067-77.
294. Sharma, R. C., and R. T. Schimke. 1996. Preparation of electrocompetent E. coli using salt-free growth medium. Biotechniques 20:42-4.
295. Shaw, G., and R. Kamen. 1986. A conserved AU sequence from the 3' untranslated region of GM-CSF mRNA mediates selective mRNA degradation. Cell 46:659-67.
296. Shen, Y., G. Kitzes, J. A. Nye, A. Fattaey, and T. Hermiston. 2001. Analyses of single-amino-acid substitution mutants of adenovirus type 5 E1B-55K protein. J Virol 75:4297-307.
297. Shenk, T. 2001. Adenoviridae: The Viruses and Their Replication. In Fields Virology, 4th ed, pp. 2264-2300. Edited by D. M. Knipe and P. M. Howley. Lippincott Williams & Wilkins.
298. Simon, R., and J. D. Richter. 1990. The degradation sequence of adenovirus E1A consists of the amino-terminal tetrapeptide Met-Arg-His-Ile. Mol Cell Biol 10:5609-15.
299. Smiley, J. K., M. A. Young, C. C. Bansbach, and S. J. Flint. 1995. The metabolism of small cellular RNA species during productive subgroup C adenovirus infection. Virology 206:100-7.
300. Smith, A., A. Brownawell, and I. G. Macara. 1998. Nuclear import of Ran is mediated by the transport factor NTF2. Curr Biol 8:1403-6.
301. Spaeny-Dekking, E. H., W. L. Hanna, A. M. Wolbink, P. C. Wever, J. A. Kummer, A. J. Swaak, J. M. Middeldorp, H. G. Huisman, C. J. Froelich, and C. E. Hack. 1998. Extracellular granzymes A and B in humans: detection of native species during CTL responses in vitro and in vivo. J Immunol 160:3610-6.
302. Spindler, K. R., and A. J. Berk. 1984. Rapid intracellular turnover of adenovirus 5 early region 1A proteins. J Virol 52:706-10.

303. Stommel, J. M., N. D. Marchenko, G. S. Jimenez, U. M. Moll, T. J. Hope, and G. M. Wahl. 1999. A leucine-rich nuclear export signal in the p53 tetramerization domain: regulation of subcellular localization and p53 activity by NES masking. Embo J 18:1660-72.
304. Stracker, T. H., C. T. Carson, and M. D. Weitzman. 2002. Adenovirus oncoproteins inactivate the Mre11-Rad50-NBS1 DNA repair complex. Nature 418:348-52.
305. Stracker, T. H., D. V. Lee, C. T. Carson, F. D. Araujo, D. A. Ornelles, and M. D. Weitzman. 2005. Serotype-specific reorganization of the Mre11 complex by adenoviral E4orf3 proteins. J Virol 79:6664-73.
306. Strom, A. C., and K. Weis. 2001. Importin-beta-like nuclear transport receptors. Genome Biol 2:REVIEWS3008.
307. Strunze, S., L. C. Trotman, K. Boucke, and U. F. Greber. 2005. Nuclear targeting of adenovirus type 2 requires CRM1-mediated nuclear export. Mol Biol Cell 16:2999-3009.
308. Stutz, F., A. Bachi, T. Doerks, I. C. Braun, B. Seraphin, M. Wilm, P. Bork, and E. Izaurralde. 2000. REF, an evolutionary conserved family of hnRNP-like proteins, interacts with TAP/Mex67p and participates in mRNA nuclear export. Rna 6:638-50.
309. Tauber, B., and T. Dobner. 2001. Adenovirus early E4 genes in viral oncogenesis. Oncogene 20:7847-54.
310. Tauber, B., and T. Dobner. 2001. Molecular regulation and biological function of adenovirus early genes: the E4 ORFs. Gene 278:1-23.
311. Taylor, S. L., N. Frias-Staheli, A. Garcia-Sastre, and C. S. Schmaljohn. 2009. Hantaan virus nucleocapsid protein binds to importin alpha proteins and inhibits tumor necrosis factor alpha-induced activation of nuclear factor kappa B. J Virol 83:1271-9.
312. Thomas, D. L., J. Schaack, H. Vogel, and R. Javier. 2001. Several E4 region functions influence mammary tumorigenesis by human adenovirus type 9. J Virol 75:557-68.
313. Tormanen, H., E. Backstrom, A. Carlsson, and G. Akusjarvi. 2006. L4-33K, an adenovirus-encoded alternative RNA splicing factor. J Biol Chem 281:36510-7.
314. Trentin, J. J., Y. Yabe, and G. Taylor. 1962. The quest for human cancer viruses. Science 137:835-41.
315. Tribouley, C., P. Lutz, A. Staub, and C. Kedinger. 1994. The product of the adenovirus intermediate gene IVa2 is a transcriptional activator of the major late promoter. J Virol 68:4450-7.
316. Trotman, L. C., N. Mosberger, M. Fornerod, R. P. Stidwill, and U. F. Greber. 2001. Import of adenovirus DNA involves the nuclear pore complex receptor CAN/Nup214 and histone H1. Nat Cell Biol 3:1092-100.
317. Tsuji, L., T. Takumi, N. Imamoto, and Y. Yoneda. 1997. Identification of novel homologues of mouse importin alpha, the alpha subunit of the nuclear pore-targeting complex, and their tissue-specific expression. FEBS Lett 416:30-4.
318. Valcarcel, J., and M. R. Green. 1996. The SR protein family: pleiotropic functions in pre-mRNA splicing. Trends Biochem Sci 21:296-301.
319. Van der Eb, A. J., and A. Zantema. 1992. Adenovirus oncogenesis. In Malignant Transformation by DNA Viruses, pp. 115-40. Edited by W. Dörfler and P. Böhm. VCH, Weinheim.
320. Vasu, S. K., and D. J. Forbes. 2001. Nuclear pores and nuclear assembly. Curr Opin Cell Biol 13:363-75.
321. Vellinga, J., S. Van der Heijdt, and R. C. Hoeben. 2005. The adenovirus capsid: major progress in minor proteins. J Gen Virol 86:1581-8.
322. Wadell, G. 1984. Molecular epidemiology of human adenoviruses. Curr Top Microbiol Immunol 110:191-220.
323. Weber, K., U. Bartsch, C. Stocking, and B. Fehse. 2008. A multicolor panel of novel lentiviral "gene ontology" (LeGO) vectors for functional gene analysis. Mol Ther 16:698-706.
324. Weber, K., U. Mock, B. Petrowitz, U. Bartsch, and B. Fehse. 2010. Lentiviral gene ontology (LeGO) vectors equipped with novel drug-selectable fluorescent proteins: new building blocks for cell marking and multi-gene analysis. Gene Ther 17:511-20.
325. Weigel, S., and M. Dobbelstein. 2000. The nuclear export signal within the E4orf6 protein of adenovirus type 5 supports virus replication and cytoplasmic accumulation of viral mRNA. J Virol 74:764-72.
326. Weinberg, D. H., and G. Ketner. 1986. Adenoviral early region 4 is required for efficient viral DNA replication and for late gene expression. J Virol 57:833-8.
327. Weis, K. 1998. Importins and exportins: how to get in and out of the nucleus. Trends Biochem Sci 23:185-9.
328. Wen, W., J. L. Meinkoth, R. Y. Tsien, and S. S. Taylor. 1995. Identification of a signal for rapid export of proteins from the nucleus. Cell 82:463-73.
329. White, E. 1998. Regulation of apoptosis by adenovirus E1A and E1B oncoproteins. Semin. Virol. 8:505-13.
330. White, E. 1993. Regulation of apoptosis by the transforming genes of the DNA tumor virus adenovirus. Proc Soc Exp Biol Med 204:30-9.
331. Whittaker, J. L., P. J. Byrd, R. J. Grand, and P. H. Gallimore. 1984. Isolation and characterization of four adenovirus type 12-transformed human embryo kidney cell lines. Mol Cell Biol 4:110-6.
332. Wickham, T. J., E. J. Filardo, D. A. Cheresh, and G. R. Nemerow. 1994. Integrin alpha v beta 5 selectively promotes adenovirus mediated cell membrane permeabilization. J Cell Biol 127:257-64.
333. Wickham, T. J., P. Mathias, D. A. Cheresh, and G. R. Nemerow. 1993. Integrins alpha v beta 3 and alpha v beta 5 promote adenovirus internalization but not virus attachment. Cell 73:309-19.

334. Wiegand, H. L., G. A. Coburn, Y. Zeng, Y. Kang, H. P. Bogerd, and B. R. Cullen. 2002. Formation of Tap/NXT1 heterodimers activates Tap-dependent nuclear mRNA export by enhancing recruitment to nuclear pore complexes. Mol Cell Biol 22:245-56.
335. Williams, J., M. Williams, C. Liu, and G. Telling. 1995. Assessing the role of E1A in the differential oncogenicity of group A and group C human adenoviruses. Curr Top Microbiol Immunol 199 (Pt 3):149-75.
336. Winberg, G., and T. Shenk. 1984. Dissection of overlapping functions within the adenovirus type 5 E1A gene. Embo J 3:1907-12.
337. Wodrich, H., T. Guan, G. Cingolani, D. Von Seggern, G. Nemerow, and L. Gerace. 2003. Switch from capsid protein import to adenovirus assembly by cleavage of nuclear transport signals. Embo J 22:6245-55.
338. Wodrich, H., D. Henaff, B. Jammart, C. Segura-Morales, S. Seelmeir, O. Coux, Z. Ruzsics, C. M. Wiethoff, and E. J. Kremer. 2010. A capsid-encoded PPxY-motif facilitates adenovirus entry. PLoS Pathog 6:e1000808.
339. Wold, W. S., J. K. Mackey, P. Rigden, and M. Green. 1979. Analysis of human cancer DNA's for DNA sequence of human adenovirus serotypes 3, 7, 11, 14, 16, and 21 in group B1. Cancer Res 39:3479-84.
340. Woo, J. L., and A. J. Berk. 2007. Adenovirus ubiquitin-protein ligase stimulates viral late mRNA nuclear export. J Virol 81:575-87.
341. Xi, Q., R. Cuesta, and R. J. Schneider. 2005. Regulation of translation by ribosome shunting through phosphotyrosine-dependent coupling of adenovirus protein 100k to viral mRNAs. J Virol 79:5676-83.
342. Xi, Q., R. Cuesta, and R. J. Schneider. 2004. Tethering of eIF4G to adenoviral mRNAs by viral 100k protein drives ribosome shunting. Genes Dev 18:1997-2009.
343. Xiao, S. H., and J. L. Manley. 1997. Phosphorylation of the ASF/SF2 RS domain affects both protein-protein and protein-RNA interactions and is necessary for splicing. Genes Dev 11:334-44.
344. Yang, U. C., W. Huang, and S. J. Flint. 1996. mRNA export correlates with activation of transcription in human subgroup C adenovirus-infected cells. J Virol 70:4071-80.
345. Yatherajam, G., W. Huang, and S. J. Flint. 2011. Export of adenoviral late mRNA from the nucleus requires the Nxf1/Tap export receptor. J Virol.
346. Yew, P. R., and A. J. Berk. 1992. Inhibition of p53 transactivation required for transformation by adenovirus early 1B protein. Nature 357:82-5.
347. Yew, P. R., C. C. Kao, and A. J. Berk. 1990. Dissection of functional domains in the adenovirus 2 early 1B 55K polypeptide by suppressor-linker insertional mutagenesis. Virology 179:795-805.
348. Yew, P. R., X. Liu, and A. J. Berk. 1994. Adenovirus E1B oncoprotein tethers a transcriptional repression domain to p53. Genes Dev 8:190-202.
349. Yolken, R. H., F. Lawrence, F. Leister, H. E. Takiff, and S. E. Strauss. 1982. Gastroenteritis associated with enteric type adenovirus in hospitalized infants. J Pediatr 101:21-6.
350. Yueh, A., and R. J. Schneider. 2000. Translation by ribosome shunting on adenovirus and hsp70 mRNAs facilitated by complementarity to 18S rRNA. Genes Dev 14:414-21.
351. Zantema, A., J. A. Fransen, A. Davis-Olivier, F. C. Ramaekers, G. P. Vooijs, B. DeLeys, and A. J. Van der Eb. 1985. Localization of the E1B proteins of adenovirus 5 in transformed cells, as revealed by interaction with monoclonal antibodies. Virology 142:44-58.
352. Zhang, Y., and R. J. Schneider. 1993. Adenovirus inhibition of cellular protein synthesis and the specific translation of late viral mRNAs. Semin. Virol. 4:229-36
353. Zhou, Z., M. J. Luo, K. Straesser, J. Katahira, E. Hurt, and R. Reed. 2000. The protein Aly links pre-messenger-RNA splicing to nuclear export in metazoans. Nature 407:401-5.
354. Zolotukhin, A. S., and B. K. Felber. 1999. Nucleoporins nup98 and nup214 participate in nuclear export of human immunodeficiency virus type 1 Rev. J Virol 73:120-7.

8 Abbreviations

Ad	adenovirus
APS	ammonium persulfate
aa	amino acid
bp	base pair
BSA	bovine serum albumin
DEPC	diethyl pyrocarbonate
dd	distilled deionized
DMSO	dimethyl sulfoxide
DTT	dithiothreitol
EDTA	ethylene diamine tetraacetic acid
ffu	fluorescence forming units
fwd	forward
g	gravitational constant
h p.i.	hours post infection
Ig	immunoglobulin
kbp	Kilo base pair
K, kDa	Kilodalton
min	minute
moi	multiplicity of infection
MOPS	3-(N-Morpholino) propane sulfonic acid
NES	nuclear export signal
NLS	nuclear localization signal
NRS	nuclear retention signal
nt	nucleotide
OD	optical density
orf	open reading frame
PBS	phosphate buffered saline
rev	reverse
rpm	rotations per minute
RT	room temperature
s	second
SDS	sodium dodecyl sulfate
TEMED	N,N,N',N'-Tetra methyl ethylene diamine
Tris	Tris (hydroxymethyl) aminomethane
U	unit
v/v	volume per volume
w/v	weight per volume
wt	wild type

Publications

Publications in scientific journals

Schmid M, Kindsmüller K, Wimmer P, Groitl P, Gonzalez R, Dobner T. (2011). The E3 ubiquitin ligase activity associated with the adenoviral E1B-55K-E4orf6 complex does not require CRM1-dependent export. J Virol. Accepted for publication.

Schmid M, Gonzalez R, Dobner T. (2011). CRM1-dependent transport supports cytoplasmic accumulation of adenoviral early transcripts. J Virol. Submitted for publication.

Schmid M, Kindsmüller K, Groitl P, Dobner T. Efficient replication of adenovirus type 5 is dependent on proteasomal degradation of p53 and Mre11. Manuscript in preparation.

Koyuncu O, **Schmid M**, Speiseder T, Gonzalez R, Dobner T. The nuclear export signal of adenovirus type 5 L4-100K is crucial for efficient virus infection. Manuscript in preparation.

Oral presentations at scientific meetings

Schmid M, Kindsmüller K, Dobner T. Regulation of nucleocytoplasmic transport in adenovirus infected cells. *Annual Retreat Virus-Host-Interaction*, Heinrich-Pette-Institut, Hamburg, Germany, 21. November 2008.

Schmid M, Kindsmüller K, Dobner T. Analysis of human adenovirus Type 5 E1B-55K and E4orf6 nucleocytoplasmic shuttling functions in productive infection. *2nd Adenovirus Workshop*, Hamburg, Germany, 11. – 13. February 2009.

Schmid M, Kindsmüller K, Dobner T. Analysis of human adenovirus Type 5 E1B-55K and E4orf6 nucleocytoplasmic shuttling functions in productive infection. *19th Annual Meeting of the Society of Virology*, Leipzig, Germany, 18. – 21. March 2009.

Schmid M, Kindsmüller K, Koyuncu O, Groitl P, Gonzalez R, Dobner T. Control of viral mRNA export by adenovirus regulatory proteins. *4th European Congress of Virology*, Cernobbio, Italy, 7. – 11. April 2010.

Schmid M, Kindsmüller K, Koyuncu O, Groitl P, Gonzalez R, Dobner T. Control of viral mRNA export by adenovirus regulatory proteins. *Annual Retreat Virus-Host-Interaction*, Heinrich-Pette-Institut, Hamburg, Germany, 5. July 2010.

Schmid M, Kindsmüller K, Koyuncu O, Groitl P, Gonzalez R, Dobner T. Control of viral mRNA export by adenovirus regulatory proteins. *Molecular Biology of DNA Tumor Viruses Conference*, Madison, Wisconsin, USA, 13. – 18. July 2010.

Schmid M, Gonzalez R, Dobner T. CRM1-dependent transport supports cytoplasmic accumulation of adenoviral early transcripts. *3rd Adenovirus Workshop*, Regensburg, Germany, 16. – 18. February 2011.

Poster presentations at scientific meetings

Schmid M, Kindsmüller K, Dobner T. Analysis of human adenovirus Type 5 E1B-55K and E4orf6 nucleocytoplasmic shuttling functions in productive infection. *19th Annual Meeting of the Society of Virology*, Leipzig, Germany, 18. – 21. March 2009.

Schmid M, Kindsmüller K, Koyuncu O, Groitl P, Gonzalez R, Dobner T. Control of viral mRNA export by adenovirus regulatory proteins. *4th European Congress of Virology*, Cernobbio, Italy, 7. – 11. April 2010.

Schmid M, Kindsmüller K, Koyuncu O, Groitl P, Gonzalez R, Dobner T. Control of viral mRNA export by adenovirus regulatory proteins. *Molecular Biology of DNA Tumor Viruses Conference*, Madison, Wisconsin, USA, 13. – 18. July 2010.

Acknowledgements

Mein ganz besonderer Dank gilt meinem Doktorvater Prof Dr. Thomas Dobner für die Bereitstellung meines überaus spannenden Themas, die zahlreichen wertvollen Anregungen und kritischen Diskussionen, sowie die fortwährende Unterstützung meiner Arbeit.

Agradezco al Prof. Dr. Ramón González por asumir una segunda opinión de mi trabajo, y además por haberme aceptado en su laboratorio, y otorgándome la posibilidad de trabajar en él. Además de todo esto, me gustaría agradecerle por las innumerables discusiones, y su hospitalidad tan generosa.

Allen dicken Dobners danke ich für die gute Zusammenarbeit und die stete Hilfsbereitschaft. Bei Peter Groitl möchte ich mich für seine Hilfe und die wertvollen Ratschläge bei verschiedenen Klonierungen bedanken. Mein besonderer Dank gilt Dr. Thomas Speiseder und Daniela Müller für die moralische als auch praktische Unterstützung m einer Arbeit. Dr. Peter Wimmer möchte ich für hilfreiche Diskussionen sowie die kritische Durchsicht des Manuskripts danken.

Me gustaría agradecer excepcionalmente a todos aquellos que hicieron mi estancia en Cuernavaca tan inolvidable.

Prof Dr. Schlüter und Dr. Maria Trusch danke ich für ihre Hilfe bezüglich der massenspektrometrischen Analysen. Des Weiteren danke ich Maria für ihre stete fachliche als auch moralische Unterstüzung und das geduldige Korrekturlesen meiner Arbeit.

Prof Dr. Jungblut und seiner Arbeitsgruppe danke ich für die aufwändige Herstellung sämtlicher 2D Gele.

Many thanks also to Dr. Avril Arthur-Goettig for reading and correcting my thesis.

Vorrei ringraziare Salvatore Tramontano per completarmi e rendermi felice.

Mein herzlichster Dank gilt meiner Familie für die fortwährende Förderung und die liebevolle Unterstützung. Insbesondere möchte ich mich bei meinen Eltern und meiner Schwester für ihre Liebe, ihr grenzenloses Verständnis und dafür bedanken, dass sie mir stets Kraft geben um weiter zu machen.

DR AVRIL ARTHUR-GOETTIG

Specializing in editing, writing, translations for biotechnology
molecular medicine and
life sciences

Roemerstrasse 25
80801 Muenchen
Germany
Tel: +49 (0)89 337 696
Fax: +49 (0)89 337 696
Email: avril@bioxpress.de

www.bioXpress.de

09.05.11

RE: The thesis submitted to the University of Hamburg
for the degree of DOCTOR OF NATURAL SCIENCES (Dr. rer. nat.)
by **Melanie Schmid**

I hereby declare as a native English speaker and professional scientific writer that I have checked this thesis for grammatically correct English and the scientific accuracy of the language.

Signed,

Dr. Avril Arthur-Goettig